ECOLE DE TECHNOLOGIE SUPÉRIEURE
UNIVERSITÉ DU QUÉBEC

MANUSCRIPT-BASED THESIS PRESENTED TO
ÉCOLE DE TECHNOLOGIE SUPÉRIEURE

IN PARTIAL FULFILLMENT OF THE REQUIREMENTS FOR
THE DEGREE OF DOCTOR OF PHILOSOPHY
Ph.D.

BY
Yamina BOUGHARI

FLIGHT CONTROL OPTIMIZATION FROM DESIGN TO ASSESSMENT APPLICATION ON THE CESSNA CITATION X BUSINESS AIRCRAFT

MONTREAL, 24TH OF JANUARY 2017

BOARD OF EXAMINERS

THIS THESIS HAS BEEN EVALUATED

BY THE FOLLOWING BOARD OF EXAMINERS

Mrs. Ruxandra Mahela Botez, Thesis Supervisor
Department of Automated Production Engineering at École de technologie supérieure

Mr. Thien-My Dao, President of the jury
Department of Mechanical Engineering at École de technologie supérieure

Mr. Guy Gauthier, Member of the jury
Department of Automated Production Engineering at École de technologie supérieure

Mr. Hekmat Alighanbari, External Evaluator
Department of Aerospace Engineering at Ryerson University

THIS THESIS WAS PRENSENTED AND DEFENDED

IN THE PRESENCE OF A BOARD OF EXAMINERS AND THE PUBLIC

1ST DECEMBER, 2016

AT ÉCOLE DE TECHNOLOGIE SUPÉRIEURE

ACKNOWLEDGMENTS

First and foremost, I would like to express my sincere gratitude to my supervisor, Prof. Ruxandra Mihaela Botez for her support throughout the duration of my research project, for her constant encouragement, for the motivation to participate at conferences and networking events, and for presenting me the great opportunity of teaching, without her continuous guidance and persistent help this dissertation would not have been possible.

Thanks to the project leader Mr Ken Dustin and his team at CAE Inc. for their support in the development of the Aircraft Research Flight Simulator at the LARCASE laboratory. Thanks are also due to Mrs Odette Lacasse and Mr Oscar Carranza at ETS for their continuing enthusiasm and support.

I am very much thankful to all past and present members of LARCASE who participated and contributed to the realization of this project, especially Georges and Florian for their suggestions, dedication and hard work, for Alejandro Murrieta, for reading some of my papers and given me valuable advices.

A great thank you to my family in Algeria, my friends, for their love, encouragement and support, to my husband Youssef, my son Mohammed Amine, for their patience, also to my step family, and special thank to Carol who took care of my child during my absences.

I owe my deepest gratitude to my mother, Auda, my father Abd El Kader and my brother Moustapha, for their continuous support, without them I would not be where I am, nor would I be the person that I am today. I also dedicate this dissertation to the memory of my uncle Mohammed.

Above all, thanks to the Great Almighty, author of knowledge and wisdom for his countless love.

FLIGHT CONTROL OPTIMIZATION FROM DESIGN TO ASSESSMENT APPLICATION ON THE CESSNA CITATION X BUSINESS AIRCRAFT

Yamina BOUGHARI

ABSTRACT

New methodologies have been developed to optimize the integration, testing and certification of flight control systems, an expensive process in the aerospace industry. This thesis investigates the stability of the Cessna Citation X aircraft without control, and then optimizes two different flight controllers from design to validation. The aircraft's model was obtained from the data provided by the Research Aircraft Flight Simulator (RAFS) of the Cessna Citation business aircraft.

To increase the stability and control of aircraft systems, optimizations of two different flight control designs were performed: 1) the Linear Quadratic Regulation and the Proportional Integral controllers were optimized using the Differential Evolution algorithm and the level 1 handling qualities as the objective function. The results were validated for the linear and nonlinear aircraft models, and some of the clearance criteria were investigated; and 2) the *H-infinity* control method was applied on the stability and control augmentation systems. To minimize the time required for flight control design and its validation, an optimization of the controllers design was performed using the Differential Evolution (DE), and the Genetic algorithms (GA). The DE algorithm proved to be more efficient than the GA. New tools for visualization of the linear validation process were also developed to reduce the time required for the flight controller assessment.

Matlab® software was used to validate the different optimization algorithms' results. Research platforms of the aircraft's linear and nonlinear models were developed, and compared with the results of flight tests performed on the Research Aircraft Flight Simulator.

Some of the clearance criteria of the optimized *H-infinity* flight controller were evaluated, including its linear stability, eigenvalues, and handling qualities criteria. Nonlinear simulations of the maneuvers criteria were also investigated during this research to assess the Cessna Citation X's flight controller clearance, and therefore, for its anticipated certification.

Keywords: Linear Fractional Representation, Flight Control Certification, Stability Analysis, Optimal Control, Heuristic Algorithm

OPTIMISATION DE LA COMMANDE DE VOL DE LA CONCEPTION A L'ÉVALUATION APPLICATION A L'AVION D'AFFAIRE CESSNA CITATION X

Yamina BOUGHARI

RÉSUMÉ

Afin d'améliorer le processus coûteux d'intégration, d'essai et de certification des systèmes de commande de vol des avions civils dans l'industrie de l'aérospatiale, de nouvelles méthodologies ont été développées pour son optimisation. Le modèle de l'avion a été obtenu à partir des données fournies par le simulateur de vol de recherche de l'avion. Dans cette thèse, on a étudié la stabilité du Cessna Citation X sans contrôle, puis deux contrôleurs différents de vol ont été optimisés a partir de leur conception jusqu' à leur validation sur l'avion Cessna Citation X.

Pour augmenter le système de stabilité et de contrôle de l'aéronef, des optimisations de deux conceptions différentes d'un contrôleur de vol ont été effectuées; d'une part, la méthode moderne de la régulation quadratique linéaire et la méthode classique de la commande proportionnelle intégrale ont été optimisées en utilisant l'algorithme de l'évolution différentielle, et en utilisant le niveau 1 des qualités de manœuvrabilités comme fonction objective. Les résultats on été validés pour les modèles linéaire et non linéaire de l'avion, et quelques critères de certification ont été évalués.

D'autre part, au lieu d'utiliser une combinaison de deux méthodes de contrôle ci haut mentionnées, la méthode de contrôle *H-infini* a été utilisée pour assurer l'obtention des systèmes d'augmentation de la stabilité et de contrôle. Pour réduire le temps entre la conception de la commande de vol et la validation, une optimisation de la conception de contrôleur a été réalisée en utilisant l'algorithme de l'évolution différentielle, et l'algorithme génétique. L'algorithme de l'évolution différentielle a montré plus d'efficacité que l'algorithme génétique; également de nouveaux outils pour la visualisation du processus de validation linéaire ont été développés pour réduire le temps requis pour l'évaluation du contrôleur de vol.

Pour valider les différents résultats obtenus par des optimisations des algorithmes, le logiciel Matlab a été utilisé dans lequel des plateformes de recherches du modèle linéaire et non linéaire de l'aéronef ont été développés et ont été comparées à des essais en vol effectués sur le simulateur de vol de recherche de l'avion.

Quelques critères de certification du contrôleur de vol conçu avec *H-infini* optimisé tel que la stabilité linéaire, les valeurs propres, et les critères de qualités de manœuvrabilités ont été évalués ; en outre, des critères de simulation de manœuvres des modèles non linéaires ont été étudiés au cours de cette recherche visant à évaluer l'avion d'affaires pour la certification future du contrôleur de vol.

Mots clés : Représentation fractionnaire linéaire, Certification du control de vol, Analyse de stabilité, Contrôle optimal, Algorithme heuristique.

TABLE OF CONTENTS

Page

LIST OF TABLES

Page

LIST OF FIGURES

Page

LIST OF ABREVIATIONS

ADMIRE	Air Data Model In Research Environement
CAS	Control Augmentation System
COFCLUO	Clearance Of Flight Control Laws Using Optimization
DE	Differential Evolution
EASA	European Aviation Safety Agency
ESS	Steady State Error
FAA	Federal Aviation Administration
FBW	Flight By Wire
FCL	Flight Control Law
FCS	Flight Control System
GA	Genetic Algorithm
GRATEUR	Aeronautical Research and Technology
GUI	Graphical User Interface
HIRM	High Incidence Research Model
HWEM	High performance short take off and vertical landing aircraft Model
LARCASE	Laboratory of avionics
LFR	Linear Fractional Representation
LFT	Linear Fractional Transformation
LQG	Linear Qudratic Gaussian
LQR	Linear Quadratic Regulation
MIMO	Multi Inputs Multi Outputs

PID	Proportional Integral Derivative
PIO	Pilot Induced Oscilation
PSO	Swarm Partical Optimization
SISO	Single Input Single Output
TAS	True Air Speed

LIST OF SYMBOLS AND UNITS OF MEASUREMENTS

A,B,C,D	State space matrices
p, q, r	Angular speeds along Ox, Oy, Oz axis
u, v, w	Speeds along the Ox, Oy, Oz axis
u(t)	Control vector
x(t)	State space vector
V	Total Aircraft Speed
X, Z, Y	Aircraft aerodynamic forces
OS	Overshoot
Ts	Settling Time
$F_l(P,K)$	Lower linear fractional transformation
K	Feedback Gain
W_1	Sensitivity weighting function
W_2	Complementary sensitivity weighting function
$\delta_e, \delta_a, \delta_r$	Elevator, aileron, and rudder deflections
θ , β, ϕ	Pitch angle, sideslip angle, and roll angle
ω_n	Natural frequency
ζ	Damping coefficient
γ	Robustness criterion
ki	Integral Gain
kp	Proportional Gain
Kw	Vertical speed Gain
Kq	Pitch rate Gain

P	Positive Semi-Definite Matrix
J	LQR Cost Function
Q	Weighting Matrix for the states
R	Weighting Matrix for control input
Δ	Block uncertainties
$V(x)$	System energy
$\mathbb{R}$	Real matrices m x n
$\mathbb{C}$	Complex matrices m x n
$\mathbb{Z}$	Integer number field
A^T	Transposition of matrix A
A^{-1}	Inverse of matrix A
A^*	Trans-conjugate of matrix A
Θ	Polytope (the variation range of each uncertainty)

INTRODUCTION

0.1 Problem Statement

The certification of an aircraft is an important and essential step in the process leading to its first flight. To prove that an aircraft is ready to fly, it must meet several criteria required by various agencies such as Transport Canada, the Federal Aviation Administration (FAA), or the European Aviation Safety Agency (EASA).

The Flight Control System (FCS) requires one of the most stringent certification processes in the aeronautical industry. The FCS is an automatic system that allows the pilot to control an aircraft during its mission, and provides for safe and economical operations. The FCS contains mechanical linkages that connect the pilot's control inputs to the aircraft control surfaces.

Flight automation has led to the development of the Fly By Wire FCS, illustrated in Figure 0-1, which replaces the mechanical linkages by electrical signals between the pilot's inputs and the control surfaces (aircraft actuators).

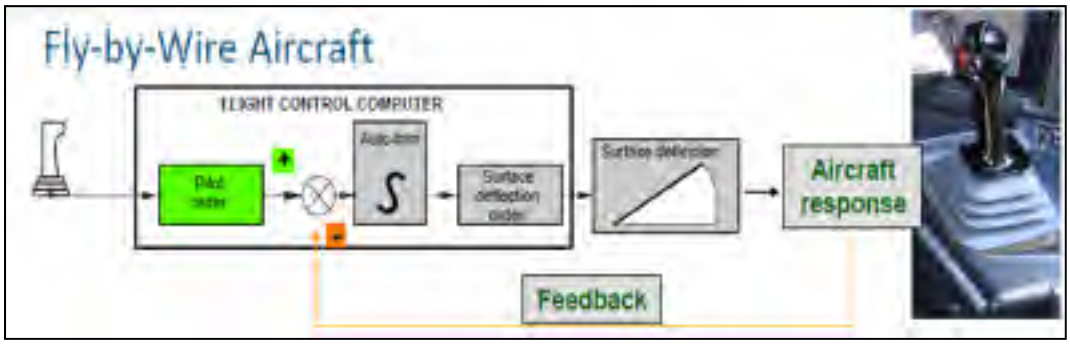

Figure 0-1 Fly-by –wire concept
Taken from (DUMOLLARD, 2014)

Civil aircraft FCS clearance is a fastidious task, especially for modern aircraft that must achieve high performance standards (C. Fielding, 2002; Nelson, 1998). Flight Control Laws (FCL), defined as the relationship between a pilot's stick input and the aircraft's response,

were developed as an important part of the FCS design. FCL clearance is considered as the last step in the certification process; with FCL clearance, an aircraft has reached a mature phase in its design, and is ready for validation and verification by means of flight tests.

However, developing FCL from concept to certification is a very expensive process in terms of money and resources. Over the last few decades, much research has been done to develop advanced methods for aircraft design and analysis that enhance the flight control law (FCL) development process. Several analysis methods are now available to address virtually any realistic design challenge and to the FCL design process. FCL design can be realized in five steps, as follows (Fielding et al., 2002):

1. The FCL architecture is defined, and the desired closed-loop specifications and the handling qualities are achieved by tuning the control law parameters. Linear analysis and nonlinear simulations are performed to assess a new FCL design's effect on an aircraft's stability and performance.
2. To assess the handling qualities of the augmented aircraft, simulations via *pilot-in-the-loop* are performed.
3. To verify if the FCL matches with the FCS hardware in the loop and operates as desired, tests are performed on a *Functional Integration Bench* known as the *Iron Bird*.
4. A clearance process verifies that the FCL fulfills all the requirements for a safe flight under a range of parameter variations and failure conditions for the entire flight envelope.
5. Flight tests are performed to validate the FCS design according to the airworthiness requirements and to assure that it meets the customer's expectations.

Designing an optimal FCL which meets all the desired requirements is an iterative and lengthy process, one that should be automated. There are several methods that address the controller optimality, but they usually employ an ad hoc technique to meet the design requirements. Due to the iterative nature of this process, an optimization algorithm is required to manage the engineering workload. At the Laboratory of Applied Research in Active Control, Avionics, and AeroServoElasticity (LARCASE), new optimizations based on

heuristic and deterministic algorithms were developed and implemented in realistic aircraft models for their identification (Ghazi, Botez et Achigui, 2015), flight trajectory optimization (Murrieta-Mendoza, Botez et Patrón, 2015), (Murrieta-Mendoza et Botez, 2015a), (Patrón, Botez et Labour, 2013), and FCL design, (Boughari et al., 2014a), (Boughari et al., 2014b; Ghazi et Botez, 2014a),(Ghazi et Botez, 2015c).

An FCL has to meet the flying qualities requirements and the closed-loop performance specifications. The main flying qualities used in FCL clearance are those that verify the linear and nonlinear aircraft maneuvers, and any that are further defined for the aircraft's longitudinal and lateral modes.

Aircraft flying qualities are provided by the "*U.S Military Specification for the Flying Qualities of Piloted Airplanes MIL-STD-1797A."* For longitudinal aircraft motion, two modes are perceived: 1) short period and 2) phugoïd mode. Three modes are perceived for aircraft lateral motion:1) the Dutch roll mode, 2) the roll mode, and 3) the spiral mode. These modes must respect some of the desired criteria required for very good flight performance, expressed in terms of the damping and time constants, as shown in Table 0.1. Very good flight performances must be met for the cruise phase, and for flight level 1, which corresponds to very good flying qualities (Standard, 1990), (Bailey et al., 2009), (Roskam, 1985). Thus the aircraft responses have to meet the criteria given in Table 0.1 for the aircraft certification.

Table 0-1 Aircraft flying qualities level 1

Criterion	Type	Limits
Short period damping	modal	$0.3 \leq \xi_{sp} \leq 2$
Phugoid damping	modal	$0.04 \leq \xi_{ph}$
Dutch roll damping	modal	$0.3 \leq \xi_{dr} \leq 2$
Roll time constant	temporal	Tr <1.4 sec

To demonstrate that an aircraft is safe to fly requires more than a verification of the handling qualities to clear the FCL, and so exhaustive stability analysis must be performed for linear and nonlinear model design over the entire flight envelope to test the robustness of the aircraft nominal model, and that of its uncertainties.

"Linear stability" aims to prove that an aircraft is stable over the whole flight envelope with sufficient phase and gain margins (gain over 6dB and phase over 45 degrees). It is evaluated for either the open-loop aircraft system by using Nichols plots, or for the closed loop by calculating the eigenvalues (negative eigenvalues) for the whole envelope. It is obvious that linear stability and flying qualities are the crucial clearance criteria which have to be fulfilled during the FCL process from design to clearance.

0.2 Objectives

The main objective in this research is the optimization of the FCL design by using some of the clearance criteria as optimization parameters, and by automating the iterative process following the development of new tools for FCL validation. This approach has been selected

based on its promise to reduce the amount of resources and costs required for this optimization.

To reach the main objectives, several sub-objectives have to be fulfilled:

1. Creation of a database of Cessna Citation X aircraft linear models that covers the entire flight envelope by using the interpolation of Linear Fractional Representation models (LFR). Altitudes and True Air Speeds (TAS) are given as flight point coordinates.
2. Development of new tools for generating a Cessna Citation X aircraft LFR model; very good visualization and analysis could be achieved using a new Graphical User Interface (GUI).
3. Analysis of the natural stability of the Cessna Citation X business aircraft on its entire flight envelope, for different weight and Xcg configurations. A unique database was created to assess the Cessna Citation X aircraft clearance for any FCL design.
4. Definition of the FCL architecture for two different modern control methods, and identification of the main parameters leading to their design optimization.
5. Definition of the desired flying qualities for both longitudinal and lateral aircraft dynamics.
6. Development and implementation of in-house evolutionary algorithms to reduce the global computation time of the FCL design.
7. Development of new tools for the visualization of the aircraft linear model's validation in its flight envelope.
8. Implementation and validation of the FCL in the aircraft nonlinear model. Carrying out tests to assess the FCL robustness for Xcg and weight variation cases due to aircraft fuel burn.
9. Evaluation of the resulting optimized FCL clearance criteria for both linear and nonlinear aircraft models.

0.3 Methodology

In this section, the Cessna Citation X business aircraft nonlinear and linear dynamics are described within the operating flight envelope. The "Stability Analysis Toolbox" used for the aircraft stability analysis is then briefly introduced.

0.3.1 Cessna Citation X business aircraft model

The algorithms for this research were developed in Matlab®. The aircraft nonlinear model for the development and validation of the FCL was built in Matlab/Simulink based on aerodynamics data extracted from a Cessna Citation X Level D Research Aircraft Flight Simulator designed and manufactured by CAE Inc., presented in Figure 0-2. According to the Federal Administration AviFation (FAA, AC 120-40B) (FAA, 1991), Level D is the highest certification level that can be delivered by the FAA Certification Authorities for flight dynamics. More than 100 flight tests were performed on the Citation X Level D Research Aircraft Flight Simulator within its flight envelope. Due to its high certification level for its flight dynamics, the RAFS was flown as a real aircraft, and its flight test data were used for this research.

Figure 0-2 Cessna Citation X Research Aircraft Flight Simulator (RAFS)

Trim and linearization routines of the nonlinear aircraft model around a fixed flight condition were developed in (Ghazi, 2014; Ghazi et Botez, 2015b),. The aircraft longitudinal and lateral equations of motion have been linearized for different flight conditions in terms of altitudes and speeds, and for different aircraft configurations in terms of mass and center of gravity positions. To validate the different models obtained by linearization, several comparisons of these models with the linear model obtained by the use of identification techniques proposed by Hamel et al (2013) were performed for different flight conditions and aircraft configurations. The results have shown that the obtained linear models are accurate, and could be further used to estimate the local behavior of the Cessna Citation X for any flight condition.

0.3.2 Aircraft dynamics

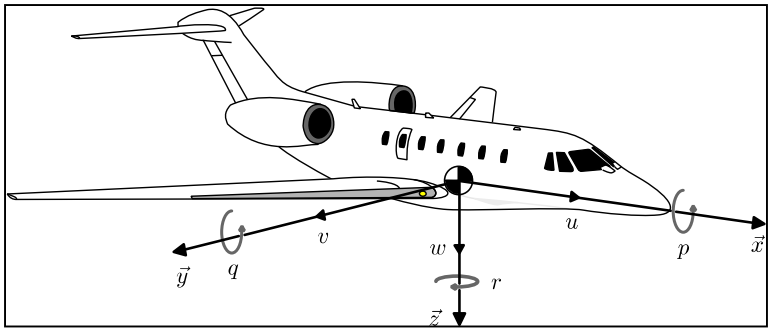

Figure 0-3 Representation of Cessna Citation X aircraft's rotation axes

The Cessna Citation X business aircraft rotation axes are represented in Figure 0-3. This aircraft can be represented using a nonlinear model, as given below:

The rates of change positions *x, y* and *z* are:

$$\dot{x} = (\cos\theta\cos\psi)u + (-\cos\varphi\sin\theta\cos\psi)v + (\sin\varphi\sin\psi + \cos\varphi\sin\theta\cos\psi)w \quad (0.1)$$

$$\dot{y} = (\cos\theta\cos\psi)u + (\cos\varphi\cos\psi + \sin\theta\sin\varphi\sin\psi)v + (-\sin\varphi\cos\psi + \cos\varphi\sin\theta\sin\psi)w \quad (0.2)$$

$$\dot{z} = (-\sin\theta)u + (\sin\varphi\cos\theta)v + (\cos\varphi\cos\theta)w \quad (0.3)$$

and the rates of change of angular positions *p, q* and *r* are:

$$p = \dot{\varphi} - \dot{\psi}\sin\theta \tag{0.4}$$

$$q = \dot{\theta}\cos\varphi + \dot{\psi}\cos\theta\sin\varphi \tag{0.5}$$

$$r = -\dot{\theta}\sin\varphi + \dot{\psi}\cos\theta\cos\varphi \tag{0.6}$$

$$\dot{\theta} = q\sin\varphi - r\cos\varphi \tag{0.7}$$

$$\dot{\varphi} = p + q\sin\varphi\tan\theta + r\cos\varphi\tan\theta \tag{0.8}$$

$$\dot{\psi} = (q\sin\varphi + r\cos\varphi)/\cos\theta \tag{0.9}$$

The rates of change of speeds are:

$$\dot{u} = \frac{X}{m} - g\sin\theta + rv - qw \tag{0.10}$$

$$\dot{v} = \frac{Y}{m} + g\sin\varphi\cos\theta - r\,u + p\,w \tag{0.11}$$

$$\dot{w} = \frac{Z}{m} - g\cos\varphi\cos\theta - pv + qu \tag{0.12}$$

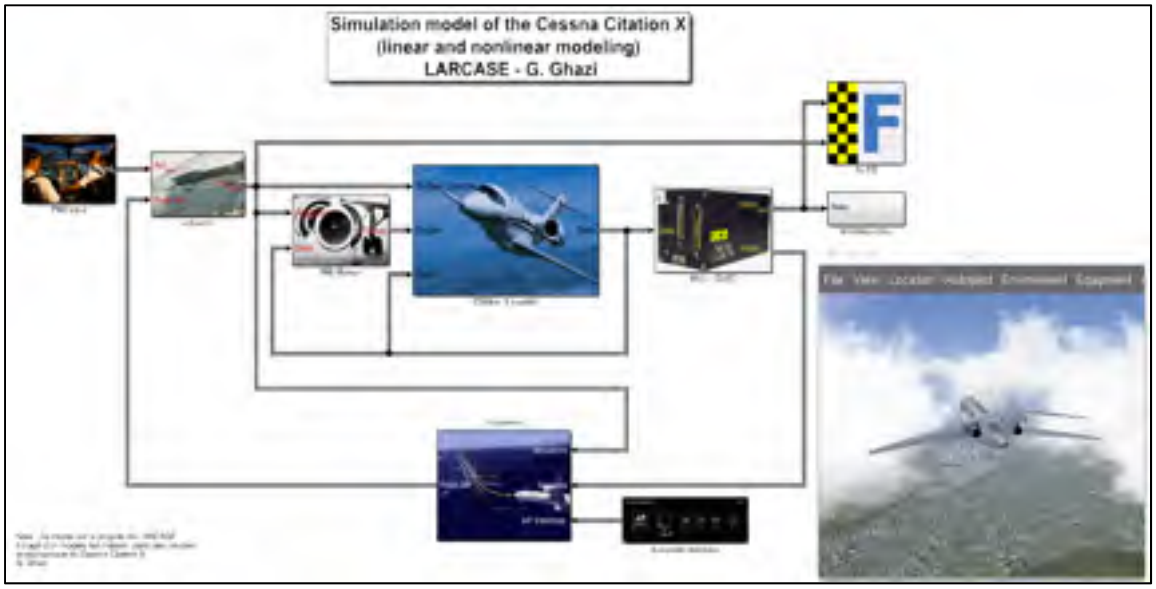

Figure 0-4 Simulation of linear and nonlinear model of the Cessna Citation X
Taken from (Ghazi, 2014)

The simulations of a Cessna Citation X linear and nonlinear model are represented in Figure 0-4. To design a controller for any aircraft, a linearization of the nonlinear aircraft model for

flight conditions within the flight envelope given by the designer is required as a first step. Following the decoupling of the linearized aircraft motion into longitudinal and lateral motions, the equations are represented in the form of the following state space system:

$$\dot{X} = Ax + Bu \tag{0.13}$$

The aircraft's longitudinal motion dynamics are given by the state space equation, using the elevator deflection as input:

$$\dot{X}_{long} = A_{long}x_{long} + B_{long}u_{long}$$

$$A_{Long} = \begin{pmatrix} X_u & X_w & X_q & -g\cos\theta \\ Z_u & Z_w & Z_q & 0 \\ M_u + M_{\dot{w}}Z_u & M_w + M_{\dot{w}}Z_w & M_q + M_{\dot{w}}u_0 & 0 \\ 0 & 0 & 1 & 0 \end{pmatrix},$$

$$B_{Long} = \begin{pmatrix} X_{\delta_e} \\ Z_{\delta_e} \\ M_{\delta_e} + M_{\dot{w}}Z_{\delta_e} \\ 0 \end{pmatrix} \tag{0.14}$$

where the state vector $x_{long}(t)$ and the control vector $u_{long}(t)$ are given by:

$$x_{long}(t) = (u \quad w \quad q \quad \theta)^T \ \ and \ \ u_{long}(t) = \delta_e \tag{0.15}$$

The aircraft's lateral motion dynamics are given by the state space equation, using the aileron and the rudder as deflection inputs:

$$\dot{X}_{lat} = A_{lat}\,x_{lat} + B_{lat}u_{lat}$$

$$A_{Lat} = \begin{pmatrix} Y_\beta/u_0 & Y_p/u_0 & -(1 - Y_r/u_0) & g\cos\theta_0/u_0 \\ L_\beta & L_p & L_r & 0 \\ N_\beta & N_p & N_r & 0 \\ 0 & 1 & 0 & 0 \end{pmatrix}, B_{Lat} = \begin{pmatrix} Y_{\delta_a}/u_0 & Y_{\delta_r}/u_0 \\ L_{\delta_a} & L_{\delta_r} \\ N_{\delta_a} & N_{\delta_r} \\ 0 & 0 \end{pmatrix} \tag{0.16}$$

where the state vector $x_{lat}(t)$ and control vector $u_{lat}(t)$are given by:

$$x_{lat}(t) = (\beta \quad p \quad r \quad \phi)^T, \; u_{lat}(t) = (\delta_a \delta_r)^T \tag{0.17}$$

The linearized model of the Cessna Citation X was obtained for 36 flight conditions using the Cessna Citation X Aircraft Flight Research Simulator tests performed at the LARCASE (Hamel, 2013). The linearized model is further decomposed into Linear Fractional Representation LFR models (Poussot-Vassal et Roos, 2011) using the *bilinear interpolation method*. Thus, these LFR models were obtained for 72 flight points expressed in terms of TAS and altitude, for 12 weight conditions as described in the following section.

0.3.3 Flight envelope using LFR models design by flight point's interpolation

The linear models' interpolation using Linear Fractional Transformation (LFT) facilitates the calculation of the state space matrices' variation with the altitude and the TAS (Poussot-Vassal et Roos, 2011). Given the data extracted from the Research Aircraft Flight Simulator provided by CAE Inc., the aircraft flight dynamics can be described for any flight condition in the flight envelope. Figure 0-5 shows the 36 flight points selected inside the flight envelope limits. These aircraft models are obtained at each 5000 ft. in altitude for 4 different speeds.

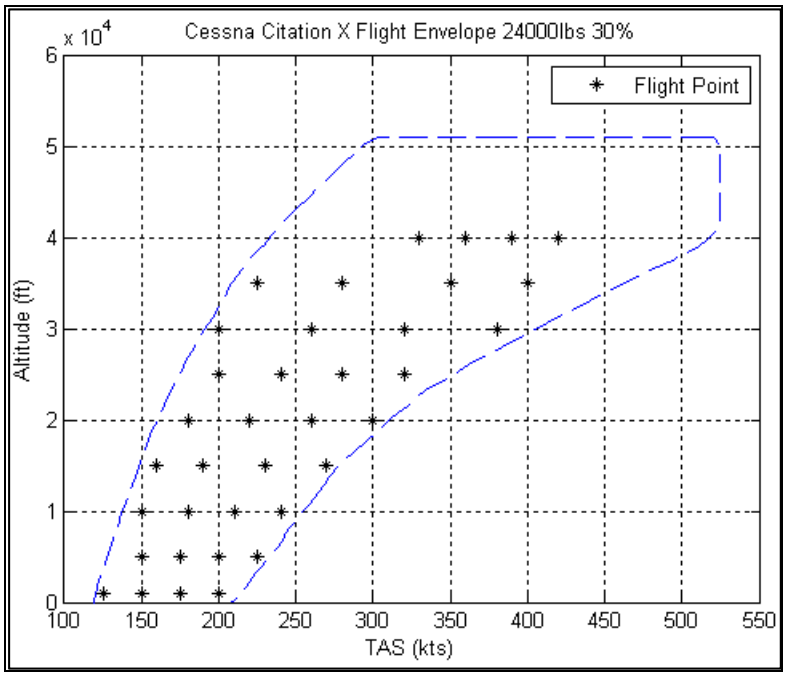

Figure 0-5 Cessna Citation X flight enveloppe

Before carrying out the interpolation, two steps need to be performed. The first step involves the definition of the region where the interpolation will be performed, for an altitude and a range of TAS, and for which the four corners of the region form the vertices. Each of these regions has lower and upper values which are defined as "bounds". The second step concerns the normalization of these bounds in order to assign a value equal to 1 or -1 to each coordinate of the vertices.

To maximize the accuracy level, the smallest possible regions have been defined, containing only 3 or 4 flight points to use as reference points for the interpolation. This definition only allows a "bilinear interpolation", for which four coefficients have to be found for each state space matrix, using equations (0.18), (0.19), and (0.20):

$$A(h,TAS) = A_{0_{4,4}} + A_{1_{4,4}}h + A_{2_{4,4}}TAS + A_{3_{4,4}}TAS \times h \tag{0.18}$$

$$B_{long}(h,TAS) = B_{0_{4,1}} + B_{1_{4,1}}h + B_{2_{4,1}}TAS + B_{3_{4,1}}TAS \times h \tag{0.19}$$

$$B_{lat}(h,TAS) = B_{0_{4,2}} + B_{1_{4,2}}h + B_{2_{4,2}}TAS + B_{3_{4,2}}TAS \times h \tag{0.20}$$

Where A is a matrix of 4 rows and 4 columns, B_{Long} is a matrix of 4 rows and 1 column, and B_{lat} is a matrix of 4 rows and 2 columns. The Least Square (LS) method is employed to minimize the relative error in these reference points.

From these results, 26 regions that cover a large part of the flight envelope are obtained, denoted by rectangles in Figure 0-5. The mesh is valid for all of the weight and X_{CG} locations presented in Figure 0-7. It can be observed from Figure 0-6 that some of the regions superimpose other regions (darker zones) due to their common reference points; for some regions, not only are their interpolations considered, but also their extrapolations.

These 26 regions' vertices lead to 72 different flight conditions obtained by means of the LFR models; these cover more space in the flight envelope, as shown in Figure 0-8.

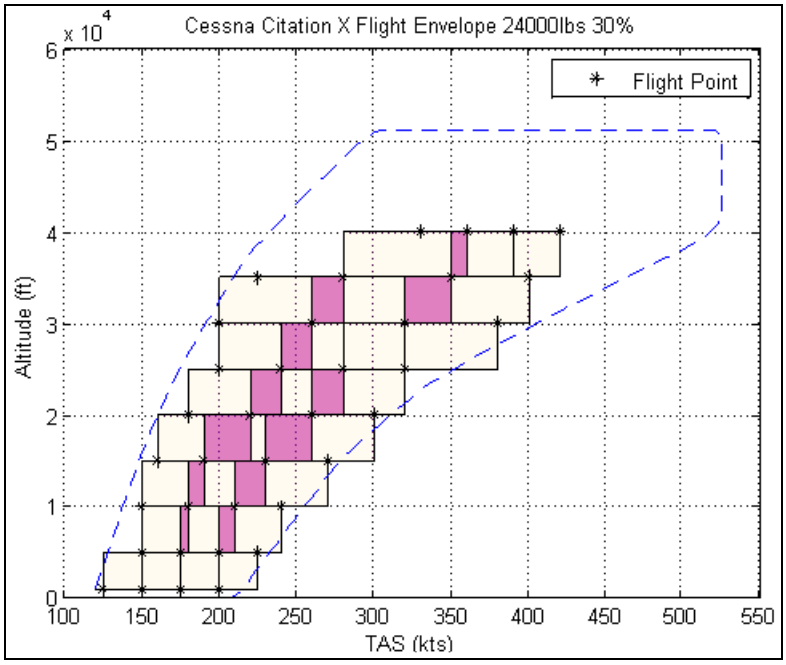

Figure 0-6 Definition of 26 regions

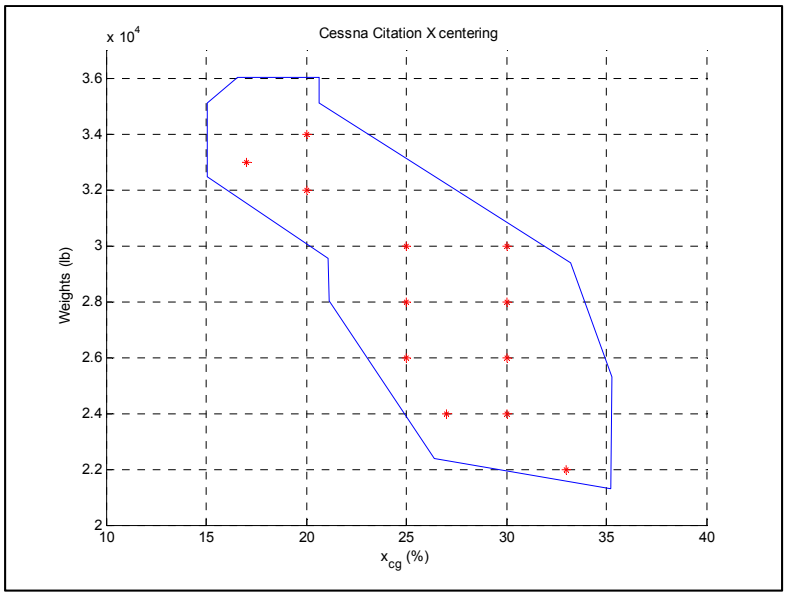

Figure 0-7 Cessna Citation X Weight/ X_{CG} conditions

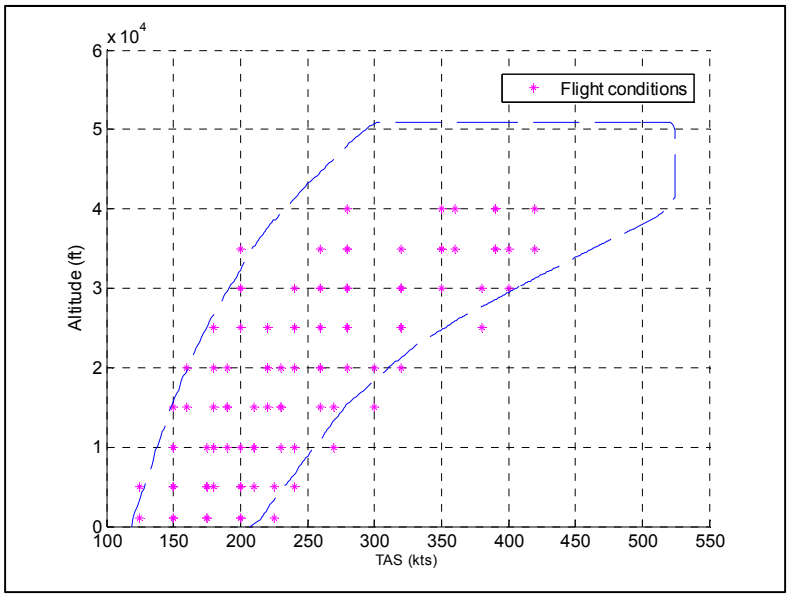

Figure 0-8 Flight points obtained by use of LFR models

0.3.4 Stability analysis interface

In order to accomplish the stability analysis, a Graphical User Interface (GUI) is used. It offers a wide choice of resolutions via three methods from published research found in (Wang et Balakrishnan, 2002), (Dettori et Scherer, 2000), and (Fu et Dasgupta, 2000). Figure

0-9 shows the window with which the user interacts; a brief description of how to manipulate the GUI is given in the following paragraph.

The GUI has two main sections; the first one is "Analysis", which contains the LFR models in “Model”, three methods for resolution in “Method”, the region that will be analyzed in “Region definition”, and “Approach”, which contains all the functions called during the analysis, classified as “ Progressive” or “Adaptive”, and the type of “Lyapunov Function”. The second section is the "Results", which stores the results data. The GUI has access to the LFR Toolbox, and to the YALMIP SDPT3.7.

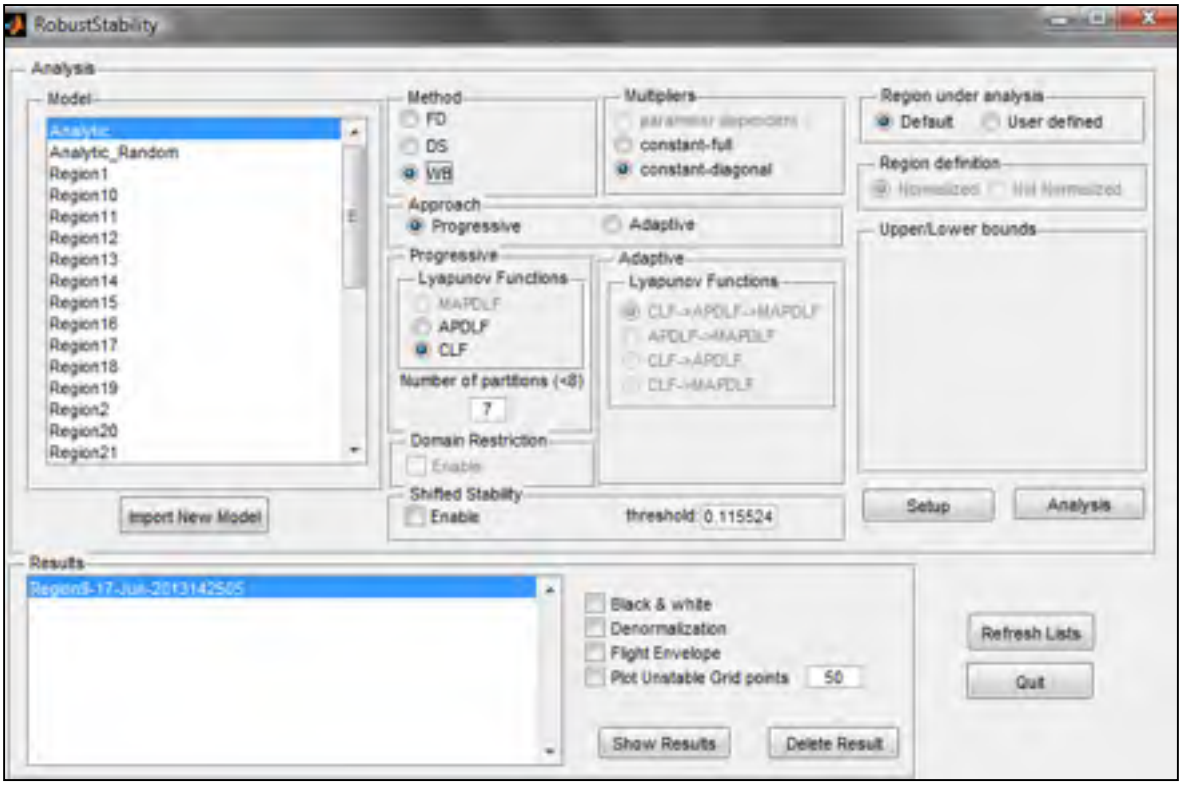

Figure 0-9 Robust Stability Toolbox

To perform the stability analysis, the desired LFR model is first selected, and then the analysis parameters method (FD, DS, and WB), which can be one of the three main methods (Wang et Balakrishnan, 2002), (Dettori et Scherer, 2000), and(Fu et Dasgupta, 2000), is

carried out, followed by the normalization of the selected region, and then some other options such as choosing the discretization number, the Lyapunov function or the approach type. Once these parameters are chosen, the stability analyses can be performed for the selected region.

CHAPITRE 1

LITTERATURE REVIEW

1.1 Aircraft Flight Control System

Flight Control System (FCS) is designed to achieve higher aircraft performance with better or acceptable flying qualities within the flight envelope specified by the designer (Pahle et al., 1996). Classical control methods usually considered Single Input, Single Output (SISO) systems for flight control while aircraft control systems required several actuators simultaneously. Thus, Multi-Inputs Multi-Outputs (MIMO) systems are of interest for designing modern control methods using the state space systems. Lacking of knowledge in FCS will limit the development of an optimal controller with high performance FCS.

During the three last decades, modern control methods gained popularity over classical methods, for their efficiency in handling Multi-Inputs Multi-Outputs (MIMO) systems especially in the aeronautical industry (Nelson, 1997b). These modern control methods were applied on the Flight By Wire (FBW) airplanes.

Use of the state space (modern control) in FBW controls does not involve complexity in computer computation, allowing improved the flight safety while reducing the pilot workload, the mechanical parts, and real time monitoring of all aircraft systems' (Samad et Annaswamy, 2011).

1.2 Flight Control Optimization

The state space equations are used for wide range of control methods (Friedland, 2012),(Skogestad et Postlethwaite, 2007). The design of optimal flight controllers relies on selecting the appropriate control method, which in turn depends on the aircraft type (civil or military), and its performance requirements (Roskam, 1985). The most popular methods are:

the Linear Quadratic Regulation Method and t the *H-infinity* method that is generally used to consider aircraft robustness requirements.

1.3 Linear Quadratic Regulation (LQR)

The advantage of the Linear Quadratic Regulation (LQR) method is that it provides the smallest possible error to both inputs and outputs while minimizing the control effort; the error corresponds to the difference between the desired and obtained value for system input and output.

In the case when the full states are measurable, the LQR method ensures a stable controller output for the nominal model, and it provides cross-terms in the flight dynamics equations. Consequently, it leads to a robust controller in the sense that the gain margin is infinite and the phase margin is greater than 60 degrees. It was illustrated in the literature by Boughari et al (2012) that LQR method has been used for the Stability Augmentation System (SAS) control, and applied on Hawker 800XP business aircraft.

In addition, the Linear Quadratic Gaussian (LQG) method has been used in (Botez et al., 2001) bomber B-52 aircraft to alleviate the gust effects. The LQR method has also been used in a longitudinal attitude controller designed for B747 aircraft (Guilong et al., 2013), and in adaptive LQR gain scheduling control is designed for remotely controlled aircraft (Mukherjee et Pieper, 2000).

In order to obtain corresponding optimal state feedback gain K in the LQR control methodology, the objective function which represents the quadratic performance index function *J* must be defined. This means the appropriate Q and R weighting matrices need to be estimated by a trial and error method, or by relying on the designer's knowledge until the desired response is found.

In order to overcome the time-consuming LQR procedure, many algorithms were developed in the last decade to optimize the LQR weighting matrices searches. Use of stochastic searching as an optimization algorithm is one of the most popular methods that have been used recently; in (Wongsathan et Sirima, 2008) , (Wongsathan et Sirima, 2009), used stochastic search method to determine LQR weighting matrices to control an inverted pendulum, and then a triple inverted pendulum. Satisfactory results were obtained by comparison of the optimal Q and R matrices with the weighting matrices obtained through "trial and error". The optimized LQR methodology using the Genetic Algorithm (GA) was applied on the buck converter to improve its voltage control response, and the distillation column control, respectively shown in (Poodeh et al., 2007) and (Jones et Hengue, 2009).
In both of those cases, the control performances that is given by weighting matrices found with a GA search provided better results than those found experimentally.

(Ghoreishi et Nekoui, 2012) used both the Genetic Algorithm (GA) and Particle Swarm Optimization (PSO) algorithms with the LQR optimization. Guo et al used optimal LQR weighting matrices analyses based on the Genetic Algorithm (GA) search (Guo et al., 2010). Stochastic search for optimal LQR control combined with integral quadratic constraints was investigated by (Lim et Zhou, 1999); while Xiong et al. (Xiong et Wan, 2010) used LQR method based on PSO algorithm for double inverted pendulum control. In (Yoon Joon et Kyung Ho, 1997), the authors investigated stochastic searching methods for the determination of the LQR weighting parameters used for nuclear reactor power control.

In (Zhu et Li, 2003), the authors have used an iterative method for solving stochastic Riccati differential equations of the LQR problem. Unfortunately, the LQR control can only provide a stability augmentation to the system, in order to perform the tracking error; a classical control method is added by using a PID control.

The PID control gain can be tuned using an ad hoc method or can be optimized using a stochastic algorithm. As illustrated by (Mitsukura, Yamamoto et Kaneda, 1997), the tuning of PID gain parameters was based on the GA, and on Fuzzy Logic in (Hyung-Soo et al.,

1999). Han, Luo et Yang (Han, Luo et Yang, 2005), used a nonlinear PID controller based on genetic tuning, while a self-tuning algorithm was investigated by the authors for linear PID controllers; this algorithm was based on frequency characteristics in (Chen, Wang et Wu, 2010). In (Chang-Hoon, Myung-Hyun et Ik-Soo, 1997), the authors have used the model identification by use of two Nyquist points to automate the PID controller tuning; in (Bandyopadhyay et Patranabis, 2001), an auto-tuning algorithm for PID controllers based on dead-beat format requirements was performed using the fuzzy inference method.

From previous researches, we can deduce that these optimized LQR and PID algorithms were mainly used in chemical industries. There is a huge amount of flight tests to be managed in the aircraft control design, thus in the aerospace industry; for this reason there is a great need in the use of the optimization algorithms that can be performed on control parameters to meet the design requirements, and to save time, and thus money, which is a part of investigation in this thesis.

1.4 *H-infinity* Controller

The aircraft's safety is dependent on its controller, as the clearance authorities need to ensure that the controller operates properly through the specified flight envelope even in presence of uncertainties related to mass, center of gravity positions, and inertia variations. The control clearance process is a fastidious and expensive task, especially for modern aircrafts that need to achieve high performance (C. Fielding, 2002) . This process aims to prove that the stability, robustness and handling requirements are satisfied against any possible uncertainties.

During the industrial clearance process, the selection of the appropriate control laws with sufficient robustness involves: the investigation of the closed-loop eigenvalues, the stability margins and the performance indices, in the presence of uncertainties. The resulting control laws are used further for the design of the Flight Control System (FCS).

The aircraft controller determination is very complex. Nonlinear methods such as Fuzzy Logic and Neural Network methods have been applied for Aircraft Identification and Control (G. Kouba, 2009),(N. Boëly, 2009). The Non- Linear Hybrid Fuzzy Logic Control on a morphing wing was explored (Grigorie et al., 2012a),(Popov et al., 2010). Due to its complexity in the Aerospace Industry, the determination of the robust Flight Control System FCS is usually carried out using linear methods applied on linear models, and it is further validated on non-linear models. In the literature, many linear control methods were used to obtain a FCS by the combination of modern control LQR method, the classical PID control method, and evolutionary algorithms that were applied successfully on the whole flight envelope of the Cessna Citation X (Boughari. et al., 20014a). However, the use of the LQR method allowed the system stabilization, while the classical PID control method was used for the tracking problem. A FCS that stabilizes and can track the reference input while taking disturbances into account was obtained by using, the *H-infinity* linear method proposed by Zames in 1983 (Zames), that had gained popularity in guarantying system robustness in the presence of uncertainties. The *H-infinity* method has been used in the Aeronautical industry to develop controllers with the aim to meet the required system specifications and needs.

One of the most important aspects of this controller is the determination of the weighting functions (W_1 and W_2), which are very important in the gains calculation. There is no specific methodology to determine these weighting functions. The literature points out that the weighting functions are determined using a trial-an-error methodology, or pure experience-based methods.

Several applications of this control method have been incorporated in the aeronautical domain, mostly for fighter jets, where a scheduled *H-infinity* controller was used for VSTOL longitudinal control (Hyde et Glover, 1993), and it has as well been used for the lateral control of an F-14 (G.J.Balas, 1998). An *H-infinity* controller design with gain scheduling approach was successfully used on a flexible aircraft where the weighting functions were not optimized, but were determined using Engineering intuition (Aouf, Boulet et Botez, 2002).

To overcome this lack of reference formulas, some guidelines were given in (Ciann-Dong, Hann-Shing et Shin-Whar, 1994b; Hu, Bohn et Wu, 1999) to determine these weighting functions. However, due to their trial and error nature the guidelines procedures may need many iterations to find acceptable results. Besides, the guidelines do not guarantee the fulfillment of the required control conditions. For this reason, a methodology to tune the weighting functions to meet the mandatory requirements is necessary.

There exist several weighting optimization methods based on mathematical algorithms, in which trade-offs were established between maximizing the stability margin and minimizing the *H-infinity* norm of the closed loop transfer function (Lanzon, 2005). These algorithms often performed on frequency-dependent optimizations, in which the iteration process demanded a considerable amount of memory allocation. To overcome this frequency-dependent optimization memory, a state space weight optimization was developed in (Osinuga, Patra et Lanzon, 2012b). However, that algorithm does not guarantee a global minimum convergence, which could lead to a poor stability margin, that could have a negative effect on a system operating in a large envelope, such as an aircraft.

A new and innovative methodology by taking advantage of both GA and DE algorithms to optimize the *H-infinity* weighting functions to develop a controller that satisfies the imposed dynamic specifications and the industrial needs is proposed in this thesis. This new approach can solve the clearance problem by reducing the complexity of needed calculations and their validation. However, this research confirms that optimization using the DE algorithm is more efficient and accurate than the optimization using the GA; Storn and Price (Storn et Price, 1997) have also shown the efficiency of the DE algorithm by the comparison of its results with genetic algorithm results.

Many global optimizations based on evolutionary principles have been used in the Control Engineering field. In the Aeronautical field, aircraft trajectory optimizations based stochastic search, such as the Genetic Algorithm (GA) were performed on several civil aircrafts (Murrieta-Mendoza et Botez, 2015a),(Patrón et Botez, 2015) as well as parameters estimation

methodologies were performed on autonomous air vehicles and in the flight testing of the aircraft intelligent flight controls (Mario, 1999),(Osinuga, Patra et Lanzon, 2012a). These new methodologies for the control of different parameters are applied in this thesis for the flight dynamics and control of the business aircraft Cessna Citation X model.

All these methods were developed in this thesis with the aim of reducing the computational complexity, and thus their time of convergence while achieving very good results. The GA and the Differential Evolution (DE) algorithms were selected to optimize the weighting function parameters.

1.5 Aircraft Clearance Criteria

The certification of an aircraft is an important and essential step in the process leading to its first flight. To prove that an aircraft is ready to fly, it must meet several criteria required by various agencies such as Transport Canada, the Federal Aviation Administration (FAA), or the European Aviation Safety Agency (EASA), and for a multitude of flight combinations in terms of center of gravity position, mass, speed, altitude and angle of attack. As in the case of any aircraft design or production process, the Flight Control Laws (FCL) have to be qualified, cleared and certified (C. Fielding, 2002).

Over the last few decades, very much research has been done to identify the FCLs' clearance criteria (Deutschland, 2003), (De Oliveira et Puyou, 2011), (Goupil et Puyou, 2013). Some of these criteria have been reformulated as robustness criteria (Popov et al., 2010), (Boughari. al., 2012, Boughari et al. 2014b, Boughari et al.2016, Ghazi et Botez, 2015). For example the target criteria for the Airbus team are the stability, turbulence, comfort and maneuver criteria (Puyou, 2007), (Favre, 1994). All of these criteria have to be evaluated in the full flight envelope for all weight and X_{CG} configurations.

A simulation technique for a flight envelope grid is commonly used. In this technique, for each grid point, the model simulation verifies if the specifications are (or not) satisfied

(Garulli et al., 2010). The main disadvantages of this technique are two-fold; firstly only local results following a partial study are obtained, and therefore, despite a significant density of the number of points, it is always possible to neglect the most critical flight cases. Secondly, the technique's execution time depends directly on the required accuracy, and therefore on the grid refinement. However, due to the time involved and the considerable design cost, analyzing a full envelope model is not feasible in this thesis because of the infinite number of cases contained within the flight envelope and the weight/ X_{CG} configurations.

To enable the use of rapid, comprehensive and effective analysis methods, parameter-varying models have been developed by incorporating their variations, also known as "uncertainties" in nominal models. These models were built for several flying conditions, and have led to the design of a new parametric method called Linear Fractional Transformation (LFT) (Becker et Packard, 1994b), (Zhou, Doyle et Glover, 1996). The use of such a method has gained the attention of aeronautical companies. It provided results which indicate to the industry that it has a promising future for the modeling of control laws' design and certification (Bates, Kureemun et Mannchen, 2003), as it is expected to reduce the number of required flight maneuvers (Puyou et Losser, 2012).

Several methods were investigated as they were used for the generation of LFT parametric models (Yan et Moore, 1996), (Cockburn et Morton, 1997), (Cockburn, 2000), (Hecker et Varga, 2003). LFT is based primarily on the way in which different types of uncertainties in the dynamic model are incorporated. For example, a parametric multiplicative uncertainty was incorporated by applying multiplicative uncertainty for a robust Gust Load Alleviation of B-52 aircraft, and analyzed using *mu –synthesis* (Aouf, Boulet et Botez, 2002). One of the two forms of uncertainties structures: unknown "unstructured" or well-defined, known as "structured uncertainties" must be chosen. These types of uncertainties have been investigated for the stabilization problem, and were further illustrated for the thrust vectoring aircraft (Ibrir et Botez, 2005).

The LFT represents one of the more challenging methods for the incorporation of aerodynamic uncertainties (Marcos et al., 2010), (Szabó et al., 2011) or of the X_{CG}, mass and inertia variations in the aircraft model. Several approaches for obtaining a good quality and reduced order of LFT models have been investigated, based on the number and complexity of parametric uncertainties (Varga et al., 1998), (Varga et Looye, 1999).

In the flight clearance process, an aircraft system with parameter uncertainties has been transformed into an LFR model using LFT, as shown in (Tang, Wei et Meng, 2011), where a robustness analysis was performed on an unmanned helicopter flight using *μ-analysis*. In (Shuai et al., 2013), the *H-infinity* control method was used for the flight clearance of a longitudinal aircraft model that had parametric uncertainties.

Flight control clearance criteria have become the focus of many studies conducted by universities and industries in the Group for Aeronautical Research and Technology in EUROPE GARTEUR project (Fielding et al., 2002). These studies were performed mainly on three aircraft fighter models, the High Incidence Research Model with feedback control HIRM+ which is a generic model, the Aero Data Model In Research Environment ADMIRE, and high performance short take off and vertical landing aircraft model called HWEM. Flight control clearance criteria has become the focus of many studies, including studies conducted by a group of universities and industries in the Group for Aeronautical Research and Technology in EUROPE GARTEUR project (Fielding et al., 2002).

These studies were performed mainly on three aircraft fighter models, the High Incidence Research Model with feedback control HIRM+ which is a generic model, the Aero Data Model In Research Environment ADMIRE, and high performance short take off and vertical landing aircraft model called HWEM, which are both realistic models. However, the flight control clearance criteria analysis results were mainly published for the HIRM+ generic model, and suggested adaptations of these criteria to civil aircrafts were only briefly discussed. Due to the lack of access to real flight control clearance data and the availability

of a level D Research Aircraft Flight Simulator, we were motivated to investigate the flight control clearance for a realistic Cessna Citation X business aircraft model.

1.6 Linear Stability Criteria

Due to the high volume of the flight clearance criteria, the “Eigenvalue Stability” criterion was selected to be investigated during this present research (Baldelli, Lind et Brenner, 2005). This criterion is expressed by a robustness analysis which was investigated at the LARCASE on both civil and military aircrafts: the HIRM, and the Hawker 800XP by using the weighting functions method (Anton, Botez et Popescu, 2013), (Anton et Botez, 2015). Normally this criterion has to be performed on the longitudinal aircraft closed loop control model to test its reliability during the aircraft flight in the presence of uncertainties. It searches through the aircraft envelope for eigenvalues with a negative real part. To evaluate this criterion, the results are compared with the natural stability of the aircraft, which means the eigenvalues for the longitudinal open loop model.

Our research shown in this thesis focuses on the Cessna Citation X open loop stability analysis. The data are provided by a level D Research Aircraft Flight Simulator; this level corresponds to the highest level flight dynamics certification and developed by CAE Inc. These data were used to develop both nonlinear and linear models of the airplane for its longitudinal and lateral motions (G.Ghazi, 2014), and to create longitudinal LFR models for 12 X_{CG} and weight configurations of the whole flight envelope using a user-friendly GUI developed during this study to automate the LFR model generation. The LFR models were further analyzed with the robustness and stability analysis toolboxes to assess the aircraft open loop stability.

1.7 Cessna Citation X Clearance Criteria Evaluation

The clearance of the flight control laws of a civil aircraft is a fastidious task, especially for modern aircrafts that need to achieve high performance (C. Fielding, 2002). This process aims to prove that the selected stability, robustness and handling requirements are satisfied

against any possible uncertainties. Because of the numerous flight test data, the parameters variations, and their uncertainties have to be provided for the clearance of the large flight envelope. To carry out this process, a detailed description of methods and procedures, which are currently used in industry, was given in (C. Fielding, 2002).

As mentioned also in the other sub-section, the presence of uncertainties is related to many factors, that are mainly dues to the mass and X_{CG} variations, aerodynamics data, control surfaces dynamics and delays, and Air Data measurements errors. To demonstrate the effects of important uncertainties, the clearance criteria are considered as robustness criteria from the Airbus team point of view (Deutschland, 2003), and were applied in linear, and nonlinear models and simulation (C. Fielding, 2002), (Seiler, Balas et Packard, 2012), and (Vincent et al., 2012).

In this thesis, the linear and the nonlinear clearance analysis of the Cessna Citation X business aircraft is addressed and evaluated for the first time, which gives to the reader a very good understanding of the criteria and visualization tools used in the assessment and clearance of the Flight Control Laws (FCL's).

CHAPITRE 2

APPROACH AND ORGANIZATION OF THE THESIS

The research presented in this thesis was performed in four main phases, which are detailed in the following four chapters from Chapter 3 to Chapter 6 subsequently:

- ✓ Stability Analysis of the Cessna Citation X Business Aircraft;
- ✓ Aircraft Control Design and Optimization of Flight Control Laws (FCL) Design using a combination of the modern Linear Quadratic Regulator (LQR) control method, the Proportional Integral (PI) classical control methods, and the differential evolution algorithm;
- ✓ Aircraft Control Design and Optimization of the FCL design using the advanced H-*infinity* robust control method; and
- ✓ Evaluations of the Linear and Non-Linear Clearance Criteria for the Cessna Citation X

During the first phase, a set of linear flight conditions composed of 36 points extracted from the flight test data performed on a level D Flight Simulator Research were interpolated using the Linear Fractional Transformation (LFT) method to create a larger database that covered the whole flight envelope, with a total of 72 flight points. This new database was used in the linear FCL design and validation for the whole research project. The Eigenvalue stability of the Cessna Citation X was also analyzed in this phase. The dynamic stability analysis of the whole Cessna Citation aircraft flight envelope using the Lyapunov function was performed on a Graphical User Interface (GUI), developed to automate the Linear Fractional Representation (LFR) generation in three ways (manual, visual, and direct). This LFR generation employed the altitude; True Air Speed TAS and Weight/Xcg were employed as uncertainties. The stability analysis was performed for a total of 12 Weight and Center of Gravity (Xcg) configurations in Chapter 3.

In the second phase, the Aircraft Flight Control System (FCS) design architecture was identified using the modern LQR control method for the Stability Augmentation System

(SAS), and then with the PI control method for error tracking. The handling qualities' requirements for the Cessna Citation X were imposed as *constraints* for the controller optimization and design.

The LQR and PI control laws were optimized using a 'Differential Evolution' (DE) stochastic search algorithm. The results obtained during this optimization were validated for both the linear and nonlinear models of a Cessna Citation X business aircraft. Robustness stability analysis on the nonlinear aircraft model was performed for 12 Xcg and weight variations; good stability results were obtained for all of these variations In Chapter 4.

The third phase consisted of defining the aircraft's controller architecture using the *H-infinity* modern control laws. This controller method was applied on both the Stability Augmentation System (SAS) and the Control Augmentation System (CAS) for an aircraft's flight, and then the handling qualities were identified using the H-*infinity* controller. The controller design was further optimized using two different stochastic search algorithms, the Genetic Algorithm (GA) and the DE (using a methodology developed in the second phase).

The results obtained with these algorithms were compared during the controller design optimization, and its 'linearized model' controller validation. Following this comparison, the DE algorithm was chosen. It performed better than the GA in its design the *H-infinity* controller, which was then further used in the 'nonlinear model' controller validation. Robustness stability analysis was performed on the nonlinear model using a set of Xcg and weight variations, and very good stability results were obtained for this set of variations.

In the fourth and final phase presented in Chapter 4, the Cessna Citation X's stability clearance linear and nonlinear criteria were evaluated for the designed flight controller using the optimized *H-infinity* control methodology. These linear and the nonlinear model stability analyses reveal that the optimal controller performs with an excellent stability in both cases.

Thus far, the phases of this research have been described in four journal papers and four conference papers. In this thesis, only the four journal papers, for which I was the main author, are included in four chapters, Chapters 3 to 6. One of these journal articles has been published; the other three will be submitted for publication in peer-reviewed scientific journals.

Dr. Ruxandra Botez, as a co-author, has supervised the realization of all the research presented here, and thus, of all the publications. In the first and second paper, Master's students Mr. Georges Ghazi and Mr. Florian Theel worked as co-authors. Georges provided the aircraft linear and nonlinear models data, and performed the nonlinear model validation by incorporating the resulting controllers in the nonlinear aircraft model and then performing the simulations. Florian contributed by performing the linear model validation and developing the visualization tools. In the third paper, Master's student Florian Theel automated the LFR generation by using a newly-designed GUI tool simplifying data easy handling. In the fourth paper, the PhD candidate Georges Ghazi performed all the nonlinear simulations.

The first research paper is presented in **Chapter 3**, and is entitled "Cessna Citation X Business Aircraft Stability Analysis using an LFR Model: Using a new GUI for the easy manipulation of the LFR models".
This paper investigates the Cessna Citation X Business aircraft's Eigenvalue stability using the linear stability criterion. The generation of LFR uncertainty models for a range of altitudes and the True Airspeeds was automated for the whole aircraft envelope using a Graphical User Interface (GUI). This newly-developed interface assists the user to visualize and understand the generation and validation of LFR models. These LFR models were further used in assessing the aircraft's longitudinal stability, which was analyzed using a method based on Lyapunov functions using another GUI developed in the Clearance of Flight Control Laws Using Optimization (COFCLUO) project (Magni, 2006). These analyzed LFR models were then rearranged in their flight envelope so that they illustrate the aircraft's stable regions (safe flight) in green and its unstable regions (unsafe flight) in red.

The research paper entitled “New Methodology for Optimal Flight Control using Differential Evolution -- Application to the Cessna X Aircraft”, is presented in **Chapter 4**.

This paper presents the Cessna X’s flight control architecture using an in-house algorithm that combines the LQR and the PI control methodologies. It also presents the handling qualities, used as constraints in the optimization problem, and a description of the in-house algorithm. The aircraft’s linear models were interpolated to cover the whole flight envelope using Matlab®.

The optimal flight control results (pitch angle and pitch rate for longitudinal controls, roll rate and roll angle for lateral controls) obtained using the proposed algorithm were validated for the whole flight envelope, for 864 aircraft linear models and for 500 nonlinear models.

Chapter 5 contains “Flight Control Clearance of the Cessna Citation X using Evolutionary Algorithms”, published in *The Proceedings of the Institute of Mechanical Engineers, Part G: Journal of the Aerospace Engineering,* in April 2016, doi: 10.1177/0954410016640821. In this paper, an *H-infinity* robust modern control methodology was applied to the controller architecture to achieve stability augmentation and tracking error control. GA and the DE algorithms were applied to optimize the weighting functions used in the controller determination, and then the performances of both these algorithms and their results were compared. The optimal pitch rate q and the roll p controllers using the DE algorithm were further validated in the flight envelope for the linear and the nonlinear aircraft models. To obtain the optimal flight control robustness, variations up to ±5% in weight and Xcg around a nominal flight condition were performed, while maintaining the aircraft controls at the same pitch rate and roll.

The last research paper is presented in **Chapter 6**, entitled “Optimal Control and New Methodologies’ Validation on the Cessna Citation X Business Aircraft Research Aircraft Flight Simulator ”.

This paper evaluates the clearance criteria for the new Cessna Citation X business aircraft flight controller, which is a part of the clearance process. This evaluation includes assessing how the flight limitations are obtained for the Cessna Citation X business aircraft from the worst parameters combinations cases. These limitations can (now) be visualized and analyzed to give precise information, in terms of altitude and TAS, on each trajectory the aircraft would be allowed to fly. The flight control laws' clearance provides information regarding the flight envelope stability margins. The eigenvalues' linear stability, the handling qualities and the nonlinear stability analysis were all investigated to assess the Cessna Citation X business aircraft from the point of view of flight control clearance and certification.

The unique contributions of the research articles presented in this thesis are the following:

- Chapter 3 contributes a stability analysis to obtain a flight envelope of the Cessna Citation X business aircraft without a controller, an envelope that shows the limits, or the worst possible parameter combinations cases in terms of altitude and TAS.
- Chapter 4 presents an optimization based on Differential Evolution of the Flight Control design, performed by combining the LQR modern control method and the PI classical method, using the time response performance and the 1st level handling qualities as the objective functions.
- In Chapter 5 demonstrates an enhanced Flight Control design by using the robust, modern *H-infinity* method, optimized by using two different evolutionary algorithms, the GA and the DE algorithm.
- Lastly, Chapter 6 details an evaluation of some of the clearance criteria used to assess a newly- designed Flight Controller certification process.

Following the structure given earlier, a complete Flight Control process, from design to clearance, was optimized by using the time and frequency response performances and the 1st level of handling qualities as an objective function, which minimizes the overall time of the process and consequently reduces the corresponding costs.

Five conference papers were also published on the research presented in this thesis. For brevity and to narrow the objectives of this document, they are not included in this thesis, although some of their contents have been cited. The research performed in these conference papers is summarized below.

In the first conference paper, “Flight Control on the Hawker 800XP Business Aircraft”, by Boughari and Botez, the LQR method was used in the Stability Augmentation System (SAS) design for the Hawker 800XP Business Aircraft. This paper was presented at the Industrial Electronic Conference IECON 2012, 38th Annual Conference of the IEEE Industrial Electronics Society, in Montreal, Quebec, Canada, on October 28th, 2012. It was also published in the conference proceedings (Boughari et all, 2012).

The second conference paper, “Business Aircraft Flight Control System using Robust *H-infinity* Controllers on Cessna Citation X”, was authored by Boughari, Ghazi, Theel, and Botez. Here the *H-infinity* control method was used on the Cessna Citation X business aircraft for designing a flight controller by using guidelines to define the shapes of parametric weighting functions. It was presented at the Canadian Aeronautical Society Institute CASI AÉRO conference, in Toronto, Ontario, Canada, on May 2nd, 2013, and later published in the conference proceedings.

“Optimal Flight Control on Cessna X Aircraft using Differential Evolution”, by Boughari, Botez, Theel, and Ghazi, is the third conference paper. It describes an optimization of the flight controller laws using a combination of the PI and the LQR methodologies, and was presented and then published in the Proceedings of the International Association of Science and Technology for Development IASTED, in Modeling, Identification and Control (MIC) Conference, Innsbruck, Austria, held on February 18th, 2014.

The fourth conference paper, entitled “Evolutionary Algorithms for Robust Cessna Citation X Flight Control”, by Boughari, Botez, Ghazi, and Theel, describes how the DE and the GA algorithms were used for a robust Flight Controller Laws design optimization using the

modern *H-infinity* method. Presented at the Society of Automotive Engineers SAE conference on the 16th of September, 2014 in Cincinnati, Ohio, this paper was also published in the SAE Conference Proceedings.

The fifth conference paper, "Optimal Control, New Methodologies Validation on the Research Aircraft Flight Simulator of the Cessna Citation X Business Aircraft", by Boughari, Ghazi, and Botez, describes an evaluation of the clearance criteria of the newly - optimized *H-infinity* controller designed via the DE algorithm. It was presented at the Science and Engineering for Reliable Energy REMOO conference proceeding in Budva, Montenegro on May 19th, 2016.

CHAPITRE 3

CESSNA CITATION X BUSINESS AIRCRAFT AEROELASTIC STABILITY FLIGHT ENVELOPE ANALYSIS USING LFR MODELS - USING A NEW GUI FOR THE EASY MANIPULATION OF LFRs

Yamina Boughari, Ruxandra Mihaela Botez, Florian Theel, Georges Ghazi,

LARCASE Laboratory of Applied Research in Active Controls, Avionics and AeroServoElasticity
ETS, 1100 Notre Dame West, Montreal, Que., Canada, H3C-1K3

This article was submitted on January 2017

Résumé

La certification du contrôle de vol d'un avion civil est une démarche très longue, et c'est ainsi un processus couteux dans l'industrie aérospatiale. Ce processus doit être examiné et prouvé d'être sécuritaire pour plusieurs milliers des combinaisons en termes de vitesses, d'altitudes, des configurations de poids par rapport au centrage X_{CG} et des angles d'attaque. Même dans ce cas, une mauvaise condition qui pourrait mener à une situation critique, peut s'échapper. Pour aborder ce problème, des modèles qui peuvent décrire la dynamique d'un avion en prenant en compte toutes les incertitudes sur une région de l'enveloppe de vol ont été développés en utilisant la Représentation Fractionnelle Linéaire. Pour investiguer la stabilité de l'avion d'affaire Cessna Citation X, les modèles de Représentation Fractionnaire Linéaire sont mis en œuvre en utilisant les vitessses et les altitudes comme des paramètres variables. Dans cet article, la stabilité en termes de valeur propre du mouvement longitudinale de l'avion est analysée dans une plage continue de l'enveloppe de vol avec la Vraie vitesse relative et l'altitude comme paramètres variables, au lieu d'analyser point par point, comme les méthodes classiques. C'est connu sous le nom de « l'enveloppe de stabilité aeroelastic », qui est nécessaire pour la certification d'avion civile, ainsi demandé par Circular Advisory "Aeroelastic Stability Substantiation of Transport Category Airplanes AC

No: 25.629-18". Dans cette nouvelle méthodologie l'analyse est exécutée dans le domaine de temps basé sur la stabilité Lyapunov et résolue par des algorithmes d'optimisation convexes en utilisant les inégalités matricielles linéaires pour évaluer la stabilité aeroelastic, qui est réduite a chercher les valeurs propres négatives dans une région d'enveloppe de vol. Il peut aussi être utilisé pour étudier la stabilité d'un système pendant un mouvement arbitraire d'un point a un autre dans l'enveloppe de vol. Une Interface Utilisateur Graphique est développée pour faciliter la génération de modèles incertains de Représentation Fractionnaire Linéaire pour l'avion Cessna Citation X en utilisant 12 configurations de poids et centrage X_{CG} ; ainsi, 26 régions de l'enveloppe de vol pour chaque configuration poids et centrage X_{CG} ont été développées pour les études du mouvement longitudinal. Finalement, « la stabilité et la robustesse » sont analysées en utilisant l'interface utilisateur graphique développé dans le projet de la certification de lois de contrôle de vol en utilisant l'optimisation (COFCLUO). Les résultats d'analyse de l'avion dans son enveloppe de vol entière sont présentés sous forme de graphiques, offrant ainsi la bonne lisibilité et les rendant facilement exploitables.

Abstract

Civil aircraft flight control clearance is a time consuming, thus an expensive process in the aerospace industry. This process has to be investigated and proved to be safe for thousands of combinations in terms of speeds, altitudes, gross weights, X_{CG} and weight configurations and angles of attack. Even in this case, a worst-case condition that could lead to a critical situation, that might be missed. To address this problem, models that are able to describe an aircraft's dynamics by taking into account all uncertainties over a region within a flight envelope have been developed using Linear Fractional Representation. In order to investigate the Cessna Citation X aircraft aeroelastic stability envelope, the Linear Fractional Representation models are implemented using the speeds and the altitudes as varying parameters. In this paper, the aircraft longitudinal eigenvalue stability is analyzed in a continuous range of flight envelope with varying parameter of True airspeed and altitude, instead of a single point, like classical methods. This is known as the aeroelastic stability envelope, required for civil aircraft certification as given by the Circular Advisory

"Aeroelastic Stability Substantiation of Transport Category Airplanes AC No: 25.629-18". In this new methodology the analysis is performed in time domain based on Lyapunov stability and solved by convex optimization algorithms by using the linear matrix inequalities to evaluate the aeroelastic stability, which is reduced to search for the negative eigenvalues in a region of flight envelope. It can also be used to assist the stability of a system during an arbitrary motion from one point to another in the flight envelope. A friendly Graphical User Interface is developed to facilitate the generation of Linear Fractional Representation uncertainty models for the Cessna Citation X aircraft using 12 weight and X_{CG} configurations; thus, 26 regions of the flight envelope are developed for different Weight/Xcg configurations to study the aircraft's longitudinal motion. Finally, the robustness stability is analyzed using the Graphical User Interface developed in the Clearance Of Flight Control Laws Using Optimization (COFCLUO) project. This project aimed to boost the aircraft safety using computer computation and was conducted by academic and industrial partners in Aeronautical Research in Europe.

A whole aircraft analysis results' for its entire envelope are presented in the form of graphs, thus offering good readability, and making them easily exploitable.

3.1 Introduction

The certification of an aircraft is an important and essential step in the process leading to its first flight. To prove that an aircraft is ready to fly, it must meet several criteria required by various agencies such as Transport Canada (TC), the Federal Aviation Administration (FAA), or the European Aviation Safety Agency (EASA); a multitude of flight combinations in terms of center of gravity position, mass, speed, altitude and angle of attack are used.

In the same way as for any aircraft design or production process, the Flight Control Laws (FCL) have to be qualified, cleared and certified (C. Fielding, 2002). Over the last decades, much research has been done to identify the FCLs' clearance criteria (Deutschland, 2003), (Fernandes De Oliveira et Puyou, 2011). Some of these criteria have been reformulated as

robustness criteria (Boughari et al., 2014a, Boughari et al., 2014b, Boughari et al., 2016), (Boughari et al., 2014d), (Ghazi et Botez, 2014 b), (Ghazi et Botez, 2015c). The target criteria for the Airbus team, for example, correspond to the Eigenvalue stability, turbulence, comfort and maneuver criteria (Puyou, 2007), (Favre, 1994). All of these criteria have to be evaluated in the full flight envelope, and for all weight and X_{CG} configurations.

A simulation technique involving a flight envelope expressed by grid of points was used. In this technique, for each grid point, the model simulation verified if the specifications were satisfied (or not) (Garulli et al., 2010). The main disadvantages of this technique were two-fold: first, the local results were obtained following a partial study (C. Fielding, 2002) , and therefore, despite a significant density of the number of points, it was always possible to neglect the most critical flight cases. Secondly, the technique's execution time depended directly on the required accuracy, and therefore on the grid refinement. However, due to the execution time involved and the considerable design cost, analyzing a full flight envelope model was not possible with the existing team computer capabilities as the number of cases contained within the flight envelope and the weight/ X_{CG} configurations, were very high.

To enable the use of rapid, comprehensive and effective analysis methods, parameter-varying models have been developed by incorporating variations, (also known as "uncertainties" in their nominal models). These models were built for several flying conditions, by use of a parametric method called Linear Fractional Transformation (LFT) (Becker et Packard, 1994a), (Zhou, Doyle et Glover, 1996). The use of such a method has gained the attention of aeronautical companies. Results were provided which indicated to the industry that there was a promising future for the modeling of control laws' design and certification (Bates, Kureemun et Mannchen, 2003), and it was expected to reduce the number of required flight maneuvers (Puyou et Losser, 2012).

Several methods were investigated with the aim to generate of the LFT parametric models (Yan et Moore, 1996), (Cockburn et Morton, 1997), (Cockburn, 2000), (Hecker et Varga, 2003). LFT is based primarily on the number of different types of uncertainties that are

incorporated in the aircraft dynamic model. For example, a multiplicative parametric uncertainty was considered for a robust Gust Load Alleviation of B-52 aircraft, and analyzed using *mu-synthesis* (Aouf, Boulet et Botez, 2000) One of the two forms of uncertainties: "unknown (or unstructured) uncertainty" structure, and well-defined, known as "structured uncertainties" could be chosen. These types of uncertainties have been investigated for the stabilization problems, and were further illustrated for the thrust vectoring aircraft (Ibrir et Botez, 2005).

The LFT method represents one of the more challenging methods for the incorporation of aerodynamic uncertainties (Marcos et al., 2010), (Szabó et al., 2011) or of the X_{CG}, mass and inertia variations in the aircraft model. Several approaches for obtaining a very good quality and a reduced order of LFT models have been investigated based on the number and complexity of parametric uncertainties (Varga et al., 1998), (Varga et Looye, 1999).

In the flight clearance process, an aircraft system with parameter uncertainties has been transformed into LFR model by using LFT, as shown in (Tang, Wei et Meng, 2011), where a robustness analysis was performed on an unmanned helicopter flight using *mu-analysis*. In (Dong et al., 2013), the *H-infinity* control method was used for the flight clearance of a longitudinal aircraft model having parametric uncertainties.

Flight control clearance criteria have become the focus of many studies conducted by universities and industries in the Group for Aeronautical Research and Technology in EUROPE GARTEUR project (C. Fielding, 2002), (Varga A, 2012). These studies were performed mainly on three aircraft fighter models, the High Incidence Research Model with feedback control HIRM+ which is a generic model, the Aero Data Model In Research Environment ADMIRE, and high performance short take off and vertical landing aircraft model called HWEM, which are both realistic models.

However, the flight control clearance criteria analysis results were mainly published for the HIRM+ generic model (C. Fielding, 2002), and suggested adaptations of these criteria to

Cessna Citation X civil aircraft. Due to the lack of access to real flight control clearance data and the availability of the level D Research Aircraft Flight Simulator at our LARCASE laboratory, we have been motivated to investigate its flight control clearance.

Due to the high volume of the flight clearance criteria tasks, the “eigenvalues stability” criterion (Baldelli, Lind et Brenner, 2005) was selected to be investigated during this present research. This criterion is applied for a robustness analysis which has been investigated at the LARCASE laboratory on both civil and military aircrafts: the Hawker 800XP, and the HIRM by using the weight functions method (Anton et Botez, 2015), (Anton, Botez et Popescu, 2013).

Normally the stability criterion has been performed on the longitudinal aircraft closed loop model to test the reliability of the flight control in the presence of uncertainties. This criterion seeks for eigenvalues with negative real parts in the aircraft envelope. To evaluate this criterion, the results have to be checked with those obtained for the natural stability of the aircraft; the eigenvalues for the longitudinal open loop system should therefore be investigated.

Our current research focuses on the Cessna Citation X open loop stability analysis. The data are provided by a Level D Research Aircraft Flight Simulator (RAFS), where Level D corresponds to the highest level flight dynamics certification by the FAA. The RAFS was designed and manufactured by CAE Inc. for the research purposes of the LARCASE team at the ETS. These data were used to develop both nonlinear and linear models of the airplane for its longitudinal and lateral motions (Ghazi et Botez, 2015a), (Ghazi, 2014). In addition, 26 longitudinal LFR models were created for 12 X_{CG} and weight configurations of the whole flight envelope. A user-friendly GUI was developed during this study to automate the LFR model generation. The LFR models were further analyzed using the robustness and stability analysis toolbox to assess the Cessna Citation X aircraft open loop stability.

The paper is organized as follows: Firstly, a presentation of the Cessna Citation X aircraft and a description of the Linear Fractional Representation (LFR) method are given. Next, the Lyapunov stability theory is detailed, and finally the aircraft stability analysis results are given and discussed.

3.2 Cessna Citation X Business Aircraft Modeling

The Cessna Citation X operates at a Mach number of 0.935; thus, it is the fastest civilian aircraft in the world. The nonlinear model for the development and validation of this aircraft's flight control system uses the Cessna Citation X's flight dynamics that is detailed in (Ghazi, 2014). This model was built in Matlab/Simulink, and is based on aerodynamics data extracted from a Cessna Citation X Level D Research Aircraft Flight Simulator designed and manufactured by CAE Inc. According to the Federal Administration Aviation (FAA, AC 120-40B), Level D is the highest certification level that can be delivered by the Certification Authorities for an aircraft's flight dynamics. More than 100 flight tests were performed on the Citation X Level D Research Aircraft Flight Simulator within its aircraft flight envelope, for the research presented in this paper.

Using trim and linearization routines developed in (Ghazi, 2014), (Ghazi et Botez, 2015a) , the aircraft longitudinal and lateral equations of motions were linearized for various flight conditions expressed in terms of altitudes and speeds, and for different aircraft configurations in terms of mass and center of gravity positions. In order to validate these different models obtained by this linearization, several comparisons of them with the linear model obtained using the identification techniques proposed in (Hamel, 2013), and (Hamel, Botez et Ruby, 2014) were performed for different flight conditions and aircraft configurations. The results have shown that the linear models were accurate and could be further used to estimate the local behavior of the Cessna Citation X for any flight condition. The linearized aircraft equations of motion are represented in the form of the following state space system (Nelson, 1998):

$$\dot{x} = Ax + Bu \tag{3.1}$$

This system is decomposed into two sub-systems representing the aircraft's longitudinal and lateral motions. Only the aircraft's longitudinal motion dynamics are considered for the stability, and are given by the state space equation, using the elevator deflections as input:

$$\dot{x}_{long} = A_{long}x_{long} + B_{long}u_{long}$$

$$A_{Long} = \begin{pmatrix} X_u & X_w & X_q & -g\cos\theta \\ Z_u & Z_w & Z_q & 0 \\ M_u + M_{\dot{w}}Z_u & M_w + M_{\dot{w}}Z_w & M_q + M_{\dot{w}}u_0 & 0 \\ 0 & 0 & 1 & 0 \end{pmatrix}, B_{Long} = \begin{pmatrix} X_{\delta_e} \\ Z_{\delta_e} \\ M_{\delta_e} + M_{\dot{w}}Z_{\delta_e} \\ 0 \end{pmatrix} \tag{3.2}$$

Where A_{long} represents the stability derivatives matrix, and B_{long} represents the control derivatives matrix; the state vector $x_{long}(t)$ and control vector $u_{long}(t)$ are given by Equation (3.3):

$$x_{long}(t) = (u \quad w \quad q \quad \theta)^T,\ u_{long}(t) = \delta_e \tag{3.3}$$

In (Ghazi, 2014) a linear model was obtained for 36 flight conditions for the Cessna Citation X business aircraft, that was based on data extracted from the Level D Research Aircraft Flight Simulator (RAFS) tests performed at the LARCASE laboratory. The models used Linear Fractional Representation (LFR) that considered their uncertainties; LFR models were obtained using the bilinear interpolation method (Magni, 2006), (Poussot-Vassal et Roos, 2012), (Hecker, Varga et Magni, 2005). The following section offers a brief description of the LFR method, and its application on the Cessna Citation X model business aircraft.

3.3 Linear Fractional Representation (LFR)

LFR changes a group of linearized models by means of their "progression". These linearized models are used to define "state matrices" by keeping a range of error known as

"uncertainties" in their design. To define the robustness of the modeling of the system analysis, the uncertainties are extracted from the state matrices coefficients', and are arranged into a block named "Δ".

This matrix "Δ" contains information about a model's fluctuations around its nominal value. The matrix can have any shape; it can be purely diagonal, and could have a format to include "structured uncertainties" or could be fully populated, and have a format known to include "unstructured uncertainties".

The matrix is of an order at least equal to the sum of all the uncertainties' repetitiveness', where "repetitiveness" reflects when an uncertainty appears more than once in the expression of a matrix' coefficients. In addition, block Δ contains as many integrators as the order of the system.

To obtain an LFR model, we consider two symbolic objects functions $K_1$and K_2 as described in (Magni, 2006), (Poussot-Vassal et Roos, 2012) :

$$K_1(\delta_1) = I_{n_1} \frac{b+\delta_1(bc-ad)}{1-a\delta_1} \tag{3.4}$$

$$K_2(\delta_2) = I_{n_2}(a\delta_2^2 + b\delta_2 + c) \tag{3.5}$$

where δ_1 and δ_2 are 1x1 symbolic objects (*a,b,c,d* are constant parameters) and I_{n_1}, I_{n_2} are identity matrices. Equation (3.4) and Equation (3.5) giving the expressions of $K_1(\delta_1)$ and $K_2(\delta_2)$ are represented in the form of two closed loops as shown in Figure 3-1(a) and 3-1(b)

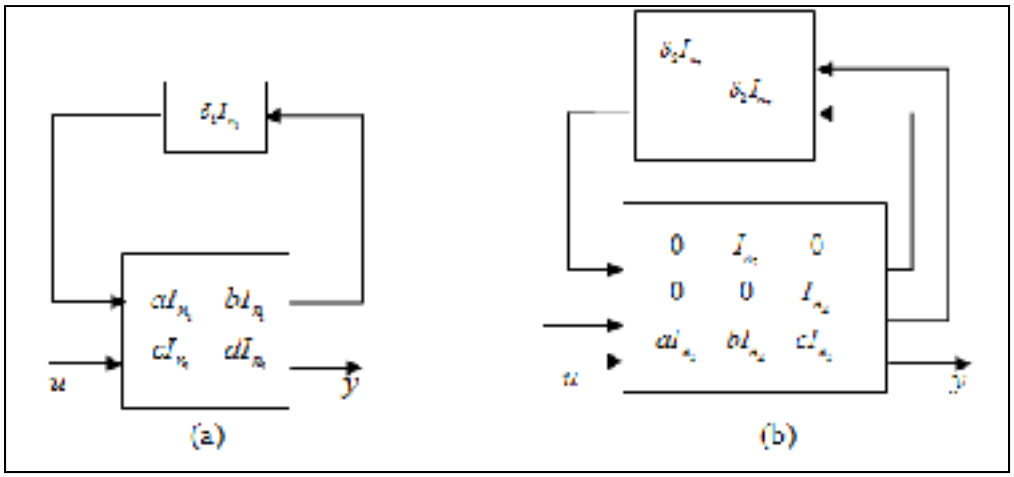

Figure 3-1 Representation of $K_1(\delta_1)$: $y = K_1(\delta_1)u$ (a) ,
and of $K_2(\delta_2)$: $y = K_2(\delta_2)u$ (b)

Figure 3-1(a), and (b) show feedback control similar to that of a state space representation, which includes transfer function matrices. The following definitions are given for LFR representation by Magni, (2006):

Definition 1: A rational symbolic object is given by the following expression

$$K\left(1/s, \delta_{1,\ldots,}\delta_q\right) \tag{3.6}$$

The transformation of the symbolic expression (3.6) into a Linear Fractional Representation (LFR) depends on the evaluation of the matrices $(A, B_1, B_2, C_1, C_2, D_{11}, D_{12}, D_{21}, D_{22})$ such that:

$$y = K\left(\frac{1}{s}, \delta_1, \ldots, \delta_q\right)u \tag{3.7}$$

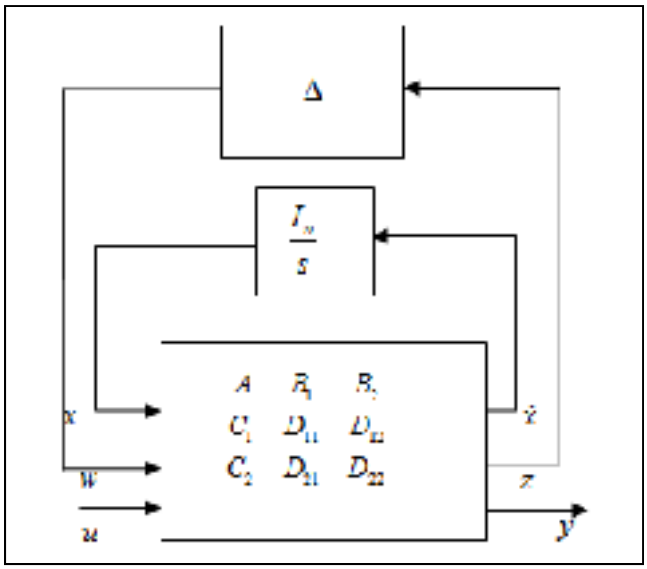

Figure 3-2 LFR of $K\left(\frac{1}{s}, \delta_1, \ldots, \delta_q\right)$

From Figure 3-2, equations (3.8) to (3.10) are obtained:

$$\dot{x} = Ax + B_1 w + B_2 u \tag{3.8}$$

$$z = C_1 x + D_{11} w + D_{12} u \tag{3.9}$$

$$y = C_2 x + D_{21} w + D_{22} u \tag{3.10}$$

Where

$$w = \Delta u \quad \text{where} \quad \Delta = \text{Diag}\left(\delta_1 I_{n_1}, \ldots, \delta_q I_{n_q}\right) \tag{3.11}$$

The LFR of $K\left(\frac{1}{s}, \delta_1, \ldots, \delta_q\right)$ is given in Figure 3-2 which shows the interconnection of the uncertainty block Δ to the block representing the dynamics, the outputs, and the inputs control.

In order to simplify the LFR, the uncertainties contain integrators ($\frac{I_n}{s}$) in addition to the parameters variations. It is obvious that the sizes of a block's uncertainties can easily reach high order. Block Δ is further written, due to the integrators addition:

$$\Delta = Diag\left(\frac{I_n}{s}, \delta_1 I_{n_1}, \ldots, \delta_q I_{n_q}\right) \tag{3.12}$$

The LFR of Δ bloc can then be illustrated as follows:

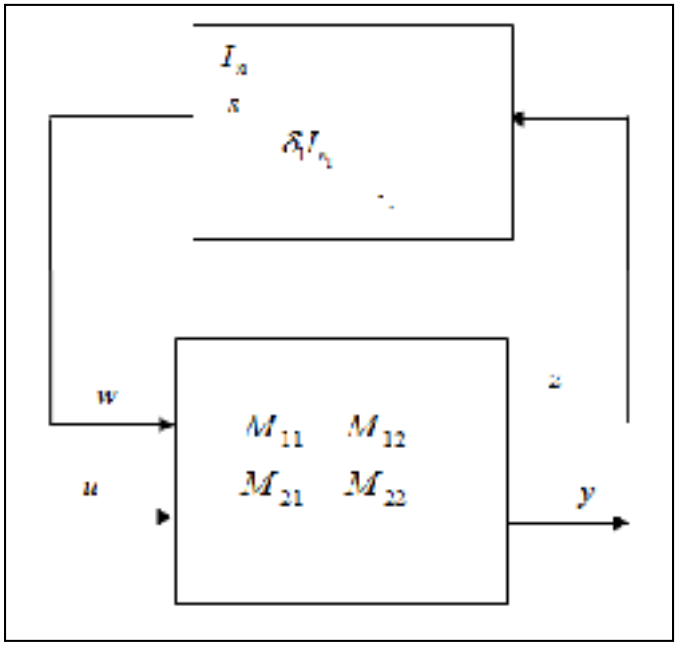

Figure 3-3 The LFR of Δ bloc

If the L Linear Fractional Representations of the block Δ given by Figure 3-2 and Figure 3-3 are compared, we can deduce that:

$$M_{11} = \begin{bmatrix} A & B_1 \\ C_1 & D_{11} \end{bmatrix}; M_{12} = \begin{bmatrix} B_2 \\ D_{12} \end{bmatrix}; \quad M_{21} = [C_2 \quad C_{21}]; M_{22} = D_{22} \tag{3.13}$$

Definition 2 :

1. *The upper Linear Fractional Transformation* $F_u(M, \Delta)$:

In Figure 3-3, the transfer function between *u* and *y* given by closing the loop of block Δ is denoted as $F_u(M, \Delta)$:

$$F_u(M, \Delta) = M_{21}\Delta(I - M_{11}\Delta)^{-1}M_{12} + M_{22} \tag{3.14}$$

where $M = \begin{bmatrix} M_{11} & M_{12} \\ M_{21} & M_{22} \end{bmatrix}$

2. *The Lower Linear Fractional Transformation* $F_l(M, K)$:

After closing the loop using $y = Ku$, the transfer function is denoted as $F_l(M, K)$:

$$F_l(M, K) = M_{12}K\,(I - M_{22}K)^{-1}M_{21} + M_{11} \tag{3.15}$$

It can be observed that all the matrices of the system interact directly or indirectly with the matrix Δ, which means that their sizes are equivalent to the sizes of bloc Δ's uncertainties. As mentioned above, the size of the uncertainty matrix can quickly become very large, which can be reflected in the size of the set of matrices in the dynamic bloc Δ. It is therefore in our interest to minimize the order of the system as much as possible in order to reduce the computation time, of our algorithm.

In order to facilitate the modeling and the use of LFR systems, a toolbox was developed by ONERA, that used Matlab® software that contained several useful features (Poussot-Vassal et Roos, 2012).

The uncertainties of altitude and True Air Speed (TAS) are the crucial parameters required to obtain an LFR model for the Cessna Citation X business aircraft, and to build a system involving uncertainties covering its whole aircraft envelope. The aircraft model is linearized for an altitude range between 0 – 51,000 ft and a TAS range of 120-425 knots. A graphical representation of the Cessna Citation X linearized model flight points within its flight envelope is given in Figure 3-4.

There are several approaches used to generate LFR models by both "direct" and "indirect" methods. The methods commonly used in research to obtain such representation were discussed in (C. Fielding, 2002) . In this paper, the LFR model based on interpolation is considered to be generated by a direct method; a database of linearized flight points is considered by using the *Trends and Bands* technique, that is illustrated in the next section.

3.3.1 LFR modeling using Trends and Bands method

To perform a Linear Fractional Transformation (LFT), the first step is to determine how the state matrices describe an uncertain model changes according to the True Air Speed (TAS) and the altitude. In the case of the Cessna Citation X aircraft, a set of linearized models expressed in the state space form, based on data extracted from the Research Aircraft Flight Simulator (RAFS) provided by CAE Inc. for different flight conditions using altitudes and TAS as variables (see Figure 3-4), are available for a set of weights and X_{CG} configurations, as shown in Figure 3-5. Matrices A and B can then be obtained for a fixed weights and X_{CG} configurations in the following form:

$$A = A(h, TAS) \tag{3.16}$$

$$B = B(h, TAS) \tag{3.17}$$

The aircraft dynamics is described for the flight envelope conditions. Figure 3-4 shows the 36 flight points selected within the flight envelope limits. The aircraft models are obtained at each 5000 ft in the flight envelope, for 4 different speeds.

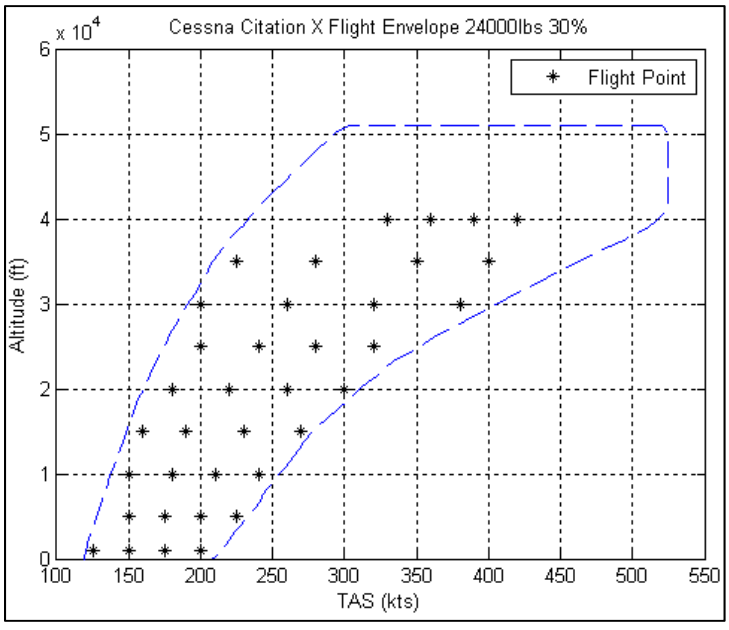

Figure 3-4 Cessna Citation X Aircraft Flight Envelope

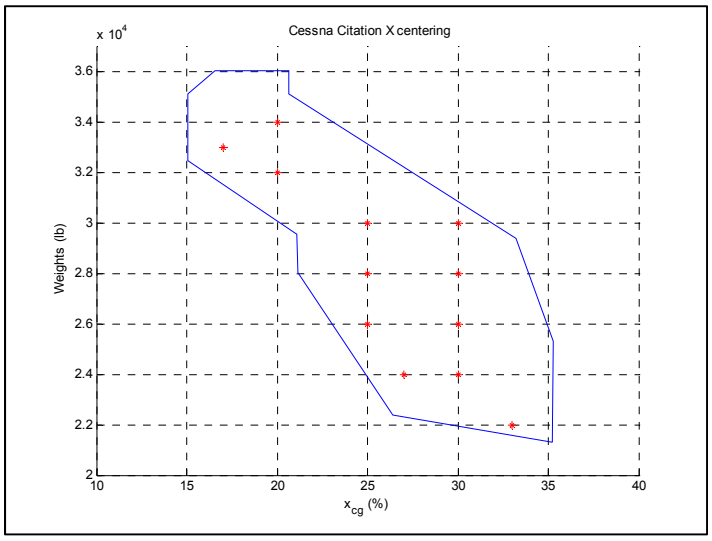

Figure 3-5 Cessna Citation X Weight/ X_{CG} conditions

Before carrying out the interpolation, two steps must be performed. The first step defines the region for an altitude and a range of TAS where the interpolation will be performed; the four (4) corners of the region form the vertices as shown in Figure 3-6. Each of the TAS ranges has a lower and an upper value, which are its bounds. The second step is the normalization of these bounds in order to attribute each coordinate of the vertices a value equal to 1 or -1.

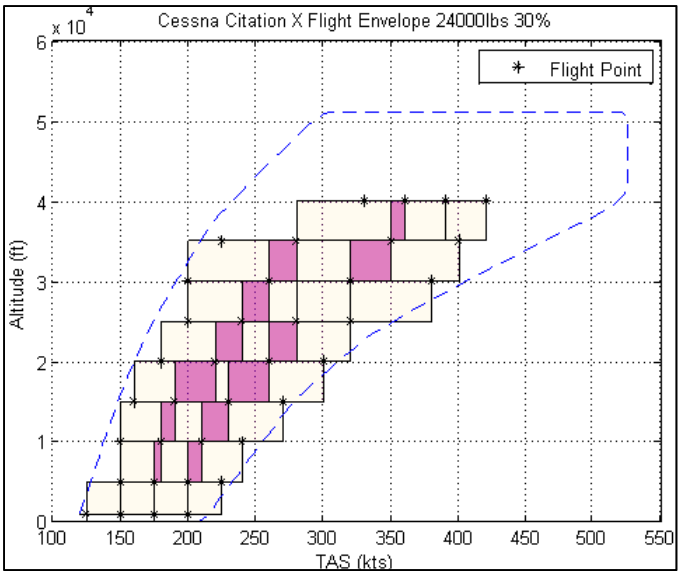

Figure 3-6 Regions Definition

3.3.2 Normalization

The function used to proceed to the regions' normalization allows the "coordinates" of the two uncertainties parameters the TAS and the altitude to be associated with a pair of normalized coordinates in the variation range. Since each region has neither the same form nor the same limits, it was necessary to develop a generic code with the aim to adapt the different values taken by these regions.

Ideally, three vertices of the region are sufficient to normalize the concerned region; this normalization reduces the system of equations to a system of three equations with three unknowns for the two (2) uncertainties.

The minimum and maximum values, as well as the positions of the two vertices, diagonally opposite one to another were associated with these values. The third vertex position is selected as one of the two remaining vertices positions. The normalized values associated with these three positions are the following: $\{[-1;-1],[-1;1],[1;1]\}$ or $\{[-1;-1],[1;-1],[1;1]\}$.

The matrix form implementation of what is shown in Equation (3.19), and allows the obtaining of the coefficients a_i, b_i, c_i for each uncertainty, by allowing the uncertainty to be given by Equation (3.18):

$$Inc_i = a_i + b_i\delta_1 + c_i\delta_2 \tag{3.18}$$

where $\delta_i \in [-1,1]$, and $i = [1,2] \in N$

$$\begin{bmatrix} Inc_{i,1} \\ Inc_{i,2} \\ Inc_{i,3} \end{bmatrix} = \begin{bmatrix} 1 & -1 & -1 \\ 1 & -1 & 1 \\ 1 & 1 & 1 \end{bmatrix} \begin{bmatrix} a_i \\ b_i \\ c_i \end{bmatrix} \text{ or } \begin{bmatrix} Inc_{i,1} \\ Inc_{i,2} \\ Inc_{i,3} \end{bmatrix} = \begin{bmatrix} 1 & -1 & -1 \\ 1 & 1 & -1 \\ 1 & 1 & 1 \end{bmatrix} \begin{bmatrix} a_i \\ b_i \\ c_i \end{bmatrix} \tag{3.19}$$

Equation (3.18) has two varying terms, which are used to define the regions of rectangular or parallelogram shapes. Thus, it is easy to move from a normalized basis to a non-normalized basis and vice versa by inverting coefficients matrix in Equation (3.19). We note that this operation it is used to obtain the determinant of the matrix presented in Equation (3.20) the normalized coordinates for each point used for interpolation are determined from Equation (3.20), which is obtained under matrix form Equation (3.18):

$$\begin{pmatrix} 1 \\ \delta_1 \\ \delta_2 \end{pmatrix} = \begin{pmatrix} 1 & 0 & 0 \\ a_1 & b_1 & c_1 \\ a_2 & b_2 & c_2 \end{pmatrix}^{-1} \begin{pmatrix} 1 \\ Inc_1 \\ Inc_2 \end{pmatrix} \tag{3.20}$$

Table 3-1 presents the coefficients values obtained from two regions' coordinates:

Table 3-1 Normalization of Coefficients and Coordinates

Classification of Interpolation Points (Step 1) '' Reference points''	Normalization of Coefficients a_i b_i c_i (Step 2)	Normalization of Coordinates (Step 3)
Point 1 : [125 ; 1000]	i=1, [137,5; 12,5 ; 0]	[-1 ; -1]
Point 2 : [150 ; 1000]	i=2, [3000 ; 0 ; 2000]	[1 ; - 1]
Point 3 : [150 ; 5000]		[1 ; 1]
Point 1 : [200 ; 5000]		[-1 ; -1]
Point 2 : [225 ; 5000]	i=1, [220; 20 ; 0]	[0.25 ; -1]
Point 3 : [240 ; 10000]	i=2, [7500 ; 0; 2500]	[1 ; 1]
Point 4 : [210 ; 10000]		[-0.5 ; 1]

To optimize the accuracy of the results, the smallest possible regions have been defined, containing only 3 or 4 flight points to use as "reference points" for the interpolation.

This definition allows performing a bilinear interpolation for which 4 coefficients must be found by using equations (3.21) - (3.23).

$$A(h,TAS) = A_{0_{4,4}} + A_{1_{4,4}}h + A_{2_{4,4}}TAS + A_{3_{4,4}}TAS \times h \tag{3.21}$$

$$B_{long}(h,TAS) = B_{0_{4,1}} + B_{1_{4,1}}h + B_{2_{4,1}}TAS + B_{3_{4,1}}TAS \times h \tag{3.22}$$

$$B_{lat}(h,TAS) = B_{0_{4,2}} + B_{1_{4,2}}h + B_{2_{4,2}}TAS + B_{3_{4,2}}TAS \times h \tag{3.23}$$

The Least Square (LS) method is employed to minimize the relative errors in the "reference points". The maximum relative errors found for the state space matrices *A* and *B* coefficients are between 10^{-13} à 10^{-15}, thus are neglected, and therefore these coefficients value are considered to be very good.

Using the reference points, which are the flight points obtained from the flight tests and shown in Figure 3-4, a number of 26 regions (rectangular) are reached, which cover a large part of the flight envelope expressed in terms of altitude and TAS. The region division is valid for all weight and balance conditions, and is presented in Figure 3-6. It can be observed from Figure 3-6 that some of the regions superimpose over other regions (darker zones) due to their common reference points; in many cases there is not only an interpolation applies but also extrapolation applies to obtain these regions.

The achievement of 26 models for 12 different X_{CG} /weight configurations takes 59.28 seconds by means of LFR, and takes 0.19 seconds by region. The computing time is acceptable following the usefulness of presented results.

The final phase of generating the LFR system is based on the last two steps: 1) obtaining the LFR system and 2) its minimization. Thus, four LFR systems are found that representing our four state space matrices (*A, B, C, D*), although the *C* and *D* matrices do not contain uncertainties. Next, an overall system is designed using the "abcd2lfr" command in Matlab® by specifying the states number which is equal to four. Information regarding the order of the system and the uncertainties' repetitiveness are presented in the following Table 3-2 for the longitudinal aircraft model design. By using the "*minlfr*" function, the order of the system can be reduced from 24 to 13 when the region used 4 reference flight points for interpolation, and from 13 or 14 to 10 when the region used 3 reference flight points as shown in Table 3-2.

Table 3-2 LFR's system order and repetitiveness

	Longitudinal LFR models	
Number of reference points used in the interpolation	3	4
System order	13 or 14	24
System order after minimization	10	13
TAS repetitiveness	3	3
Altitude repetitiveness	3	6

A comparison of a full order LFR system with a reduced system results is shown in Figure 3-7 for a given weight and X_{CG} configuration, and for medium altitudes regions; results are shown for regions 15 to 18 for the other 22 regions are given in the Appendix. This comparison demonstrates that the reduction of the system preserved its main characteristics, where the full-order LFR system poles (blue circles) are perfectly consistent with those of the reduced order LFR system poles (red crosses).

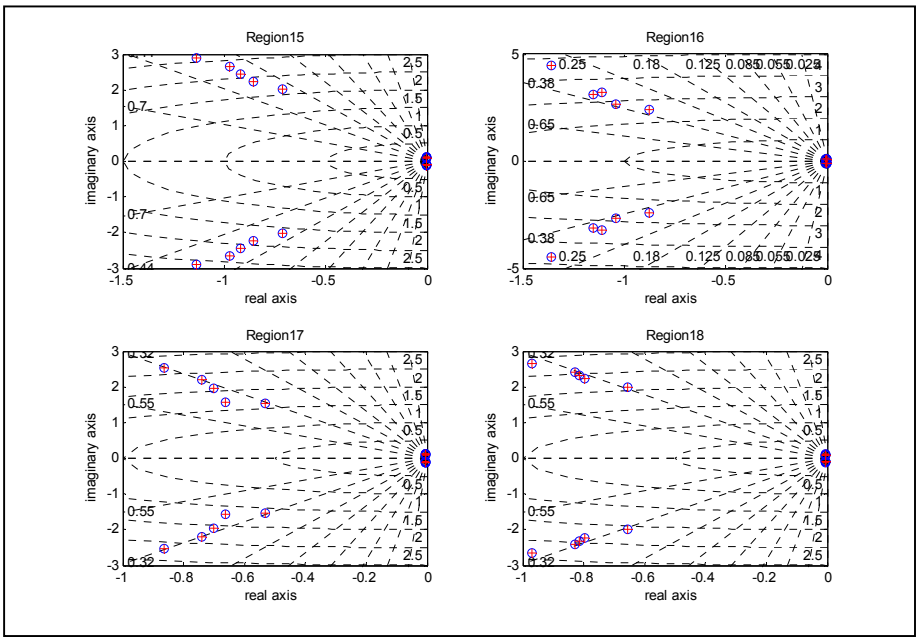

Figure 3-7 Full-order LFR system versus a reduced-order LFR system

To automate the Cessna Citation X aircraft's LFR model generation, and for a better visualization, a GUI was developed to encompass all these steps from the beginning of the research, and is presented in the next Section.

3.3.3 The Graphical User Interface GUI

A user-friendly Graphical User Interface (GUI) was developed, showing the major steps for the generation of the LFR models, their reduction, and their validations. As shown in Figure 3-8, it is possible to determine the type of interpolation: bilinear or biquadratic, the type of model: lateral or longitudinal, the X_{CG} location terms, and the definition of the regions.

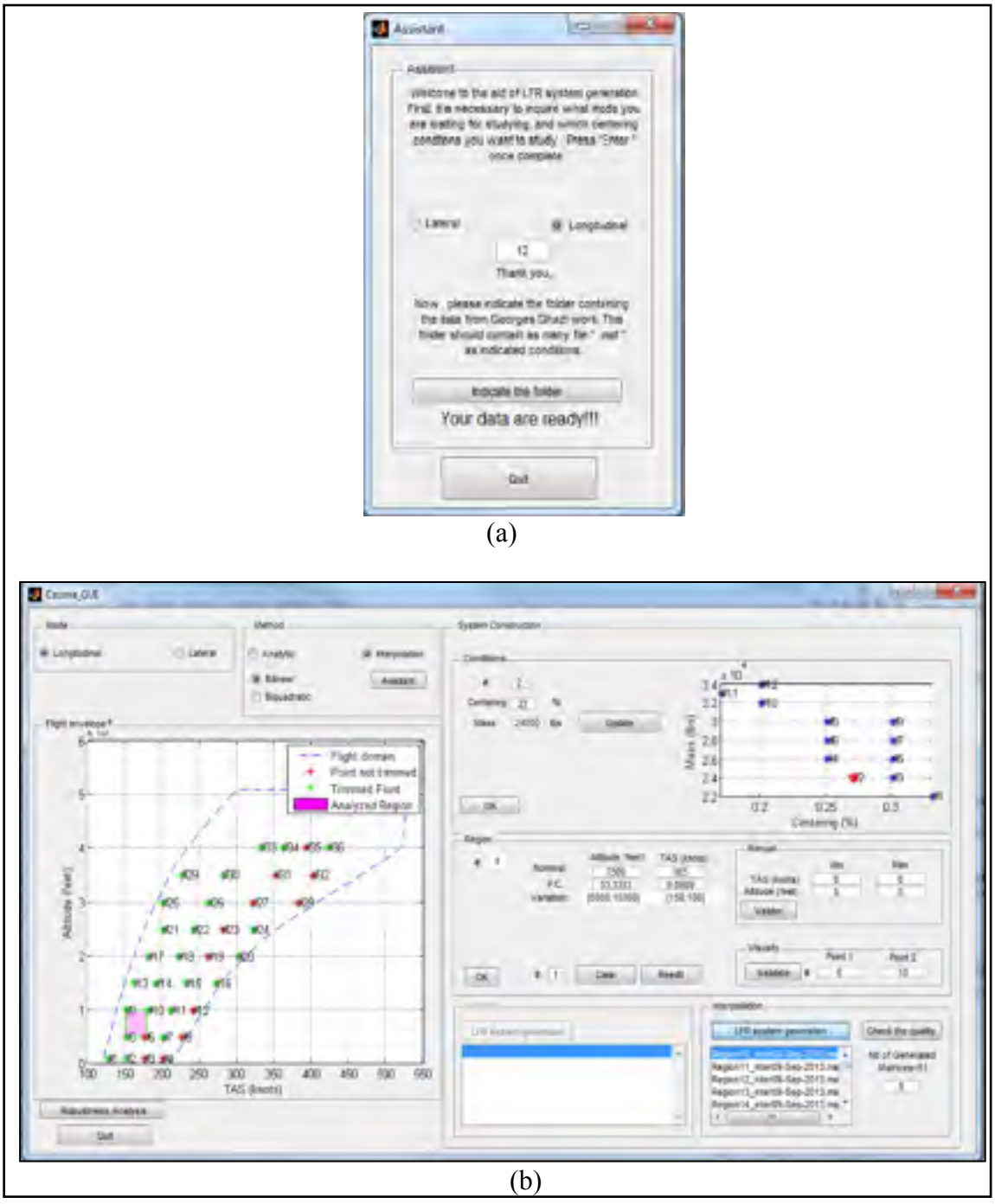

Figure 3-8 (a) and (b) Graphical User Interface for generating the Cessna Citation X LFRs.

To subdivide the flight envelope into regions, the following three ways are offered by using the GUI:

1. "Manually" -- by specifying “the upper and lower bounds of each uncertainty”. The "Submit" button associated with the manual method must be chosen to show the nominal values and the percentage of the uncertainties, corresponding to each parameter (TAS and altitude). By clicking on "OK", the selected region appears in a colored square shape in the flight envelope, as shown in Figure 3-8 (b);
2. "Visually" -- by specifying the “opposite diagonal vertices”. The flight points are numbered by use of two numbers, a region would be constructed (by assuming that the two points are not displayed on the same axis). It is necessary to click the "Submit" button on the GUI to display the nominal value and the percentage of uncertainty associated with each parameter. By clicking on "OK", the corresponding region appears on the flight envelope;
3. "Directly" -- by “filling the nominal value of each parameter and the percentage of uncertainties, and by confirming their selection, the corresponding region appears on the flight envelope;

Two additional options were added on the GUI, that were:

1. "Clear": Entering the region number in the box provided for this purpose, and then clicking the "Delete" button caused the disappearance of region from the flight envelope;
2. "Reedit": After choosing the region to redefine, and after validating its new coordinates, clicking on the " Re-edit " button will display the changes of the region in the flight envelope;

Once all informations have been provided, the interface allows us to build a minimized LFR model corresponding to each region that is specified by clicking on the button "Generate LFR systems". The border of the regions becomes green, and newly-created regions will appear in the “dialog box” used by the interpolation method with their names in the following format: "Region (number of region) _interp (dd-mm-yyyy) .mat".

It will further be possible to check the quality of the interpolation -- as shown in the Results Section -- by choosing the number of points to be randomly created for interpolation purpose. Whether there are one or more display windows open, these windows can contain a maximum of four graphs. To leave the interface, simply click on the button "Exit". This interface provides a helpful real-time visualization, and it has very good modularity.

A single Graphical User Interface (GUI) as shown in Figure 3-8 (a) that can only be opened from the previous interface was created to facilitate the organization of the data. Indeed, it has been observed that there can be too much information to handle, given the large number of centering and flight points. This GUI classifies state space matrices in the longitudinal or lateral models, centering and flight points.

In addition, the flight envelope is generated by providing information on each flight point's trim conditions of the model. "Green" highlighting means that the model is trimmed at this flight point, and "red" highlighting refers to a flight point for which no equilibrium condition was found.

It was possible to accurately develop the Cessna Citation X aircraft's dynamic longitudinal LFR models by means of the state matrix interpolation method using this GUI. The results are very good, and that are further used to study the aircraft's longitudinal natural dynamics stability.

3.4 Stability Analysis

After the development and testing of the Graphical User Interface (GUI), the aircraft LFR models could be created easily. A stability analysis using this interface that was developed by researchers at the University of Siena within the framework of the project "Clearance of Flight Control Laws Using Optimization" (Varga A, 2012),(Magni, 2006), (Poussot-Vassal et Roos, 2012) was performed on the 26 LFR models generated for a longitudinal aircraft model for each weight and X_{CG} location.

Before dealing with the stability analysis, some concepts are introduced on the determination of stability, based on linear algebra, and on the positive or negative condition of a matrix. A matrix $\mathbf{A} \in \mathbb{R}^{n \times n}$ is defined as "positive" if for each vector $x \in \mathbb{R}^{n}$, the quadratic Equation (3.24) is positive (Rugh, c1996):

$$x^T \mathbf{A} x \geq 0, \forall x \in \mathbb{R} \tag{3.24}$$

One of the properties associated with this definition is that the matrix can be defined as "broadly positive" if and only if all its eigenvalues are positive. If **A** is positive, then the values of the **A** spectrum set are all strictly positive. This strictly positivity can be written under the quadratic form as shown in Equation (3.25):

$$x^T \mathbf{A} x > 0, \forall x \in \mathbb{R} \tag{3.25}$$

3.4.1 Lyapunov stability

Next, the Lyapunov stability direct method is presented. Suppose that a system has an equilibrium point x_e. The system's measured energy, noted by $V(x)$, always positive, is defined. The steady state is chosen as the origin of the system, i.e. $V(x_e)$. If the energy evolution in the vicinity of this point is decreasing, $\frac{d}{dt}V(x) < 0$, it means that the system converges to a stable state. This notion of energy convergence is the basis of the Lyapunov stability theory (Bacciotti et Rosier, 2006) . A local equilibrium can thus be defined at the point x_e; that is associated with a stability condition, as shown in Figure 3-9.

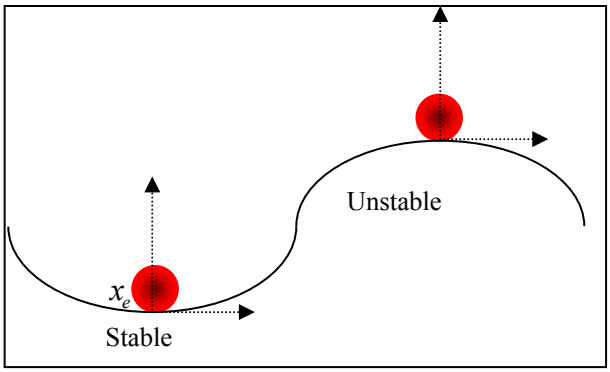

Figure 3-9 Equilibrium condition

For a system containing uncertainties, that are represented by a parameter vector α, the stability in the asymptotic sense is satisfied if there is a real-value function, and a continuously differentiable $V(x,\alpha)$ such as :

$$\begin{cases} V(0,\alpha) = 0 \\ V(x,\alpha)_{\|x(t)\|\to\infty} \to \infty \\ V(x,\alpha) > 0, \ x \neq 0 \\ \dot{V}(x,\alpha) < 0, \ x \neq 0 \end{cases} \tag{3.26}$$

Adapted from (Bacciotti et Rosier, 2006)

3.4.2 Quadratic Stability

The challenge of this method is to determine the Lyapunov function with the aim to satisfy the system of four equations (3.26). Previous research shown in (Papachristodoulou et Prajna, 2002), (Kharitonov et Zhabko, 2003), (Corless, 1994) focused mainly on the candidate functions shown in the next Equation.(3.27):

$$V(x,\alpha) = x^T P(\alpha) x \tag{3.27}$$

with $P > 0, \forall \alpha \in \Theta$

A system is represented using Equation (3.27) where Θ represents the variation range of each uncertainty. *P* is commonly chosen to be fixed. If such a function exists, then the system has a "quadratic stability" which is valid for all the uncertain parameters vectors. The robustness of the system is considered to be excellent in such a case.

The Lyapunov function presented in Equation (3.27) gives the required condition for a linear system to be considered "quadratically stable". The Lyapunov stability criterion given in Equation (3.29) lies in the existence of a positive and symmetric definite matrix $P^T = P > 0$:

$$\dot{x} = Ax \tag{3.28}$$

$$\mathbf{A}^T P + P\mathbf{A} < 0 \tag{3.29}$$

Adapted from (Lavretsky et Wise, 2012)

The matrix *P* is obtained by determining its $\frac{n(n+1)}{2}$'s coefficients. The Equation (3.29) belongs to the class of Linear Matrix Inequalities (LMI). Different toolboxes were developed to automate the resolution process of this type of equations, and to reduce the engineer's task. In this paper, the toolbox called YALMIP (Lofberg, 2004) coupled with the solver SDPT3 (Garulli et al., 2010), (Toh KC, 2012) will be used.

3.4.3 Resolution Method

In the literature, three different methods can be distinguished by the structure of the Lyapunov function that each one of them chooses. The first method focuses primarily on determining a Lyapunov function constant called Wang-Balakrishnan method (Wang et Balakrishnan, 2002), while the two other methods focus on dependent parameters functions to refine the solution search; these are Dettori-Scherer (Dettori et Scherer, 2000) and Fu-Dasgupta methods (Fu et Dasgupta, 2000).

The Wang-Balakrishnan method was selected to perform the system stability analysis in this paper. The latter is detailed in the following system:

$$\dot{x}(t) = A(\theta)x(t) \tag{3.30}$$

An uncertain system given by Equation (3.30) is considered, where x is the state space vector, $\theta \in \mathbb{R}^{n_\theta}$ is the parameters' vector, and $A \in \mathbb{R}^{n \times n}$ is the aircraft dynamics, and this system can be defined by equations (3.31) and (3.32) :

$$A(\theta) = A + B\Delta(\theta)(I - D\Delta(\theta))^{-1} \tag{3.31}$$

where
$$\Delta(\theta) = diag(\theta_1 I_{s_1}, \dots, \theta_1 I_{s_1}) \tag{3.32}$$

Taken from (Garulli et al., 2010)

An equivalent Linear Fractional Transformation (LFT) of Equation (3.31) is given by equations (3.33), (3.34), and (3.35) :

$$\dot{x}(t) = Ax(t) + Bu(t) \tag{3.33}$$

$$y(t) = Cx(t) + Du(t) \tag{3.34}$$

$$u(t) = \Delta(\theta)y(t)) \tag{3.35}$$

Taken from (Garulli et al., 2010)

with $u \in \mathbb{R}^d, y \in \mathbb{R}^d$, $d = \sum_{i=1}^{n_\theta} s_i$, and A, B, C, D are real matrices of appropriate dimensions. Matrix A is assumed to be Hurwitz type for the stability analysis of the LFR system. θ is an uncertain parameter vector, which belongs to Θ a hyper- rectangular with vertices of 2^{n_θ} as $Ver\,[\Theta]$, and $\dot{\theta}(t) = 0$ the uncertain parameters that are time invariant.

The system of equations is represented by equations (3.33), (3.34), and (3.35) and following conditions are mentioned:

- If there exists a common quadratic Lyapunov function for all matrices A(θ), where $\theta \in \Theta$, then this function is quadratically stable;
- If A(θ) is Hurwitz for all $\theta \in \Theta$, the system is robustly stable;

3.4.3.1 Wang-Balakrishnan method

The system expressed by equations. (3.36), (3.37), and (3.38) presents a "quadratic stability", because its dynamics is given by a symmetric matrix defined as positive: $P \in \mathbb{R}^{n \times n}$, $P = P^T > 0$ and $M \in \mathbb{R}^{d \times d}$, $M = M^T > 0$, and expressed as follows :

$$\begin{bmatrix} A^T P + PA + C^T MC & PB(\theta) + C^T MD(\theta) \\ B(\theta)^T P + D(\theta)^T MC & -M + D(\theta)^T MD(\theta) \end{bmatrix} < 0 \quad (3.36)$$

where $B(\theta) = B\Delta(\theta)$ (3.37)

and $D(\theta) = D\Delta(\theta)$ (3.38)

Taken from (Garulli et al., 2010)

Thus, the existence of such matrices can prove with certainty the stability of a system. An alternative to this theorem that uses parameter-dependent Lyapunov functions is given by equations. (3.39) and (3.40); and the demonstration of this theorem is given in detail in (Wang et Balakrishnan, 2002).

$$V(x) = x^T Q(\theta)^{-1} x \quad (3.39)$$

whith

$$Q(\theta) = Q_0 + \sum_{j=1}^{n_\theta} \theta_j Q_j \quad (3.40)$$

3.4.4 Stability analysis interface

In order to accomplish the aircraft stability analysis, a Graphical User Interface is used, which eases and greatly facilitates the analysis task. It offers a wide choice of resolutions via three methods from published research found in (Wang et Balakrishnan, 2002), (Dettori et Scherer, 2000), and (Fu et Dasgupta, 2000). Figure 3-10 shows the window with which the user interacts; a brief description of how to manipulate the GUI for the stability analysis is given in the following paragraph.

There are two main sections in the GUI, the first one is "Analysis" contains the LFR models in “Model”, in “Method” three methods for resolution are given, “Region definition” the region that will be analyzed, and “Approach” which contains all functions called during the analysis as “ Progressive” or “Adaptive” and the type of “Lyapunov Functions”.

The second is the "Results" stores the results data. Furthermore, the GUI has access to the LFR Toolbox, and to the YALMIP SDPT3.7.

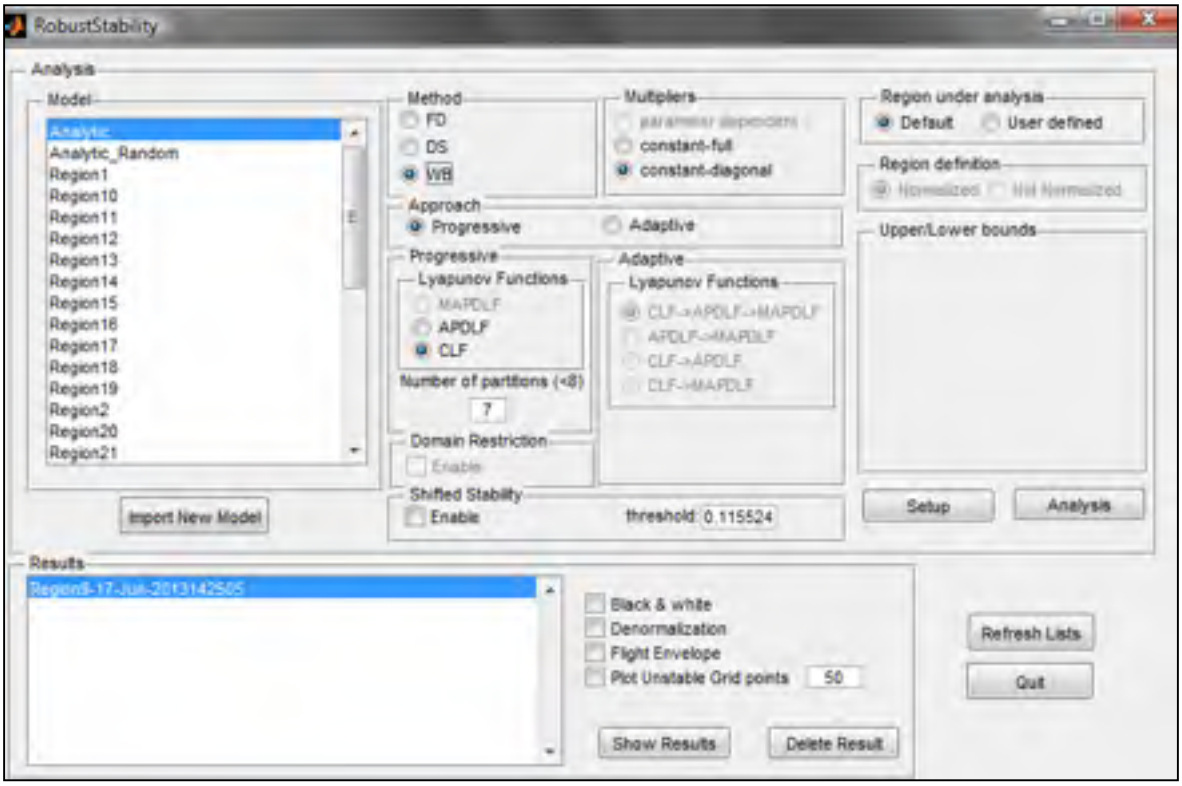

Figure 3-10 Robust Stability Toolbox

To perform the stability analysis, the obtained LFR model is firstly selected, and secondly the analysis parameters method Fu-Dasgupta (FD), Dettori-Scherer (DS), and Wang-Balakrishnan (WB), is chosen. The theory of the Wang-Balakrishnan method, is chosen, as it regards the normalization of the selected region. Other options exist such as the choice of the discretization number, the Lyapunov functions’ shape. After these parameters are validated, the stability analysis can be done for the selected region of the flight envelope.

3.5 Analysis of Results

3.5.1 LFR results validation

The results generated by LFR models must be evaluated (Varga A, 2012). To assess the accuracy of these results outside our interpolated points, any number of points can be randomly generated, we have chosen 40 as an example**,** were randomly created from our interpolations, and they were compared with our reference points (representing the four (4) vertices of the region), for the 26 regions, we obtained 40 points for each of region.

It can be ensured that the interpolated points have a relative proximity with those references points, and remain in the area formed by these reference points. Figure 3-11 shows the eigenvalues results (imaginary versus real eigenvalues) for a given X_{CG} location and for 9 medium altitudes (regions 10 to 18), while Figure 3-12 gives the eigenvalues results for the highest altitudes (regions 24 and 25), while the results obtained for the other regions are given in Appendix. Only the positive side of the imaginary axis is shown in these symmetrical figures. Each pole pair is represented by a cross and circles. The color “blue” is associated with the points used as reference points, and the “red” color indicates the randomly-generated interpolated matrices.

It can be observed that the quality of the interpolations is satisfied for the whole flight envelope, with the exception of the two regions (24 and 25) where it might be a problem for some X_{CG} locations. Indeed, at high altitudes, as shown in Figure 3-12, the interpolation of points seems to be more delicate and the pole pairs associated with the randomly-generated matrices appear to show some signs of disparity with the reference points, as indicated in Figure 3-12.

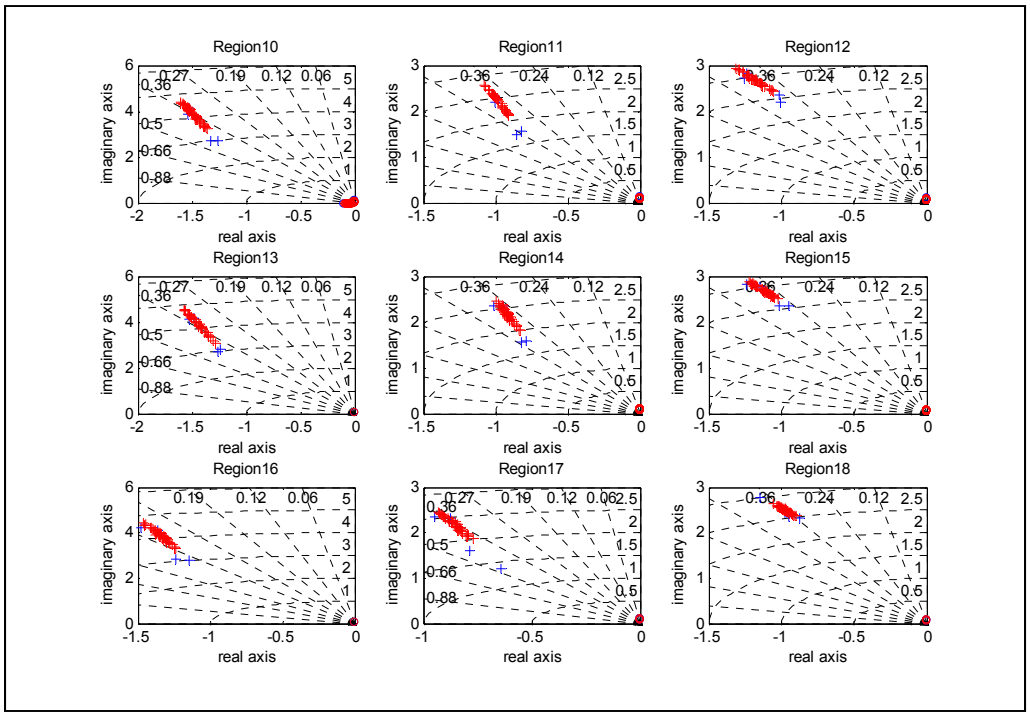

Figure 3-11 Comparison of eigenvalues for interpolated flight points with the reference values for medium altitudes (between 15,000 ft and 30,000 ft)

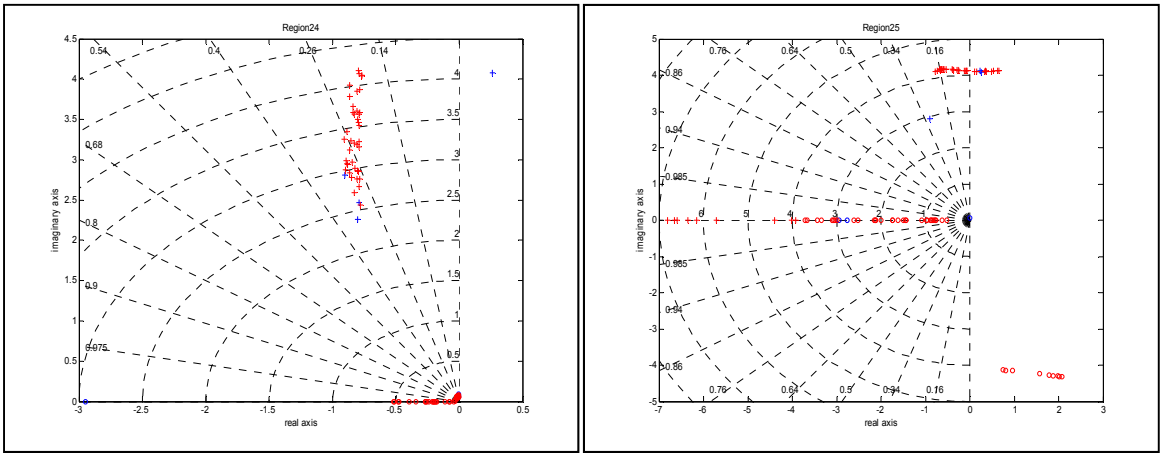

(a) (b)

Figure 3-12 Comparison of eigenvalues for the interpolated flights points with the reference values at the highest altitudes (between 35,000 ft and 40,000 ft)

This dissimilarity is most critical for region 25, which has isolated poles represented by circles and red crosses, especially in its lower right corner and on its pure real axis in Figure 3-12(b). Regarding region 24 shown in Figure 3-12(a), two poles seem isolated from the rest

of the poles. Even though the results obtained for the other X_{CG} locations are not presented here, these results are of a similar type for the remaining 11 weight/ X_{CG} configurations. After analyzing all graphs, the quality of these results allows us to validate the interpolations made for our entire flight envelope for all X_{CG} locations, except for regions 24 and 25 at the highest altitudes. Those results still need to be analyzed, but they will be considered "less reliable" if inconsistencies persist.

3.5.2 Stability analysis results

The interface allows the number of times that the region will be sub-divided to be freely selected in the analysis. Whenever a region is discretized, it is sub-divided in four smaller sub-regions; each sub-region is analyzed, and possibly discretized at its turn, and so on until the 7^{th} order of discretization. This choice directly influences the results' accuracy, but it also affects the execution time.

A compromise between the quality and the quantity of results had to be found. We have chosen to discretize a single region having a very high instability. A first analysis was launched that allowed the maximum possible discretization, which was seven (7), which meant that the uncertainty domain (region) was going to be bisected 7 times representing potentially $2^7 = 128$ tiles per side, . For a model with 2 uncertainties, the region (uncertainty domain) was meshed a number of $2^7 \text{x}\, 2^7 = 16{,}384$ tiles, which meant, that the region was subdivided in 4 sub-regions each time until reaching the 7 times, that was equivalent to $\sum_{k=0}^{7} 4^k = 16{,}384$ tiles, that were obtained in the worst cases (in the proximity of instability). The results analyses are presented in Figure 3-13 and Figure 3-14.

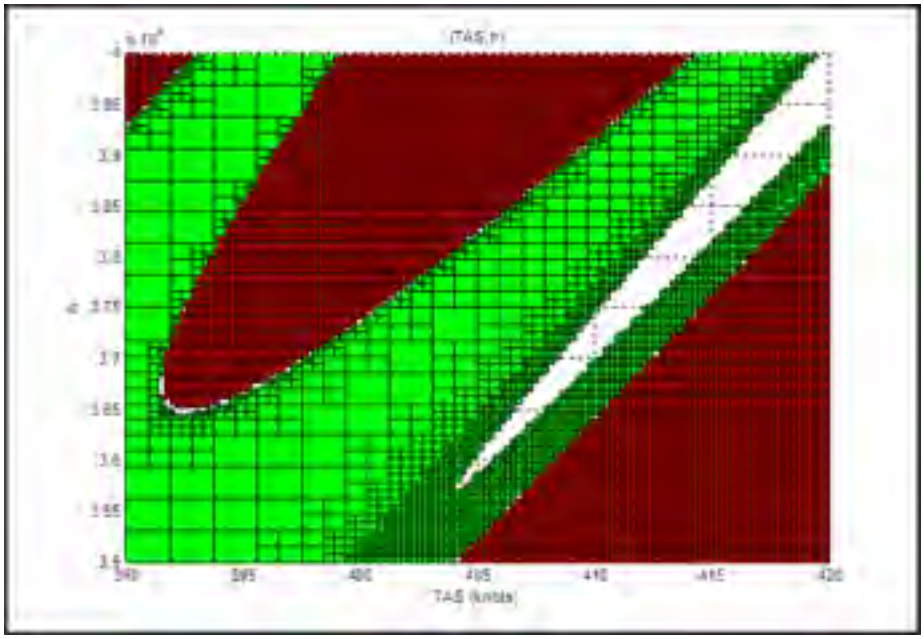

Figure 3-13 Results for the single region with 7th order discretization (altitude= 35,000ft -40,000 ft and TAS= 390 – 420 knots)

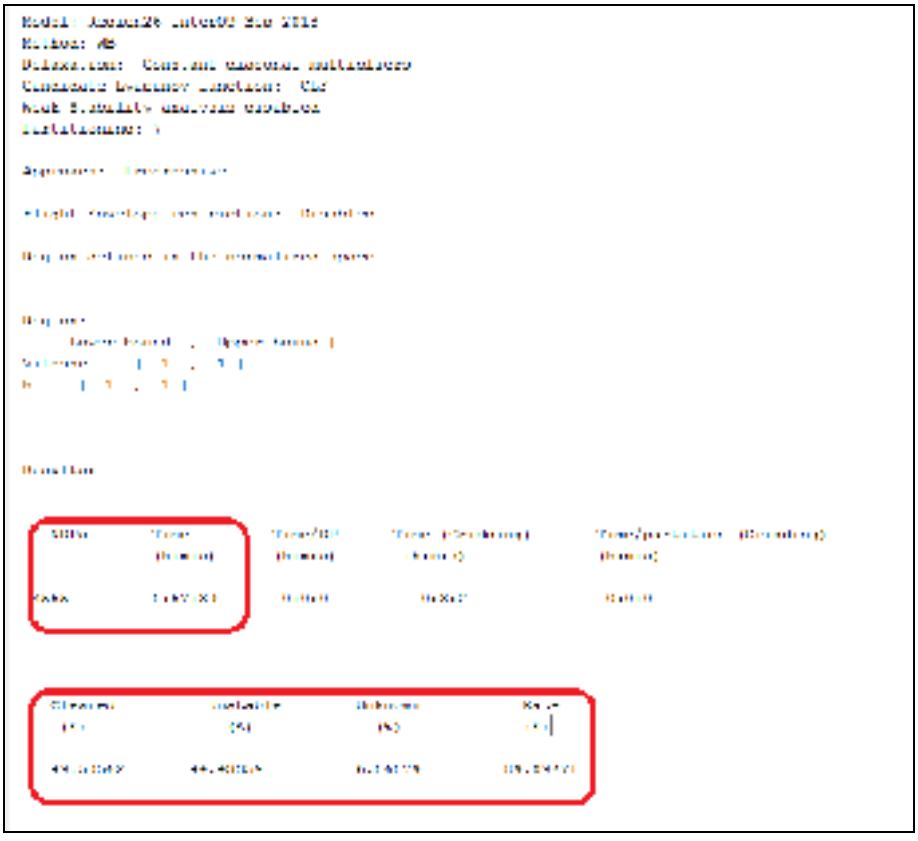

Figure 3-14 Results of a completed stability analysis

Figure 3-14, and Figure 3-16 show the results when a region's analysis has been completed by 7^{th} and 5^{th} order discretization, respectively. These figures obtained using the Matlab command summarize the information about the region; in fact the method selected, the candidate Lyapunov function, the approach, the order of discretization, and the bounds of the normalized uncertainties used in the LFR model are indicated.

The results represent the Number of Optimizations denoted by NOPs that have been solved (they correspond to the number of tiles attempted to be cleared, that is expressed by the sum of the number of the "green" plus the number of "red" tiles), therefore to the time taken for the region analysis. These results are presented graphically in Figures 3-13 and 3-15, where they indicate the sub-regions where the analysis has been cleared; ; the stable sub-regions were in "green", the unstable sub-regions were in "red", and the unknown sub-regions were in "white"; when the sub-regions (tiles) are unknown so denoted in "white", the aircraft cannot be trimmed for its corresponding altitudes h and TAS; the results were expressed in percentages (%) of the area of the analyzed region in Figures 3-14 and 3-16. The "Rate" value indicates the ratio of the cleared (the stable (green) plus the unstable (red)) part to the neutral "white" part of the region.

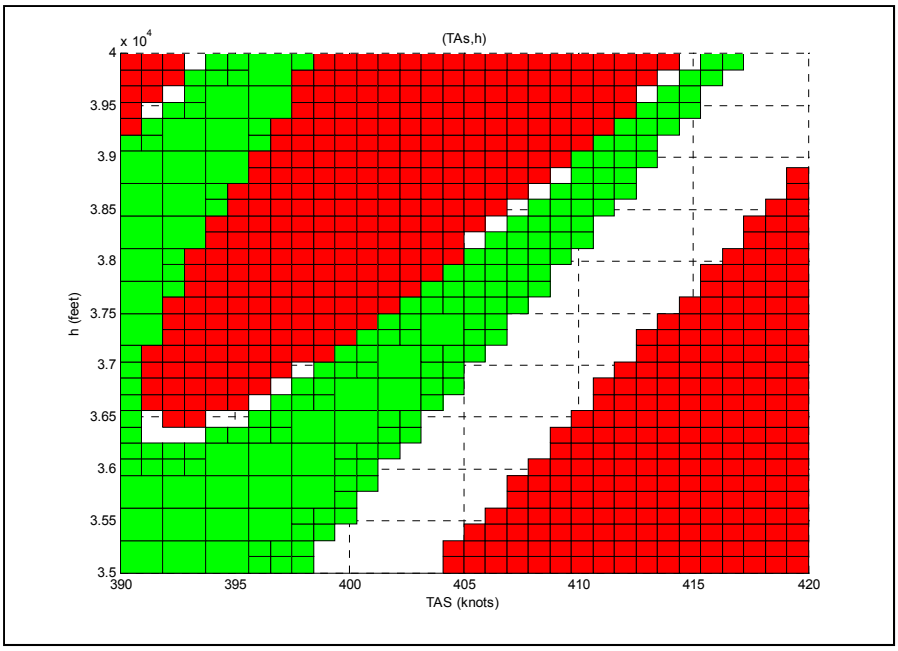

Figure 3-15 Region with 5th order discretization
(altitude 35000ft -40000 ft and TAS 390 – 420 knots)

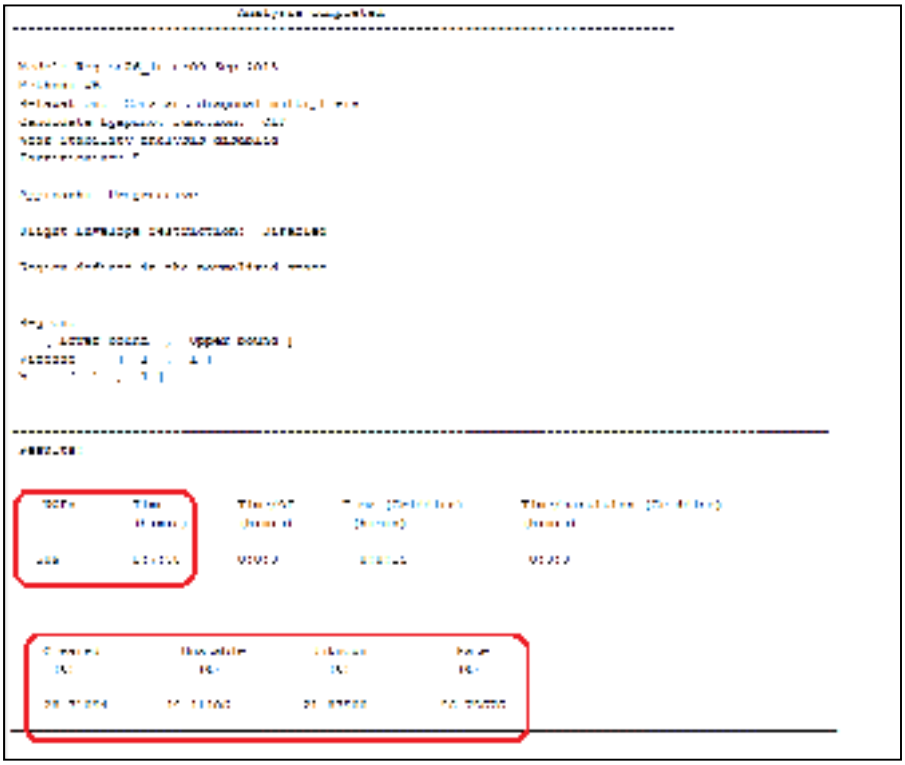

Figure 3-16 Results of 5th order discretization of the region

Four hours took to complete the computations need for the results analysis. The 26 LFR models defined by interpolation for 12 weight/ X_{CG} configurations have been analyzed for the stability of the longitudinal aircraft model. These results indicate that it was not necessary to obtain a very high discretization order of the regions' subdivisions.

Achieving a 7th order discretization results were obtained for "2" uncertainties $2^7 = 128$ maximum tiles per side. Given the fact that the largest region defined in Figure 3-13 is 80 knots wide and 5,000 ft high, and that a tile precision is represented by 0.625 knots and 39.0625 ft, then a computation time of almost 57 min is required to analyze the entire region, and to solve 4555 (NOPs) optimizations for this region (this number was computed by the Stability Analysis software which represents the sum of the stable and the unstable sub-regions or "tiles"). The system discretization was reduced from the 7th order to a 5th order as shown in Figure 3-15, which means that a maximum resolution of 2.5 knots and 156.25 ft per region was applied. This discretization reduced highly the computing time for the region from 57 min in its 7th order of discretization (Figure 3-14) to almost 8 min in its 5th order of discretization, the time that takes to analyze the entire region, and to solve 509 (NOPs) optimizations (this number was computed by the Stability Analysis software which represents the sum of the stable and the unstable sub-regions or "tiles") as shown in Figure 3-16. The results produced by the 7th order discretization are of course better than those obtained from a 5th order discretization, especially in terms of "Rate". The rate of 6.06% is obtained in the 7th order discretization while the rate of 21.87% is obtained in the 5th order discretization, which means that the unknown area in the region with 5th order descretization is larger than in the region with 7th order of descretization. The computing time was used to choose between these two orders of discretization. The studies considering discretization of up to $2^5 = 32$ elements per variation range of each uncertainty (h, and *TAS*) were carried out, and seemed to be a very good compromise for the Cessna Citation X stability analysis due to its "very good natural stability".

The system discretization was reduced to a 5^{th} order, which was equivalent to a maximum resolution of 2.5 knots and 156.25 feet per region. This discretization reduced highly the computing time under 8 min in order to solve 509 optimizations. The results produced by 7^{th} order discretization are of course better than those obtained from a 5^{th} order discretizations, especially in terms of "rate percentage". The rate of 6.06% is obtained in the 7^{th} order discretization while the rate of 21.87% is obtained in the 5^{th} discretization orders, which means the unknown area in the region with 5^{th} order discretization is larger than the region with 7^{th} order of discretization. The computing time was used to choose between these two discretizations.

The studies with discretizations of up to $2^5 = 32$ elements per variation range of each uncertainty were carried out, and seem to be a very good compromise for the Cessna Citation X stability analysis due to its very good natural stability

3.5.2.1 Results of the aircraft longitudinal model stability analysis

Figures 3-17 and 3-18 show the stability analysis results obtained for two different weight and X_{CG} positions using the Wang-Balakrishnan method based on the Lyapunov constant functions, and the 5^{th} order discretization. The results obtained for other five different weight/ X_{CG} configurations are given in Appendix I.

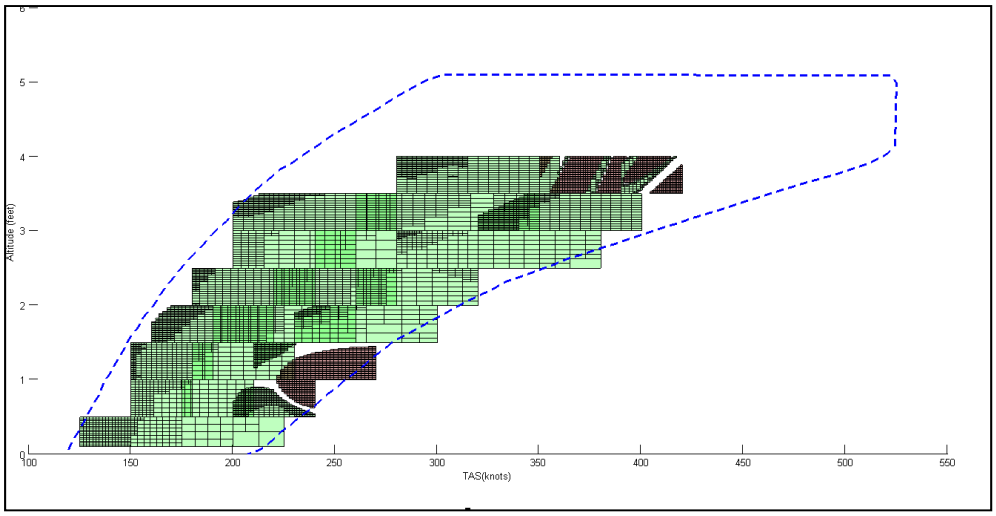

Figure 3-17 Stability analysis of a longitudinal model for 3rd weight/ XCG configuration (24000lbs/30%)

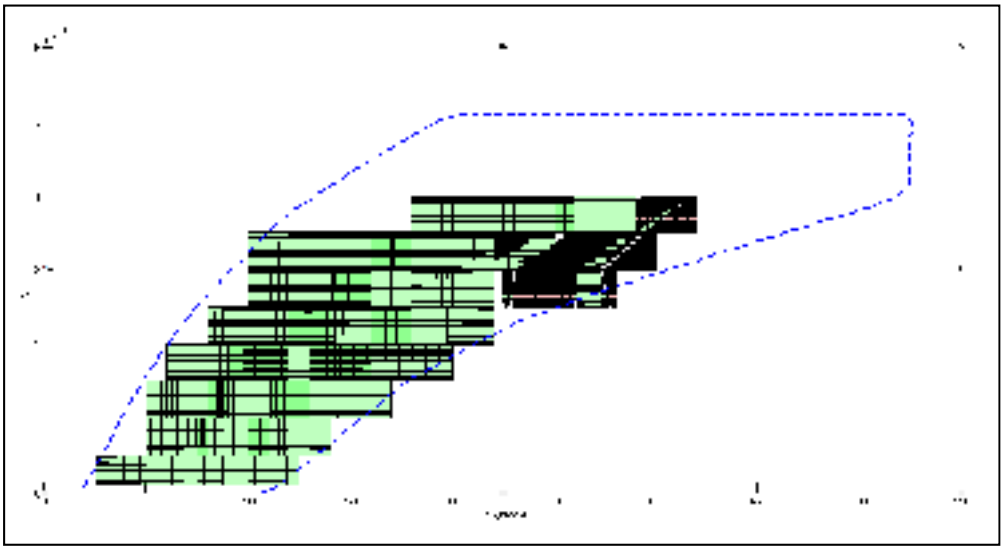

Figure 3-18 Stability analysis of a longitudinal model for 7th weight/ X_{CG} configuration (28000lbs/30%)

Firstly, the continuity between regions is found. Indeed, the instability zone, located for low altitude and average speed, that is and shown in Figure 3-17, covers two distinct regions, and therefore two different interpolated models. The “red” area stops at the border between the two models, and this is marked for unstable regions. Figure 3-18 illustrates this fact by revealing a peak discretization on the back of the flight envelope and along the stall limit from the lowest to the highest altitude.

Secondly, some conflicts are discussed that appear in the superposed regions. The results of these recovering areas are not consistent, and are sometimes contradictory. The regions are not only built by interpolating, but also by extrapolating data for the left upper and the right lower peaks. In all cases, “incoherence” is caused by extrapolation; the model does not describe the reality accurately. Therefore, the area(s) presenting an extrapolation situation must be neglected.

3.6 Conclusion

The aim of the clearance process was to demonstrate that a set of selected criteria expressing desired stability and handling requirements was fulfilled in the presence of all possible sources of uncertainties. The stability criterion can be reformulated to be a clearance criterion, as mentioned by Airbus and can be classified in four classes: 1) the aeroelastic stability, 2) turbulence, 3) comfort, and 3) maneuvers criteria. Only the aeroelastic stability envelope criterion was presented for the longitudinal Cessna Citation X business aircraft in the open loop system, which was the basis for any Cessna Citation X flight controller design validation and clearance.

Future work will evaluate the aeroelastic stability of the Cessna Citation X longitudinal closed loop aircraft model by using a *H-infinity* controller developed during an earlier work (Boughari et al., 2016), to show if the interaction of the flight controller with the Cessna Citation X would induce any instability.

The generation and validation of Cessna Citation X LFR models were automated in this research using a Graphical User Interface (GUI), which offered the user a very good visualization tool that facilitated the manipulation of LFRs models, and therefore, it provided a very good understanding of its validation process.

The longitudinal model natural stability (open loop system without a controller) has been made for the 26 interpolated regions, and it was also a very good tool for validating the LFR

models. The analysis indicated the regions reliability in representing the aircraft dynamics in its whole envelope for all its uncertainty parameters values. This analysis highlighted the importance of the work that was performed for the exploitation of results in this research. The only disadvantage of this method was that it was still requires a relatively long time calculation, of almost four hours for the entire flight envelope. However, practical aspects of this study were considered in the aircraft stability analysis, by using the low order discretizations. In this paper, 5^{th} order discretization was applied.

Acknowledgements

This work was performed at the LARCASE (Laboratory of active controls, avionics and aeroservoelasticity research). We would like to thank to the project leader Mr Ken Dustin and his team at CAE Inc. for their support in the development of the Aircraft Research Flight Simulator at the LARCASE laboratory.

This simulator was obtained thanks to research grants that were approved by the Canada Foundation for Innovation (CFI) and the Ministère de Développement de l'Économie, de l'Innovation et de l'Exportation MDEIE. In addition, this research was funded by the Natural Sciences and Engineering Research Council of Canada NSERC in the frame of Canada Research Chair Programs; Dr Ruxandra Botez is Canada Research Chair Holder in Aircraft Modeling and Simulation Technologies. Thanks are also due to Mrs Odette Lacasse and Mr Oscar Carranza at ETS for their continuing enthusiasm and support

CHAPITRE 4

NEW METHODOLOGY FOR OPTIMAL FLIGHT CONTROL USING DIFFERENTIAL EVOLUTION- APPLICATION TO THE CESSNA CITATION X AIRCRAFT - VALIDATION ON AIRCRAFT RESEARCH FLIGHT LEVEL D SIMULATOR

Yamina Boughari, Ruxandra Mihaela Botez, Florian Theel, Georges Ghazi,

LARCASE Laboratory of Applied Research in Active Controls, Avionics and AeroServoElasticity
ETS, 1100 Notre Dame West, Montreal, Que., Canada, H3C-1K3

This article was submitted on January 2017

Résumé

Les réglages des gains optimaux appropriés au Système d'Augmentation de Stabilité (SAS), et au Système d'Augmentation de Contrôle de (CAS) sont des tâches complexes et de longue durée qui dépendent de la connaissance du système par l'ingénieur. Lorsque ces tâches reposent sur le réglage des gains, comme dans le cas d'un contrôleur Proportionnel Intégrateur et Dérivé PID, ou sur les matrices de pondérations, comme dans le cas de la méthode de Régulation Quadratique Linéaire (LQR), un processus d'essai et d'erreur est habituellement utilisé pour la détermination des matrices de pondération, qui est généralement une longue procédure.

Dans le cadre de cette recherche, le modèle linéaire de l'avion Cessna Citation X est présenté pour des différentes conditions de vol et pour 12 conditions de poids / X_{CG} nécessaires pour couvrir l'enveloppe de vol de l'avion. La loi de contrôle des vols a été optimisée et conçue pour cette enveloppe de vol en combinant l'algorithme d'évolution déférentielle (DE), la méthode LQR et le contrôleur proportionnel intégral (PI). Les contrôleurs optimaux a été utilisé pour atteindre des caractéristiques dynamiques satisfaisantes par rapport aux exigences de qualité de vol et de conception du Système d'Augmentation de la Stabilité (SAS) et de Contrôle (CAS) de l'avion Cessna Citation X.

Le contrôleur Intégrateur Proportionnel PI a été ensuite utilisé dans le système d'augmentation de contrôle. À la fois, la matrice de pondération de la méthode LQR et les paramètres du contrôleur PI ont été optimisés en utilisant la méthode de l'évolution différentielle. Ensuite, le nombre de contrôleurs utilisés pour contrôler l'avion dans son enveloppe de vol a été optimisé en utilisant les caractéristiques LFR. En outre, la conception et la validation des contrôleurs sur l'enveloppe de vol ont été automatisés à l'aide d'une interface graphique qui offre au concepteur la souplesse nécessaire pour modifier les exigences de conception et de valider le contrôleur sur toute l'enveloppe de vol de l'avion et réduire la complexité du processus de conception de la Loi de contrôle des vols.

L'algorithme meta-heuristique utilisé dans cet article a fourni de très bons résultats avec une grande fiabilité et efficacité. Dans le but de réduire le temps et le couts de la conception de la loi de contrôle, cet algorithme a été utilisé sous cette forme pour optimiser la régulation quadratique linéaire et le contrôleur proportionnel intégral (PI) dans le contrôle de l'avion, en utilisant une seule fonction objective pour les deux optimisations.

Abstract

Setting the appropriate controllers for aircraft Stability Augmentation System (SAS), and Control Augmentation Systems (CAS) are complicated and time consuming tasks. As in the Linear Quadratic Regulator method gains are found by selecting the appropriate weights or as in the Proportional Integrator Derivative control by tuning gains. A trial and error process is usually employed for the determination of weighting matrices which is normally a time consuming procedure.

The Cessna Citation X aircraft linear model was presented for different flight conditions, and at 12 X_{CG} locations to cover the aircraft’s flight envelope. Flight Control Law were optimized and designed for this flight envelope by combining the Deferential Evolution (DE) algorithm, the LQR method, and the Proportional Integral (PI) controller. The optimal controllers were

used to reach satisfactory aircraft's dynamic and safe flight operations with respect to the stability and control augmentation system's handling qualities, and design requirements.

The Differential Evolution algorithm was used in this research to optimize the LQR method, and the PI gains and to automate the tuning operation. Then the number of controllers used to control the aircraft in its flight envelope was optimized using the LFRs features. Furthermore the design and the clearance of the controllers over the flight envelope were automated using a Graphical User Interface, which offers to the designer, the flexibility to change the design requirements, and to validate the controller over the whole aircraft flight envelope, and consequently to reduce the Flight Control Law design process complexity.

The meta-heuristic algorithm used here has given very good results with great reliability and efficiency. In the aim of reducing time and costs of the Flight Control Law design, one fitness function has been used for both optimizations, and using design requirements as constraints.

4.1 Introduction

The certification authorities need to ensure that the Flight Control System (FCS) operates properly through the specified flight envelope, when the safety of the new generations of aircrafts, which are fully Flight By Wire relay importantly on its FCS, the. The Flight Control Law (FCL) from design to clearance process is a time consuming process, and it costs, especially for civil aircrafts that need to achieve higher safety. This process aims to prove that the aircraft's robustness and flying requirements are satisfied.

The use of the aircraft flying qualities as requirements criteria in the flight control design is rarely, if ever carried out in the practice (Tischler, 1996). Usually the flight control design is achieved and implemented as a part of avionics system, when the flying qualities are a part of aerodynamics.

Flight control systems are designed to accomplish high aircraft performance with good or acceptable flying qualities within the flight envelope specified by the designer. However, in the real world the selection of a control law is commonly based on the experience of the engineers and the pilots in charge (Pratt, 2000). The flying qualities were considered for the first time in flight testing of the aircraft prototype, this process worked until the Fly By Wire technology were be implemented in the modern aircrafts, where the problem of the PIO appears and there were a loss of aircraft.

The flight control development is an iterative process, which start from the definition of the requirements and the flying qualities, followed by the evaluation of the control law design, and concepts, then the resulting controllers were implemented in the linear and non linear models for simulation, and validation, ending by the last step which is the control laws optimization via flight tests.

There are many ways in which the design of optimal flight control laws can be done using modern methods, such as the Linear Quadratic Regulation (LQR); the advantage of the LQR method is that it provides the smallest possible error to both its input and outputs while minimizing the control effort, where the error corresponds to the difference between the desired and the obtained value for system input and output. In case full states are measurable the LQR method ensures the obtaining of a stable controller for the nominal model, and provides cross-terms in the flight dynamics equations, and further, automatically leads to a robust control in the sense that the gain margin is infinite and the phase margin is greater than 60 deg. This is shown in (Boughari et Botez, 2012a) where the LQR method has been used for the Stability Augmentation System (SAS) control, and applied on Hawker 800XP business aircraft, and to alleviate gust effects in (Botez et al., 2001) on bomber aircraft.
The LQR method has also been used in a longitudinal attitude controller designed for B747 aircraft (Guilong et al., 2013), and in adaptive control for remotely controlled aircraft (Mukherjee et Pieper, 2000).

To obtain the corresponding optimal state feedback gain K; the objective function which represents the quadratic performance index function *J* must be defined. This means the appropriate Q and R weighting matrices need to be found by a trial and error method or by relying on the designer's knowledge until the desired response is found.

In the same way a PID controller was tuned (Grigorie et al., 2012b), and in (Grigorie et al., 2012c) for a linear model of a morphing wing relying on the engineer's experience, and validated on its nonlinear model.

In order to overtake the time-wasting during the trial and error method, many algorithms were developed in the last decades to optimize the controller performances. Using stochastic searching as an optimization algorithm is one of the most popular methods that have been used recently. Both Genetic Algorithm (GA) and Particle Swarm Optimization (PSO), were used in the LQR optimization in(Chen et Zhang, 2009),(Ghoreishi et Nekoui, 2012). In (Guo et al., 2010), (Zeng et al., 2012), the optimal LQR weights matrices analyses were based on the Genetic Algorithm (GA) search. Using the GA, the optimized LQR gains were used to improve the buck converter's (Poodeh et al., 2007), and the distillation column control in (Jones et Hengue, 2009); in both those instances, better results of the control performances were found than those based on experience. By using the GA and PSO algorithms ; in (Wongsathan et Sirima, 2008), and (Xiong et Wan, 2010) an inverted pendulum and double inverted pendulum were controlled successfully.

In (Zhi, Luo et Liu, 2012), the authors have used a shift function combined with Neural Network to improve a PID tuning algorithm for mobile robots. A social algorithm known as the 'small world phenomenon' was used in (Xiaohu et al., 2008) to search for the shortest path that could be taken by an algorithm for PID parameters tuning. The tuning of PID parameters was based on Fuzzy Logic in (Hyung-Soo et al., 1999), (Bandyopadhyay et Patranabis, 2001). In (Saad, Jamaluddin et Darus, 2012), (Han, Luo et Yang, 2005), and (Mitsukura, Yamamoto et Kaneda, 1997), the authors used a PID controller based on genetic tuning.

Recently many researches were curried on in the flight control domain, to optimize and automate the controller performances using modern control methods such as in (Boughari et al, 2014b), and (Boughari et al , 2016) the weighting functions that described the H-infinity controller were optimized using GA and DE algorithms the resulting controllers were successfully cleared over the entire flight envelope, however the H-infinity controller is of high order, which made it difficult in real implementation. Hence the LQR method offered relatively simple controllers of law order, as the LQR controller performance rely on the weighting matrices selection, then it became interesting to automate the weighting searches processes, as shown in (Kukreti et al, 2016), where the LQR was genetically optimized for UAV control under wind disturbance, and gave good results in both performance and robustness , and (Boughari et al, 2014a) the authors optimized the performance of the controller using the LQR method, with the meta-heuristic Differential Evolution, the controllers were cleared for each flight condition in the Cessna Citation X aircraft flight envelope. In (Ghazi et al,2014), and (Ghazi et al,2015b), LQR gains were optimized by using the Genetic Algorithm and were applied on Lynx helicopter, and lateral control on Cessna Citation X business aircraft, the robustness of the controllers was assisted by the guardian map theory, the optimized controllers show a very good results, in other hand, the application of the guardian map is a very long time computation, which made the guardian map method less desirable to clear the controller for the entire flight envelope. So the main contributions of this paper firstly, is to apply an evolutionary algorithm such as the Differential Evolution (DE) algorithm to optimize the Flight Control Laws, by combining the LQR modern control method for Stability Augmentation and the classical PI control method for the Control Augmentation System in one objective function, and secondly to consider some of the design specifications and flying qualities requirements as constraints in the design problem, finally to optimize the number of the controllers used in the flight envelope as well as assisting the controller robustness by using the LFRs features, where the flight envelope is divided to 26 regions, and one controller is calculated for each region, therefore a set of 26 controllers is then applied to control the center and the 4 vertices of each region, which lead to a relatively certain robustness of the controller. Furthermore these controllers are used to enhance

Cessna Citation X business aircraft controllability according to the flying qualities requirements. Furthermore, to ease the design engineer's work, the whole process is automated using a Graphical User Interface, to overcome to the time consuming process due to its iterative nature

The main contributions of this paper firstly, is to apply an evolutionary algorithm such as the Differential Evolution (DE) algorithm to optimize the Flight Control Laws, by combining the LQR modern control method for stability augmentation and the classical PI control method for the Control Augmentation System in one objective function, and secondly to consider some of the design specifications and flying qualities requirements as constraints in the design problem, and finally to optimize the number of the controllers used in the flight envelope by using the LFRs features, where the flight envelope is divided to 26 regions, and one controller is calculated for each region, therefore a set of 26 controllers is then applied to control the center and the 4 vertices of each region, which lead to a relatively certain robustness of the controller. Furthermore these controllers are used to enhance Cessna Citation X business aircraft controllability according to the flying qualities requirements. Furthermore, to ease the design engineer's work, the whole process is automated using a Graphical User Interface, to overcome to the time consuming process due to its iterative nature.

4.2 Problem Statement

4.2.1 Aircraft control architecture using LQR and PI

The main idea of this study is to use the Differential Evolution Algorithm to search for the appropriate weighting matrices Q and R, where the LQR method is based on them; the optimal controller used as SAS is further obtained by solving the well known Ricatti equation. Then a second optimization follows to find the optimal CAS by using the PI method.

The linear longitudinal and lateral models of Cessna Citation X aircraft dynamics are given by using the state space matrices, also actuators and sensors dynamics are given. The SAS is used to stabilize the system response accordingly to the flying qualities requirements, and the CAS is used as tracking controller as shown in the aircraft closed loop architecture given in Figure 4-1.

In the following sections, useful theories that will be utilized in this work are presented: the Cessna Citation X dynamics, the differential evolution algorithm search, the LQR design and the Proportional Integral tracking controller.

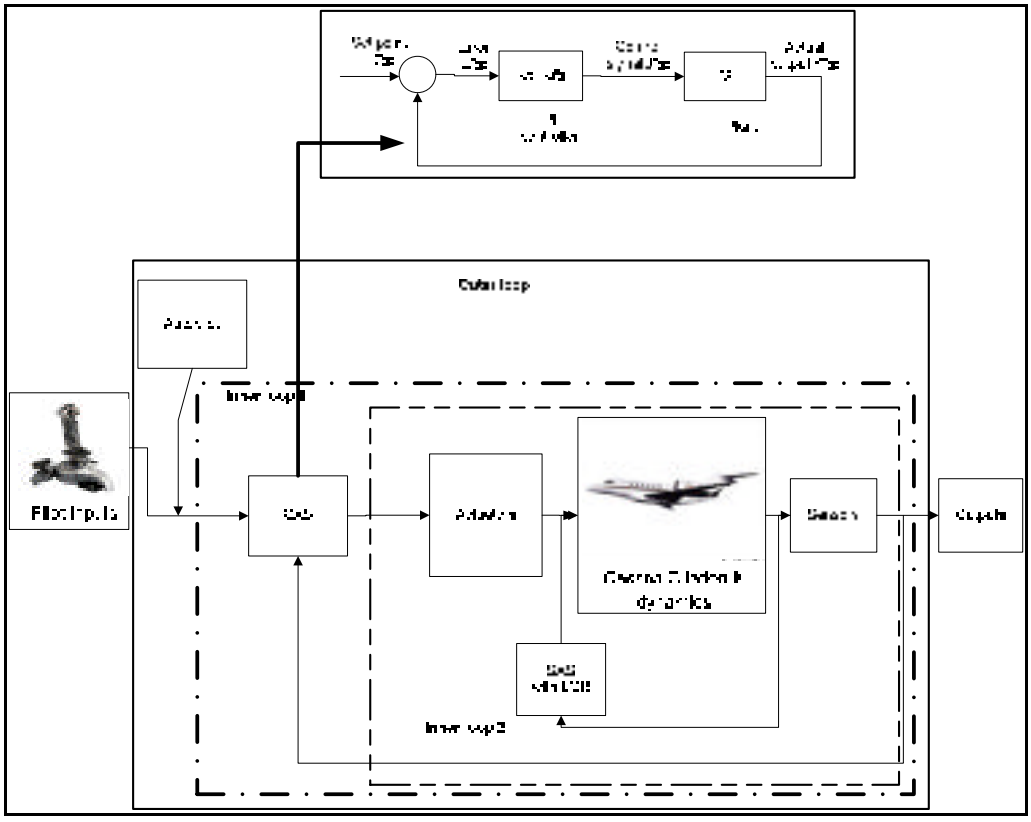

Figure 4-1 Closed loop representation of the Cessna Citation X business aircraft

4.2.2 Cessna Citation X business aircraft

The Cessna Citation X is the fastest civil aircraft in the world, as it operates at its speed upper limit given by Mach number of 0.935. The longitudinal and lateral motions of this business aircraft are described, as well as its flight envelope and the flying qualities requirements.

The aircraft nonlinear model for the development and validation of the flight control system used the Cessna Citation X flight dynamics, and was detailed by Ghazi (2014). This model was built in Matlab/Simulink based on aerodynamics data extracted from a Cessna Citation X Level D Research Aircraft Flight Simulator designed and manufactured by CAE Inc. According to the Federal Administration Aviation (FAA, AC 120-40B), the Level D is the highest certification level that can be delivered by the Certification Authorities for the flight dynamics. More than 100 flight tests were performed on the Citation X Level D Research Aircraft Flight Simulator within the aircraft flight envelope.

Using trim and linearization routines developed by Ghazi and Botez in (Ghazi et Botez, 2015b), the aircraft longitudinal and lateral equations of motions have been linearized for different flight conditions in terms of altitudes and speeds, and different aircraft configurations in terms of mass and center of gravity positions. In order to validate the different models obtained by linearization, several comparisons of these models with the linear model obtained by use of identification techniques as proposed in (Hamel, 2013) were performed for different flight conditions and aircraft configurations. Results have shown that the obtained linear models were accurate and could be further used to estimate the local behavior of the Cessna Citation X for any flight conditions.

4.2.3 Aircraft, actuators and sensors dynamics

4.2.3.1 Aircraft dynamics

The Cessna Citation X aircraft's rotation and translation axes are illustrated in Figure 4-2.

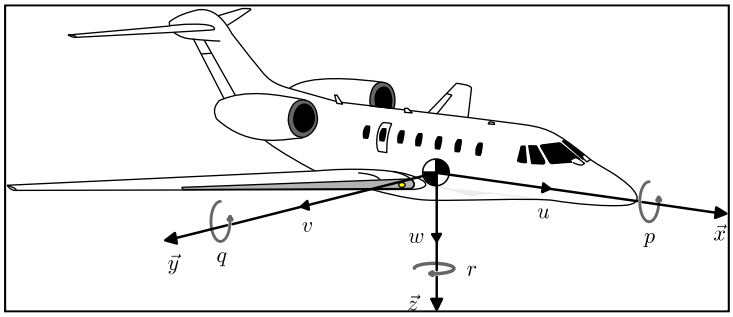

Figure 4-2 Representation of Cessna Citation X aircraft's rotation (body) axes

The motion of an aircraft can be represented with a nonlinear model (Nelson, 1998). To design a controller for any aircraft, a linearization of the nonlinear aircraft model for flight conditions within the flight envelope given by the designer is required as a first step. Following the decoupling of the linearized aircraft motion into longitudinal and lateral motions, and their dynamics are given in the form of the state space matrices as follows:

$$\dot{x} = Ax + Bu \tag{4.1}$$

The aircraft's longitudinal motion dynamics are given by the state space equation, using the elevator as input as follows:

$$\dot{x}_{long} = A_{long}x_{long} + B_{long}u_{long}$$

$$A_{Long} = \begin{pmatrix} X_u & X_w & X_q & -g\cos\theta \\ Z_u & Z_w & Z_q & 0 \\ M_u + M_{\dot{w}}Z_u & M_w + M_{\dot{w}}Z_w & M_q + M_{\dot{w}}u_0 & 0 \\ 0 & 0 & 1 & 0 \end{pmatrix},$$

$$\mathrm{B_{Long}} = \begin{pmatrix} \mathrm{X_{\delta_e}} \\ \mathrm{Z_{\delta_e}} \\ \mathrm{M_{\delta_e} + M_{\dot{w}} Z_{\delta_e}} \\ 0 \end{pmatrix} \quad (4.2)$$

where the state vector $x_{long}(t)$ and control vector $u_{long}(t)$ are given by:

$$x_{long}(t) = (u \quad w \quad q \quad \theta)^T \ , \ u_{long}(t) = \delta_e \quad (4.3)$$

The aircraft's lateral motion dynamics are given by the state space equation, using the aileron and the rudder as inputs:

$$\dot{x}_{lat} = A_{lat}\, x_{lat} + B_{lat} u_{lat}$$

$$A_{Lat} = \begin{pmatrix} Y_\beta/u_0 & Y_p/u_0 & -(1 - Y_r/u_0) & g\cos\theta_0/u_0 \\ L_\beta & L_p & L_r & 0 \\ N_\beta & N_p & N_r & 0 \\ 0 & 1 & 0 & 0 \end{pmatrix}, B_{Lat} = \begin{pmatrix} Y_{\delta_a}/u_0 & Y_{\delta_r}/u_0 \\ L_{\delta_a} & L_{\delta_r} \\ N_{\delta_a} & N_{\delta_r} \\ 0 & 0 \end{pmatrix} \quad (4.4)$$

where the state vector $x_{lat}(t)$ and control vector $u_{lat}(t)$are given by:

$$x_{lat}(t) = (\beta \quad p \quad r \quad \phi)^T, \ u_{lat}(t) = (\delta_a \delta_r)^T \quad (4.5)$$

The Cessna Citation X linear model is obtained for 36 flight conditions based on the Aircraft Flight Research Simulator tests performed at the LARCASE laboratory (Hamel, 2013). The linearized model is interpolated using the bilinear method (Poussot-Vassal et Roos, 2011). These models in turn give 72 flight conditions described in the following section, for 12 weight conditions represented in Figure 4-3.

4.2.3.2 Actuators and sensors dynamics

The actuators dynamics is provided from the literature by Ghazi (2014) and are given as second order transfer functions; their damping and frequencies are mentioned in Table 4-1.

$$\frac{\omega^2}{s^2 + 2\zeta\omega s + \omega^2} \tag{4.6}$$

Table 4-1 Actuators dynamics characteristics

Actuator	Frequency ω [rad/sec]	Damping ζ	Angle[$^\circ$]	Rates[$^\circ$/s]
Elevators	60	0.7	± 20	±30
Rudder	60	0.7	±20	±30
Ailerons	60	0.7	±60	±30

For all the accelerometers and gyroscopes, the sensors dynamics are expressed by second order transfer functions, with their frequencies of 40 rad/sec, and damping of 0.7.

4.3 Flight Conditions Interpolation

Given the data extracted from the Aircraft Flight Research Simulator provided by CAE Inc., the aircraft dynamics are described for all of the flight envelope conditions.

Figure 4-3 shows the 36 points obtained for straight uniform flight level inside the flight envelope limits, which were selected to be trimmed. The aircraft models are obtained at each 5000 ft in the flight envelope and at 4 different speeds.

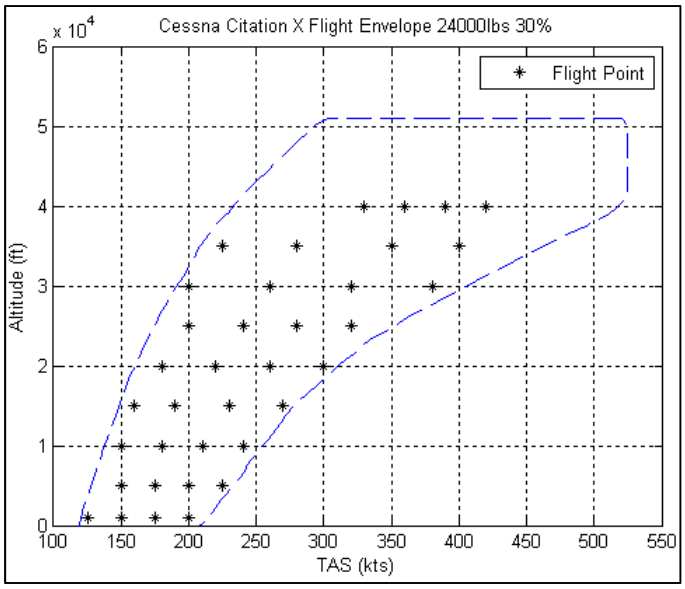

Figure 4-3 Cessna Citation X Aircraft Flight Envelope

Before carrying out the interpolation, two steps must be performed. The first step defines the region for an altitude and a range of TAS where the interpolation will be performed; the four corners of the region forms the vertices. Each of these ranges has a lower and upper value, which are the bounds. The second step is the normalization of these bounds in order to attribute each coordinate of the vertices to a value equal to 1 or -1.

To optimize the accuracy, the smallest possible regions have been defined, containing only 3 or 4 flight points to use as reference points for the interpolation. This definition only allows a bilinear interpolation, for which 4 coefficients must be found, using equations (4.7), (4.8) and (4.9), where Equation (4.7) was used for both longitudinal and lateral matrices A.

$$A_{long/lat}(h, TAS) = A_{0_{4,4}} + A_{1_{4,4}}h + A_{2_{4,4}}TAS + A_{3_{4,4}}TAS \times h \quad (4.7)$$

$$B_{long}(h, TAS) = B_{0_{4,1}} + B_{1_{4,1}}h + B_{2_{4,1}}TAS + B_{3_{4,1}}TAS \times h \quad (4.8)$$

$$B_{lat}(h, TAS) = B_{0_{4,2}} + B_{1_{4,2}}h + B_{2_{4,2}}TAS + B_{3_{4,2}}TAS \times h \quad (4.9)$$

The Least Square (LS) method is employed to minimize the relative error in these reference points. The maximum errors found for the state space matrices A and B are negligible, and has a value of $3.97\ 10^{-11}\%$, therefore the results are good.

From these results, 26 regions are obtained, which covers a large part of the flight envelope. The mesh is valid for all of the weight and balance conditions presented in Figure 4-5. It can be observed from Figure 4-4 that some of the regions superimpose others (darker zones) due to the common reference points, and in many cases there is not only interpolation but also extrapolation.

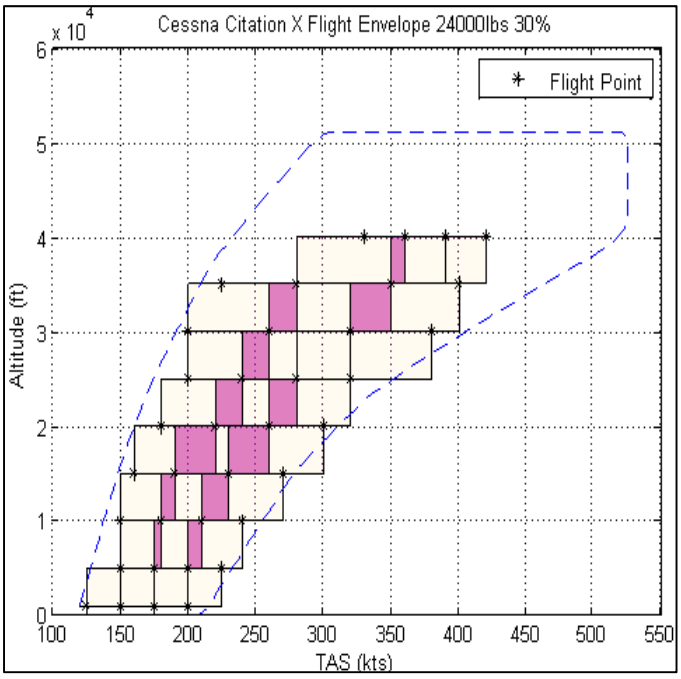

Figure 4-4 Region definition

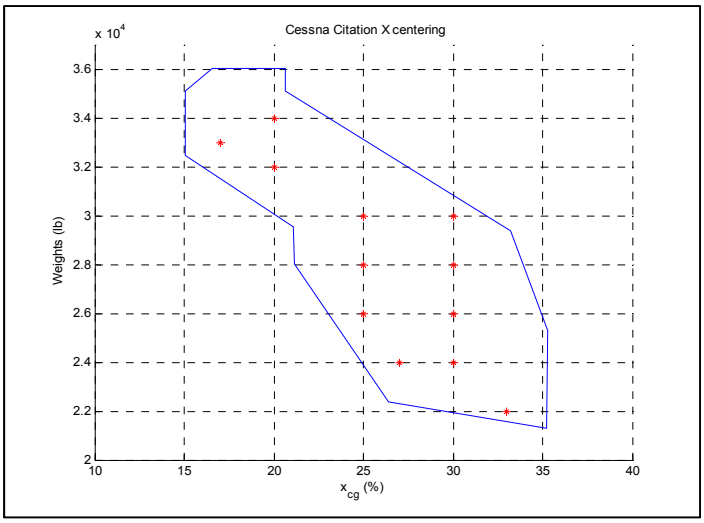

Figure 4-5 Cessna Citation X Weight/ X_{CG} conditions

These regions are presented by LFR models, where the center of each region is used to calculate a controller that can be applied on the 4 vertices of the region, which lead to an optimization of the number of controller used to control the aircraft in its flight envelope, and to ensure a relatively certain robustness against the altitude (h) and the airspeed (TAS) variations.

All vertices of these 26 regions lead to 72 different flight points to be analyzed shown by Figure 4-6, which make it possible to more closely approximate the flight envelope limits.

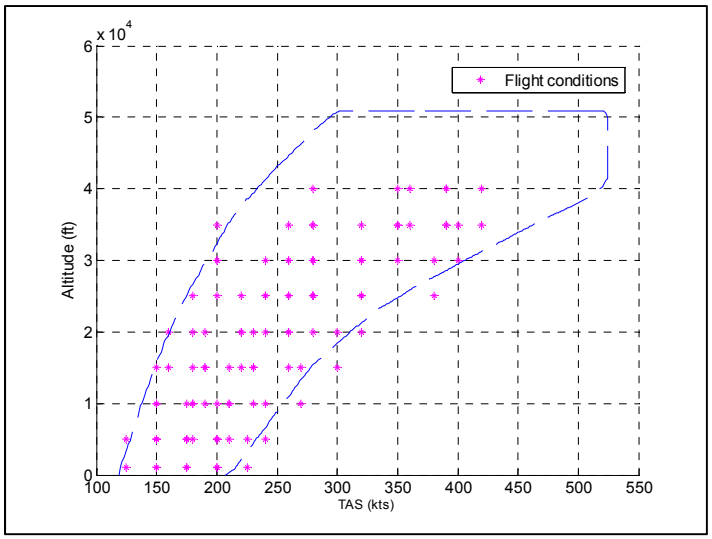

Figure 4-6 Flight points obtained by LFR models

4.4 Design Specifications and Requirements

The aircraft Flight Control System required airworthiness and handling qualities requirements that should be considered in the Flight Control Law design. These criteria are intended for satisfactory flight performance, and safety. In this research some of the flying qualities and time response specifications have been considered in the optimization problem for the flight controller design, Table 4-2 presents the desired flying qualities, and temporal criteria expressed in terms of damping (Nelson, 1978), overshoot, steady state error, time constant, and settling time required for the longitudinal and lateral modes; the criteria were provided in the U.S « Military specification for the Flying Qualities of Piloted Airplanes MIL-STD-1797A».

Table 4-2 Aircraft flying qualities and temporal criteria

Criteria	Type	Limits
Overshoot	Temporal	OS<30%
Steady state error	Temporal	ess≤2%
Settling time	Temporal	Ts≤4s
Short period damping	Modal	$0.3 \leq \zeta_{sp} \leq 2$
Phugoid damping	Modal	$0.04 \leq \zeta_{ph}$
Dutch roll damping	Modal	$0.3 \leq \zeta_{dr} \leq 2$
Roll time constant	Temporal	Tr<1.4 sec

4.5 Differential Evolution

The Differential Evolution (DE) algorithm was developed in 1995 by Price and Storn (Price, 1996; Storn et Price, 1996), and has been used in global optimization in many domains. The DE algorithm is a meta-heuristic optimization algorithm that uses real values (which do not need any encoding and decoding operations) to represent problem parameters. The key concept of DE is its use of a differential operator to generate the mutant vector which allows population diversity. Flow charts given in Figure 4-7 summarize the DE algorithm used to search for the optimal LQR and PI gains.

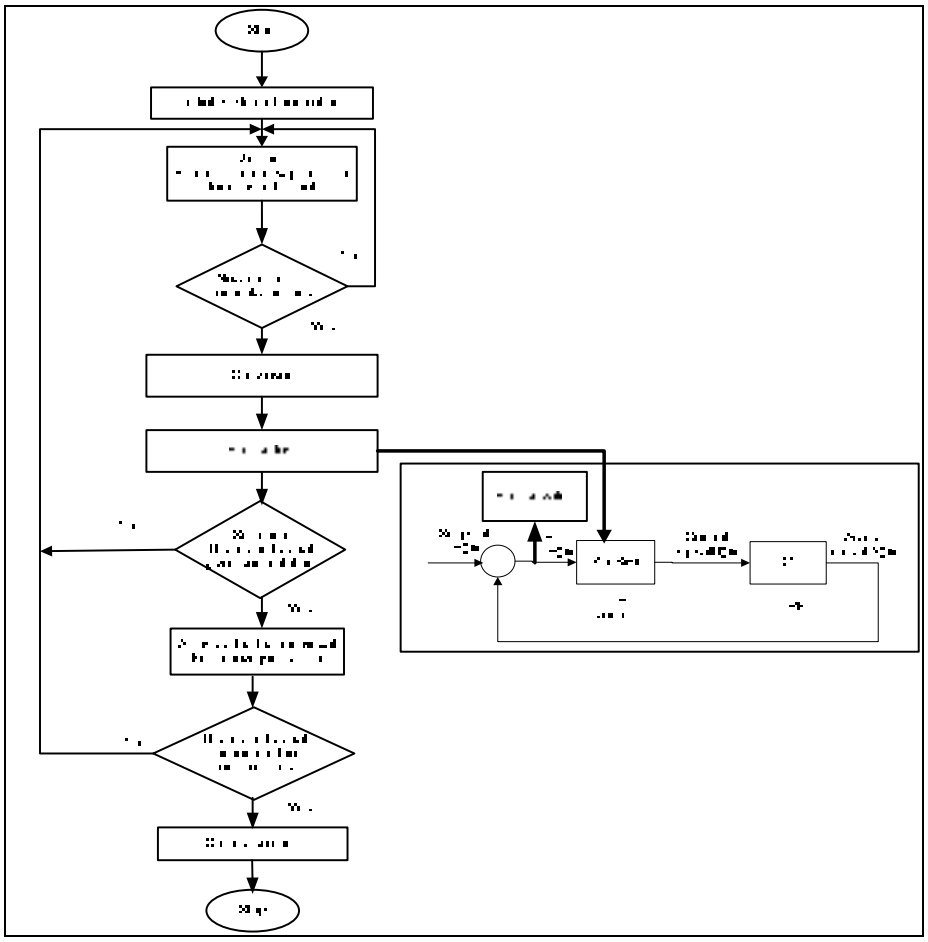

Figure 4-7 LQR weighting matrices and PI tuning optimization using DE algorithm

4.5.1 Initialisation phase

In this phase, the number iterations or generations is fixed, the dimension of the problem is then determined according to the fitness function parameters number. Next, a vector is formed by the parameters to be optimized; at each generation, the i^{th} vector is described as**:**

$$\vec{X}_{iG} = [x_{1,iG}, x_{2,iG}, x_{3,iG}, \ldots\ldots, x_{D,iG}] \tag{4.10}$$

The population is initialized at random in its search space, where each parameter is limited by a lower and upper value. These boundaries are represented in vectors given by equations (4.10) and (4.11):

$$\vec{X}_{imin} = \left[x_{1,imin}, x_{2,imin}, x_{3,imin}, \ldots\ldots, x_{D,imin}\right] \tag{4.11}$$

$$\vec{X}_{imax} = \left[x_{1,imax}, x_{2,imax}, x_{3,imax}, \ldots\ldots, x_{D,imax}\right] \tag{4.12}$$

The j^{th} component of the i^{th} vector is initialized as:

$$x_{j,i,0} = x_{j,min} + rand_{i,j}[0,1].\left(x_{j,max} - x_{j,min}\right) \tag{4.13}$$

where $0 \leq rand_{i,j}[0,1] \leq 1.$

Once the initialization phase is completed, the next step is the mutation operation

4.5.2 Mutation

In DE algorithm, the "Mutation" is when different vectors change their parameters between them. So the "donor vector" is obtained from the differential mutation operation. Each "donor" vector is created from its corresponding i^{th} "target" vector. In the current population a sampling of three different parameter vectors $\vec{X}_{r_1^i,G}$, $\vec{X}_{r_2^i,G}$, $\vec{X}_{r_3^i,G}$ at random is performed in the current population; each i^{th} "target" vector is used to create its corresponding "donor" vector. For each "mutant" vector $\vec{X}_{r_i^i,G}$, three different indices $r_1^i, r_2^i,$ and $r_3^i,$ are from the range$[1, NP]$at random, where *NP* is the population number. Then the difference between two different vectors is weighted by a scalar F selected at random to finally obtain the "donor" vector V_{iG}, as defined in equation (4.13):

$$V_{IG} = \vec{X}_{r_1^i,G} + F * \left(\vec{X}_{r_2^i,G} - \vec{X}_{r_3^i G}\right) \tag{4.14}$$

4.5.3 Crossover

In the operation of the "crossover", a "trial" vector $\vec{U}_{IG}$ results from the operation of exchanging components between the "donor" and the "target" vectors, which improve the population diversity:

$$\vec{U}_{IG} = \left[u_{1,iG}, u_{2,iG}, u_{3,iG}, \dots, u_{D,iG}\right] \tag{4.15}$$

There exist two crossovers: the exponential and the binomial.

Two integers n and L are chosen arbitrarily in the exponential crossover from the interval $[1, D]$, where D represents the dimension, which is the number of parameters subject to optimization, and then the trial vector is given as follows:

$$u_{j,iG} = v_{j,iG} \quad \text{for} \quad j = \langle n \rangle_D, \langle n+1 \rangle_D, \dots., \langle n+L-1 \rangle_D \tag{4.16}$$

$$\textit{Else} \quad u_{j,iG} = x_{j,iG} \quad \text{and} \quad j \in [1, D] \tag{4.17}$$

where $\langle . \rangle$ refers to the modulo function with modulus D. While in the binomial crossover the trial vector is given as:

$$u_{j,iG} = v_{j,iG} \tag{4.18}$$

$$\text{if} \quad rand_{i,j}[0,1] \leq \text{Cr} \ \text{ or } \ j = j_{rand} \tag{4.19}$$

$$\textit{Else} \quad u_{j,iG} = x_{j,iG}$$

After the population diversity has been assured with the crossover step, a selection operation is performed as detailed in the next phase.

4.5.4 Selection

The operation of "selection" determined if the "target" or "trial" vectors survive in the next generation or not, and thus maintain a constant population size. The "selection" operation is outlined as:

$$\vec{X}_{i,G+1} = \vec{U}_{i,G} \quad \text{if} \quad f(\vec{U}_{i,G}) \leq f(\vec{X}_{i,G}) \tag{4.20}$$

$$\text{Else} \qquad \vec{X}_{i,G+1} = \vec{X}_{i,G} \tag{4.21}$$

Where $f(\vec{X}_{i,G})$ is the objective function or the "fitness" to be converged using an iteration process.

4.5.5 Iteration

The operations (Initialization, mutation, crossover and selection) listed above are repeated until the termination criteria have been met. These criteria are related to the maximum number of generations and to the convergence of fitness functions.

4.6 Linear Quadratic Regulation (LQR) Method

The LQR control algorithm is one of many optimal controls methods described in (Dorato, c1995),(P.Albertos, 2004) and used in an optimal way to stabilize the controlled system in(Lee et al., 2011),(Turoczi, 2009).The LQR used as a control method in this context zimplies that a cost function must be determined in order to balance between the actuators' effort and the aircraft's responses.

The weighting matrices Q and R need to be selected. Q represents the weighted state space matrix, R represents the weighted control inputs' matrix, $x(t)$ and $u(t)$ denote the state space and input matrices of the aircraft. These matrices are selected to minimize the cost function J given by the following equation:

$$J = \frac{1}{2}\int_0^{\infty}[x^T(t)Qx(t) + u^T(t)Ru(t)] \tag{4.22}$$

The Q matrix is of $m \times m$ and the R matrix is of $n \times n$ dimensions, as follows:

$$Q = \begin{bmatrix} q_{11} & \cdots & q_{1m} \\ \vdots & \ddots & \vdots \\ q_{m1} & \cdots & q_{mm} \end{bmatrix}, R = \begin{bmatrix} r_{11} & \cdots & r_{1n} \\ \vdots & \ddots & \vdots \\ r_{n1} & \cdots & r_{nn} \end{bmatrix}$$

These Q and R matrices are used to determine the matrix P which is positive semi-definite by use of the Ricatti equation (Dorato, c1995):

$$PA + A^TP - PBR^{-1}B^TP + Q = 0 \tag{4.23}$$

From equation (4.23) the gain vector K is then found by using the next Equation (4.24):

$$K = R^{-1}B^TP \tag{4.24}$$

The control vector is then determined as follows:

$$u = -K(Q, R)x(t) \tag{4.25}$$

4.7 Tracking Control with PI Optimization

The aircraft dynamics' stability augmentation system (SAS) uses the LQR method to attenuate the undesired effects mainly on its longitudinal (phugoid) and lateral Dutch Roll modes in the presence of possible perturbations. Next, to follow the reference signals the PI gains are used in the control augmentation system (CAS).

Where k_p indicates proportional gain, and as k_i indicates the integral gain. The use of PI gains reduces the overshoot and eliminates the steady state error in order to improve the

system response. Using the experimentation process to find the optimal values for these two gains can be quite time-consuming for a full flight envelope.

Trial and error process and other types of methods for tuning PID gains using meta-heuristic algorithms are available, such as the genetic algorithm GA (Neath et al., 2013; Tan et al., 2011a), the swarm particle optimization PSO (Kanojiya et Meshram, 2012; Rahimian et Raahemifar, 2011), the Fruit Fly optimization algorithm (Jiuqi, Peng et Xin, 2012).

Nonlinear methods such as fuzzy logic and neural network methods have also been applied to identification and control (G. Kouba, 2009), and (N. Boëly, 2009), hybrid fuzzy logic (Grigorie et al., 2012a), (Grigorie et al., 2012d) real time optimization used on a morphing wing by (Popov et al., 2010). Other parameter estimation and control methodologies were used and validated during flight tests (Mario, 1999), (Frost, Taylor et Bodson, 2012; Perhinschi et al., 2005).

All of these methods were developed with the aim of reducing the computation time while achieving satisfactory results. For this work, the DE algorithm was selected to tune the PI controller parameters, applied on a business aircraft.

4.8 DE Algorithm for Solving the LQR-PI Problem

The optimal controller is found using the following algorithm given by the flow charts in Figure 4-7 mentioned in Section 4.3:

Set the population number *NP*; formed by the parameters of the weighting matrices *Q* and *R* (only the diagonal parameters are considered), and the PI proportional integral gains, $\mathrm{k_i}, \mathrm{k_p}$; from the initial vector:

$$\vec{X}_{IG} = \left[q_{1,iG}, q_{2,iG}, q_{3,iG}, \dots, q_{m,iG}, r_{1,iG,\dots}, r_{n,iG}, k_i, k_p\right] \tag{4.26}$$

Each of these parameters belongs to an interval with lower and upper bounds. The optimal controller is found first by choosing the appropriate Q, R, $, k_i, k_p$ parameters and then performed a system time domain simulation to obtain the characteristics of a system's response. The iteration process continues if the satisfactory characteristics are not reached, until one of the stopping conditions is achieved.

4.8.1 Objective function

One objective function was used for both LQR and PI algorithms to give the desired time response specifications of the closed loop system, and to be minimized in order to obtain the optimal solution. The settling time T_s , the natural frequency ω_n , the damping ζ, the overshoot OS and the Integral Square Error (ISE) are shown in the next equation giving the expression of fitness:

$$fitness = 10 * (ISE) + 10 * (OS) + 10 * (Ts) + 10(\omega_n) + 10 * (\xi) \quad (4.27)$$

The optimized controller is not offering only an infinite gain margin, but also a good phase margin; both of them were given for some controls over than 60 deg. that can be shown by the results given below in the following sections.

4.9 Simulation Results Analysis

Simulations were performed firstly on the linearized model (longitudinal and lateral) of Cessna Citation X business aircraft, for which its flight dynamics model is represented using state space matrices for multiple flight conditions. Then, the Stability Augmentation System (SAS) is established using the LQR design approach, and is applied on the aircraft to enhance its response.

Furthermore, the tracking reference signal is ensured by using the PI controller as Control Augmentation System (CAS). This process was automated using a Graphical User Interface

as shown in Figure 4-8, which facilitate to the design engineer the manipulation of some parameters such as the design requirements (flying qualities, time response specifications), the parameter to be controlled (pitch rate *q,* pitch angle *theta,* and roll rate *p*), and to visualize the responses for the entire flight envelope.

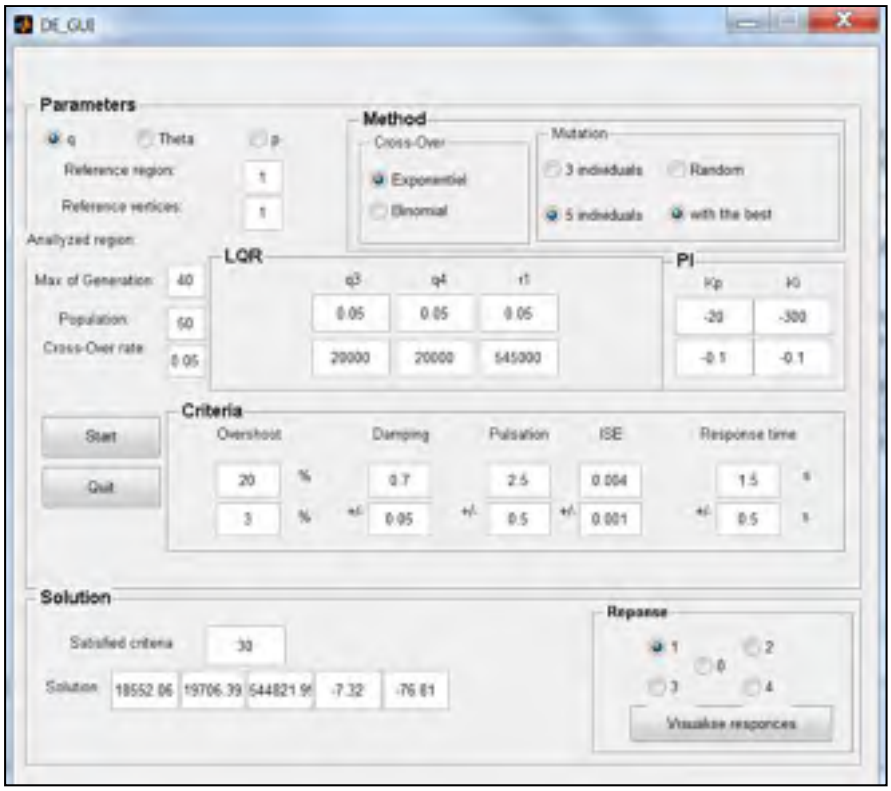

Figure 4-8 GUI used in the controller design and optimization

The validation of results was performed using the nonlinear aircraft model. The nonlinear model, the Cessna Citation X was formed by the aircraft's, actuators', and sensors' dynamics. The dynamics of the aircraft, actuators and sensors are given in the Section "Actuators and sensors dynamics". To control the augmented system, two internal loops were added: the first internal loop represented by the SAS, and the CAS formed the second internal loop; the autopilot dynamics was modeled in the external loop.

First, the LQR weighting matrices were optimized for 36 flight conditions extracted from the Cessna Citation X Flight Simulator as given in (Yamina Boughari, 2014) and then further

generalized for 72 flight conditions obtained using the interpolation method, than a second optimization is performed for tuning the PI controller. Both the PI and the LQR parameters were optimized by using the differential evolution described in Section 4.5.

After the obtaining of optimal weighting matrices, the SAS and the CAS were computed for each flight condition, and aircraft configuration. The results obtained by the algorithm were given under the form of a set of gains for each inner loop (pitch angle control loop, pitch rate control loop, etc.).

These gains were next exported into the Matlab's curve Fitting Toolbox in order to compute an interpolation model. Figure 4-9 shows an example of interpolation of the feedback gains K_q and K_w with respect to the altitude h and airspeed V_{TAS} for the 4th X_{CG} location 30%. In Figure 4-9, the data points represent the results obtained with the algorithm, and the surface represents the interpolated model for K_q (Figure 4-9.a) and for K_w (Figure 4-9.b).

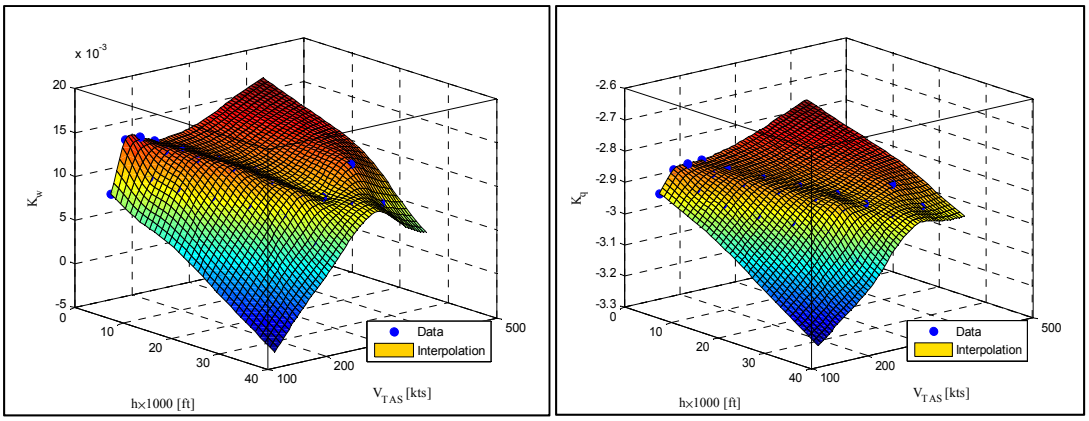

(9.a) (9.b)

Figure 4-9 Gains scheduling with respect to the altitude and airspeed

This process was repeated for all the gains for each loop and for each aircraft mass and center of gravity position.

The results were next formatted into different 4-D Lookup Tables in order to allow the linear interpolation for any altitude, airspeed, mass and center of gravity position. The next section presents the results obtained for each loop.

4.9.1 Results validation

4.9.1.1 Linear validation

Simulations of both aircraft motions were performed for all CG locations and flight conditions given above in Figures 4-4 and 4-5. The controlled system was then simulated in the time domain to reach the satisfactory dynamic characteristics of the aircraft. The results were given for each region, delimited by four vertices which lead to 72 fight conditions as explained in Section 4.3, and for each centering, as shown in Figures 4-10,4-13 , 4-16, and 4-19.

Pole-zero map responses were obtained for pitch angle, pitch rate, roll rate and roll angle as shown in Figures 4-11, 4-14, 4-17, and 4-20, where handling quality requirements parameters were superimposed over results.

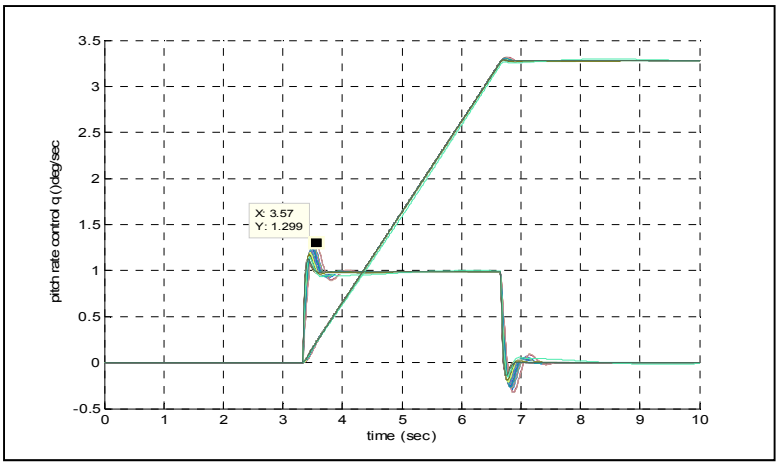

Figure 4-10 Pitch rate q (deg/sec) control and
the resulting pitch angle θ (deg)

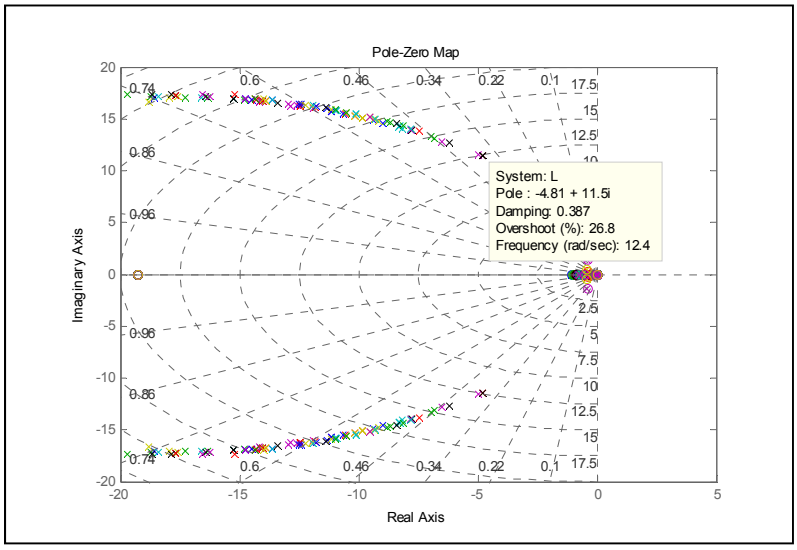

Figure 4-11 Pole zero map for pitch rate control *q*(deg/sec)

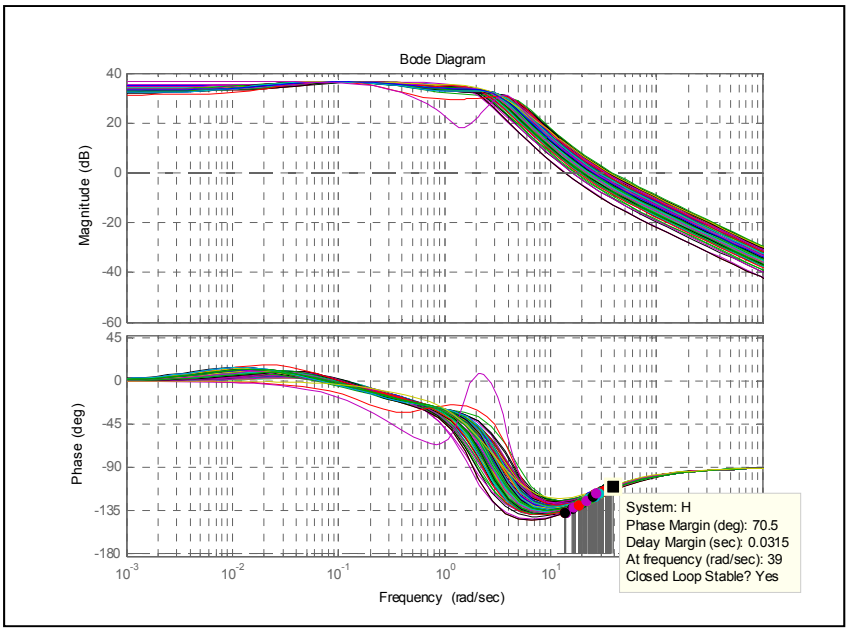

Figure 4-12 Bode diagram for pitch rate q (deg/sec) control

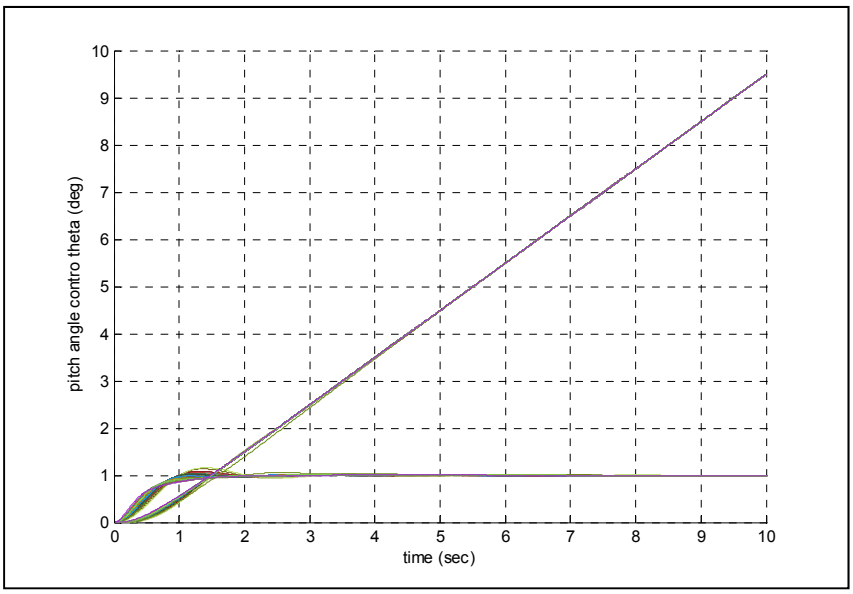

Figure 4-13 PI Tracking reference for pitch angle θ(deg)

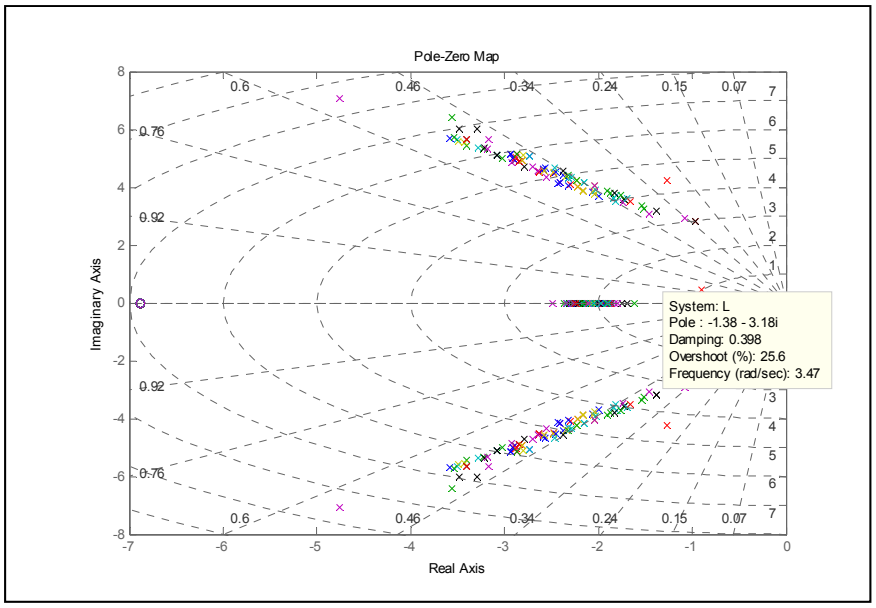

Figure 4-14 Pole zero map for pitch angle θ (deg) control

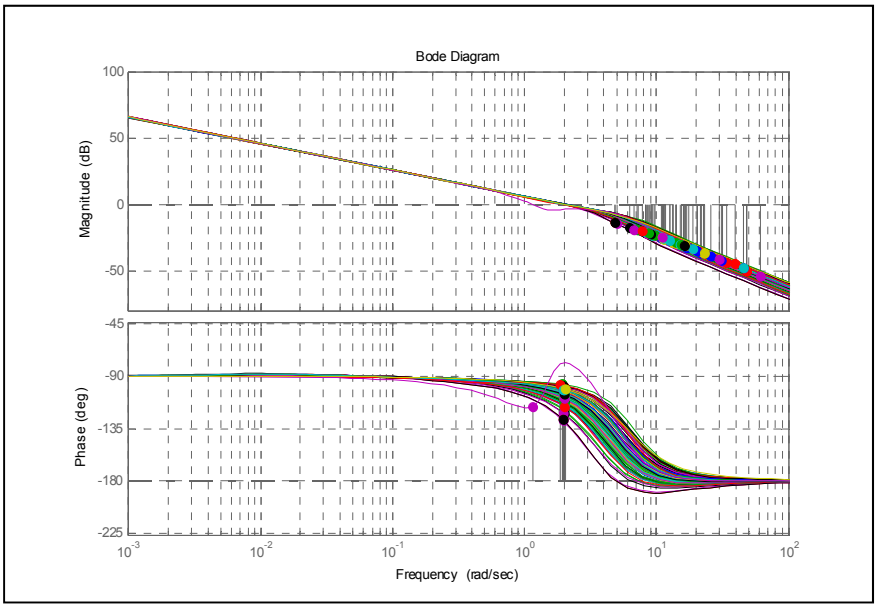

Figure 4-15 Bode diagram for pitch angle θ (deg) control

Previous research was done in (Yamina Boughari, 2014), where the LQR and PI control were achieved for 36 flight conditions and 12 centre of gravity locations and showing good stability and command tracking of the aircraft. Also the system successfully tracks the reference signals when the control is generalized for 72 flight conditions for all aircraft

motions (Figure 4-10, Figure 4-13, Figure 4-16 and Figure 4-20). Bode diagram is plotted for each control to assess its stability margins in Figures 4-12, 4-15, 4-18, and 4-21, which confirms what was said previously in Section 4.3 that the resulting controller gives an infinite gain margin and secure phase margin.

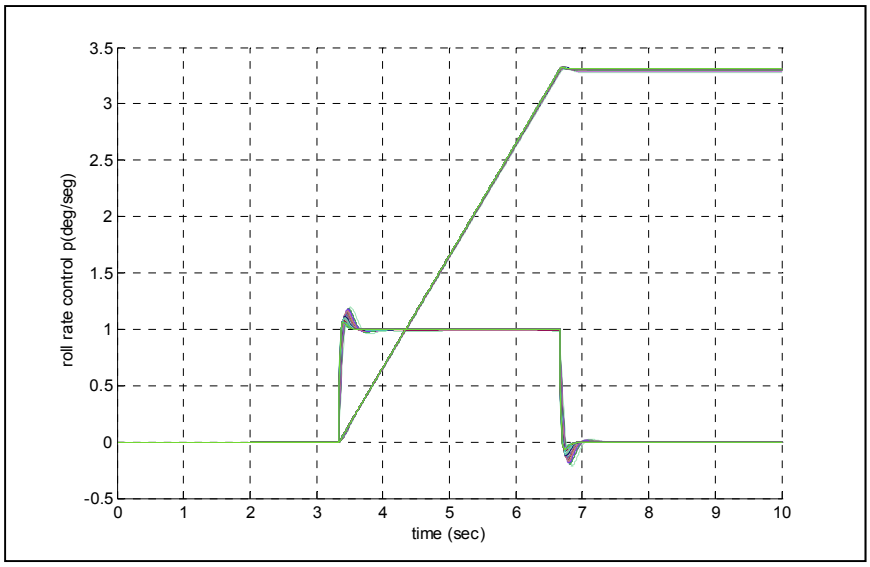

Figure 4-16 Tracking references for roll rate *p* (deg/sec)

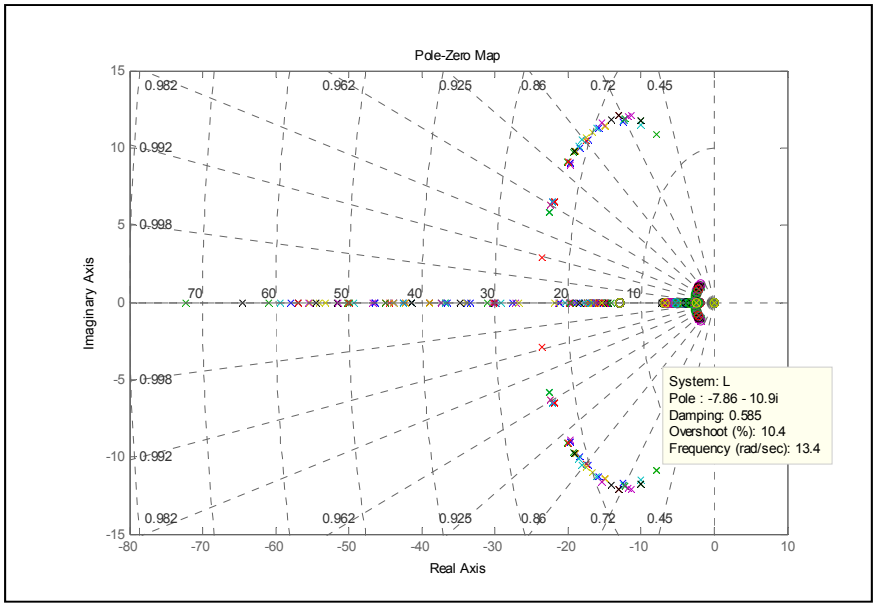

Figure 4-17 Pole zero map for roll rate *p* (deg/sec)

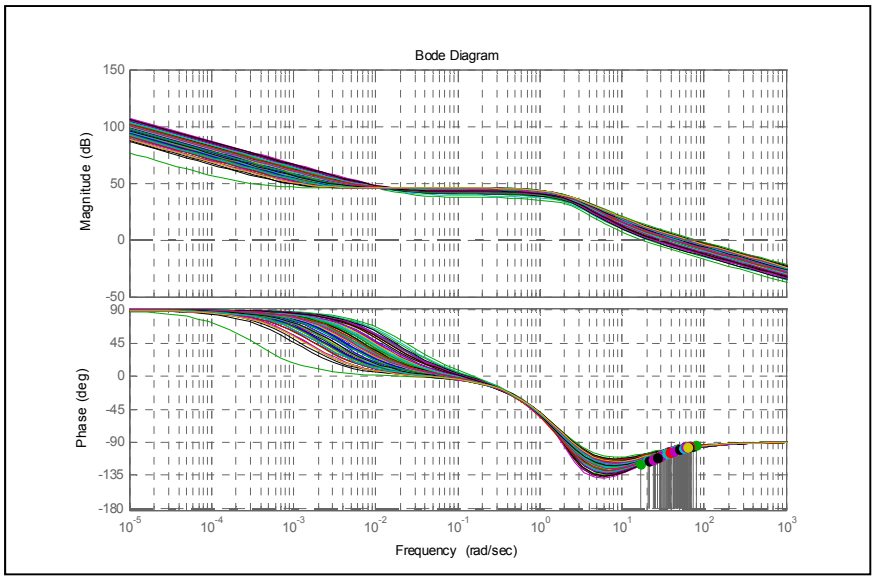

Figure 4-18 Bode diagram for roll rate p (deg/sec)

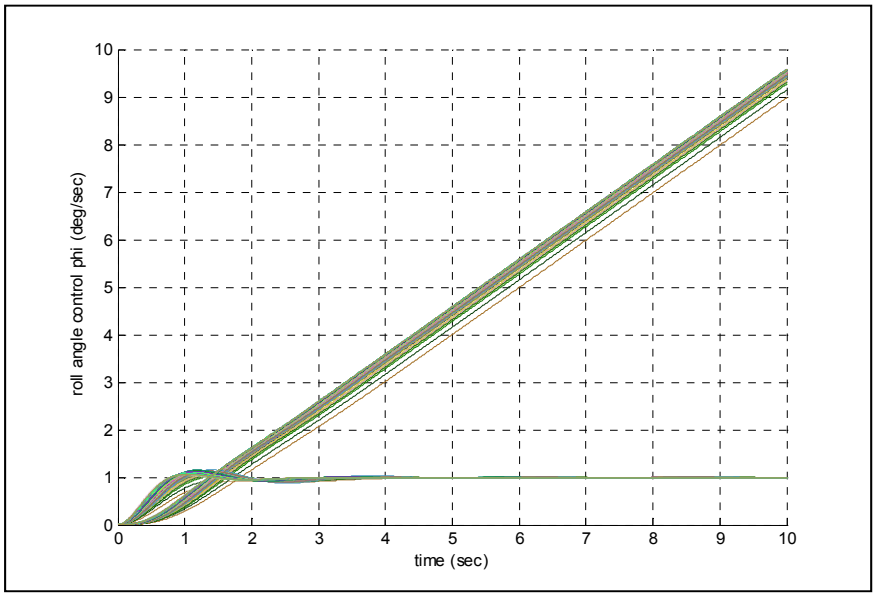

Figure 4-19 Roll angle ϕ (deg) control and the resulting roll rate p(deg/sec)

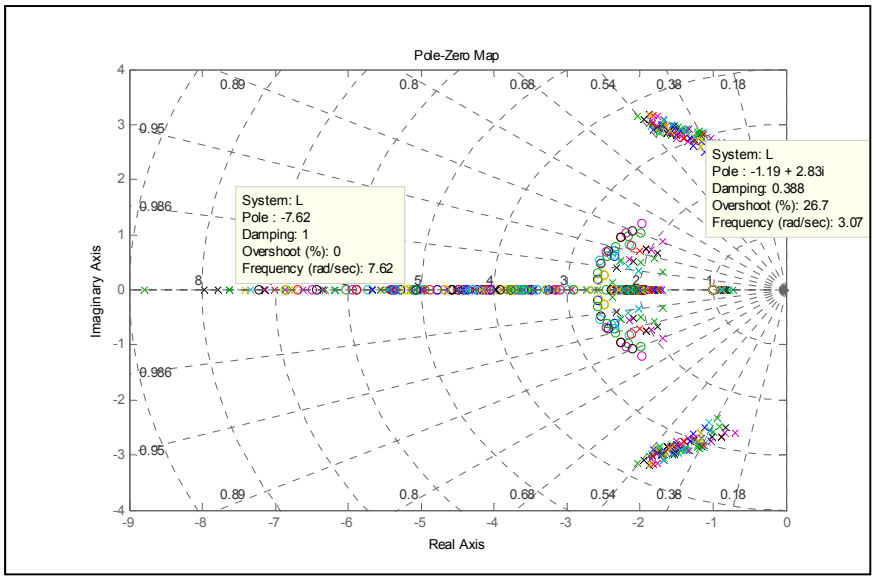

Figure 4-20 Pole Zero map of roll angle ϕ (deg)

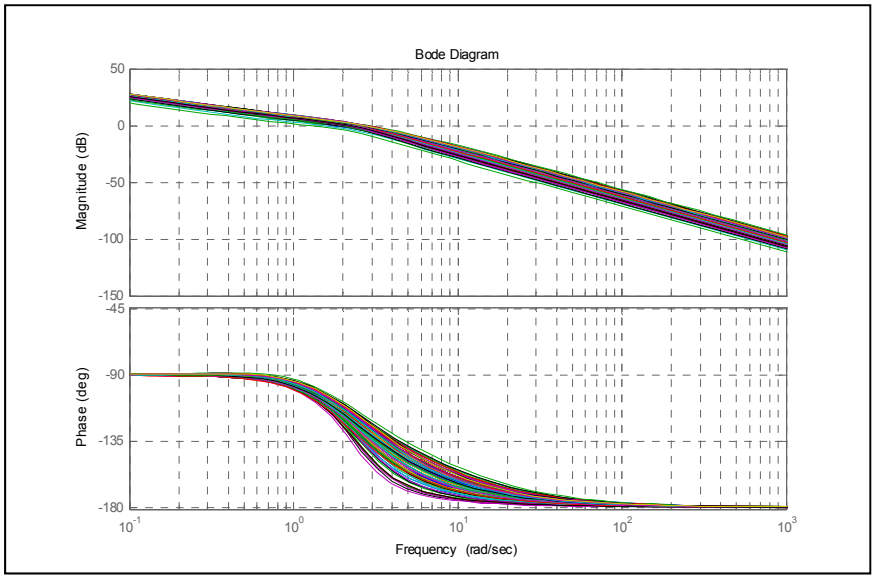

Figure 4-21 Bode diagram of roll angle ϕ (deg)

These results have been validated using a linear model for all of the flight conditions. The steady state error is less than 2% for pitch rate q, pitch angle θ, and both roll rate p and roll angle φ, while the overshoot is less than 30% for all responses, and the settling time *Ts* is less than 2 sec; therefore , the system is stable and behaves as desired, and all the

performance criteria are reached. Generally, the optimal controllers with LQR-PI gains are more suitable for their stability performance and simplicity of integration in the FCL design.

4.9.1.2 Nonlinear validation

Simulations were performed for more than 500 flight points at different mass and centering conditions on the nonlinear model of the Cessna citation X aircraft. The results are shown in Figures 4-22, 4-23, 4-24, and 4-25 for pitch angle, pitch rate, roll angle and roll rate controls; all of these responses track the command given as input. The nonlinear simulations demonstrate the efficiency and the reliability of the optimal controllers.

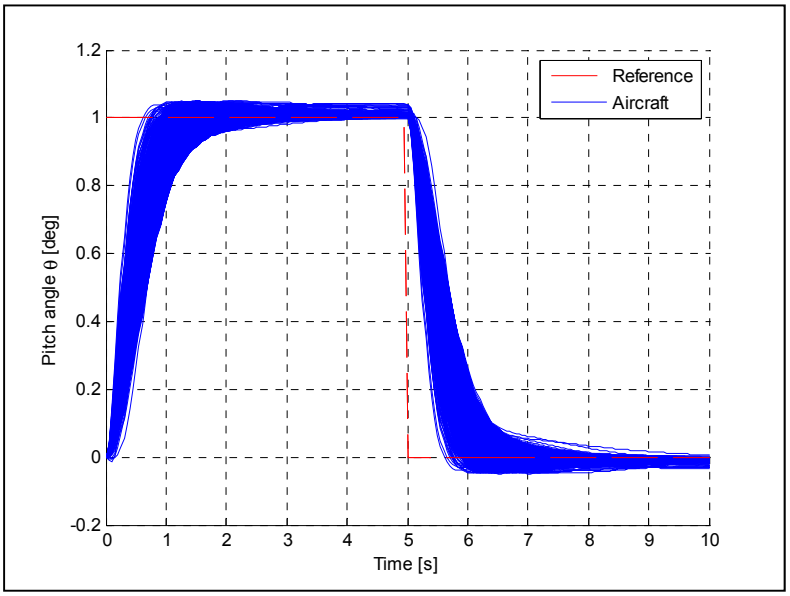

Figure 4-22 Pitch angle θ(deg) control of the nonlinear aircraft model

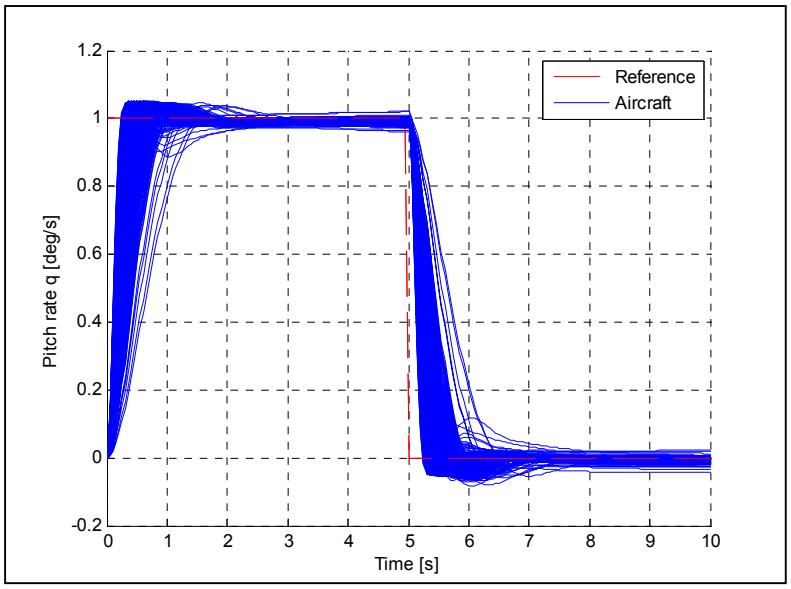

Figure 4-23 Pitch rate q(deg/sec) control of
the nonlinear aircraft model

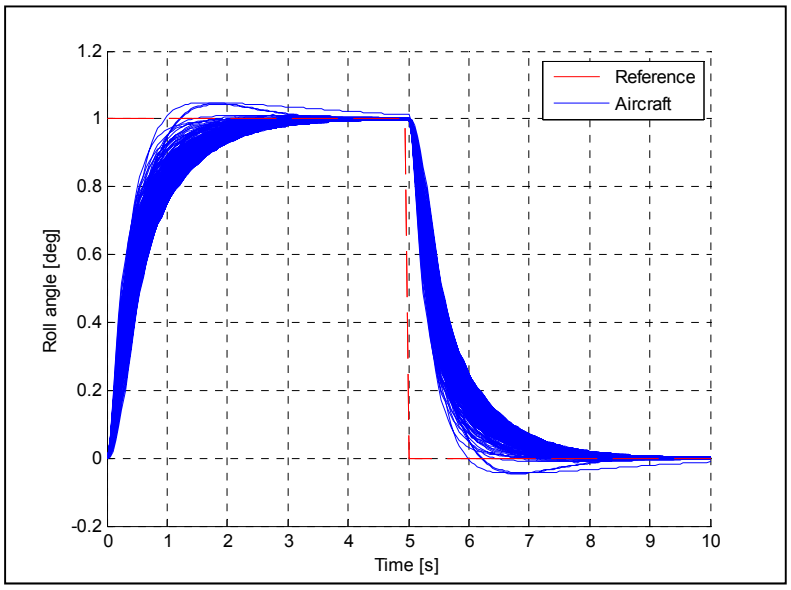

Figure 4-24 Roll angle φ(deg) control of
the nonlinear aircraft model

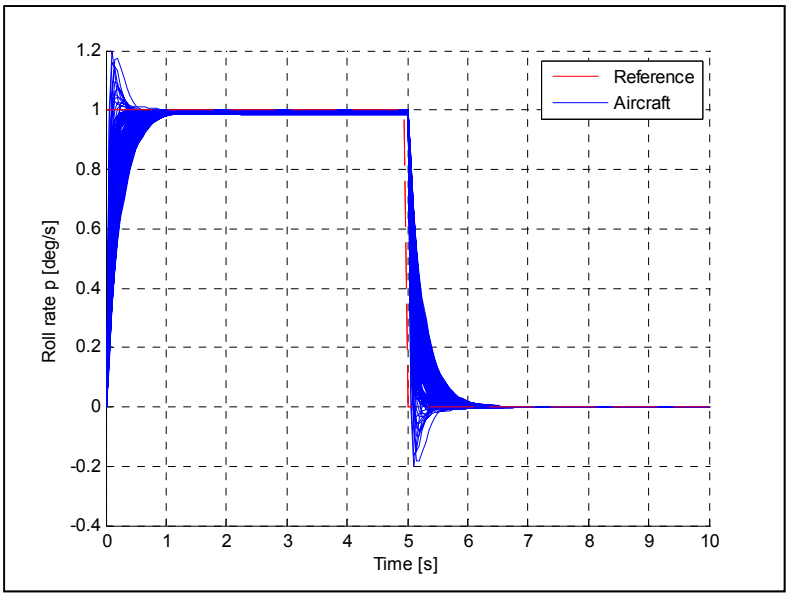

Figure 4-25 Roll rate *p* (deg/sec) control of the nonlinear aircraft model

4.10 Conclusion

Before the first flight and the aircraft certification, an airplane must pass a multitude of tests. Some of these tests involve the aircraft control laws, which assess whether an aircraft is able to fly safely in a variety of conditions.

In this research, some of the FCL design requirements were considered in the FCL optimization problem, these requirements were based on a selected set of flying quality criteria, and a desired temporal ones chosen from the designer experience usually used in aircraft control design in the Aeronautical Industry.

In this research, a multi-objectives optimization was presented. First the SAS design was optimized by combining the Differential Evolution algorithm (DE) with the LQR method, secondly the DE was used to tune the PI gains for the CAS design in one objective function.

The optimized controllers were then validated on 72 flight conditions of the linear model over 12 X_{CG},and weight configurations selected to cover the entire envelope, and with the aircraft nonlinear model. Furthermore the aircraft's closed loop performances were improved according to the flying qualities and temporal dynamic response specifications given in Table 4-2. The DE algorithm shows a minimum time computing, and demonstrates a high efficiency and reliability in global optimization with minimum time convergence.

The optimized controller parameters were used in the validation of the linear aircraft models in its entire envelope. Furthermore, the controller number was also optimized by using the LFR features, were the controller is calculated for the center of each region represented by LFR model and applied on the 4 vertices of the region, which means that the 72 flight points are controlled by 26 controllers which correspond to the number of flight envelope regions.
Due to the complexity of the FCL design and its iterative nature a Graphical User Interface was developed to carry on the optimization, and the clearance of the FCL in the entire envelope. This computing tool offered the flexibility to change the design requirements if needed before a new optimization.

Using more Complex handling quality and airworthiness requirements in the optimization problem could be a subject of future research.

Acknowledgements

This research was carried out at the LARCASE (Laboratory of active controls, avionics and aeroservoelasticity research). We express our gratitude to the CAE Inc. team, and especially to Mr Ken Dustin for their support in the development of the Aircraft Research Flight Simulator at the LARCASE laboratory. Also thanks are due to the research grants approved by the Canadian Foundation of Innovation (CFI) and MDEIE. We also wish to thank to Mrs Odette Lacasse, and to Mr Oscar Carranza at ETS for their support related to the flight simulator research and development.

CHAPITRE 5

FLIGHT CONTROL CLEARANCE OF CESSNA CITATION X USING EVOLUTIONARY ALGORITHMS

Yamina Boughari, Ruxandra Mihaela Botez, Georges Ghazi, Florian Theel

LARCASE Laboratory of Applied Research in Active Controls, Avionics and AeroServoElasticity
ETS, 1100 Notre Dame West, Montreal, Que., Canada, H3C-1K3

This article was published in *The Proceedings of the Insitute of Mechanical Engineers, Part G: Journal of the Aerospace Engineering,* in April 2016, doi: 10.1177/0954410016640821.

Résumé

Dans cet article, un simulateur de vol de recherche d'aéronef équipé avec une dynamique de vol de niveau D (le plus haut niveau) a été utilisé pour recueillir des données d'essais en vol et de développer de nouvelles méthodologies de contrôle. Les changements dans la masse et dans la position du centre de gravité de l'avion sont affectées par la consommation de carburant, ce qui résulte dans des incertitudes dans la dynamique de l'avion.

Un contrôleur robuste a été conçu et optimisé à l'aide de la méthode *H-infini* et deux différents algorithmes méta-heuristiques; afin d'assurer des qualités de vol acceptables dans l'enveloppe de vol spécifiée malgré la présence des incertitudes. Les fonctions de pondération *H-infini* ont été optimisées en utilisant à la fois l'algorithme génétique (GA), et l'algorithme de l'évolution différentielle DE. L'algorithme DE a révélé une grande efficacité et a donné des excellents résultats en un minimum de temps par rapport à l'algorithme génétique. De bonnes caractéristiques dynamiques des systèmes d'augmentation de contrôle et de stabilité longitudinale et latérale avec un bon niveau de qualités de vol ont été atteintes.

Le contrôleur optimal a été utilisé sur le modèle linéaire de l'avion Cessna Citation X pour plusieurs conditions de vol en couvrant toute son enveloppe de vol. La nouveauté de la

nouvelle fonction objective utilisée dans cette recherche est qu'elle combine à la fois le critère de performance dans le domaine temporel et le critère de robustesse dans le domaine fréquentiel, ce qui a conduit à l'obtention des bonnes qualités de vol de niveau 1 de l'avion. L'utilisation de cette nouvelle fonction objective permet de réduire considérablement le temps de calcul des deux algorithmes et d'éviter l'utilisation d'autres méthodes de calcul plus complexes. La même fonction objective a été utilisée dans les deux algorithmes évolutionnaires (DE et GA), puis leurs résultats concernant la validation du modèle linéaire dans des points de vol ont été comparés.

Enfin, l'analyse de la robustesse a été réalisée sur le modèle non linéaire, en faisant varier la masse et la position du centre de gravité. De nouveaux outils ont été développés pour valider les résultats obtenus pour les deux modèles d'avion linéaires et non linéaires. On a conclu que de très bonnes performances de l'avion d'affaire Cessna Citation X ont été obtenues dans cette recherche.

Abstract

In this paper, an Aircraft Research Flight Simulator equipped with Flight Dynamics Level D (highest level) was used to collect flight test data and develop new controller methodologies. The changes in the aircraft's mass and center of gravity position are affected by the fuel burn, leading to uncertainties in the aircraft dynamics.

A robust controller was designed and optimized using the *H-infinity* method and two different metaheuristic algorithms; in order to ensure acceptable flying qualities within the specified flight envelope despite the presence of uncertainties. The *H-infinity* weighting functions were optimised by using both: the Genetic Algorithm (GA), and the Differential Evolution algorithm DE. The DE algorithm revealed high efficiency and gave excellent results in a short time with respect to the GA. Good dynamic characteristics for the longitudinal and lateral stability control augmentation systems with a good level of flying qualities were achieved.

The optimal controller was used on the Cessna Citation X aircraft linear model for several flight conditions that covered the whole aircraft's flight envelope. The novelty of the new objective function used in this research is that it combined both time-domain performance criteria and frequency-domain robustness criterion, which led to good level aircraft flying qualities specifications.

The use of this new objective function helps to reduce considerably the calculation time of both algorithms, and avoided the use of other computationally more complicated methods. The same fitness function was used in both evolutionary algorithms (DE and GA), then their results for the validation of the linear model in the flight points were compared. Finally, robustness analysis was performed to the non-linear model by varying mass and gravity center position. New tools were developed to validate the results obtained for both linear and nonlinear aircraft models. It was concluded that very good performance of the business Cessna Citation X aircraft was achieved in this research.

5.1 Introduction

The aircraft's safety relays importantly on its controller, the clearance authorities need to ensure that the controller operates properly through the specified flight envelope even in presence of uncertainties such as mass, center of gravity positions, and inertia variations. The control clearance process is a fastidious and expensive task, especially for modern aircrafts that need to achieve high performance (C. Fielding, 2002) .This process aims to prove that the selected stability, robustness and handling requirements are satisfied against any possible uncertainty.

During the industrial clearance process, the selection of the appropriate control laws with sufficient robustness involves: the investigation of the closed-loop eigenvalues, the stability margins and the performance indices, in the presence of uncertainties. The resulting controller is used further for the design of the Flight Control System (FCS).

The aircraft controller determination is very complex. Nonlinear methods such as Fuzzy Logic and Neural Network methods have been applied for Aircraft Identification and Control (G. Kouba, 2009),(N. Boëly, 2009). The non linear Hybrid Fuzzy Logic Control on a morphing wing was explored in (Grigorie et al., 2012a),(Popov et al., 2010). Due to its complexity in the Aerospace Industry, the determination of the robust Flight Control System FCS is usually carried out using linear methods applied on linear models, and it is further validated using non-linear models. In the Literature many linear control methods were used to obtain an FCS such as the LMI (Linear Matrix Inequality) approach, which has been used to achieve a robust control design of an uncertain aircraft system (Ibrir et Botez, 2005), Adaptive controls have been used for disturbance rejection (Balas et Frost, 2014a), (Balas et Frost, 2014b), (Balas et Frost, 2013), other optimal algorithms were investigated for gust load alleviation and further tested on different aircrafts (Frost et al., 2015), (Frost, Taylor et Bodson, 2012), (Frost et Balas, 2012), (Aouf, Boulet et Botez, 2000b). Then on-line parameter estimations and identifications methods were used to improve the flight control capabilities (Perhinschi et al., 2002a), (Campa et al., 2002), (Perhinschi et al., 2002b) by its recovering in presence of disturbances.

To obtain a flight control system by taking disturbances into account, the *H-infinity* linear method proposed by Zames (1983) had gained popularity as a way to guarantee robustness in the presence of uncertainties. The *H-infinity* method has been used in the industry to develop controllers to meet the required specifications and needs. One of the most important aspects of this controller is the determination of the weighting functions (W_1 and W_2), which are very important in the gains determination. There is no specific methodology to determine these weighting functions. The literature points out that the weighting functions are determined using a trial-an-error methodology, or by pure experience-based methods.

Several applications of this control method have been incorporated in the aeronautical domain, mostly for fighter jets, where a scheduled *H-infinity* controller was used on VSTOL longitudinal control (Hyde et Glover, 1993), and it has as well been used on the lateral control of an F-14 (G.J.Balas, 1998). An *H-infinity* controller design with gain scheduling

approach was successfully used on a flexible aircraft where the weighting functions were not optimized but were determined using engineering intuition (Aouf, Boulet et Botez, 2002). To overcome this lack of reference formulas, some guidelines were given in (Ciann-Dong, Hann-Shing et Shin-Whar, 1994a), (Hu, Bohn et Wu, 1999) to determine these weighting functions.

However, due to its trial and error nature the guidelines procedure may take many iterations to find acceptable results: Besides, the guidelines do not guarantee fulfillment of the required conditions. For this reason, a methodology to tune the weighting functions to meet the mandatory requirements is necessary.

There exist several weighting optimization methods based on mathematical algorithms, in which trade-offs were arranged between maximizing the stability margin and minimizing the *H-infinity* norm of the final closed loop transfer function (Lanzon, 2005).

These algorithms often performed on frequency-dependent optimizations, in which the iteration process demanded a considerable amount of memory allocation. To overcome this frequency-dependent optimization memory, a state space weight optimization was developed in (Osinuga, Patra et Lanzon, 2012b). However, that algorithm does not guarantee a global minimum convergence, which could lead to a poor stability margin, especially important in a system operating in a large envelope, such as an aircraft.

This paper proposes a new and innovative methodology by taking advantage of both GA and DE algorithms to optimize the *H-infinity* weight functions to develop a controller that satisfies the imposed dynamic specifications and the industrial needs. This new approach can solve the clearance problem by reducing the complexity of calculation and validation. However, this research aims to confirm that the DE algorithm optimization is more efficient and accurate than the GA optimization; Storn and Price (Storn et Price, 1997) have also shown the efficiency of the DE algorithm by its comparison with genetic algorithm.

Many global optimizations based on evolutionary principles have been used on control engineering field, In the aeronautical field, aircraft trajectory optimizations based stochastic search, such as the Genetic Algorithm (GA) were performed on several civil aircrafts (Murrieta-Mendoza et Botez, 2015b), (Patrón et Botez, 2015) as well as parameters estimation performed on autonomous air vehicle and flight testing for intelligent flight controls (Mario, 1999), (Osinuga, Patra et Lanzon, 2012a). These new methodologies to estimation and control different parameters will be applied in future for the flight dynamics and control of the business aircraft Cessna Citation X. All of these methods were developed with the aim of reducing the computational complexity and time of convergence while achieving satisfactory results. For this study, the GA and the Differential Evolution DE algorithms were selected to optimize the weighting function parameters.

The following section presents a brief description of the Cessna Citation X, then the description of the nonlinear and linear aircraft models, followed by the Cessna Citation X's flying qualities. Section three contains a short presentation of the *H-infinity* theory. The weight-selection methods are mentioned in the fourth section, both the differential evolution and the genetic algorithms, followed by their application to the *H-infinity* problem in section five. Our simulation and results' analysis are exposed in section six, followed by conclusions. Preliminary results are presented by Boughari et al (2014b).

5.2 Cessna Citation X Business Aircraft

The Cessna Citation X is the fastest business aircraft in the world; it operates at a Mach number of 0.935. The longitudinal and lateral motions of the business aircraft, its flight envelope, and its flying qualities requirements are described below.

The Cessna Citation X aircraft was selected for this work because the Aircraft Flight Research Simulator Level D was available at LARCASE laboratory. The Level D is the highest Flight Dynamics certification level. The availability of this flight simulator makes possible the validation of the numerical results with real flight test data.

In order to analyze the stability of an aircraft, its model must be first identified. The model identification can be done in by using a combination of fuzzy logic and neural networks methods as performed on the F/A–18 aircraft in (Boely, Botez et Kouba, 2011). A new system identification for the business Cessna Citation X aircraft has been developed in 2013 at LARCASE laboratory (Hamel; 2013); this system was compared with a linearized Cessna Citation X model obtained using aircraft simulator data.

5.2.1 Aircraft dynamics

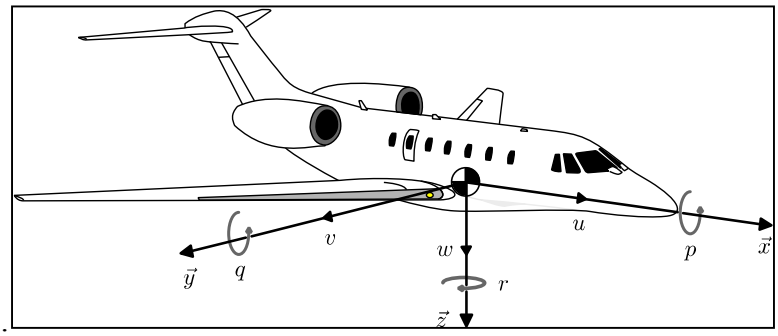

Figure 5-1 Representation of Cessna Citation X aircraft's rotation axes

The Cessna Citation X rotation axes are represented in Figure 5-1, the aircraft nonlinear model is given in the literature by (Nelson, 1998). To design a controller, a linearization of the aircraft nonlinear model is required, for flight conditions within the flight envelope given by the designer. Following the decoupling of the linearized aircraft in two longitudinal and lateral motions, the equations are represented in the form of the following state space system:

$$\dot{x} = Ax + Bu \tag{5.1}$$

This system is decomposed into two sub-systems representing the aircraft's longitudinal and lateral motions. The aircraft's longitudinal motion dynamics are given by the state space equation, using the elevator as input:

$$\dot{x}_{long} = A_{long}x_{long} + B_{long}u_{long}$$

$$A_{Long} = \begin{pmatrix} X_u & X_w & X_q & -g\cos\theta \\ Z_u & Z_w & Z_q & 0 \\ M_u + M_{\dot{w}}Z_u & M_w + M_{\dot{w}}Z_w & M_q + M_{\dot{w}}u_0 & 0 \\ 0 & 0 & 1 & 0 \end{pmatrix},$$

$$\mathrm{B_{Long}} = \begin{pmatrix} \mathrm{X_{\delta_e}} \\ \mathrm{Z_{\delta_e}} \\ \mathrm{M_{\delta_e} + M_{\dot{w}}Z_{\delta_e}} \\ 0 \end{pmatrix} \quad (5.2)$$

Where the state vector $x_{long}(t)$ and control vector $u_{long}(t)$ are given by:

$$x_{long}(t) = (u \quad w \quad q \quad \theta)^T \ , \ u_{long}(t) = \delta_e \quad (5.3)$$

The aircraft's lateral motion dynamics are given by the state space equation, using the aileron and the rudder as inputs. Where the state vector $x_{lat}(t)$ and control vector $u_{lat}(t)$are given by:

$$x_{lat}(t) = (\beta \quad p \quad r \quad \phi)^T, \ u_{lat}(t) = (\delta_a \delta_r)^T \quad (5.4)$$

The linear model of the Cessna Citation X was obtained for 36 flight conditions using the Cessna Citation X Aircraft Flight Research Simulator tests performed at LARCASE (Hamel, 2013). The linearized model is further decomposed in Linear Fractional Representation LFR models (Poussot-Vassal et Roos, 2011) using the *bilinear interpolation method*. Thus, these models are obtained for 72 flight points, and 12 weight conditions described in the following section.

5.2.2 LFR models design by flight point's interpolation

The linear models interpolation using Linear Fractional Transformation (LFT) facilitates the calculation of the state space matrices variation with the altitude and the TAS (Poussot-

Vassal et Roos, 2011). Given the data extracted from the Aircraft Flight Research Simulator provided by CAE Inc., the aircraft flight dynamics can be described for any flight condition in the flight envelope. Figure 5-2 shows the 36 flight points chosen inside flight envelope limits. These aircraft models are obtained at each 5000 ft. in altitude, and for 4 different speeds.

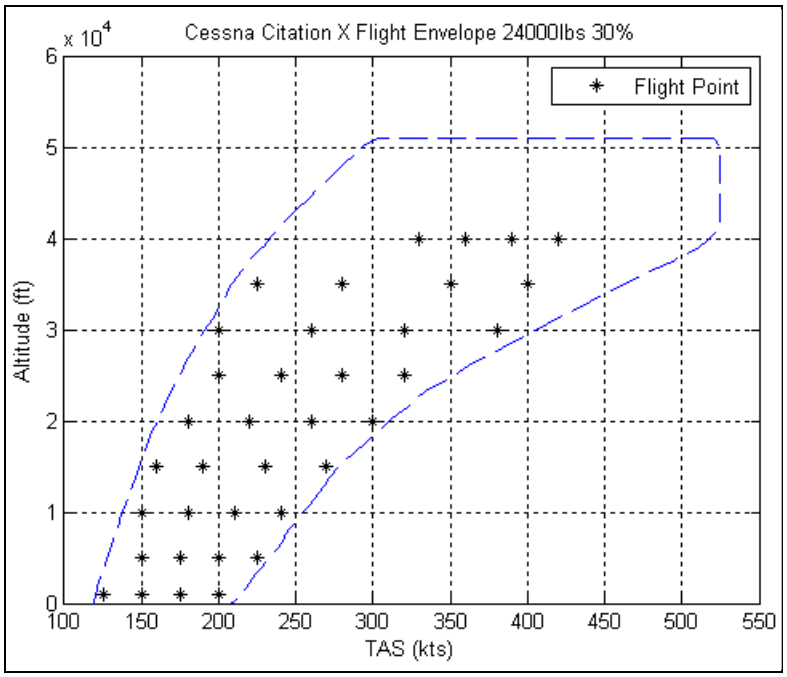

Figure 5-2 Cessna Citation X flight enveloppe

Before carrying out the interpolation, two steps need to be performed. The first step regards the definition of the region for an altitude and a range of TAS, where the interpolation will be performed, and for which the four corners of the region form the vertices.

Each of these ranges has lower and upper values which are the bounds. The second step regards the normalization of these bounds in order to attribute each coordinate of the vertices a value equal to 1 or -1.

To optimize the level of accuracy, the smallest possible regions have been defined, containing only 3 or 4 flight points to use as reference points for the interpolation. This

definition only allows a bilinear interpolation, for which 4 coefficients have to be found, using equations (5.8), (5.9), and (5.10):

$$A(h,TAS) = A_{0_{4,4}} + A_{1_{4,4}}h + A_{2_{4,4}}TAS + A_{3_{4,4}}TAS \times h \tag{5.8}$$

$$B_{long}(h,TAS) = B_{0_{4,1}} + B_{1_{4,1}}h + B_{2_{4,1}}TAS + B_{3_{4,1}}TAS \times h \tag{5.9}$$

$$B_{lat}(h,TAS) = B_{0_{4,2}} + B_{1_{4,2}}h + B_{2_{4,2}}TAS + B_{3_{4,2}}TAS \times h \tag{5.10}$$

Where A is a matrix of 4 rows and 4 columns, B_{long} is a matrix of 4 rows and 1 column, and B_{lat} is a matrix of 4 rows and 2 columns. The Least Square (LS) method is employed to minimize the relative error in these reference points (Biskri et al., 2006). From Table 5-1, it can be observed that the maximum errors found for the state space matrices A and B are negligible, therefore results are good.

Table 5-1 Maximum relative error

	Longitudinal mode	**Lateral mode**
A	$1.04\ 10^{-11}\%$	$1.97\ 10^{-11}\%$
B	$3.05\ 10^{-12}\%$	$3.97\ 10^{-11}\%$

From these results, 26 regions denoted by rectangles in Figure 5-3 are obtained, that cover a large part of the flight envelope. The mesh is valid for all of the weight and X_{CG} locations presented in Figure 5-4. It can be noticed from Figure 5-3 that some of the regions superimpose others (darker zones) due to the common reference points, and in some cases there is not only the interpolation considered, but also the extrapolation.

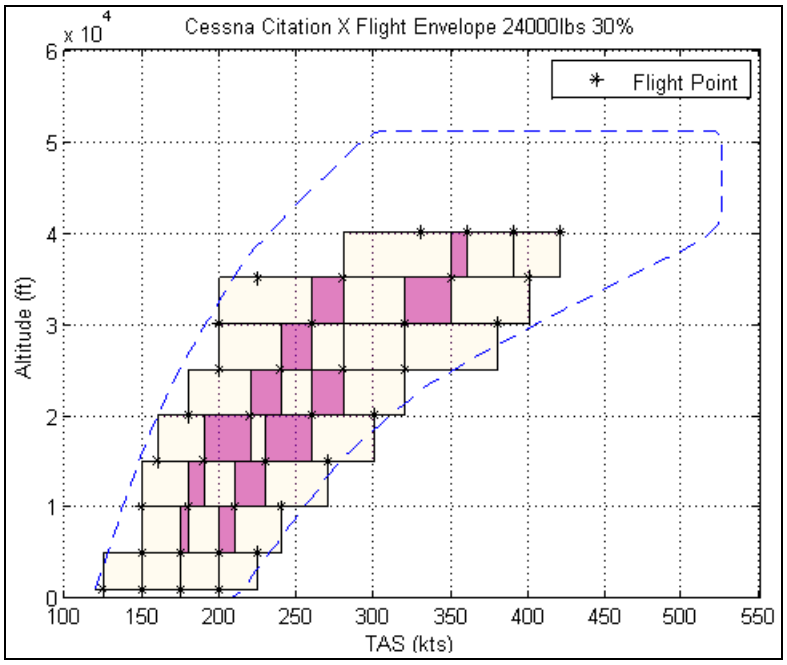

Figure 5-3 Definition of 26 regions

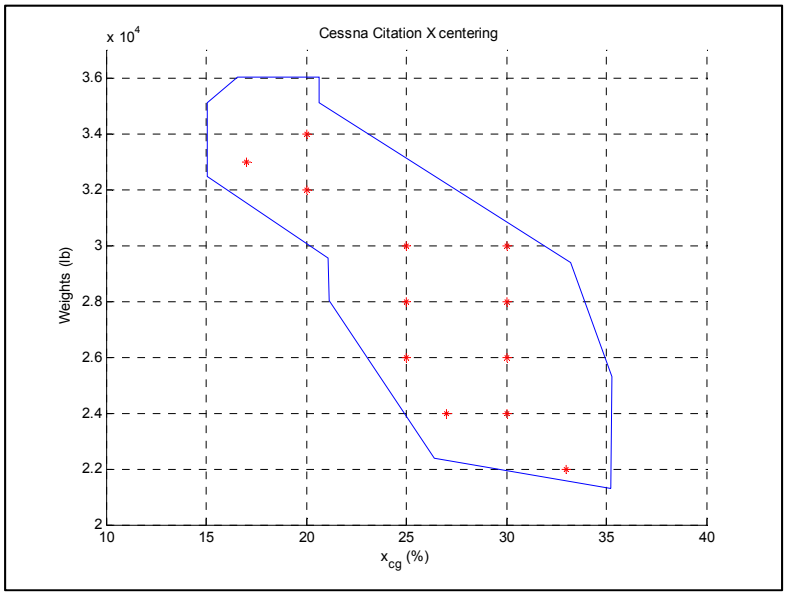

Figure 5-4 Cessna Citation X Weight/ X_{CG} conditions

All of these 26 regions' vertices lead to 72 different flight points that can be controlled. Figure 5-5 shows these 72 conditions obtained by means of the LFR models, which makes it possible a close approximation of the flight envelope limits.

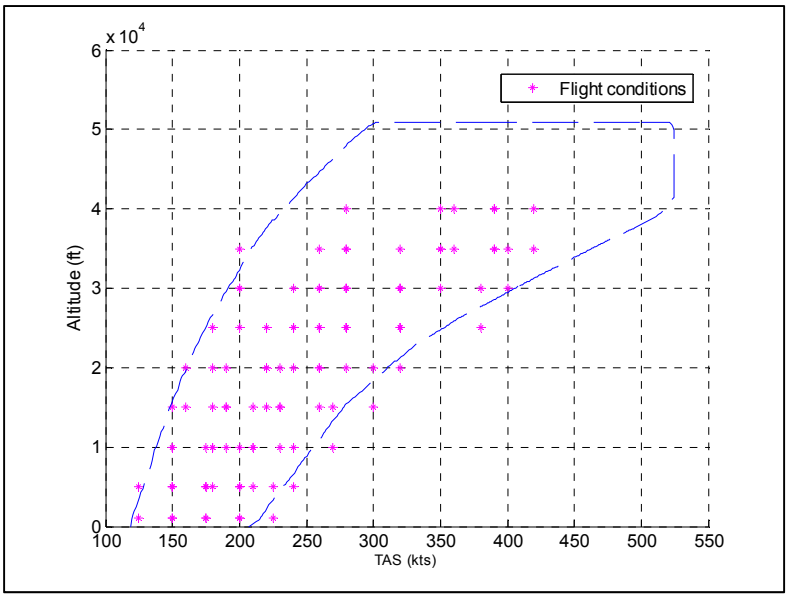

Figure 5-5 Flight points obtained by LFR models

5.2.3 Flying quality's level 1

The flying qualities are provided by the *U.S '' Military Specification for the Flying Qualities of Piloted Airplanes MIL-STD-1797A ''*. For the aircraft longitudinal motion, two modes are perceived: 1) short period and 2) phugoïd mode. Three modes are perceived for the lateral aircraft motion:1) the Dutch roll mode, 2) the roll mode, and 3) the spiral mode. These modes need to respect some of the desired criteria, which are required for satisfactory flight performance, and are expressed in terms of damping, and time constant as shown in Table 5-2. These flying qualities are given for the cruise phase or phase B, and for the flight level 1 which corresponds to very good flying qualities (Jackson EB, 2009), (Roskam, 1988). Thus the aircraft responses have to meet the criteria given in Table 5-2 for the aircraft certification

Table 5-2 Aircraft flying qualities level 1

Criterion	Type	Limits
Short period damping	modal	$0.3 \leq \xi_{sp} \leq 2$
Phugoïd damping	modal	$0.04 \leq \xi_{ph}$
Dutch roll damping	modal	$0.3 \leq \xi_{dr} \leq 2$
Roll time constant	temporal	Tr <1.4 sec

5.3 *H-infinity* Theory

H∞ represents a modern approach to characterize closed-loop performance, by measuring the size of the closed-loop transfer function matrices, and the way in which the control objectives can be fixed to minimize closed-loop transfer functions (Zames et Wang, 1991).

5.3.1 Definition of the standard *H-infinity* robust control problem

The Linear Fractional Transformation LFT technique is a configuration to describe how the relationship between the input and the output, is affected by uncertainty as shown in Figure 5-6. The LFT is used to formulate the Standard *H-infinity* configuration, ***P(s)*** denotes the generalized plant which contains the disturbance model and the interconnection structure between the plant and the controller ***K(s)***. ***w*** denotes all the external (disturbances, noise and command) inputs and ***z*** denotes all of the external outputs expressed in terms of error signals, to be minimised, including both the performance and the robustness measures. The control input is denoted by ***y,*** and ***u*** denotes the control signal's vectors. The objective is to find a stabilizing controller that minimizes the output ***z,*** which means that it minimizes the *H-infinity* norm of the closed loop transfer function from ***w*** to ***z***.

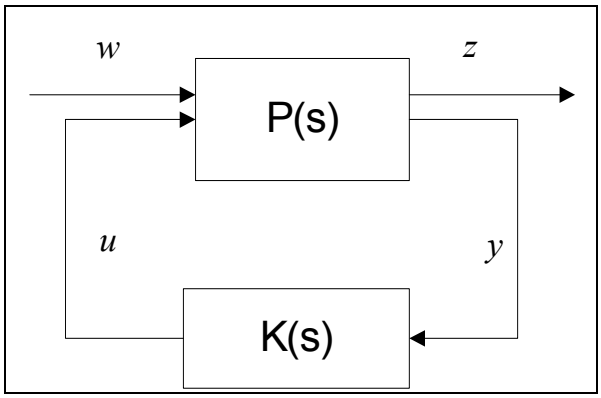

Figure 5-6 Standard *H_infinity* configuration

The generalized plant ***P(s)*** can be written as:

$$P(s) = \begin{bmatrix} P_{11}(s) & P_{12}(s) \\ P_{21}(s) & P_{22}(s) \end{bmatrix} \tag{5.11}$$

The transfer function between ***z*** and ***w*** can be written as follows (D.-W. Gu, 2005):

$$z = (P_{11} + P_{12}K(I - P_{22}K)^{-1}P_{21})w \tag{5.12}$$

$$z = F_l(P, K)w \tag{5.13}$$

Where $F_l(P, K)$ is the lower linear fractional transformation of ***P*** and ***K.*** The H_∞ optimization problem design is then formulated as given in (D.-W. Gu, 2005):

$$min_{Kstabilizing} \|F_l(P, K)\|_\infty \tag{5.14}$$

5.3.2 Definition of the mixed sensitivity *H-infinity* problem

The mixed sensitivity *H-infinity* optimization is one of several practical optimization problems in industry, where its cost function is a combination of other two cost functions,

such as a control signal's energy limitation and a good tracking reference as shown in Figure 5-7. In order to keep the system internally stable, these cost functions will be optimized for a set of stabilizing controllers using the state space gain defined in Equation (5.15) and in (Walker, Turner et Gubbels, 2001):

$$min_{Kstabilizing} \left\| \begin{bmatrix} (\mathrm{I} + \mathrm{GK})^{-1} \\ \mathrm{K}(\mathrm{I} + \mathrm{GK})^{-1} \end{bmatrix} \right\|_{\infty} \tag{5.15}$$

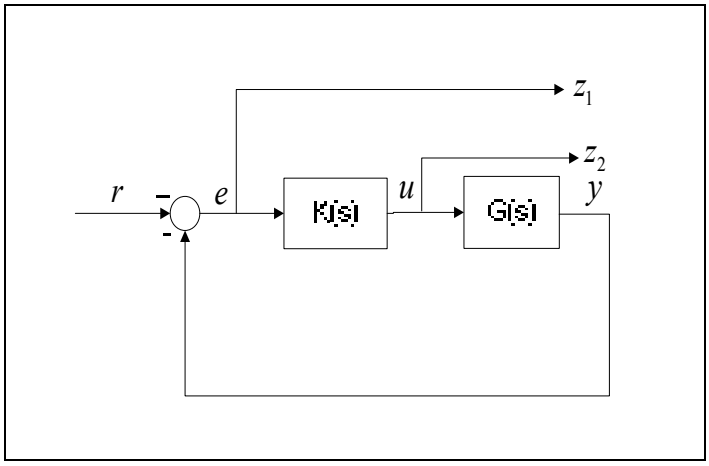

Figure 5-7 Mixed sensitivity *H-infinity* configuration

Weighting functions are often used to respect the design specifications in the closed loop system (control input signal limitations and good tracking). Thus, Equation (5.15) can be rewritten as function of both weighting functions W_1 and W_2 as follows:

$$min_{Kstabilizing} \left\| \begin{bmatrix} \mathrm{W}_1(\mathrm{I} + \mathrm{GK})^{-1} \\ \mathrm{W}_2\mathrm{K}(\mathrm{I} + \mathrm{GK})^{-1} \end{bmatrix} \right\|_{\infty} \tag{5.16}$$

In practice, a stabilizing controller is found by iterations using the lowest achievable value γ. Equation (5.16) then becomes:

$$min_{Kstabilizing} \left\| \begin{bmatrix} W_1(\mathrm{I} + \mathrm{GK})^{-1} \\ W_2\mathrm{K}(\mathrm{I} + \mathrm{GK})^{-1} \end{bmatrix} \right\|_{\infty} < \gamma \tag{5.17}$$

where γ is the robustness criterion given as the maximum value of the $\infty - norm$ of the system's closed loop transfer function (D.-W. Gu, 2005).In Equation (5.17),W_1 is used to shape the sensitivity function $(\mathrm{I} - \mathrm{GK})^{-1}$ and W_2 to shape the complementary sensitivity function given as $\mathrm{K}(\mathrm{I} - \mathrm{GK})^{-1}$, which characterize the disturbances and controls. In addition, K is the state space gain calculated from the *H-infinity* method, while W_1, and W_2represent the weighting functions, appropriately chosen using guidelines given by (Beaven, Wright et Seaward, 1996):

$$W_1 = \frac{\mathrm{as+b}}{\mathrm{cs+d}} \tag{5.18}$$

$$W_2 = \frac{1}{\alpha_{\delta a}} \tag{5.19}$$

So the *H-infinity* problem will be then reduced to define W_1, and W_2.

5.4 Differential Evolution and Genetic Algorithms

This research aims to optimize the determination of weighting functions given by equations (5.18) and (5.19), using both Genetic and Differential Evolution algorithms, in which one fitness function will be defined and used for the optimization process.

5.4.1 Objective Function for DE algorithm and GA

The same objective function to be minimized is used in both GA and DE optimization methods, in order to obtain the optimal solution calculated by the *H-infinity* algorithm. In these algorithms, the objective function gives the designer specifications for the desired closed loop time response of the system using Overshoot(OS), Integral Square Error (ISE) and the frequency domain robustness criterion (γ) as shown in the next equation:

$$\mathrm{fitness} = 10 * (ISE \leq 0.002) + 10 * (OS \leq 35\%) + 10 * (\gamma \leq 1) \tag{5.20}$$

5.4.2 Differential Evolution algorithm

The Differential Evolution (DE) algorithm has been developed in 1995 by Price and Storn (Price, 1996; Storn et Price, 1996)**,** and has been used in global optimization in many disciplines as shown in (Rogalsky, Kocabiyik et Derksen, 2000; Tijani et al., 2011; Wu et Tseng, 2010; Yamina Boughari, 2014; Yu et Zhang, 2012). The DE algorithm is a heuristic optimization algorithm that uses real values, thus there is no need for coding and decoding operations to represent problem parameters. The key concept of DE is its use of a differential operator to diversify the *population*. This section gives a detailed presentation of the DE algorithm along with the genetic algorithm.

5.4.2.1 Initialization phase

In this phase, the *number of generations* is selected as one of the termination criteria. The problem dimension is set according to the number of parameters forming the *fitness function*. Next, the parameters to be optimized are represented in a vector form; at each generation, the i^{th} vector is described (Price, 1996) as:

$$\vec{X}_{iG} = \left[x_{1,iG}, x_{2,iG}, x_{3,iG}, \ldots\ldots, x_{D,iG}\right] \tag{5.21}$$

The population is initialized randomly within the search space constrained by the lower and higher boundaries for each parameter. These boundaries are represented in vectors given by equations (5.21) and (5.22):

$$\vec{X}_{imin} = \left[x_{1,imin}, x_{2,imin}, x_{3,imin}, \ldots\ldots, x_{D,imin}\right] \tag{5.22}$$

$$\vec{X}_{imax} = \left[x_{1,imax}, x_{2,imax}, x_{3,imax}, \ldots\ldots, x_{D,imax}\right] \tag{5.23}$$

The j^{th} component of the i^{th} vector is initialized as:

$$\mathrm{x_{j,i,0}} = \mathrm{x_{j,min}} + \mathrm{rand_{i,j}}[0,1].\left(\mathrm{x_{j,max}} - \mathrm{x_{j,min}}\right) \tag{5.24}$$

where $0 \leq \text{rand}_{i,j}[0,1] \leq 1.$

The next step after the finalization of the initialization step is the mutation operation.

5.4.2.2 Mutation

"Mutation" is the operation of changing parameters between different vectors. In the DE algorithm, a random choice of three different parameter vectors $\vec{X}_{r_1^i,G}, \vec{X}_{r_2^i,G}, \vec{X}_{r_3^i,G}$ is performed in the current population; for each i^{th} "target" vector $\vec{X}_{r_1^i,G}$, a corresponding "donor" vector is created, which results from the combination of the "target" vector and a "weighted difference" between two parameter vectors $\vec{X}_{r_2^i,G}, \vec{X}_{r_3^i,G}$ by a randomly chosen scalar F, where $F \in [0,2]$. The "mutant" vector $\vec{V}_{iG}$ so called the "donor" vectors is defined in Equation (5.24) (Rogalsky, Kocabiyik et Derksen, 2000) as follows:

$$V_{IG} = \vec{X}_{r_1^i,G} + F * \left(\vec{X}_{r_2^i,G} - \vec{X}_{r_3^i G}\right) \tag{5.25}$$

5.4.2.3 Crossover

To improve the diversity of the population, a "crossover" operation is performed, from which the "mutant" and the "target" vectors exchange their components to create the "trial" vector $\overrightarrow{U}_{IG}$:

$$\overrightarrow{U}_{IG} = \left[u_{1,iG}, u_{2,iG}, u_{3,iG}, \ldots, u_{D,iG}\right] \tag{5.26}$$

There are two types of crossover operation: the exponential (two points modulo) and the binomial (uniform). In the exponential crossover the trial vector is given as follows:

$$u_{j,iG} = v_{j,iG} \quad \text{for} \quad j = \langle n \rangle_D, \langle n+1 \rangle_D, \ldots., \langle n+L-1 \rangle_D \tag{5.27}$$

Otherwise

$$u_{j,iG} = x_{j,iG} \quad \text{for} \quad j \in [1, D] \tag{5.28}$$

Where $\langle . \rangle$ denotes the modulo function with modulus D. The "modulus operator" is the remainder after the arithmetic division that is used as a function in the program to reduce a generated number to a random one in a smaller range of values. D refers to the number of parameters to be optimized or the parameters dimensions range, in which two integers L and n where randomly generated from the range $[1, D]$. The trial vector in the binomial crossover is given as:

$$u_{j,iG} = v_{j,iG}, \quad \text{if} \quad rand_{i,j}[0,1] \leq Cr \quad \text{or} \quad j = j_{rand} \tag{5.29}$$

Otherwise

$$u_{j,iG} = x_{j,iG} \tag{5.30}$$

Where the crossover rate $Cr \in [0\ 1]$, $rand_{i,j}[0,1]$ is a random number distributed uniformly, and $j_{rand} \in [1,2, \dots, D]$ is an index randomly chosen to ensure that the resultant trial vector $\vec{U}_{iG}$, considers in its expression at least one component from the donor vector:

$$\vec{V}_{iG} = [v_{1,iG}, v_{2,iG}, \dots \dots \dots, v_{D,iG}] \tag{5.31}$$

At the end of the population diversity step, a selection operation is performed as detailed in the next phase.

5.4.2.4 Selection

Using the "selection" operation, we can determine if the "trial" or "target" vectors survive in the next generation or not, and thus a constant population size is kept. The selection operation is outlined as:

$$\vec{X}_{i,G+1} = \vec{U}_{i,G} \text{ if } f(\vec{U}_{i,G}) \leq f(\vec{X}_{i,G}) \tag{5.32}$$

Else $\vec{X}_{i,G+1} = \vec{X}_{i,G}$ if $f(\vec{U}_{i,G}) > f(\vec{X}_{i,G})$ (5.33)

where $f(\vec{X}_{i,G})$ is the objective function or the" fitness" to be converged using iteration process.

5.4.2.5 Iteration

The operations listed above (Initialization, mutation, crossover and selection) are repeated until the termination criteria are met, which consist of:

1. The maximum number of generations required by the user; or
2. The convergence of the fitness function given in the objective function for DE and GA Section

The *H-infinity* weighting functions optimization for longitudinal and lateral control using DE algorithm is summarized as follows:

Set a population number as NP formed by the weighting functions W_1 and W_2.The parameters from the initial vector are:

$$\vec{X}_{IG} = [a_{q,iG}, b_{q,iG}, c_{q,iG}, d_{q,iG}, \alpha_{\delta e,iG}] \quad (5.34)$$

Where a, b, c, d, are the coefficients of W_i functions defined in equations (5.18) and (5.19). Each of these parameters belongs to an interval defined by a lower and an upper bound; for example, $a_{q,iG} \in \left[\underline{a_{q,iG}}, \overline{a_{q,iG}}\right]$ belongs to an interval in which $\underline{a_{q,iG}}$ represents the lower bound and $\overline{a_{q,iG}}$ represents the higher bound. The optimal gain is obtained by choosing the appropriate W_1 and W_2 parameters and then by simulating the control system in the time domain to obtain satisfactory characteristics of the system's response. If the satisfactory characteristics are not reached, the iteration process continues, until one of the two termination criteria is achieved.

Weighting functions parameters for lateral control are calculated by the same way. All the weighting functions used in longitudinal and lateral controls are determined using the DE algorithms once, and another time with GA.

5.4.3 Genetic Algorithm applied to the *H-infinity* method

The genetic algorithm (GA) is an evolutionary computation and a powerful stochastic search and optimization technique that has become the most-recognized and used technique in the last few years based on the genetic principles. This algorithm has been successfully applied to aeronautical problems, such as control (Ghazi et Botez, 2015c; Manocha et Sharma, 2009; Schirrer et al., 2010; Shi et al., 2006; WANG et al., 2010b), optimal trajectory research (Felix Patroto et al., 2013; Patron et al., 2013; Wang et al., 2010a; Wongsathan et Sirima, 2009; Wu et Xiao, 2010; Yang et al., 2006; Zakaria et al., 2011a), and others field (Tan et al., 2011b; Zakaria et al., 2011b). The GA is a stochastic search algorithm that finds solutions using Darwin's theory of natural selection; it is an iterative process done until the desired solution is found, in which each iteration represents a generation; where the best individual is examined according to its fitness. In this research, the real coded genetic algorithm is considered, in which the "individual" defines a string of real parameters without performing "binary coding" or "decoding". The different steps of the GA are:

1. Initial *population*: To start the evolution process a *population* is randomly created. For an optimal control problem, a *population* P_p of *N* individuals is created, where *N* was chosen to be equal to 50, and each individual is represented by two chromosomes corresponding to the coefficients of the two weighting functions (W_1, W_2). For the optimisation of the pitch rate weighting functions W_q, , the individual is the following:

$$Individual = \left[\alpha_{\delta e,1} a_1 \;\; b_1 \;\; c_1 \;\; d_1 \;\right] \tag{5.35}$$

where $a_{q,1}$, $b_{q,1}, c_{q,1}, d_{q,1}, \alpha_{\delta e,1}$ are weighting functions coefficients of the pitch rate.

2. Individuals evaluation: To quantify the adaptation degree of an individual, a fitness function evaluates the robustness and the performance of the resulting controller using the weighting functions (W_1, W_2) estimated for the individual. The *population* is further sorted from the best-fitted individual to the worst.

3. Crossover: To perform a crossover, an operator randomly chooses two individuals in the current *population* (parents) and crosses their chromosomes to create new individual (children). Two different types of crossover methods are used to improve the diversity of individuals and their genes to obtain diverse results. The first type of crossover methods regards the uniform crossover. This method creates a random binary mask that decides if two chromosomes can be crossed (see Figure 5-8).

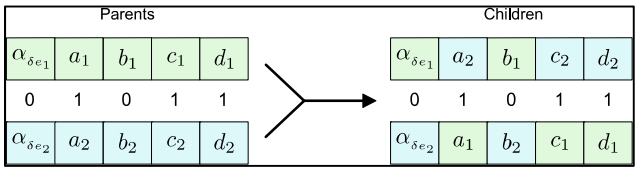

Figure 5-8 Example of uniform crossover

The second method consists in dividing the parents into two or three sections, and each section is crossed to obtain two individuals. Figure 5-9 shows two examples:

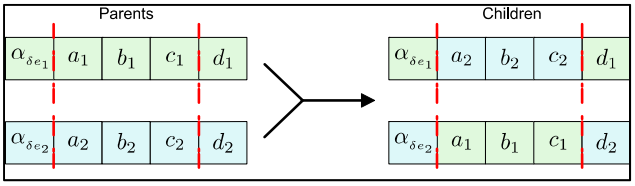

Figure 5-9 Example of crossover by section

4. Mutations: A “mutation” is performed by changing the chromosome structure. To create a mutation in an individual, two genes are randomly selected and permuted, as shown in Figure 5-10.

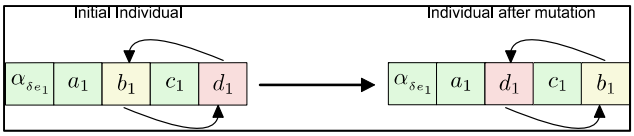

Figure 5-10 Example of mutation

5. Elitist selection: The process of natural selection promotes the most fitted individuals according to Darwin's theory. The elitist selection can be defined as follows: from one generation to another, a portion of the most fitted individuals will be guaranteed to always survive preserving its genetic information. These individuals can be discarded only if a better individual emerges from a given generation. This method has a fast convergence, which can penalize the diversity of individuals. To overcome the diversity problem, the crossover is done by considering all the *population*, but with more 'chances' given to the better-fit individual. Thus, even the less fitted individuals can contribute to the creation of the new generation. To illustrate the iteration process of a genetic algorithm search, the following steps are considered in a GA as shown below:

Step 1: The weighting functions are represented as an individual of fixed length; some parameters are defined, such as the size of the individual *population*, the crossover and the mutation probabilities.

Step 2: The performance of an individual is quantified by defining a fitness function, which selects chromosomes that will be mated.

Step 3: The random initial population is set.

Step 4: The *H-infinity* norm of each individual is computed and the gain control K is found.

Step 5: The fitness of each individual is evaluated.

Step6: A pair of individuals is selected according to the probability of their fitness.

Step 7: The next generation is reproduced by creating a pair of offspring Individuals.

Step8: The best individuals were preserved from the initial population, and with the new individuals are inserted into the new population.

Step 9: Starting at step 6, the process is repeated until the sizes of the new and the initial populations are equal.

Step10: The initial population is replaced with the new population.

Step 11: If the termination criteria has been satisfied, obtain the solution, if not Return to step 4 and repeat the process.

Two flowcharts summarize the DE and GA algorithms, presented below in Figure 5-8 and Figure 5-9.

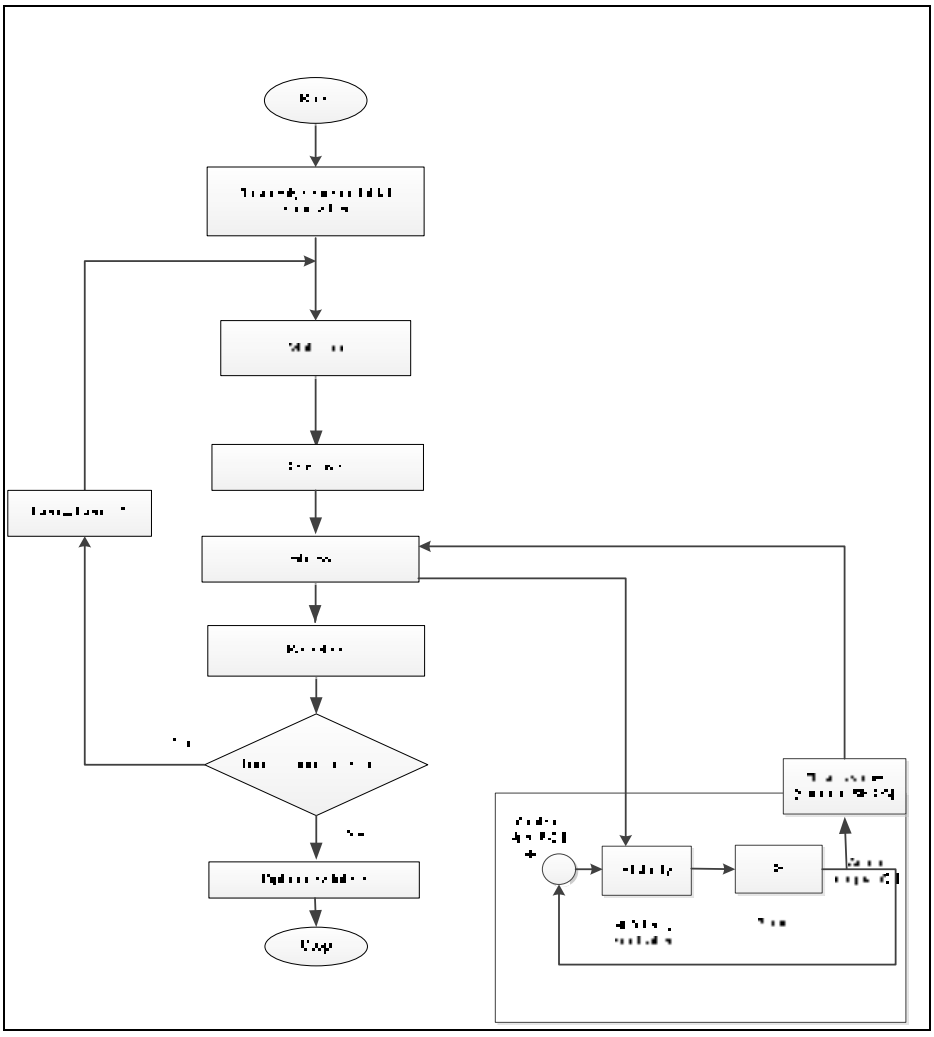

Figure 5-11 *H*-infinity optimization the Differential Evolution DE algorithm

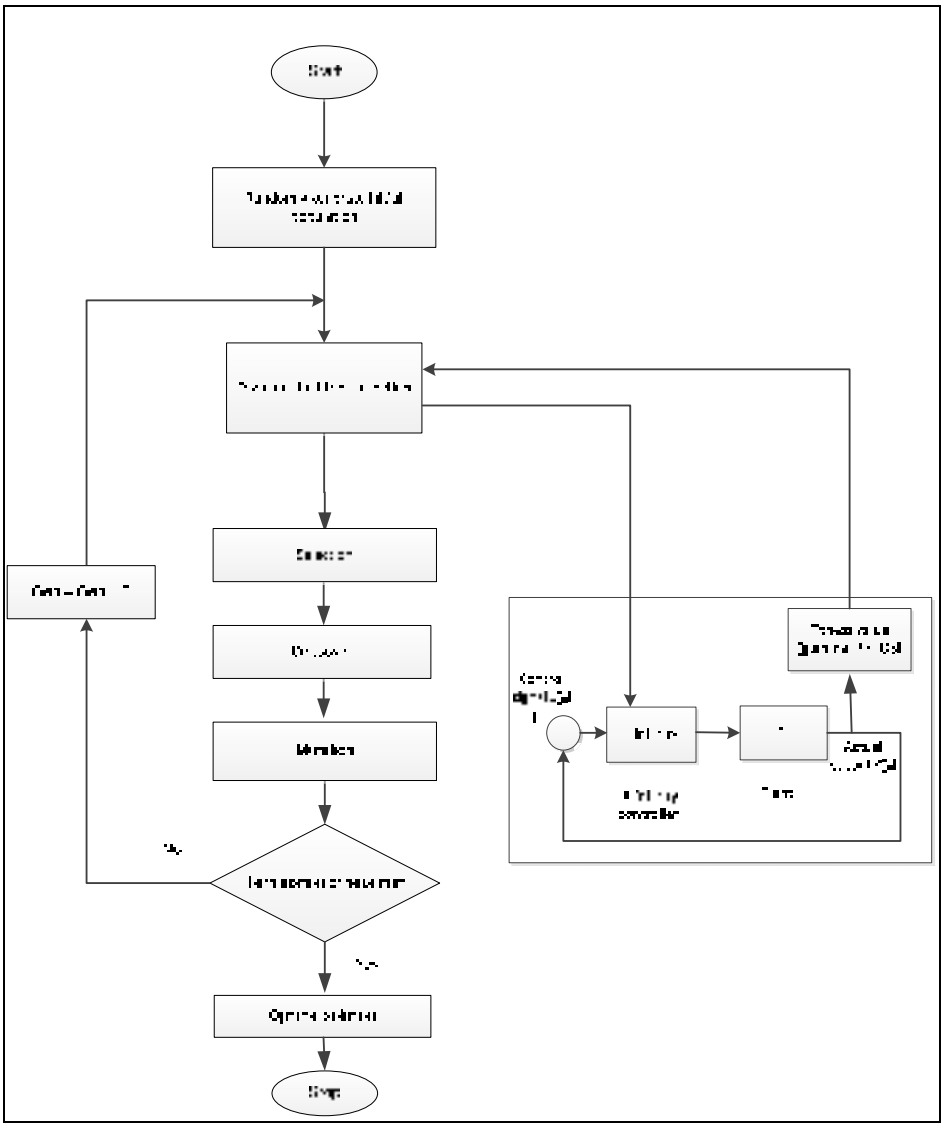

Figure 5-12 *H*-infinity optimization using
the Real-valued Genetic Algorithm

5.5 Presentation of Results

The open loop of the Cessna Citation X business aircraft is composed of aircraft dynamics, actuators and sensors, while in the aircraft's closed loop, the actuators' limits, and the performances weighting functions are considered in the Control Augmentation System (CAS), as in the simulation shown in Figure 5-13.

The business aircraft Cessna Citation X is represented in the state space form for its longitudinal and lateral motions. Robust control using the *H-infinity* design is then applied on the Cessna Citation X to improve its stability and its time response.

Closed loop simulations of the Cessna Citation X longitudinal and lateral aircraft mode were performed for the whole flight envelope. The results presented below were obtained for 12 centering configurations, using 72 flight conditions obtained from both the Cessna citation X Flight simulator and the interpolation method.

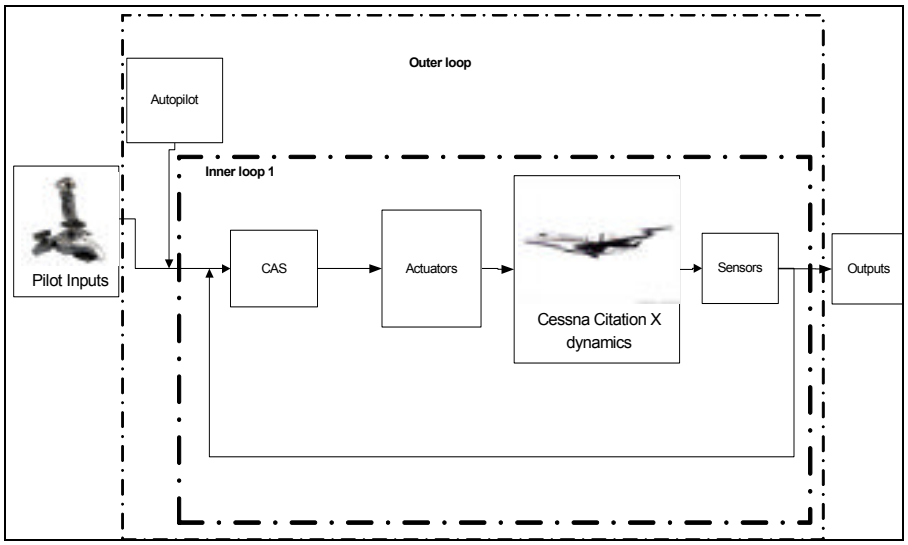

Figure 5-13 Closed loop representation of Cessna Citation X business aircraft

5.5.1 GA and DE algorithm optimization results

The Genetic and DE algorithms best fitness and the mean fitness functions during generations are presented in Figure 5-14 and Figure 5-15. Figures 5-14 and 5-15 show that the DE algorithm best fitness value converge faster than the GA best fitness value (with running time 91.63 sec and the solution given at the 5^{th} generation) with respect to the fitness function of the GA (running time 131.18 sec and the solution given at 8^{th} generation). The mean fitness value approximates the best fitness value at 3^{rd} generation in DE, and the 4th generation in GA, and it can be noticed that the mean fitness varied from maximum value of

2000 until a minimum value of 0.12856 which demonstrate the diversity of the population. Mostly the convergence of the two algorithms is obtained before reaching the 20th generation, which confirms the performance and the efficiency of the two algorithms.

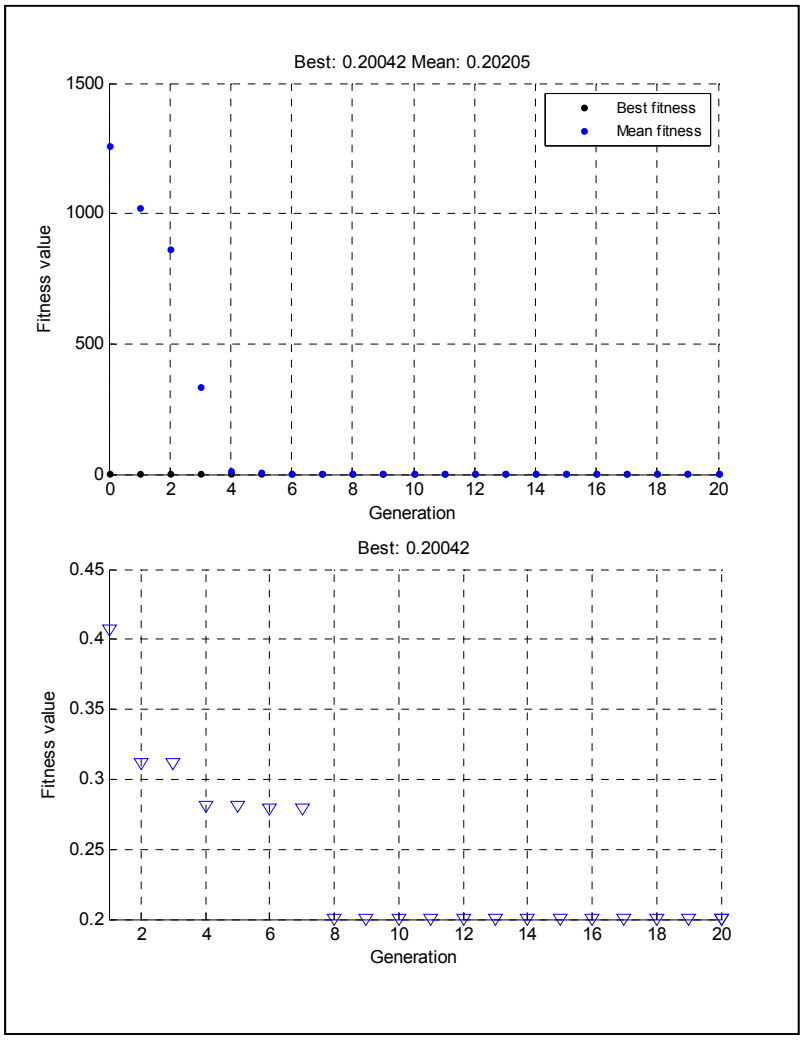

Figure 5-14 The mean fitness versus the best fitness and the best fitness value for GA

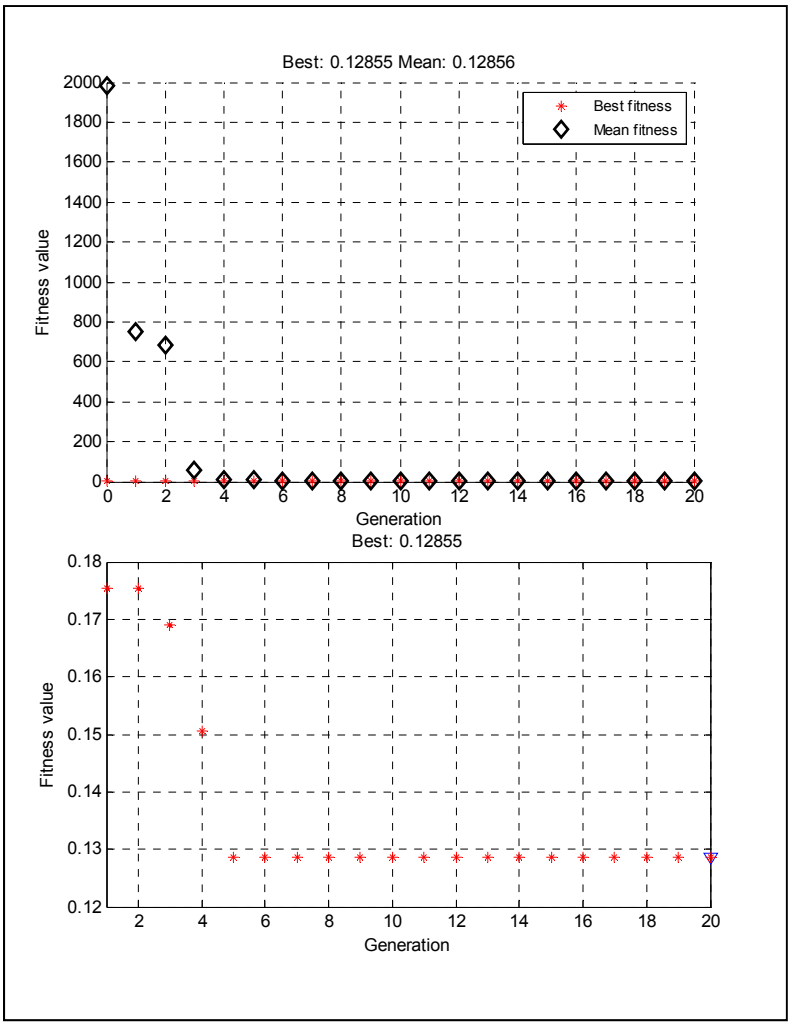

Figure 5-15 The mean fitness versus the best fitness and the best fitness value for DE

5.5.2 Results for 72 flight conditions

The simulation was performed for 72 flight conditions for each X_{CG} location. Where the results are presented below:

Table 5-3 represents the weighting functions given by the optimization using the DE algorithm. The optimization is performed for a population size of 50, and the search range for each longitudinal weighting parameter $(a_q, b_q, c_q, d_q, \alpha_{\delta e})$ and lateral weighting

parameter($a_\varphi, b_\varphi, c_\varphi, d_\varphi, \alpha_{\delta a}$) is defined as$[5 * 10^2; 10^7]$. The results are shown for the 20th generation.

Table 5-3 Weighting function optimization results

Weight fnction	DE algorithm	Genetic algorithm *GA*
Range of q weighting function coefficients	$[5 * 10^2; 10^7]$	$[5 * 10^2; 10^7]$
W_q,and W_{δ_e}weighting function solutions	$W_q = \frac{1715s + 221476}{1.66 * 10^6 s + 223992}$ $W_{\delta_e} = \frac{1}{1421997}$	$W_{q=}$ $\frac{800s + 641200}{1.6398 * 10^6 s + 1.1476 * 10^6}$ $W_{\delta_e} = \frac{1}{4.4029 * 10^6}$
Range of φ weighting function coefficients	$[0; 150]$	$[0; 150]$
W_φ and W_{δ_a}weighting functions solutions	$W_\varphi = \frac{0.0037s + 70.4}{8.89s + 0.0009}$ $W_{\delta_a} = \frac{1}{129.27}$	$W_\varphi = \frac{0.7932s + 66.8216}{0.1416s + 0.0028}$ $W_{\delta_a} = \frac{1}{137.2602}$
Generation number	≤ 20	≤ 20

Table 5-4 Mean γ values

Centring condi-tions	1	2	3	4	5	6	7	8	9	10	11	12
γ_q	0.99	0.99	0.99	0.99	0.99	0.99	0.99	0.99	0.99	0.99	0.99	0.99
γ_φ	0.96	0.96	0.96	0.97	0.97	0.99	1.00	1.04	1.04	1.09	1.09	1.09

Table 5-4 shows that the robustness criteria is not strictly less than or equal to one for higher weights than 30,000 lb which means that the system is robust for a certain range of uncertainties, and beyond this range the system may not be robust. In addition, during the

flight tests performed on the Cessna X Flight Research Simulator at the LARCASE Laboratory, the aircraft has shown a lateral dynamics sensibility and high altitudes coupling. Furthermore, in practice it is not evident for a heavy weight aircraft to fly at high altitudes, where the aircraft shows a robustness index gamma slightly greater than 1 for lateral control at high altitudes and weights as shown in Table 5-4.

As shown in Figure 5-16, time responses and pole zero map with handling qualities superimposed are given for pitch rate q. Some responses show an overshoot (*OS*) of a maximum of 20%. On the other hand, Figure 5-17 shows responses presenting the worst handling qualities for pitch controller, where new tools are presented in Figures 5-18, 5-19(a) and (b), which consists of the flight points positions in the flight envelope for which the worst handling qualities are visualized, and their coordinates are given in the text file generated by the Matlab code.

It can be noticed that in Figure 5-18(b) there are six flight points, and in the listing in Figure 5-19(b) there are nine points, because of the fact that there are 72 flight points in the flight envelope, that are tested for 12 X_{CG} locations; some of these points (as the ones shown in Figure 5-19(b) with the same colored arrow) present the same flight points with different X_{CG} locations; these flight points present the same vertex as indicated by the red arrow or a shared vertex between two adjacent regions as indicated by the black arrow and shown in Figure 5-3.

In the same way, for the roll angle ϕ control, Figure 5-20 shows time responses and pole zero map with handling qualities superimposed. Where some responses show an overshoot (*OS*) of a maximum of 18%, Figure 5-21 (a) and (b) presents the same flight points positions, but there are differences in number; they are given in Table 5-5 for both GA and DE algorithms, where we can see that the flight points number are different. Finally the responses presenting the worst handling qualities are shown in Figure 5-22.

Globally, the aircraft longitudinal and lateral motions are stabilized with the H∞ controller. For both the controls the pitch angle rate q, and the roll angle φ, the resulting response satisfies the handling qualities level 1 with damping ration and natural frequency within the limits according to Table 5-2 for both the lateral and longitudinal motions, and the imposed time domain performance, the integral square error (*ISE*) less than 2%, *OS* of 30%.

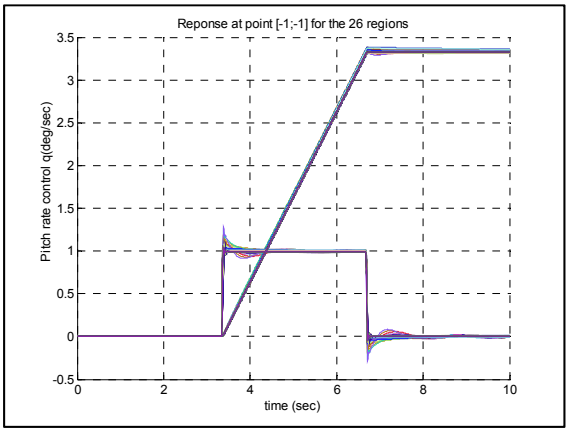

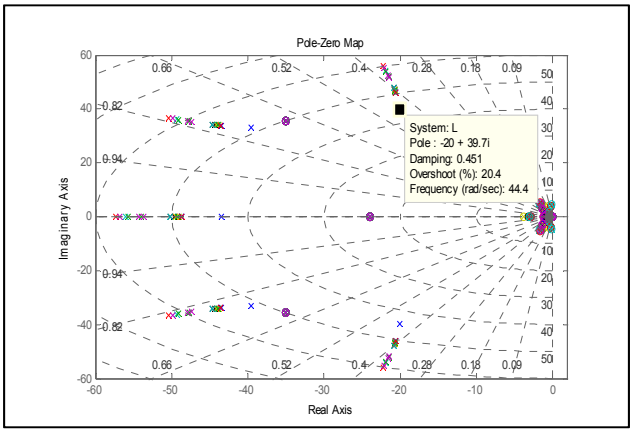

a) Pitch rate responses ***q*** b) Pole zero maps

Figure 5-16 Responses for pitch rate presenting good handling qualities for 1st XCG position (22000 lb/33%)

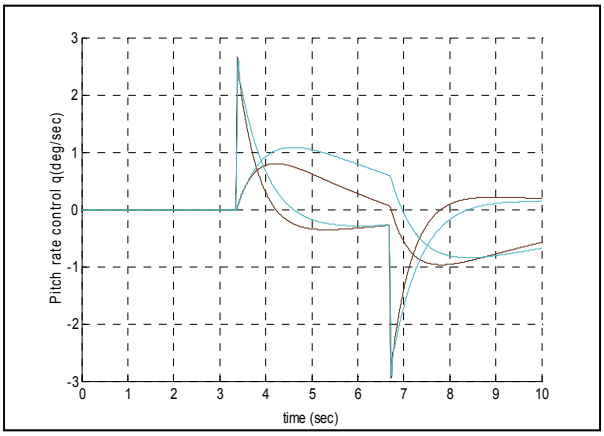

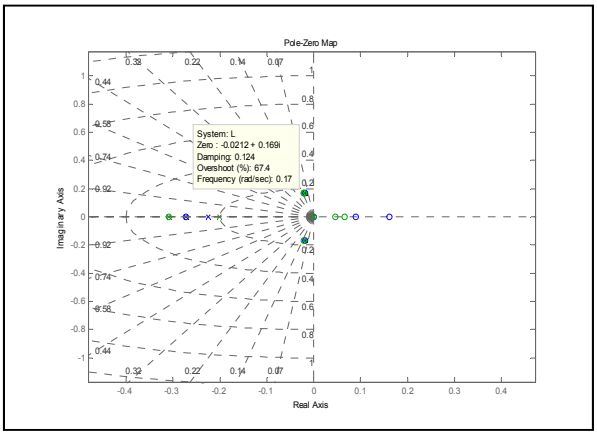

a) Pitch rate responses *q* b) Pole zero maps

Figure 5-17 Response for pitch rate *q* presenting the worst handling qualities for the entire envelope

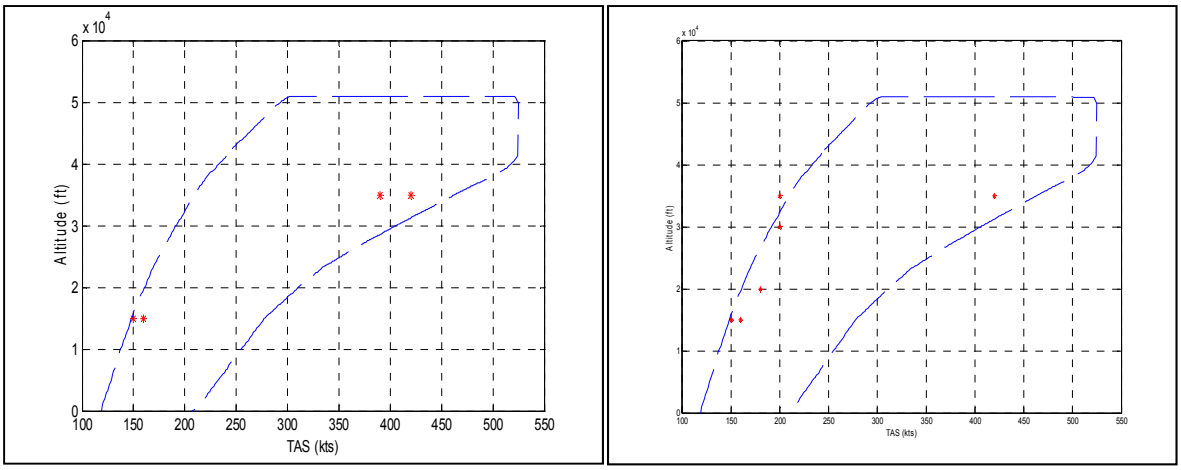

a) DE algorithm b) Genetic Algorithm

Figure 5-18 Flight points where the handling qualities for the pitch rate q control are the worst

Region	vertex	Centering
25	4	1
27	4	7
5	1	12
11	3	17

a) The DE algorithm

Region	vertex	Centering
25	4	1
27	4	7
5	1	7
14	3	12
11	3	11
5	1	11
11	3	17
17	1	11
11	3	17

b) The GA algorithm

Figure 5-19 Flight points coordinates

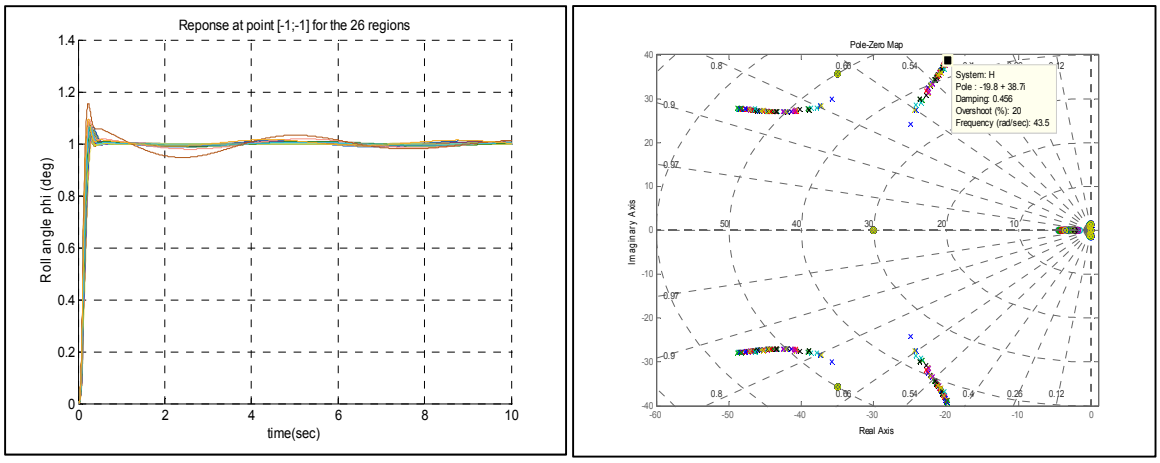

a) Roll angle responses φ b) Pole zero maps

Figure 5-20 Responses of the roll angle φ for the entire envelope presenting good handling qualities

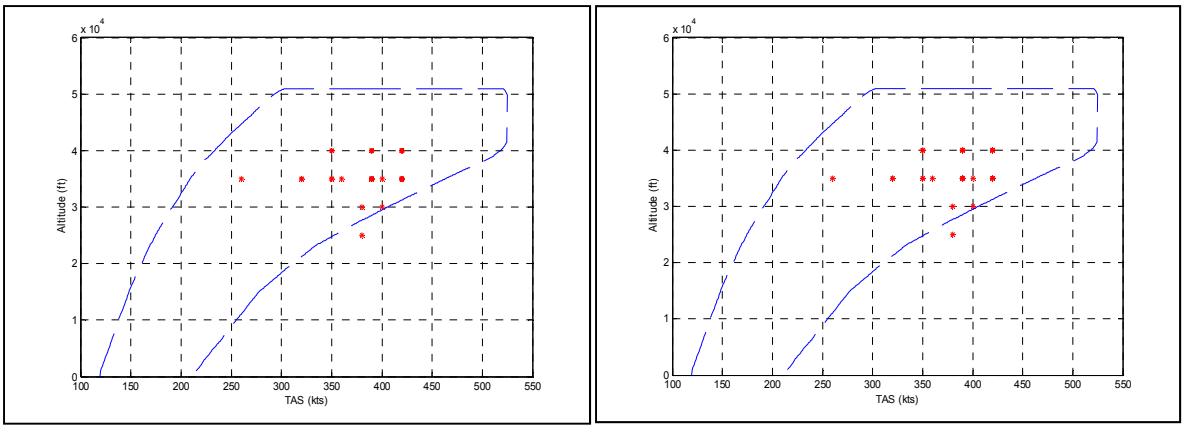

a) The Differential Evolution algorithm b) The Genetic Algorithm

Figure 5-21 Flight points where the handling qualities for the roll angle φ control are the worst

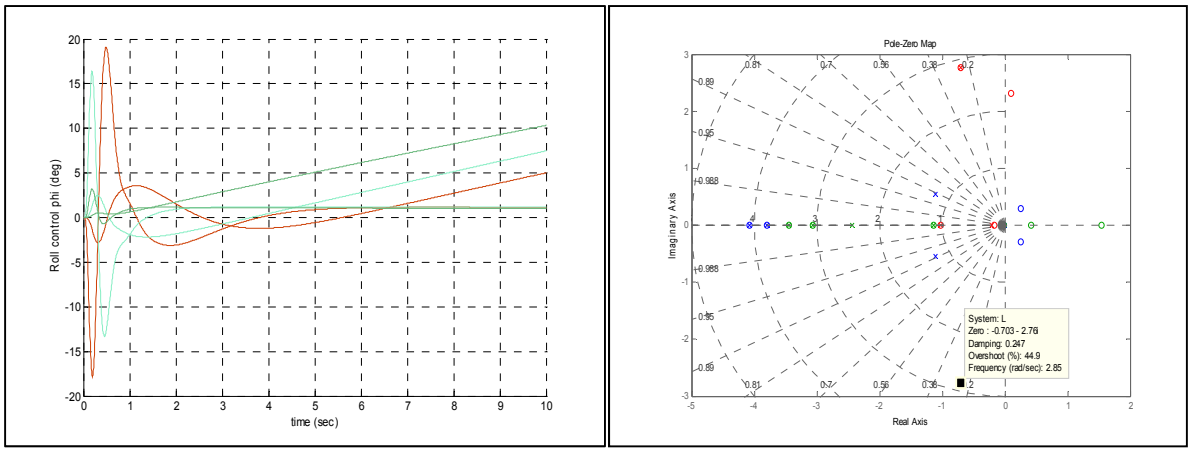

a) Roll angle φ b) Pole zero maps

Figure 5-22 Flight points presenting the worst handling qualities for the roll angle control φ

Table 5-5 Flight points with the worst handling qualities

Controls	Flight points with the worst handling qualities for the DE algorithm	Flight points with the worst handling qualities for the GA
Pitch rate *q*	4/864 (0.5%)	9/864 (1.04%)
Roll angle φ	13/864 (1.5%)	18/864 (2%)

Table 5-5 shows the flight points (within the flight envelope) for which the worst handling qualities were obtained by using optimized weighting functions for both the GA and DE algorithms. The resulting weighting functions have been validated using a linear model for almost all of the flight conditions, except for a few flight conditions which are shown by numbers and percentages for pitch angle rate q and roll angle φ. These few flight conditions belong to either very high loads or high speeds, or to low loads and low speed cases; which means flight points at the limit of the flight envelope. They present an overshoot *OS* higher than 30% and a long settling time *Ts* which reduces the controllability (handling quality level); excess weights can affect the structural limits given by the designer; high speeds can affect the aerodynamic forces and can lead to aircraft failure (loss of control surfaces). Moreover, if we compare the two algorithms, it can be deduced that the results obtained by using the DE algorithm are more accurate than those obtained by the GA optimization.

The *H-Infinity* method thus gives a controller that approximates the good handling qualities level 1 for both longitudinal and lateral motions as given in Table 5-2, improves the aircraft's stability, and its dynamic performance'. This is the first time that such research was performed on the flight control clearance using a real business aircraft model for its validation. In this research different flight conditions were used to cover the entire flight envelope to validate the *H-Infinity* controllers. In the previous researches performed in the aeronautical filed only one controller (X_{CG} location) was optimized for unmanned aircrafts or helicopters.

5.5.3 Non-linear validation

Finally, to prove the efficiency of the optimized controller and its robustness against uncertainties, a nonlinear validation was performed using the Cessna Citation X aircraft's non-linear model developed to simulate a real aircraft dynamics, using the Cessna Citation X Research Simulator data. A simulation of a pitch angle rate q and roll angle φ controls responses were performed, with the results as shown respectively in figures 5-23, 5-25 for the altitude of 2000 ft, TAS of 230 knots and load of 26000 lb, and varying mass shown in figures 5-24 and 5-26.

It can be seen that the pitch angle rate q and roll angle φ responses remain stable during the simulation, and that all the performance criteria are reached; therefore the system is robust as desired.

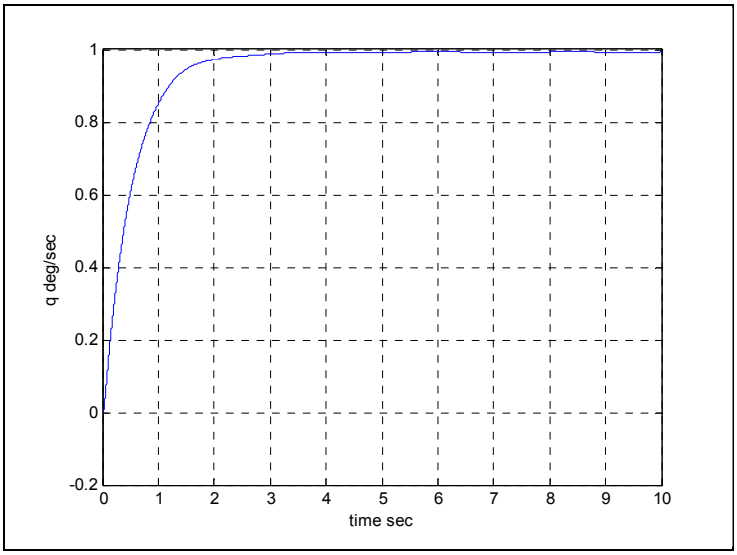

Figure 5-23 Pitch angle rate ***q*** hold control responses using nonlinear aircraft model

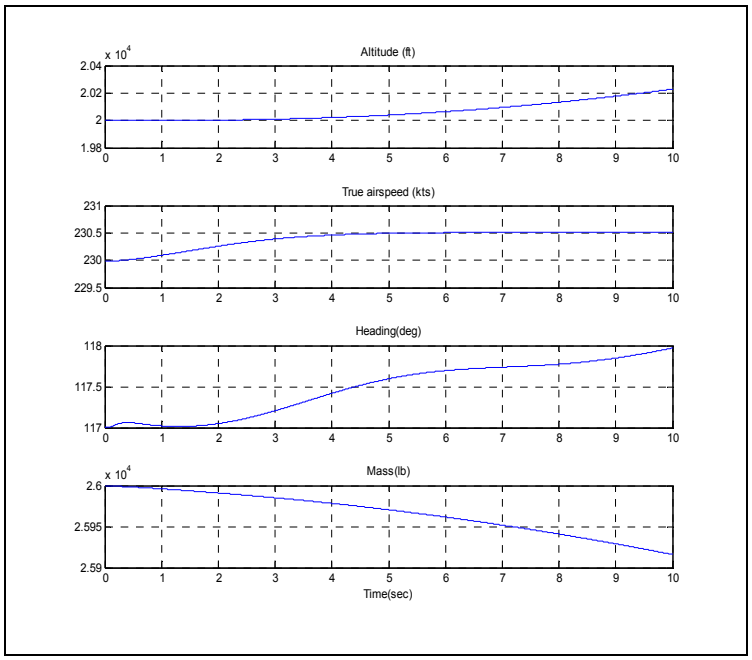

Figure 5-24 Altitude, true airspeed, heading and masse variation responses using nonlinear aircraft model

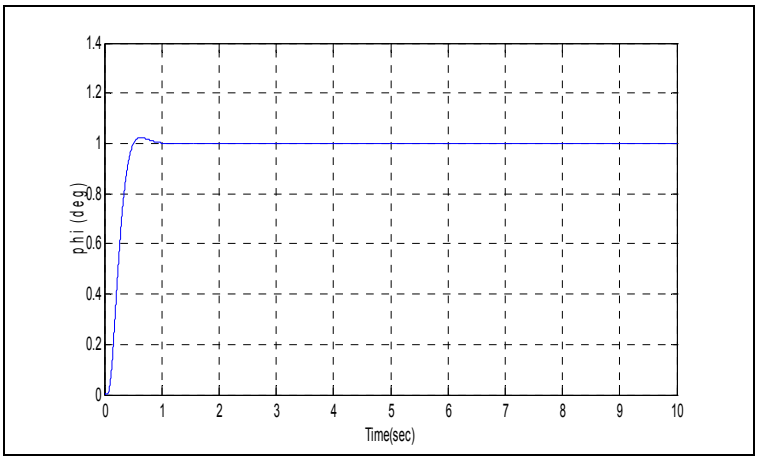

Figure 5-25 Roll angle φ control responses
on a nonlinear aircraft model

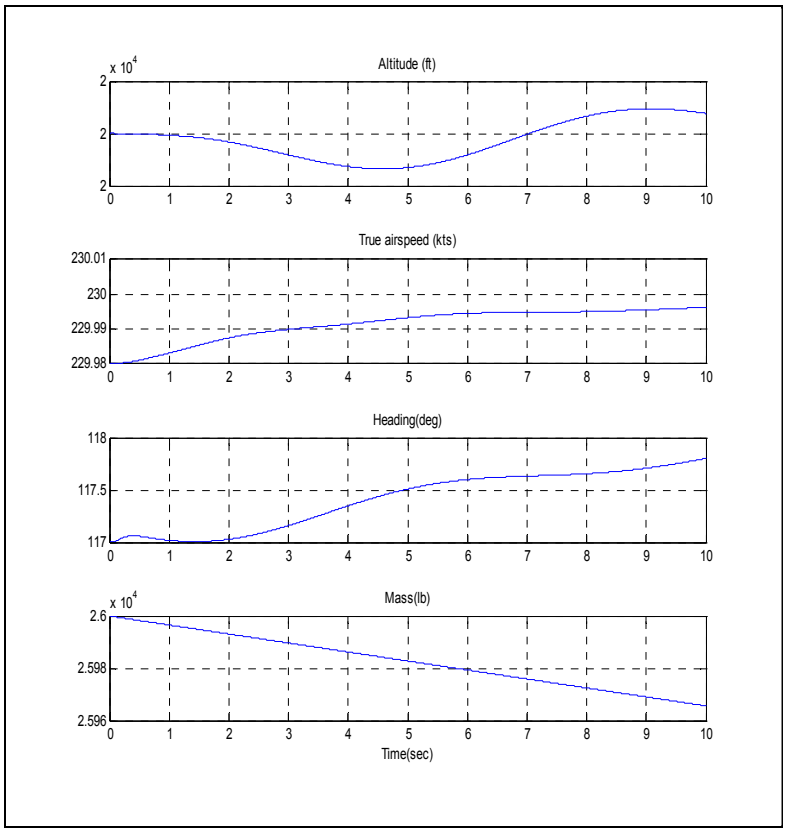

Figure 5-26 Altitude, true airspeed, heading and mass
variation responses on a nonlinear aircraft model

5.5.4 Robustness analysis of H-infinity controller

Figures 5-27 and 5-28 show robustness results for the *H-infinity* controller. The tests were performed on the nonlinear model of the Cessna Citation X that takes into account the nonlinear dynamics, actuators, sensors, saturations and signal processing times. A total of 160 tests were performed by generating uncertainty of +/- 5% on the mass and the center (position of center of gravity) with respect to a nominal condition for which the controller was obtained. The selection of the nominal flight condition and uncertainties were random. The results obtained on pitch rate control and roll angle control are presented in the following figures.

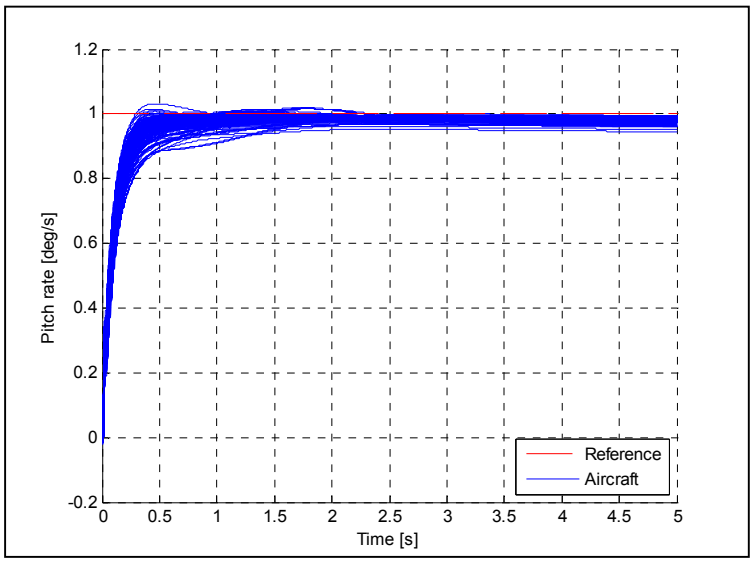

Figure 5-27 Pitch rate *q* response using mass and the center variation

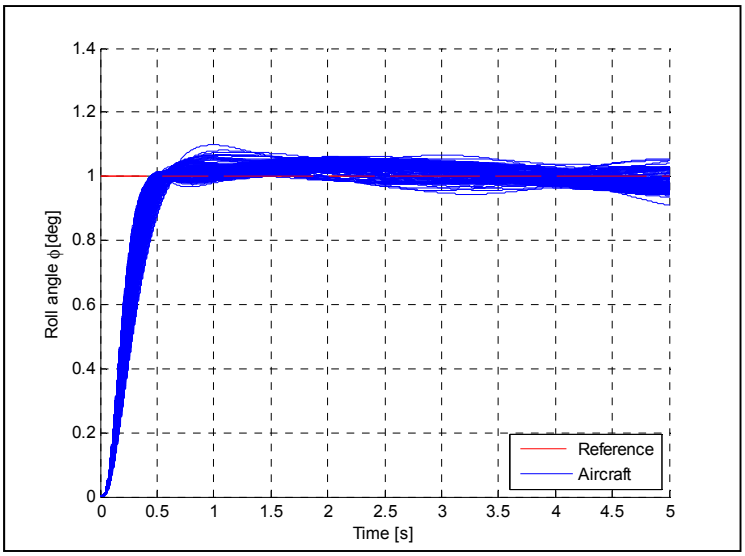

Figure 5-28 Roll angle φ response using mass and the center variation

The results reveal that the pitch rate, and roll angle controls are stable with respect to the mass, and center of gravity position variations, where their variations are stable and included in the acceptable range.

5.6 Conclusion

This paper presented a new application of evolutionary robust design controller, which aims to develop controllers providing robustness against disturbances and uncertainties that are present in the real environment.

In this study, the weighting functions were determined using two different evolutionary algorithms, the Differential Evolution (DE) and the Genetic Algorithms (GA); one of their greatest advantages is that no prior knowledge is required about the control method. Using these evolutionary algorithms over conventional optimizations improves the reliability, and effectiveness of the clearance process due to their flexibility and adaptability.

Combined with the *H-infinity* method, the proposed objective function helps to reduce considerably the calculation time of both algorithms DE and GA, rather than the use of more complicated methods. However, the solution given by the DE algorithm optimization is more efficient and accurate than the GA optimization for the clearance process. The efficiency of the optimization based clearance is due to its flexibility by concerning the formulation of the clearance criteria (as the handling qualities, robustness, and time performance criteria).

Simulations were performed using the resulting optimal gains for the Cessna Citation X aircraft's longitudinal and lateral motions, for 12 centering (X_{CG} positions) and 72 flight conditions, selected to cover the whole flight envelope. The optimized feedback gains enhanced the aircraft's closed-loop performances, according to handling qualities level 1, and designer specifications, while the Differential Evolution (DE) and Genetic Algorithms (GA) demonstrated a high efficiency in global optimization with minimum time convergence. In this research, new tools have been developed to validate the results of linear and nonlinear models, which provide a clear and accurate analysis for the user, and to facilitate the controller's certification process.

Acknowledgements

This work was performed at the LARCASE (Laboratory of active controls, avionics and aeroservoelasticity research). We would like to thank to the project leader Mr Ken Dustin and his team at CAE Inc. for their support in the development of the Aircraft Research Flight Simulator at the LARCASE laboratory. This simulator was obtained thanks to research grants that were approved by the Canada Foundation for Innovation (CFI) and the Ministère de Développement de l'Économie, de l'Innovation et de l'Exportation MDEIE. In addition, this research was funded by the Natural Sciences and Engineering Research Council of Canada NSERC in the frame of Canada Research Chair Programs; Dr Ruxandra Botez is Canada Research Chair Holder in Aircraft Modeling and Simulation Technologies. Thanks are also due to Mrs Odette Lacasse and Mr Oscar Carranza at ETS for their continuing enthusiasm and support.

CHAPITRE 6

OPTIMAL CONTROL NEW METHODOLOGIES VALIDATION ON THE RESEARCH AIRCRAFT FLIGHT SIMULATOR OF THE CESSNA CITATION X BUSINESS AIRCRAFT

Yamina Boughari, Georges Ghazi, Ruxandra Mihaela Botez

LARCASE Laboratory of Applied Research in Active Controls, Avionics and AeroServoElasticity
ETS, 1100 Notre Dame West, Montreal, Que., Canada, H3C-1K3

This article was accepted on the 23rd January 2017 in the *International Journal on Contemporary Energy*

Résumé

Dans cet article, Les critères de la certification de l'avion Cessna Citation X ont été analysés pour un nouveau contrôleur de vol. Ce contrôleur de vol a été conçu et optimisé en utilisant une combinaison de la méthode H-infini et de l'algorithme de l'évolution différentielle, lors d'une recherche précédente. La stabilité linéaire, les valeurs propres, et les critères de manœuvrabilité, en plus des critères d'analyse non linéaires ont été investigués au cours de cette recherche visant à évaluer l'avion d'affaires dans le but de certifier sa commande de vol. Les gains optimisés fournissent une bonne marge de stabilité, l'analyse des valeurs propres montre que l'avion se comporte presque avec une grande stabilité et une très bonnes qualités de vol du modèle d'avion linéaire dans toute son enveloppe de vol. De plus l'avion montre une robustesse en dépit de la variation de masse de centre de gravité.

Abstract

In this paper, the Cessna Citation X clearance criteria were evaluated for a new Flight Controller. This Flight Controller was designed and optimized using a combination of the *H-infinity* method and the Differential Evolution algorithm, during a previous research. The linear stability, eigenvalue, and handling qualities criteria in addition of the nonlinear

analysis criteria were investigated during this research to assess the business aircraft for flight control clearance and certification. The optimized gains provide good stability margins, as the eigenvalue analysis shows that the aircraft has a high stability, and a very good flying qualities of the linear aircraft models are ensured in its entire flight envelope, its robustness is demonstrated with respect to uncertainties due to the mass and canter of gravity variations.

6.1 Introduction

The clearance of the flight control laws of a civil aircraft is a fastidious process, especially for modern aircrafts that need to achieve high performance as shown in (C. Fielding, 2002) . This process aims to prove that the selected stability, robustness and handling requirements are satisfied against any possible uncertainties. Because of the high number of data, the parameters variations and their uncertainties have to be provided for the clearance of the large flight envelope. To carry out this process, a detailed description of methods and procedures, which are currently used in industry, was given by Udo Korte (Korte, 2002). The presence of uncertainties is related to many factors such as the mass and X_{CG} variations, aerodynamics data values, control surfaces dynamics and delays, and Air Data measurements errors (Boughari et Botez, 2012a). To demonstrate the effects of important uncertainties, the clearance criteria are considered as robustness criteria from the Airbus team point of view (Goupil et Puyou, 2013), and were applied in linear and nonlinear analysis. As well as in the simulation, of HIRM+ generic model and HWEM the realistic model aircrafts as given in (C. Fielding, 2002), a benchmark of high- fidelity generic civil aircraft was developed by Airbus for advanced flight control, and fault diagnosis research in (Goupil et Puyou, 2013). In (Menon, Bates et Postlethwaite, 2007) a stochastic robust flight control was applied to the highly uncertain nonlinear HIRM aircraft model and compared its robustness of flight control laws with other competitive flight control laws by using the Nichols plot. The research presented in (Slier Michiel., et al, 2003), highlighted the importance of the clearance task, where it summarized five (5) new analysis techniques applied to solve a benchmark clearance problem, researches and results of one of these 5 new techniques was presented extensively in (Varga A, et al, 2012), this technique is known as the clearance based

optimization technique. Linear and nonlinear Cessna Citation X business aircraft benchmark was developed at Laboratory of Active Controls, Avionics and AeroServoElasticity LARCASE in (Ghazi, 2014b; Ghazi et Botez, 2015c) by using a Cessna Citation X Level D Research Aircraft Flight Simulator designed and manufactured by CAE Inc. This benchmark was used for advanced flight control design and clearance (Boughari, et al 2014a), (Boughari, et al 2014b) for robust control analysis in (Ghazi, et Botez, 2015)-(Ghazi, et Botez, 2014), and for new identification methods designed and developed in (Hamel et al 2013, Hamel, et al 2014, Ghazi, et al,2015).

The clearance analysis of the linear and nonlinear Cessna Citation X business aircraft is addressed for the first time in this paper, which gives to the reader an excellent understanding of the criteria and visualization tools used in the assessment of the flight control laws. The aircraft linear model with actuators, and sensors dynamics are detailed, and then a brief description of the clearance criteria theory is listed. Analysis of results and conclusions is further given.

6.2 Cessna Citation X Aircraft, Actuators and Sensors Dynamic

The Cessna Citation X is the fastest civil aircraft in the world, as it operates at its speed upper limit given by Mach number of 0.935. The longitudinal and lateral motions of this business aircraft are described, as well as its flight envelope and the flying qualities requirements.

The aircraft nonlinear model for the development and validation of the flight control system used the Cessna Citation X flight dynamics, and was detailed in (Ghazi, 2014), (Ghazi et Botez, 2015a). This model was built in Matlab/Simulink based on aerodynamics data extracted from a Cessna Citation X Level D Research Aircraft Flight Simulator designed and manufactured by CAE Inc.

According to the Federal Administration Aviation (FAA, AC 120-40B),(FAA, 1991), the Level D is the highest certification level that can be delivered by the Certification Authorities

for the flight dynamics. More than 100 flight tests were performed on the Citation X Level D Research Aircraft Flight Simulator within the aircraft flight envelope to validate linear model in (Ghazi, 2014), and tests were performed extensively in order to identify the Cessna Citaion X aircraft model in (Hamel, 2013; Hamel, et al, 2014), and the engine model as in (Ghazi, et al, 2015).

Using trim and linearization routines developed by Ghazi and Botez in (Ghazi et Botez, 2015b), the aircraft longitudinal and lateral equations of motions have been linearized for different flight conditions in terms of altitudes and speeds, and different aircraft configurations in terms of mass and center of gravity positions. In order to validate the different models obtained by linearization, several comparisons of these models with the linear model obtained by use of identification techniques as the ones proposed in (Hamel, 2013) were performed for different flight conditions and aircraft configurations. Results have shown that the obtained linear models were accurate and could be further used to estimate the local behavior of the Cessna Citation X for any flight conditions.

6.2.1 Aircraft dynamics

The aircraft's dynamics is represented firstly by nonlinear equations representing the equations of motion in the three axis (x, y, z) as given in (Nelson, 1998), and secondly these nonlinear equations are linearized, the longitudinal and lateral motions are decoupled for each equilibrium point, which means that the longitudinal motion dynamics can be represented for each flight condition or equilibrium point under the form of the following state space equation, using the elevator as deflection angle input :

$$\dot{x}_{long} = A_{long}x_{long} + B_{long}u_{long} \tag{6.1}$$

$$A_{Long} = \begin{pmatrix} X_u & X_w & X_q & -g\cos\theta \\ Z_u & Z_w & Z_q & 0 \\ M_u + M_{\dot{w}}Z_u & M_w + M_{\dot{w}}Z_w & M_q + M_{\dot{w}}u_0 & 0 \\ 0 & 0 & 1 & 0 \end{pmatrix},$$

$$\mathrm{B_{Long}} = \begin{pmatrix} \mathrm{X_{\delta_e}} \\ \mathrm{Z_{\delta_e}} \\ \mathrm{M_{\delta_e} + M_{\dot{w}} Z_{\delta_e}} \\ 0 \end{pmatrix} \tag{6.2}$$

where the state vector $x_{long}(t)$ and the control vector $u_{long}(t)$ are given by:

$$x_{long}(t) = (u \quad w \quad q \quad \theta)^T \ , \ u_{long}(t) = \delta_e \tag{6.3}$$

In the same way the aircraft's lateral motion dynamics is also given by the state space equation, using the aileron and the rudder as deflection angle inputs:

$$\dot{x}_{lat} = A_{lat}\, x_{lat} + B_{lat} u_{lat}$$

$$A_{Lat} = \begin{pmatrix} Y_\beta/u_0 & Y_p/u_0 & -(1 - Y_r/u_0) & g\cos\theta_0/u_0 \\ L_\beta & L_p & L_r & 0 \\ N_\beta & N_p & N_r & 0 \\ 0 & 1 & 0 & 0 \end{pmatrix}, B_{Lat} = \begin{pmatrix} Y_{\delta_a}/u_0 & Y_{\delta_r}/u_0 \\ L_{\delta_a} & L_{\delta_r} \\ N_{\delta_a} & N_{\delta_r} \\ 0 & 0 \end{pmatrix} \tag{6.4}$$

where the state vector $x_{lat}(t)$ and the control vector $u_{lat}(t)$are given by:

$$x_{lat}(t) = (\beta \quad p \quad r \quad \phi)^T, \quad u_{lat}(t) = (\delta_a \delta_r)^T \tag{6.5}$$

The linear model of the Cessna Citation X is obtained for 36 flight conditions using the Cessna Citation X Aircraft Flight Research Simulator tests performed at our laboratory LARCASE (Hamel, 2013). The linearized model is further decomposed using the Linear Fractional Representation LFR method as explained (Poussot-Vassal et Roos, 2011) using the bilinear interpolation method is used to present 26 regions of the flight envelope by LFR models as shown in Figure 6-1(a). Thus, 72 flight points represented by state space models

are obtained for each Xcg and weight configuration for a total of 12 Xcg and weight configurations shown in Figure 6-1 (b).

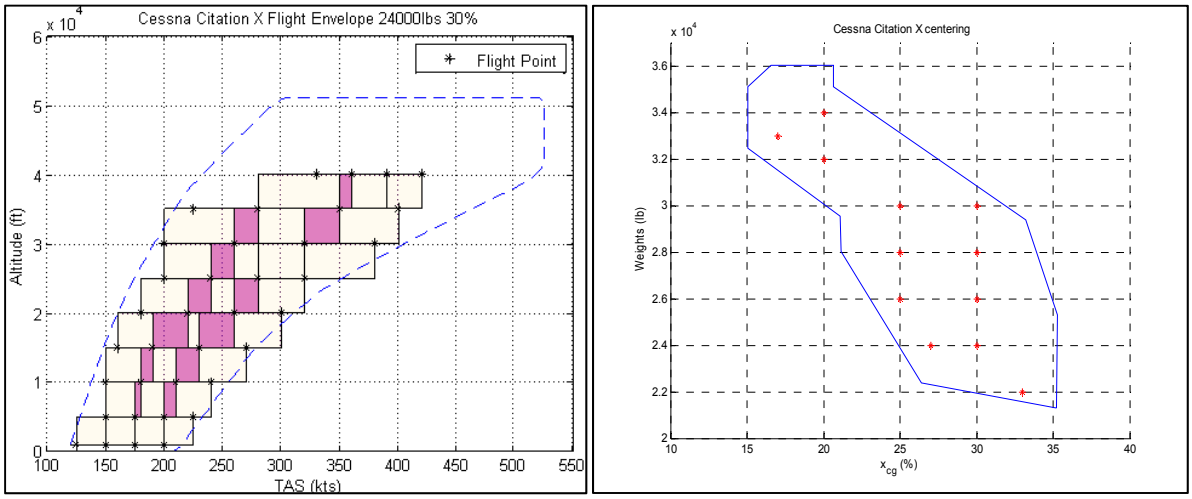

(a) (b)

Figure 6-1 (a) Flight envelope with LFR regions;(b)Weight versus X_{CG} envelope

6.2.2 Actuators and sensors dynamics

The actuators dynamics are provided from the literature by Ghazi (2014), and are given as second order transfer function; their damping and frequencies are mentioned in Table 6-1.

$$\frac{\omega^2}{s^2+2\zeta\,\omega s+\omega^2} \tag{6.6}$$

Table 6-1 Actuators dynamics characteristics

Actuator	Frequency ω [rad/sec]	Damping ζ	Angle [$^\circ$]	Rates[$^\circ$/s]
Elevators	60	0.7	$\pm$20	$\pm$30
Rudder	60	0.7	$\pm$20	$\pm$30
Ailerons	60	0.7	$\pm$60	$\pm$30

6.3 Flight Controller

The flight controller is designed, and optimized using a combination of the Hinfinity control method and the Differential Evolution algorithm, where the objective function used in the previous research combined both time domain performance criteria and frequency-domain robustness criterion, which led to good level aircraft flying qualities specifications and reduce considerably the time computing, this method is given in detailed in (Boughari et al., 2014c; Boughari et al., 2016).

6.4 Clearance Criteria

6.4.1 Linear stability and Eigenvalue analysis

The aim of the aircraft clearance and certification is to prove that the aircraft is stable over its full flight envelope, with sufficient margin stabilities, in the presence of uncertainties as. An overview of 5 new techniques for analysing the stability and robustness were considered in the industry in (Slier Michiel., et al, 2003). The basic theory of the linear stability was given in (Mack, 1975). While methodologies and results on these new techniques were presented in (Bates, Kureemun et Mannchen, 2003; De Oliveira et Puyou, 2011; Slier Michiel., et al, 2003; Garulli et al., 2010; Puyou, 2007). The weight functions method was applied on the business Hawker 800 XP, and on the HIRM aircrafts to assess their stability in (Anton et Botez, 2015; Anton, Botez et Popescu, 2013). In this paper linear stability margins for the pitch, and roll open-loop frequency responses were investigated for the Cessna Citation X business aircraft using Bode and Nichols plots.

The unstable eigenvalues either of the unaugmented aircraft or augmented closed-loop system must be identified for the worst cases (Stevens et Lewis, c2003). During this research, the open loop eigenvalues are identified by using “the robustness stability”, and analyzed using the GUI developed by the COFCLUO project (Garulli, 2015). In addition the closed loop eigenvalues are investigated by using zero poles map.

6.4.2 Linear, Nonlinear handling qualities, and Nonlinear analysis

The linear handling quality analysis is presented in time domain, and frequency domain criteria in (Jackson EB, 2009).

The time domain criteria are given by :

- ✓ Pitch acceleration peak time, pitch rate peak time, pitch rate overshoot/dropback, roll mode time constant, and time to bank.

The frequency domain responses and results, which are the most used to assess the linear handling criteria are defined in (Jackson EB, 2009):

- ✓ Pitch/bank attitude frequency response;
- ✓ The pitch/bank average phase rate, and the absolute amplitude should assess the resistance to Pilot Induced Oscillation (PIO);
- ✓ Frequency and damping of short period mode, dutch roll and Flight Control System (FCS) modes and their relationships with flight tests data parameters were given in (Botez et Rotaru, 2007).
- ✓ Closed-loop pitch axis bandwidth (Neal Smith), the open-loop pitch axis bandwidth (Hoh), and phase and gain margin criterion (Roger).

A civil aircraft should have good handling requirements in addition of the stability ones. The aircraft certification and assessment has to give the proof that the aircraft is capable to accomplish the flight easily with excellent handling qualities given by level 1 which is defined as the highest by the American military specification F-8785C (Jackson EB, 2009) among 3 levels of flying qualities. Also the non linear analysis has to investigate problems encountered in the linear analysis, and to evaluate the aircraft stability, handling and control in the presence of nonlinearities.

6.4.3 Pitch control , and Rapid roll

The aircraft maneuvers are usually evaluated in modern flight control according to (C. Fielding, 2002), which means that the load factor and angle of attack are proportional to the

pitch command (stick deflection). By using different inputs types (pull/push, step, and ramp), the required aircraft response trajectory should not exceed a given limit in the nominal aircraft model including added uncertainties.

The rapid roll control mode is a very important criterion to be checked for the nominal aircraft model or in presence of uncertainties. The maximum roll rates/overshoots, roll angle overshoot, maximum sideslip generated during roll, and the load factor have to be verified.

6.5 Analysis of Results

Closed loop simulations of the Cessna Citation X longitudinal and lateral aircraft linear and nonlinear models, were performed for the whole flight envelope. The results presented below were obtained for 12 X_{CG} and weight configurations, by using of 72 flight conditions obtained from both the Cessna Citation X flight simulator, and by using the interpolation method.

6.5.1 Stability analysis results

The phase margin for 26 regions (where each region is obtained for a number of 4 flight conditions) representing the entire flight envelope as shown in Figure 6-2. It can be noticed that the phase margin of almost the entire envelope is between 60 deg, and 90 deg, which is stable. If the results obtained for different weight and Xcg conditions are compared, we can see that they decreases for some flight conditions of heavy Gross Weights, high True Air Speeds (TAS), and Altitudes (h) above 35000 feet and 300 knots, and for those beyond the flight envelope limits. Detailed Bode and Nichols plots are shown in Figure 6-3, where the gain margin for almost the entire envelope is higher than 6 dB, which leads to the conclusion that good stability margins are ensured by the new optimized controller.

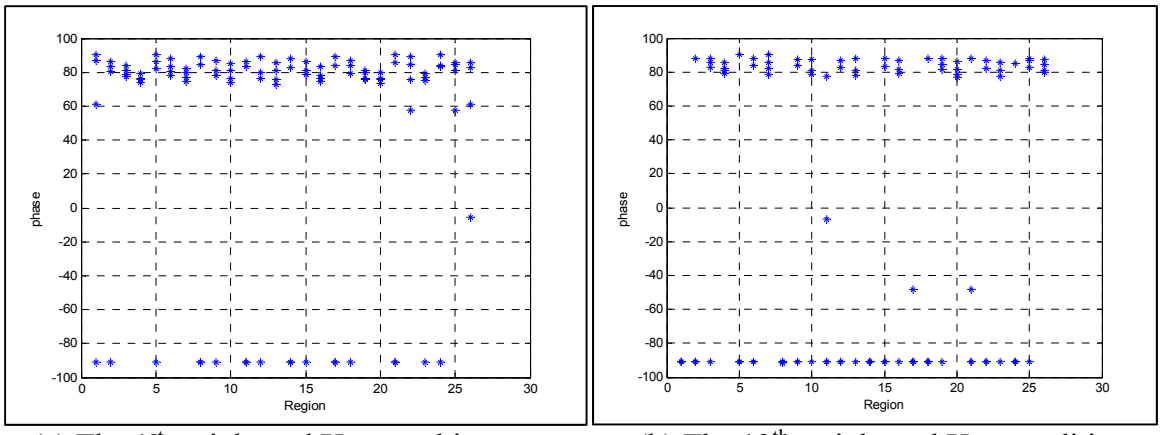

(a) The 1st weight and X_{CG} condtion (b) The 12th weight and X_{CG} condition

Figure 6-2 Minimum phase margin versus flight conditions per region for all Angle of attack (up to 14 deg)

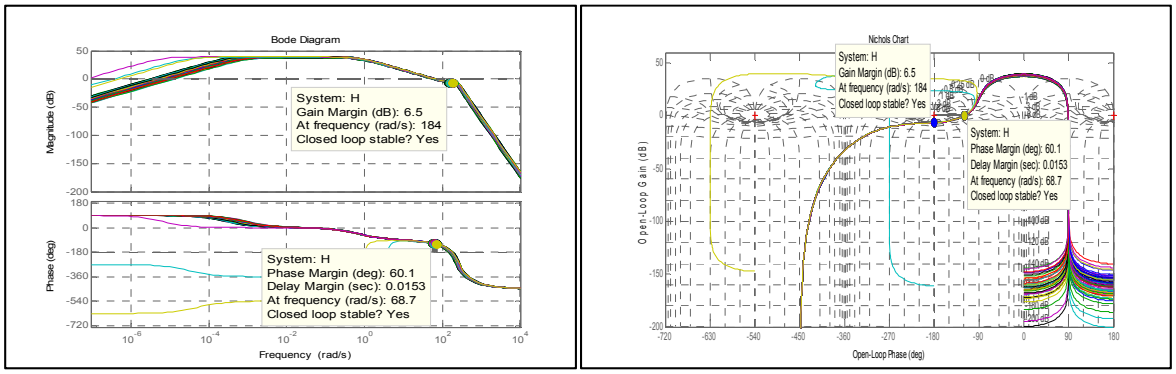

(a) Bode diagram (b) Nichols diagram

Figure 6-3 Bode diagram and Nichols

6.5.2 Eigenvalue results

The aircraft open loop eigenvalues are analyzed using the Lyapunov function given by the "Stabilty and Robustness" toolbox developed during COFCLUO project (developed in Europe in 2011), for a given weight and Xcg condition as shown in Figure 6-4. It can be deduced that the behaviour of the aircraft is "naturally stable" except for the region of very high altitudes and True Air Speeds (TAS), which is already shown by the stability margins results given in the Figure 6-2 and Figure 6-3, and also for other worst combination of parameters (altitude h and TAS). The closed loop eigenvalues are presented by pole zero

maps and are shown in Figure 6-5(b), where all flight conditions are given in the left half plan of the pole- zero map, which means that the new controller stabilizes the aircraft.

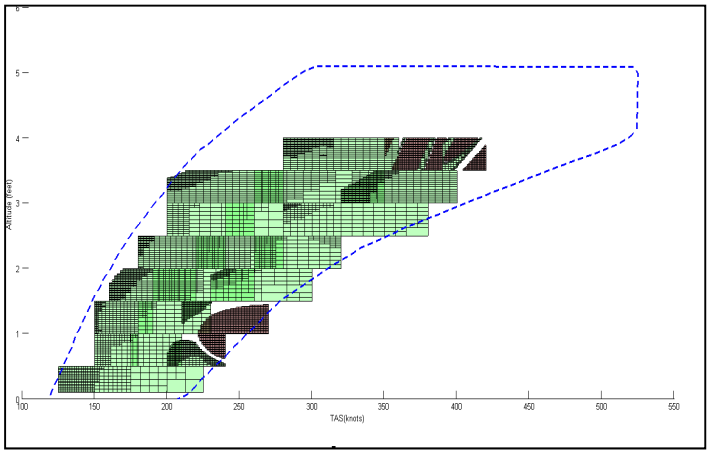

Figure 6-4 Aircraft stability analysis
using Lyapunov function.

6.5.3 Handling qualities analysis results

The aircraft longitudinal and lateral motions are stabilized with the *H-infinity* controller. For both controls the pitch angle rate q, and the roll angle ϕ, the resulting response shown for pitch rate control are shown in Figure 6-5: the flying qualities level 1 are satisfied as they have the damping ratio, and natural frequency within the limits given by (Jackson EB, 2009) for both lateral and longitudinal motions, and the imposed time domain performance, given by the Integral Square Error (ISE) less than 2%, and overshoot (OS) of less than 30%, which means that the optimized gains are very satisfactory, they ensure a very good flying qualities of level 1. The results in Table 6-2 show the percentage of the cleared flight envelope according to the Flying qualities level 1, by using the new optimized controller in both the pitch and roll angle controls.

Table 6-2 Flight points with the good handling qualities over the flight envelope

Controls	Flight points with the good handling qualities using the DE algorithm
Pitch rate q	860/864 (99.5%)
Roll angle φ	851/864 (98.5%)

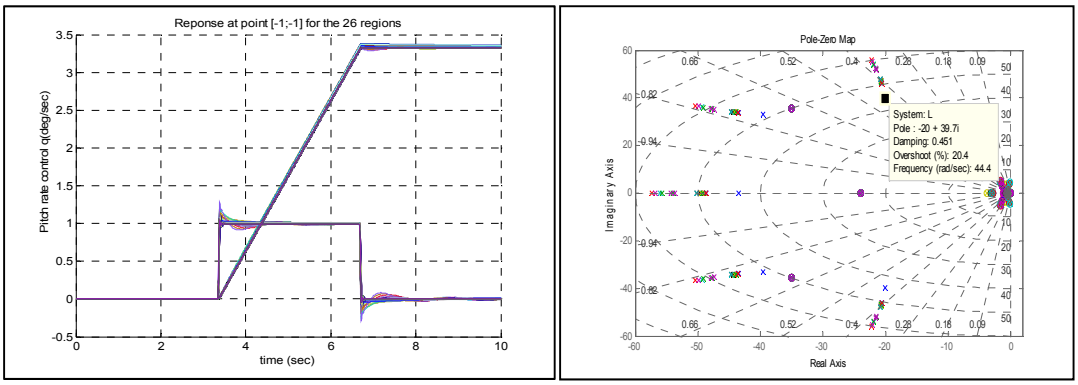

(a) (b)

Figure 6-5 (a) Time response for the pitch rate q and (b) the resulting pitch angle and pole, zero map

6.5.4 Nonlinear analysis results

Finally, to prove the efficiency of the optimized controller, its robustness against uncertainties, and the effects of nonlinearities, a nonlinear validation was performed using the Cessna Citation X aircraft's non-linear model developed to simulate a real aircraft dynamics. A simulation of a pitch angle rate q and roll angle ϕ controls responses were performed, and the results were shown respectively in Figure 6-6, and Figure 6-7 for the altitude of 2000 ft, TAS of 230 knots and load of 26000 lb, and varying mass.

It can be seen that the pitch angle rate q and roll angle ϕ hold responses remained stable during the simulation despite the mass variation, and that all the performance criteria were reached.

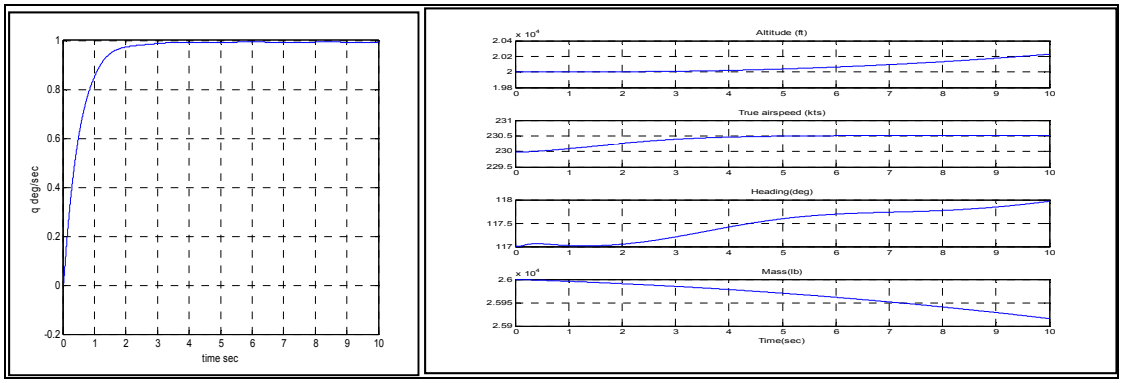

Figure 6-6 Pitch angle rate q hold control responses and the resulting altitude, true airspeed, heading and mass variation responses of the nonlinear aircraft model

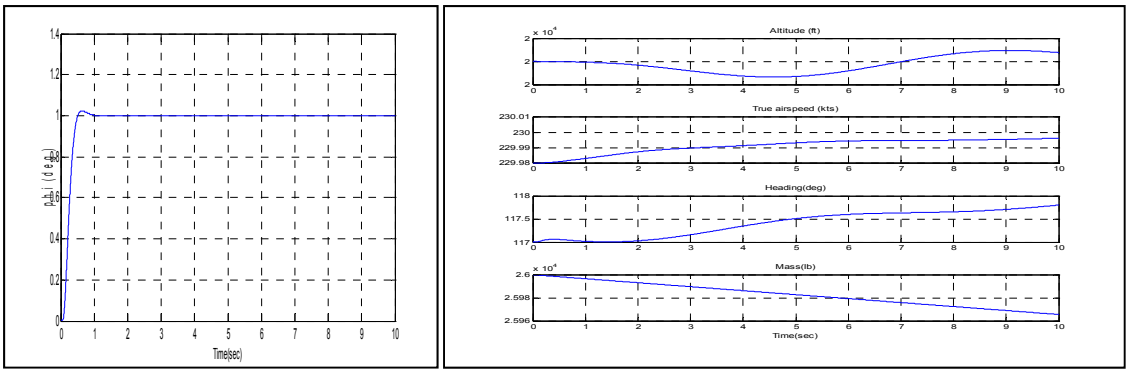

Figure 6-7 Roll angle ϕ control responses of the nonlinear aircraft model

Figure 6-8 (a) and (b) show robustness results for the nonlinear model of the Cessna Citation X with H∞ controller by taking into account the nonlinear dynamics, actuators, sensors, saturations and signal processing times. A total of 160 tests were performed by generating uncertainties of +/- 5% on the mass and the center (position of center of gravity) with respect to a nominal condition for which the controller was obtained. The selection of the nominal flight condition and uncertainties were random. The results revealed that the pitch rate, and roll angle controls were stable with respect to the mass, and center of gravity position variations; the variations were stable and further included in the acceptable range.

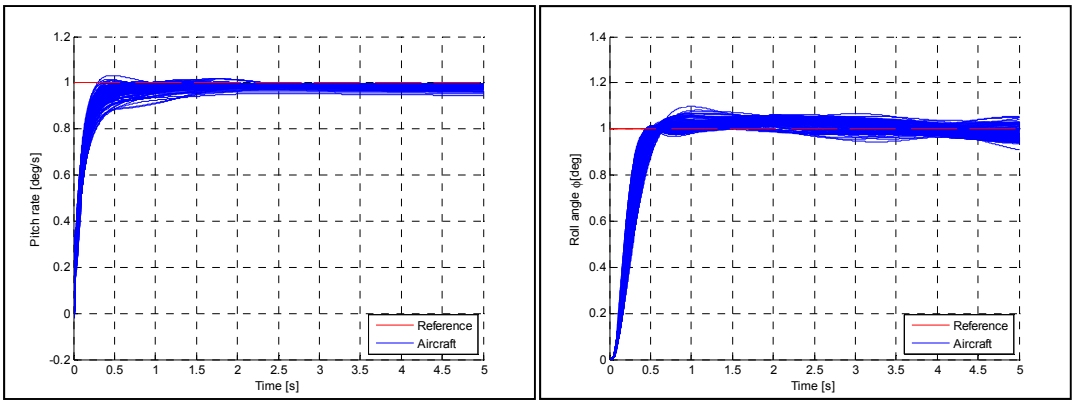

(a) (b)

Figure 6-8 Pitch rate q (a) and Roll (b) response using mass and X_{CG} variation

6.6 Conclusion

In this paper, the clearance criteria for the new flight controller of Cessna Citation X business aircraft were evaluated, which is a part of the certification process. The clearance addressed how flight limitations were derived for the Cessna Citation X business aircraft from the worst cases parameters combinations, such as True airspeed (TAS) and altitude (h), and they could be visualized and analyzed to give precise information on the direction, which the aircraft was allowed to fly. These limitations were clearly shown by the eigenvalues analysis, where the stability of the aircraft could be analyzed in its flight envelope limits. The flight control laws design optimization provided gains that have ensured very good stability margins in terms of phases and gains, these gains also provided to the aircraft very good flying qualities of Level 1. Regarding the manoeuvres such as the pitch and roll hold, their stability and robustness in presence of uncertainties dues to the mass and center of gravity variations were tested on the nonlinear aircraft model, and the obtained results were found to be very good.

The new optimized controller had ensured its stability and robustness against mass variations to the Cessna Citation X business aircraft which has led to safe control flight operations.

DISCUSSION OF RESULTS

This section presents a summary and discussion of the results of an evaluation of the stability and control of a Cessna Citation X business aircraft using its RAFS.

The aircraft non linear and linear models were built in Matlab/Simulink based on aerodynamic data extracted from a Cessna Citation X Level D Research Aircraft Flight Simulator (RAFS). More than 100 flight tests were performed on the Citation X Level D RAFS within the aircraft's flight envelope to validate its nonlinear model. The RAFS was designed and manufactured by CAE Inc. According to the Federal Aviation Administration (FAA, AC 120-40B), the Level D is the highest certification level that can be delivered by the Certification Authorities for the flight dynamics of an aircraft.

The Cessna Citation X's linear longitudinal model was used in the stability analysis of its open loop system (without controller) for various airspeeds, altitudes, and weight / X_{CG} ratios. The linearized aircraft model was used in the design and validation of the flight control laws for both longitudinal (pitch rate, pitch angle) and lateral (roll rate and roll angle) motion models by using the LQR and the PI methods, where the controller gains were optimized using the Differential Evolution (DE). Furthermore, the design of the *H-infinity* robust controllers (pitch rate and roll controllers) were optimized by investigating the DE algorithm and the Genetic Algorithm (GA) performances.

The first research paper analyzed the Eigenvalue stability envelope of the Cessna Citation X. By generating a set of LFR-based uncertainties models, the stability analysis of the whole Cessna Citation aircraft in its flight envelope was performed for 12 Weight and Center of Gravity (X_{CG}) configurations, using the Lyapunov function. The automation of the LFR models' generation, developed in three different ways (directly, manually, visually) presents a very good interactive process that facilitates the generation of reduced LFR models as well as their validation with the full order model. The stability results have shown that the Cessna Citation was stable for most of the regions in its flight envelope, except for high altitude near

the stall limits, especially for high TAS, where the aircraft exhibited instability for three weight and X_{CG} configurations. The Cessna Citation X business aircraft flight envelope should therefore be limited, for safety reasons, in terms of altitude, TAS, and for those three weight/ X_{CG} configurations.

In the second research paper presented by Chapter 4, a flight control design optimization methodology based on the Differential Evolution (DE) algorithm was performed by using a combination of the LQR modern control and the PI classical control methods. The 1st level of handling qualities and the time response performance were used as an objective function. The gain scheduling of the different controllers indicate their smoothness. The results of the different control methodologies were expressed in terms of time, frequency responses, and pole zero maps. For the entire flight envelope, the 1st level of handling qualities and the time response performances were satisfied, the stability margins (phase and gain margins) of the different controllers were sufficient, and only varied slightly between flight conditions in terms of altitude and TAS. The aircraft controls were validated for more than 500 nonlinear flight cases in terms of weight and X_{CG} configurations, while the control tracked the reference command, and thus very good results were obtained.

In the third research paper, presented in Chapter 5, another flight control design optimization was performed by using the robust *H-infinity* modern control method. The performances of two different evolutionary algorithms were compared using the DE and the GA algorithms, where the frequency and the time responses performances were also considered in the objective function.

The resulting controllers were validated for more than 800 flight conditions in terms of altitude and TAS; covering the entire aircraft flight envelope. New tools were developed to assess the clearance of the optimized flight controller in its aircraft flight envelope. The results obtained by the DE algorithm were more efficient and accurate than those from the GA algorithm; the DE algorithm's results cleared the flight envelope for pitch rate control at 99.5%, and at 98.5% for the roll angle control, while in the GA the clearance of the pitch rate

controller was 98.96%, and that of the roll controller was 98%. The computation time for the DE algorithm was less than for the GA by almost 40 sec, as shown the example in Chapter 5.

The roll hold control and the pitch rate hold control were performed on the nonlinear model for several flight conditions; both for controls tracked the reference inputs. Robustness tests were performed for a total of 160 flight cases by generating uncertainties of +/- 5% of the weight and of the X_{CG} center (position of center of gravity) with respect to a nominal condition for which the controller was obtained. The results show that both hold controls remained stable throughout these uncertainties.

In the fourth paper presented by Chapter 6, some of the linear and nonlinear criteria were evaluated for the newly- optimized flight controllers, such as the linear stability (eigenvalue) criterion, stability margins' criterion, linear handling qualities, and the nonlinear simulation criteria. All of these criteria were satisfied, indicating that the Cessna Citation X was stable and presented very good handling qualities.

CONCLUSION AND RECOMMENDATIONS

Several different issues were addressed in this thesis, and now several conclusions can be made: working with real aircraft data is a definite advantage, there is an optimal combination of handling qualities' requirements and the time response performance in the objective function of controller optimization problems, the evolutionary algorithms GA and DE have been proven to offer reliably high performance, LFR model based uncertainties are clearly useful in stability analyses, and the advantages of using *LQR* and *H-infinity* methodologies have been demonstrated.

The opportunity to work with a Level D Research Aircraft Flight Simulator RAFS in our LARCASE laboratory allowed us to manipulate real aircraft data, and to use them for the linear and nonlinear model validations. The RAFS is equipped with high dynamics certified at the highest level D by the FAA.

An airplane must pass a multitude of tests prior to its certification. Some of these tests involve the development of aircraft flight control laws that assess whether an aircraft is able to fly safely in a variety of conditions. Some of the aircraft flight control design criteria are based on the handling qualities' requirements used in aircraft Flight Control Law (FCL) clearance criteria in the aeronautical industry, while other criteria are based on the desired time and frequency response performances and the designer's experience. The combination of these criteria, considered as "objective functions" in the optimization algorithms, considerably reduces the computation time needed to reach the optimal (or sub-optimal) controller solution. The resulting controllers can thus verify the most important linear handling qualities requirements in FCL clearance criteria.

Aircraft state space models need to cover a wide range of flight points over the entire flight envelope, and thus require significant amount of computing time to assess the stability of each model. LFR model based uncertainties would be extremely useful for representing real aircraft model parameter variations over their entire flight envelopes, thereby allowing for

very good stability and its robustness analysis, as required by the FCL clearance criteria. However, the generation and the automation of LFR models is one of the most critical steps in the analysis of the clearance criteria; there are many methods for generating LFR models depending on their parameter variations, that should be analyzed in the stability problem.

In this thesis, the Trend and Band numerical method was used. It is based on a set of the state space models' variation in terms of altitude, TAS and weight/Xcg configurations. This method performed perfectly for the Eigenvalu stability envelope case study.

The most widely-known advantages of the Differential Evolution (DE) and the Genetic Algorithms (GA) are that their application does not require prior knowledge about the control method type, and their reliability, as the controller gains are globally optimized with minimum time convergence.

By combining evolutionary algorithms such as DE and GA with control methods with respect to conventional optimizations to develop an ad hoc method improves the reliability and the effectiveness of the clearance process due to their flexibility and adaptability-. The efficiency of the optimization-based clearance criteria is due to its flexibility in terms of the formulation of the clearance criteria, expressed as the handling qualities, robustness, and time performance criteria.

In this thesis, the LQR method was used in stability augmentation systems which were able to guarantee good stability margins for the Cessna Citation X aircraft linear and nonlinear models. However, this LQR method assumed that all states were measurable, which was not realistic all the time, and consequently required an observer. Furthermore, the LQR could be combined with a PI controller to obtain the control augmentation system, which could lead to a degradation of the aircraft system's stability margins.

The *H-infinity* control method was applied to both stability and control augmentation systems, so that a robust controller with very good stability in terms of phase and gain

margins could be obtained. This controller rejects the disturbance, which means that the *H-infinity* control design always assumes the aircraft model plus its filters and actuators, as well as the worst case in the presence of perturbations.

While *LQR* controllers give simple and practical gains, and their scheduling is very smooth, it is the *H-infinity* that is well suited for robust control design with disturbance rejection.

The stability criterion can be reformulated to be a clearance criterion. As indicated by Airbus, it can be classified in four classes: 1) Eigenvalue stability, 2) turbulence, 3) comfort, and 3) maneuvers criteria (Puyou, 2007). Only two of these criteria were investigated here:

- ✓ The Eigenvalue stability criterion of the longitudinal model of the Cessna Citation X business aircraft for weight/Xcg, and altitude and TAS variations without a controller; in **Chapter 3**.
- ✓ The roll and pitch maneuvers, tested on more than 160 nonlinear models. The results are shown in **Chapter 5** and **Chapter 6.**

Future work could include investigating the aeroelastic stability and the robustness of the Cessna Citation X longitudinal closed loop aircraft model by using a *H-infinity* controller as developed in this thesis to show if the interaction of the flight controller with the Cessna Citation X would induce any instability. The aircraft's lateral stability in the presence of turbulence, as well as the comfort criteria and yaw control maneuver analysis could also be the objects of future studies.

APPENDIX A

CESSNA CITATION X BUSINESS AIRCRAFT USING UN LFR MODELS - USING A NEW GUI FOR THE EASY MANIPULATION OF LFRs

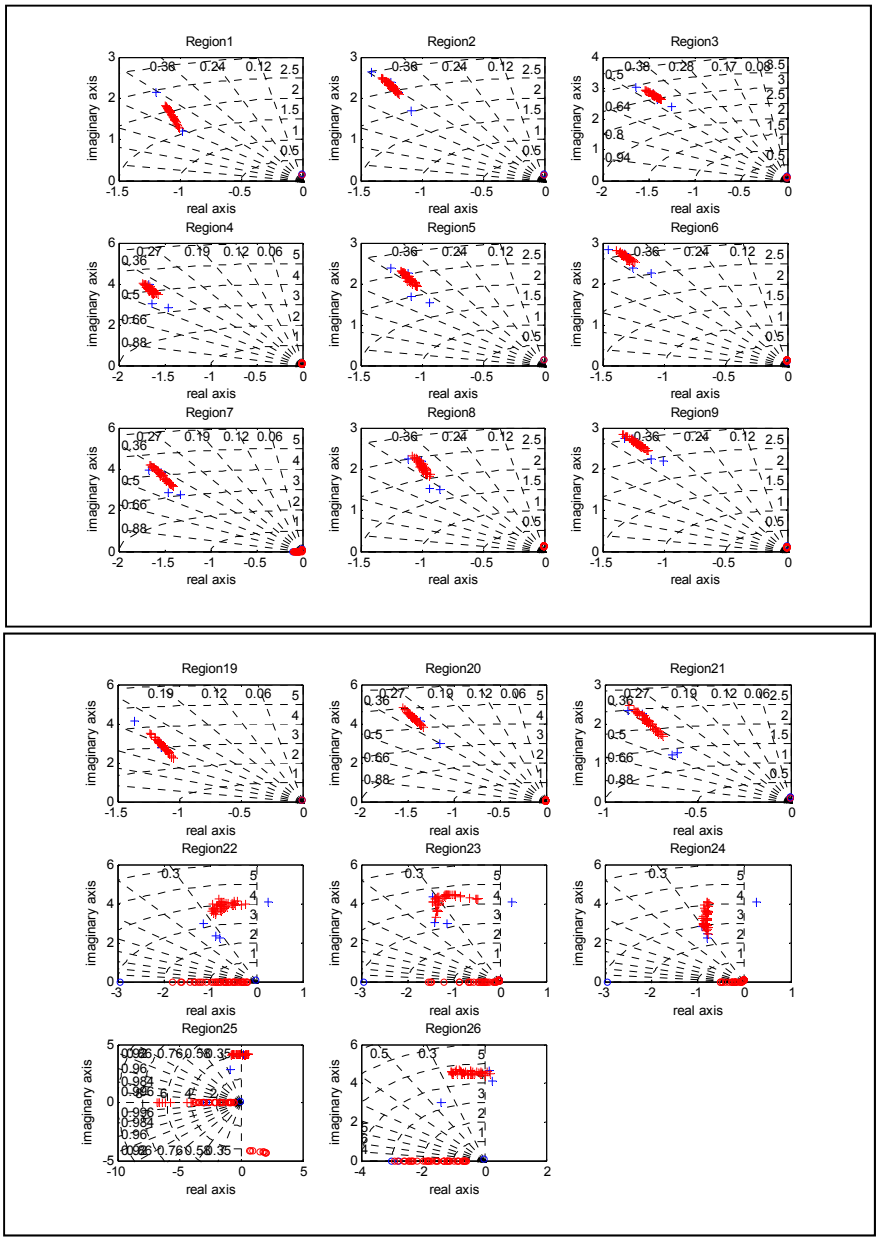

Figure A1 Comparison of eigenvalues for interpolated flight points with the reference values for low altitudes (0 -15000 ft) and high altitudes (30000 -40000 ft)

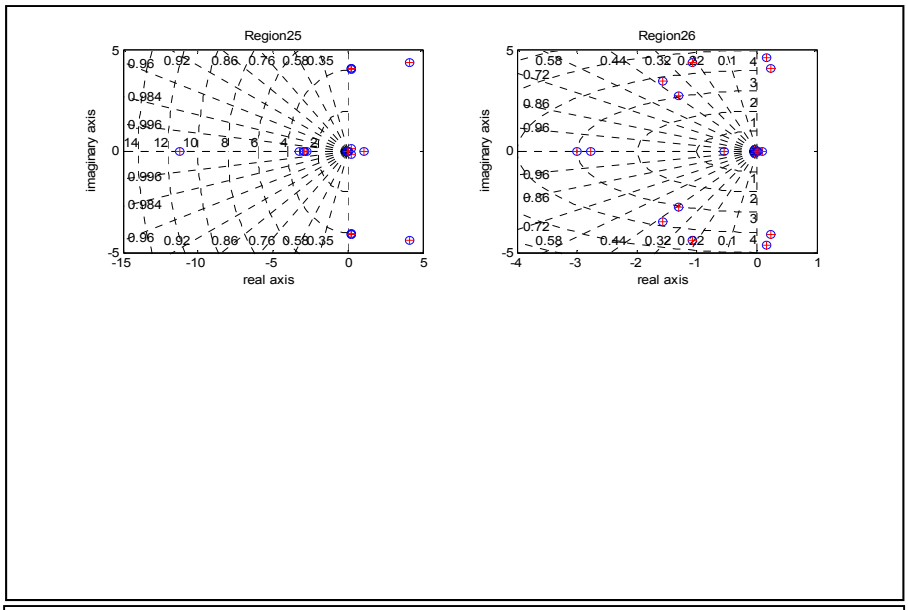
Region25
Region26
imaginary axis
real axis

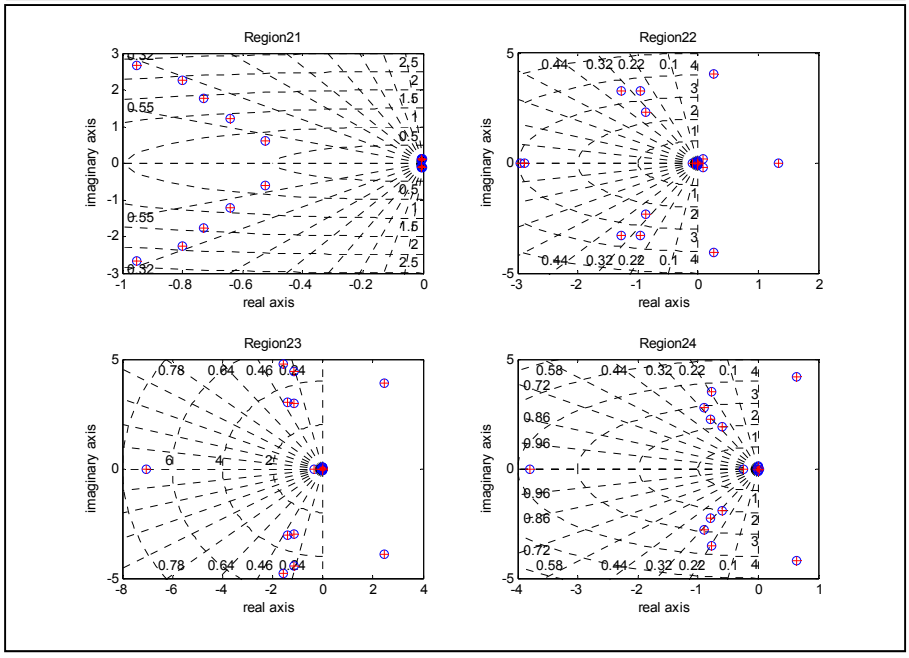
Region21
Region22
Region23
Region24
imaginary axis
real axis

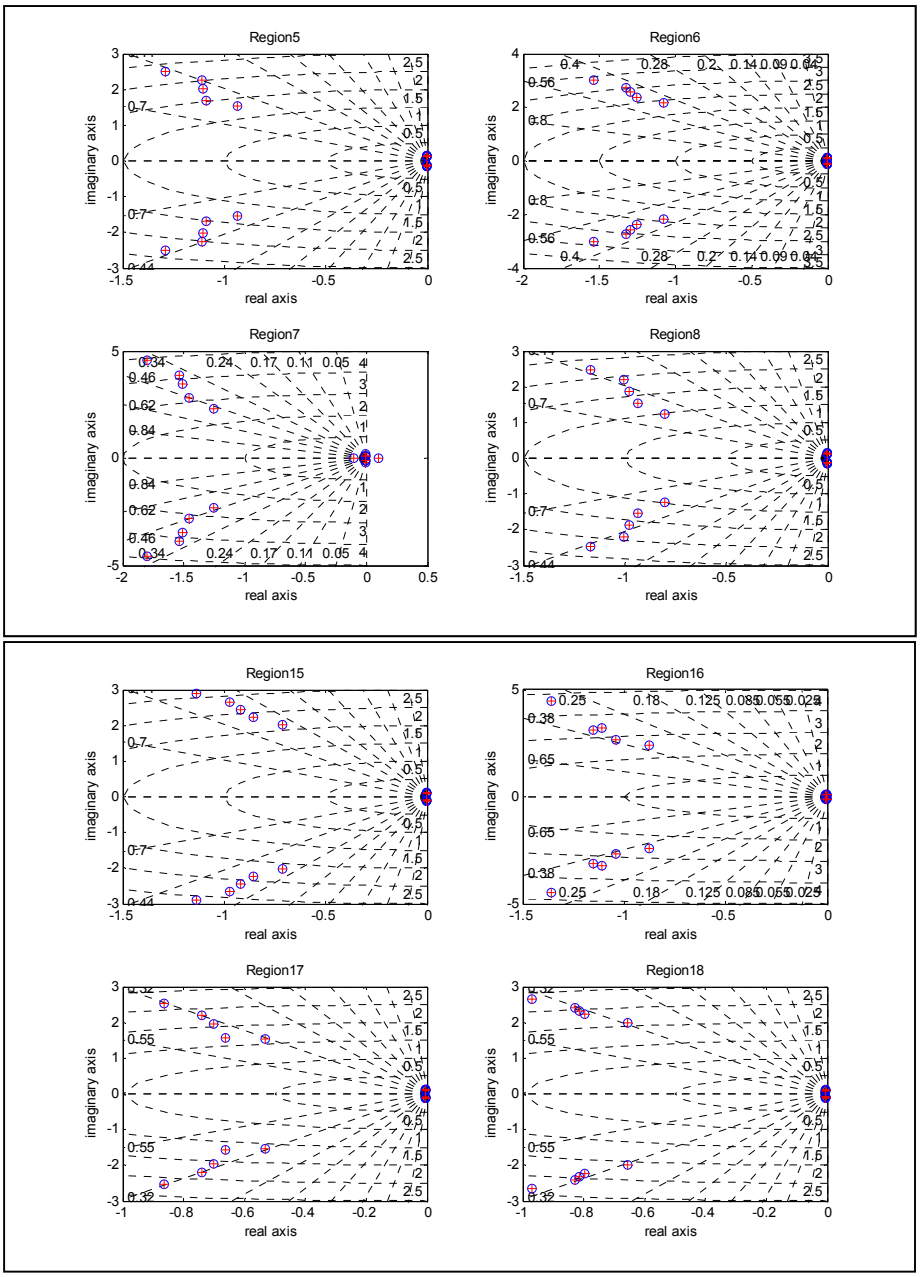

Figure A2 (24000lbs/30%) weight X_{CG} configuration comparison of full and reduced LFR order

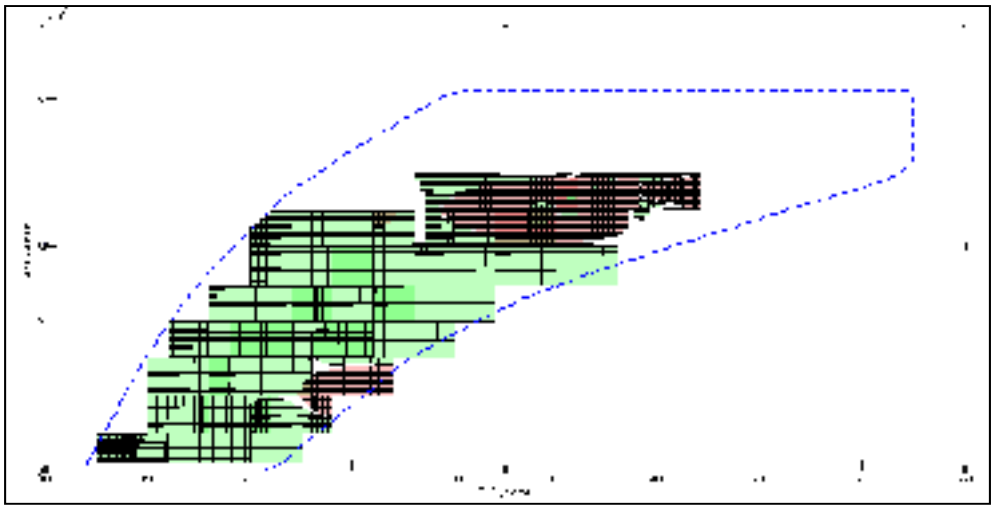

Figure A3 Stability analysis of a longitudinal model for the weight/ X_{CG} configuration (22000lbs/33%)

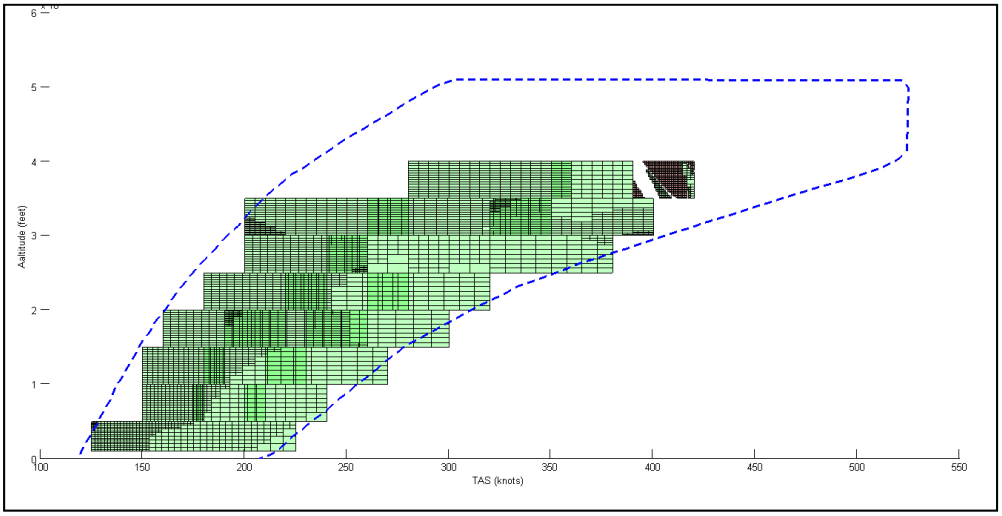

Figure A4 Stability analysis of a longitudinal model for the weight/ X_{CG} configuration (26000lbs/25%)

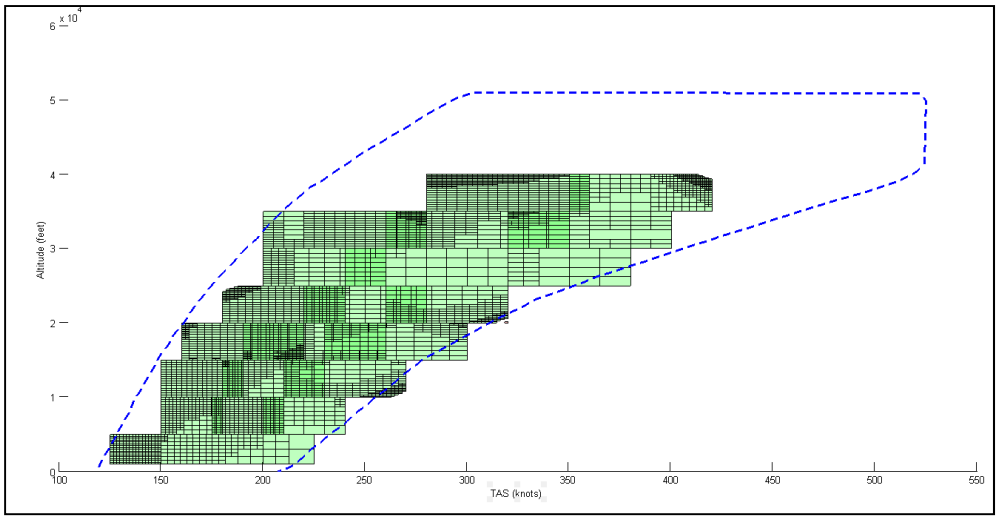

Figure A5 Stability analysis of a longitudinal model for the weight/ X_{CG} configuration (26000lbs/30%)

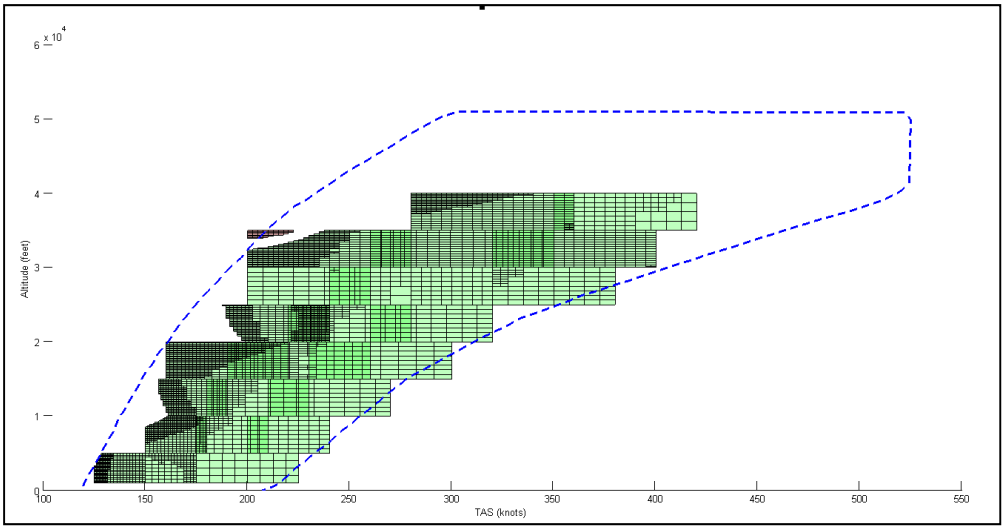

Figure A6 Stability analysis of a longitudinal model for the weight/ X_{CG} configuration (32000lbs/20%)

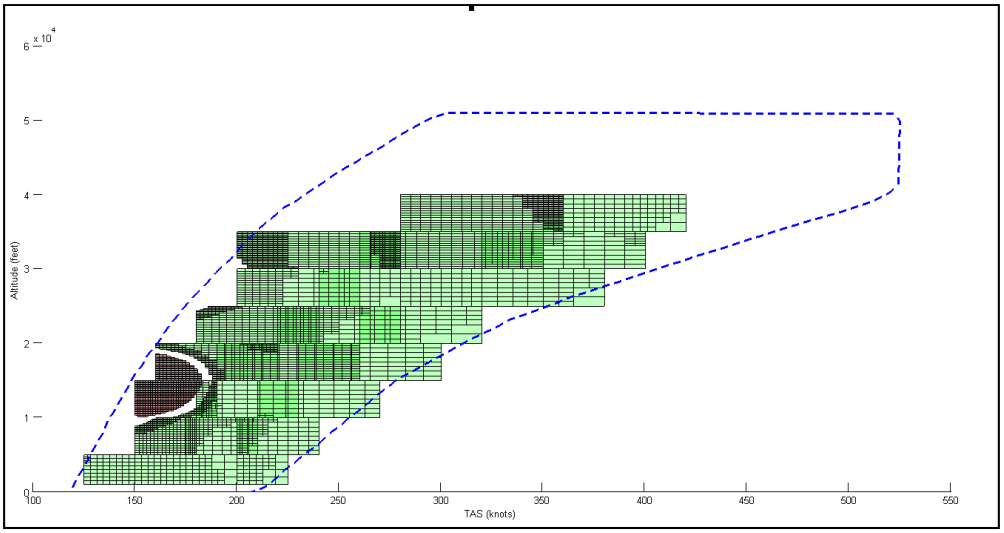

Figure A7 Stability analysis of a longitudinal model for the weight/ X_{CG} configuration (34000lbs/20%)

LIST OF REFERENCES

Anton, N., et R. M. Botez. 2015. « Weight Functions Method for Stability Analysis Applied as Design Tool for Hawker 800XP Aircraft ». *Aeronautical Journal,* vol. 119, nº 1218, p. 981-998.

Anton, N., R. M. Botez et D. Popescu. 2013. « Application of the Weight Function Method on a High Incidence Research Aircraft Model ». *Aeronautical Journal,* vol. 117, nº 1195, p. 897-912.

Aouf, N., B. Boulet et R. Botez. 2000. « H2 and H-optimal Gust Load Alleviation for a Flexible Aircraft ». In *Proceedings of 2000 American Control Conference (ACC 2000),* (Danvers, MA, USA *28-30 June 2000*.), Vol. 3, p. 1872-1876. Coll. « Proceedings of the 2000 American Control Conference. ACC (IEEE Cat. No.00CH36334) »: American Autom. Control Council. < http://dx.doi.org/10.1109/ACC.2000.879526 >.

Aouf, N., B. Boulet et R. Botez. 2002. « A Gain Scheduling Approach For a Flexible Aircraft ». In *American Control Conference, 2002. Proceedings of the 2002*. (Alaska, États-Unis, May 2002). Vol.6, p. 4439-4442,: IEEE.

Bacciotti, A., et L. Rosier. 2005. *Liapunov Functions and Stability in Control Theory*. Berlin Heidelberg : Springer-Verlag Berlin Heidelberg. 237 p.

Balas, Mark J, et Susan A Frost. 2013. « Discrete-Time infinite-Dimensional Adaptive Control and Rejection of Persistent Disturbances: To D or not to D? ». In *Control & Automation (MED), 2013 21st Mediterranean Conference.* (Plathania- Chania, Crete, Greece, June 25-28 2013), p. 1042-1049. New York: IEEE.

Balas, Mark J, et Susan A Frost. 2014a. « Direct Adaptive Control for Infinite-dimensional Symmetric Hyperbolic Systems ». *Procedia Computer Science,* vol. 36, p. 549-555.

Balas, Mark J, et Susan A Frost. 2014b. « Robust Adaptive Model Tracking for Distributed Parameter Control of Linear Infinite-dimensional Systems in Hilbert Space ». *IEEE/CAA Journal of Automatica Sinica,* vol. 1, nº 3, p. 294-301.

Baldelli, D. H., R. Lind et M. Brenner. 2005. « Nonlinear Aeroelastic/Aeroservoelastic Modeling by Block-oriented Identification ». *Journal of Guidance, Control, and Dynamics,* vol. 28, nº 5, p. 1056-64.

Bandyopadhyay, R., et D. Patranabis. 2001. « A New Auto-tuning Algorithm for PID Controllers Using Dead-beat Format ». *ISA Transaction*, vol. 40, nº 3, p. 255-66.

Bates, Declan G, Ridwan Kureemun et Thomas Mannchen. 2003. « Improved Clearance of a Flight Control Law Using μ-analysis Techniques ». *Journal of guidance, control, and dynamics,* vol. 26, nº 6, p. 869-884.

Beaven, RW, MT Wright et DR Seaward. 1996. « Weighting Function Selection in the H∞ Design Process ». *Control Engineering Practice,* vol. 4, nº 5, p. 625-633.

Becker, G., et A. Packard. 1994. « Robust Performance of Linear Parametrically Varying Systems Using Parametrically-dependent Linear Feedback ». *Systems & Control Letters,* vol. 23, nº 3, p. 205-215.

Biskri, Djallel Eddine, Ruxandra Mihaela Botez, Nicholas Stathopoulos, Sylvain Therien, Martin Dickinson et Alexandre Rathe. 2006. « New Mixed Method for Unsteady Aerodynamic Force Approximations for Aeroservoelasticity Studies ». *Journal of aircraft,* vol. 43, nº 5, p. 1538-1542.

Boely, N., R. M. Botez et G. Kouba. 2011. « Identification of a Non-Linear F/A-18 Model by the Use of Fuzzy Logic and Neural Network Methods ». *Proceedings of the Institution of Mechanical Engineers, Part G (Journal of Aerospace Engineering),* vol. 225, nº G5, p. 559-574.

Botez, R. M., I. Boustani, N. Vayani, P. Bigras et T. Wong. 2001. « Optimal Control Laws for Gust Alleviation ». *Canadian Aeronautics and Space Journal,* vol. 47, nº 1, p. 1-6

.

Botez, R. M., et M. Rotaru. 2007. « Relationships Between Flying Qualities and Flight Tests Parameters for the F/A-18 Aircraft ». *Aeronautical Journal,* vol. 111, nº 1118, p. 281-282

Boughari, Yamina, et Ruxandra Botez. 2012. « Optimal Flight Control on the Hawker 800 XP Business Aircraft ». In *IECON 2012 - 38th Annual Conference on IEEE Industrial Electronics Society*. (Montreal, Oct. 25-28, 2012), p. 5471-5476.

Boughari, Yamina, Ruxandra Mihaela Botez, Florian Theel et Georges Ghazi. 2014a. « Optimal Flight Control on Cessna Citation X Aircraft Using Differential Evolution ». In *IASTED International Conference on Modelling, Identification and Control, MIC*. (Innsbruck, Austria, Feb.17-19, 2014), p. 189-198. Coll. « Proceedings of the IASTED International Conference on Modelling, Identification and Control »: Acta Press. < http://dx.doi.org/10.2316/P.2014.809-052 >.

Boughari, Yamina, Ruxandra Botez, Georges Ghazi et Florian Theel. 2014b. « Evolutionary Algorithms for Robust Cessna citation X Flight Control ». In *SAE 2014 Aerospace Systems and Technology Conference, ASTC 2014,*. (Cincinnati, OH, United states Sept. 23-25, 2014), September Vol. 2014-September, p. Boeing Company; GE Aviation; IBM Corporation; L-3 Cincinnati Electronics; TTI Family of Companies.

Coll. « SAE Technical Papers »: SAE International. < http://dx.doi.org/10.4271/2014-01-2166 >.

Boughari, Yamina, Ruxandra Mihaela Botez, Georges Ghazi et Florian Theel. 2016. « Flight Control Clearance of the Cessna Citation X Using Evolutionary Algorithms ». *Proceedings of the Institution of Mechanical Engineers, Part G: Journal of Aerospace Engineering*, p. 0954410016640821.

Campa, Giampiero, Marcello Napolitano, Brad Seanor et Mario G Perhinschi. 2002. « Online Parameter Estimation Techniques Comparison Within a Fault Tolerant Flight Control System ». *Journal of Guidance, Control, and Dynamics,* vol. 25, nº 3, p. 528-537.

Chang-Hoon, Shin, Yoon Myung-Hyun et Park Ik-Soo. 1997. « Automatic Tuning Algorithm of the PID Controller Using Two Nyquist Points Identification ». In. (Tokyo, Japan, July 29, 1997), p. 1225-8. Coll. « *SICE '97. Proceedings of the 36th SICE Annual Conference. International Session Papers (IEEE Cat. No.97TH8323)* »: Soc. Instrum. & Control Eng. < http://dx.doi.org/10.1109/SICE.1997.624987 >.

Chen, Jian, et Chi-jian Zhang. 2009. « Control of Triple Inverted Pendulum Based on LQR Coefficients Optimization ». *Computer Engineering and Applications*, vol. 45, nº 29, p. 245-248.

Chen, Xiaoxia, Changyou Wang et Huazhu Wu. 2010. « PID Controllers Parameters Self-Tuning Algorithm Based on Frequency Characteristic ». In. (Piscataway, NJ, USA, Mar. 13, 2010), vol.2, p. 891-4. Coll. « *2010 International Conference on Measuring Technology and Mechatronics Automation (ICMTMA 2010)* »: IEEE. < http://dx.doi.org/10.1109/ICMTMA.2010.511 >.

Ciann-Dong, Yang, Ju Hann-Shing et Liu Shin-Whar. 1994b. « Experimental Design of H Weighting Functions for Flight Control Systems ». *Journal of Guidance, Control, and Dynamics,* vol. 17, nº 3, p. 544-552.

Cockburn, Juan C. 2000. « Multidimensional Realizations of Systems with Parametric Uncertainty ». In *Proceedings of MTNS*.

Cockburn, Juan C, et Blaise G Morton. 1997. « Linear Fractional Representations of Uncertain Systems ». *Automatica,* vol. 33, nº 7, p. 1263-1271.

Corless, M. 1994. « Robust Analysis and Design with Quadratic Lyapunov Functions ». In *Proceedings of the 12th Triennial World Congress of the International Federation of Automatic Control,*. (Oxford, UK, 18-23 July 1993), p. 181-184. Coll. « Automatic Control. World Congress 1993. Proceedings of the 12th Triennial World Congress of the International Federation of Automatic Control. Vol.2. Robust Control, Design and Software »: Pergamon.

Cortellessa, Vittorio, Bojan Cukic, Diego Del Gobbo, Ali Mili, Marcello Napolitano, Mark Shereshevsky et Harjinder Sandhu. 2000. « Certifying Adaptive Flight Control Software ». In *Proceedings, ISACC 2000: The Software Risk Management Conference*, (Northern Virginia, USA. Sept. 24-26, 2000).

D.-W. Gu, P. Hr.Petkov and M.M Konstatinov. 2005. *Robust Control Design with Matlab*. Coll. « Springer ». 393 p.

Da Fonseca Neto, J. V., et C. P. Bottura. 1999. « Parallel Genetic Algorithm Fitness Function Team for Eigenstructure Assignment via LQR Designs ». In *Proceedings of the 1999. Congress on Evolutionary Computation-CEC99,*. (Piscataway, NJ, USA. July 6-9, 1999, vol. 2, p. 1035-42. Coll. « Proceedings of the 1999 Congress on Evolutionary Computation-CEC99 (Cat. No. 99TH8406) »: IEEE. < http://dx.doi.org/10.1109/CEC.1999.782537 >.

De Oliveira, Rafael Fernandes, et Guilhem Puyou. 2011. « On the Use of Optimization for Flight Control Laws Clearance: a practical approach ». *IFAC Proceedings Volumes,* vol. 44, nº 1, p. 9881-9886.

Dettori, Marco, et Carsten W Scherer. 2000. « New Robust Stability and Performance Conditions Based on Parameter Dependent Multipliers ». In *Decision and Control, 2000. Proceedings of the 39th IEEE Conference on*. (Sydney,NSW, Dec. 12-15, 2000), vol. 5, p. 4187-4192. IEEE.

Deutschland, Airbus. 2003. « New Analysis Techniques for Clearance of Flight Control Laws ». En line, 20 p. <http://reports.nlr.nl/xmlui/bitstream/handle/10921/574/TP-2004-147.pdf?sequence=1 >. Consulté le 20 septembre 2015

Dong, Shuai, Zhisheng Wang, Yongji Wang, Lei Liu et Liuli Ou. 2013. « Tracking Performance Analysis of Flight Control System Based on *H-infinity* Theory ». *International Journal of Modelling, Identification and Control,* vol. 19, nº 3, p. 290-298.

Dorato, Peter Abdallah, C. T. (Chaouki T.) ; Cerone, Vito (Ed). c1995 *Linear-Quadratic Control : an Introduction* Englewood Cliffs, N.J. : Prentice-Hall, 205 p.

DUMOLLARD, Yannick. 2014. « Introduction to Fly By Wire Aircraft and New Technology ». Presentation. p. 53. On line < http://aviation-africa.eu/sites/default/files/events/105%20SIASA%20-%20Introduction%20Fly%20By%20Wire%20Aircraft%20and%20New%20Technology.pdf >. Consulté le 30-06-2016.

FAA, AC. 1991. « 120-40B," ». *Airplane Simulator Qualification*.

Favre, C. 1994. « Fly-By-Wire for Commercial Aircraft: the Airbus Experience ». *International Journal of Control,* vol. 59, nº 1, p. 139-157.

Félix Patrón, Roberto Salvador, et Ruxandra Mihaela Botez. 2015. « Flight Trajectory Optimization Through Genetic Algorithms for Lateral and Vertical Integrated Navigation ». *Journal of Aerospace Information Systems,* vol. 12, nº 8, p. 533-544.

Felix Patron, Roberto Salvador, Aniss Kessaci, Ruxandra Mihaela Botez et Dominique Labour. 2013. « Flight Trajectories Optimization Under the Influence of Winds Using Genetic Algorithms ». In *AIAA Guidance, Navigation, and Control (GNC) Conference,* (Boston, MA, United states, Aug. 19- 22, 2013.), p. Draper Laboratory. American Institute of Aeronautics and Astronautics Inc.

Felix Patron, Roberto Salvador, Adrien Charles Owono, Ruxandra Mihaela Botez et Dominique Labour. 2013. « Speed and Altitude Optimization on the FMS CMA-9000 for the Sukhoi Superjet 100 Using Genetic Algorithms ». In *2013 Aviation Technology, Integration, and Operations Conference,* (Los Angeles, CA, United states, Aug. 12-14, 2013). American Institute of Aeronautics and Astronautics Inc.

Fernandes De Oliveira, Rafael, et Guilhem Puyou. 2011. « On the Use of Optimization for Flight Control Laws Clearance: A Practical Approach ». In *18th IFAC World congress,* (Milano, Italy August 28- September 2, 2011). PART 1 vol. 18, p. 9881-9886. Coll. « IFAC Proceedings Volumes (IFAC-PapersOnline) »: IFAC Secretariat. < http://dx.doi.org/10.3182/20110828-6-IT-1002.00462 >.

Fielding, Chris, Andras Varga, Samir Bennani et Michiel Selier. 2002. *Advanced Techniques for Clearance of Flight Control Laws*, 283. Springer Science & Business Media. 449 p.

Friedland, Bernard. 2012. *Control System Design: an Introduction to State-Space Methods*. Courier Corporation. 528 p.

Frost, Susan A, Marc Bodson, John J Burken, Christine V Jutte, Brian R Taylor et Khanh V Trinh. 2015. « Flight Control with Optimal Control Allocation Incorporating Structural Load Feedback ». *Journal of Aerospace Information Systems,* vol. 12, nº 12, p. 825-834.

Frost, Susan A, Brian R Taylor et Marc Bodson. 2012. « Investigation of Optimal Control Allocation for Gust Load Alleviation in Flight Control ». In *AIAA Atmospheric Flight Mechanics Conference*. (Menneapolis, Minnisota, USA. Aug.13-16, 2012), p. 4858. Guidance, Navigation, and Control and Co-located Conferences. AIAA.

Frost, Susan, et Mark Balas. 2012. « Evolving Systems: An Outcome of Fondest Hopes and Wildest Dreams ». In Guidance, Navigation, and Control Conference, (Menneapolis,

Minnisota, USA. Aug.13-16, 2012), p. 4438. Guidance, Navigation, and Control and Co-located Conferences. AIAA.

Fu, Minyue, et Soura Dasgupta. 2000. « Parametric Lyapunov functions for uncertain systems: The multiplier approach ». *Advances in linear matrix inequality methods in control*, p. 95-108.

Kouba, G., R. M. Botez, N. Boëly. 2009. « Identification of F/A-18 Model from Flight Tests using the Fuzzy Logic Method ». In *Proceedings of the 47th AIAA Aerospace Sciences Meeting Including The New Horizons Forum and Aerospace Exposition*. (Orlando, FL, USA., 5-8 January 2009).

Balas G.J., A K.Packard, J.Renffrow,C.Mllaney, et R. T M'Closeky,. 1998. « "Control of The F-14 Aircraft Lateral-directional Axis During Powered Approach" ». *Journal of Guidance, Control, and Dynamics,* vol. 21, p. 899-908.

Garulli, Andrea, Alfio Masi, Simone Paoletti, and Ercüment Türkoglu. 2015. LFR RAI User's Guide. Technical Report. Coll. « Tech. Rep »: DII, Universit`a di Siena, Via Roma 56, 53100 Siena, Italy. 21 p. <http://www.dii.unisi.it/~garulli/lfr_rai/lfr_rai_users_guide.pdf >. Consulté le 03-09-20015

Garulli, Andrea, Alfio Masi, Simone Paoletti, Ercüment Türkoglu et Clément Roos. 2010. *D2. 3.5 Final Report WP2. 3*. Technical Report COFCLUO project, 41 p.< http://www.dii.unisi.it/~garulli/lfr_rai/D2.3.5.pdf>. Consulté le 03-09-2015

Ghazi, Georges. 2014. « Développement d'une Plateforme de Simulation et d'un Pilote Automatique- Application aux Cessna Citation X et Hawker 800XP ». Master University of Quebec-École Polytechnique de Montréal. 212 p.

Ghazi, Georges, et Ruxandra Botez. 2015a. « Development of a High-Fidelity Simulation Model for a Research Environment ». In *SAE AeroTech Congress and Exhibition, AEROTECH 2015*. (Seattle, WA, United states. Sept. 22-24, 2015), September Vol. 2015-September. Coll. « SAE Technical Papers »: SAE International. < http://dx.doi.org/10.4271/2015-01-2569 >.

Ghazi, Georges, Ruxandra Botez et Joseph Messi Achigui. 2015. « Cessna Citation X Engine Model Identification from Flight Tests ». *SAE International Journal of Aerospace,* vol. 8, nº 2015-01-2390, p. 203-213.

Ghazi, Georges, et Ruxandra Mihaela Botez. 2014. « New Robust Control Analysis Methodology for Lynx Helicopter and Cessna Citation X Aircraft using Guardian maps, Genetic Algorithms and LQR Theories Combinations ». In *70th American Helicopter Society International Annual Forum 2014,*. (Montreal, QC, Canada May

20-22, 2014) Vol. 4, p. 3138-3146. Coll. « Annual Forum Proceedings - AHS International »: American Helicopter Society.

Ghazi, Georges, et Ruxandra Mihaela Botez. 2015b. « Lateral Controller Design for the Cessna Citation X with Handling Qualities and Robustness Requirements ». In *62nd Canadian Aeronautical Society Institute CASI Aeronautics Conference and AGM,* (Montreal, Quebec, Canada, May, 19-21, 2015).

Ghoreishi, S. Amir, et Mohammad-Ali Nekoui. 2012. « Optimal Weighting Matrices Design for LQR Controller Based on Genetic Algorithm and PSO ». In *2011 International Conference on Material Science and Information Technology, MSIT2011,*. (Singapore, Singapore Sept. 16-18, 2011) Vol. 433-440, p. 7546-7553. Coll. « Advanced Materials Research »: Trans Tech Publications. < http://dx.doi.org/10.4028/www.scientific.net/AMR.433-440.7546 >.

Goupil, Ph, et Guilhem Puyou. 2013. « A High-Fidelity Airbus Benchmark for System Fault Detection and Isolation and Flight Control Law Clearance ». *EUCASS Proceedings Series,* vol. 6, p. 249-262.

Grigorie, T. L., R. M. Botez, A. V. Popov, M. Mamou et Y. Mebarki. 2012a. « A Hybrid Fuzzy Logic Proportionalintegral-Derivative and Conventional on-off Controller for Morphing Wing Actuation Using Shape Memory Alloy Part 1: Morphing System Mechanisms and Controller Architecture Design ». *Aeronautical Journal,* vol. 116, n° 1179, p. 433-449.

Grigorie, T. L., A. V. Popov, R. M. Botez, M. Mamou et Y. Mebarki. 2012b. « On-off and Proportional-Integral Controller for a Morphing Wing. Part 1: Actuation Mechanism and Control Design ». In. (55 City Road, London, EC1Y 1SP, United Kingdom), 2 vol. 226, p. 131-145. Coll. « *Proceedings of the Institution of Mechanical Engineers, Part G: Journal of Aerospace Engineering* »: SAGE Publications Ltd. < http://dx.doi.org/10.1177/0954410011408226 >.

Grigorie, T. L., A. V. Popov, R. M. Botez, M. Mamou et Y. Mebarki. 2012c. « On-off and Proportional-Integral Controller for a Morphing Wing. Part 2: Control Validation - Numerical Simulations and Experimental Tests ». In. (55 City Road, London, EC1Y 1SP, United Kingdom), vol. 2, 226, p. 146-162. Coll. « *Proceedings of the Institution of Mechanical Engineers, Part G: Journal of Aerospace Engineering* »: SAGE Publications Ltd. < http://dx.doi.org/10.1177/0954410011408271 >.

Grigorie, Teodor Lucian, Ruxandra Mihaela Botez, Andrei Vladimir Popov, Mahmoud Mamou et Youssef Mébarki. 2012d. « A Hybrid Fuzzy Logic Proportional-Integral-Derivative and Conventional On-off Controller for Morphing Wing Actuation Using Shape Memory Alloy, Part 2: Controller Implementation and Validation ». *The Aeronautical Journal,* vol. 116, n° 1179, p. 451-465.

Guilong, Zhang, Yang Lingyu, Zhang Jing et Han Chan. 2013. « Longitudinal Attitude Controller Design for Aircraft Landing with Disturbance using ADRC/LQR ». In. (Piscataway, NJ, USA), p. 330-5. Coll. « *2013 IEEE International Conference on Automation Science and Engineering (CASE)* »: IEEE. < http://dx.doi.org/10.1109/CoASE.2013.6653919 >.

Guo, Yi-Feng, Zhao-Dong Xu, Qing Tu et Cheng-Song Ran. 2010. « Optimal Analysis for Weight Matrices in LQR Algorithm Based on Genetic Algorithm ». *Zhendong yu Chongji/Journal of Vibration and Shock,* vol. 29, nº 11, p. 217-220.

Hamel, C., Sassi, A., Botez, R., Dartigues, C., . 2013. « Cessna Citation X Aircraft Global Model Identification From Flight Tests ». *SAE International Journal of Aerospace* vol. 6, nº 1, p. 106-114.

Hamel, Clement, Ruxandra Botez et Margaux Ruby. 2014. « Cessna Citation X Airplane Grey-box Model Identification Without Preliminary Data ». In *SAE 2014 Aerospace Systems and Technology Conference, ASTC 2014,*. (Cincinnati, OH, United states, Sept. 23- 25, 2014), September Vol. 2014-September, Coll. « SAE Technical Papers »: SAE International. < http://dx.doi.org/10.4271/2014-01-2153 >.

Han, Hua, An Luo et Yong Yang. 2005. « Nonlinear PID Controller Based on Genetic Tuning Algorithm ». *Kongzhi yu Juece/Control and Decision,* vol. 20, nº 4, p. 448-454.

Hecker, Simon, et Andras Varga. 2003. « Generalized LFT-based Representation of Parametric Uncertain Models ». In *European Control Conference (ECC),*(Cambridge, UK, Sept. 1-4, 2003). p. 763-768. IEEE.

Hecker, Simon, Andras Varga et Jean-Francois Magni. 2005. « Enhanced LFR-toolbox for Matlab ». *Aerospace Science and Technology,* vol. 9, nº 2, p. 173-180.

Hu, Jiankun, Christian Bohn et H. R. Wu. 1999. « Practical H Weighting Functions and their Application to Real-time Control of a Pilot Plant ». In *Proceedings of the 1999 American Control Conference (99ACC),*. (San Diego, CA, USA, June 2- 4, 1999) Vol. 2, p. 920-924. Coll. « *Proceedings of the American Control Conference* »: IEEE.

Hyde, R. A., et K. Glover. 1993. « The Application of Scheduled H Controllers to a VSTOL Aircraft ». *IEEE Transactions on Automatic Control,* vol. 38, nº 7, p. 1021-1039.

Hyung-Soo, Hwang, Choi Jeong-Nae, Lee Won-Hyok et Kim Jin-Kwon. 1999. « A Tuning Algorithm for the PID Controller Utilizing Fuzzy Theory ». In. (Waschington, DC, USA, July, 10-16, 1999), vol.4, p. 2210-15. Coll. « *IJCNN'99. International Joint Conference on Neural Networks. Proceedings (Cat. No.99CH36339)* »: IEEE. < http://dx.doi.org/10.1109/IJCNN.1999.833404 >.

Ibrir, Salim, et Ruxandra Botez. 2005. « Robust Stabilization of Uncertain Aircraft Active Systems ». *Journal of Vibration and Control,* vol. 11, nº 2, p. 187-200.

Jackson EB, Bilimoria KD, Mueller ER, Frost CR, Alderete TS. 2009. « Cooper-Harper Experience Report for Spacecraft Handling Qualities Applications ». *National Aeronautics and Space Administration, Langley Research Center*. 72 p. < http://www.aviationsystemsdivision.arc.nasa.gov/publications/shaq/NASA_Pub_2009_Bailey.pdf >.

Jiuqi, Han, Wang Peng et Yang Xin. 2012. « Tuning of PID Controller Based on Fruit Fly Optimization Algorithm ». In *Mechatronics and Automation (ICMA), 2012 International Conference on*. (Chengdu, China, Aug. 5-8, 2012), p. 409-413.

Jones, Karl O., et Wilfried Hengue. 2009. « Distillation Column Control Using Genetic Algorithms for LQR Design ». In *International Conference on Computer Systems and Technologies and Workshop for PhD Students in Computing, CompSysTech'09,* (Ruse, Bulgaria, June 18-19, 2009), vol. 433, p. IIIA.191-IIIA.196. Coll. « *ACM International Conference Proceeding Series* »: Association for Computing Machinery. < http://dx.doi.org/10.1145/1731740.1731789 >.

Kanojiya, R. G., et P. M. Meshram. 2012. « Optimal Tuning of PI Controller for Speed Control of DC Motor Drive using Particle Swarm Optimization ». In *Advances in Power Conversion and Energy Technologies (APCET), 2012 International Conference on*. (Mylavaram, Andhra Pradesh, India. Aug. 2-4 2012), p. 1-6.

Kharitonov, V. L., et A. P. Zhabko. 2003. « Lyapunov-Krasovskii Approach to the Robust Stability Analysis of Time-delay Systems ». *Automatica,* vol. 39, nº 1, p. 15-20.

Korte, Udo. 2002. « Tasks and Needs of the Industrial Clearance Process ». In *Advanced Techniques for Clearance of Flight Control Laws*. p. 13-33. Springer.

Kukreti, S., Kumar, M., K. Cohen. 2016. "Genetically tuned LQR based path following for UAVs under wind disturbance". *In Unmanned Aircraft Systems (ICUAS)*, 2016 *International Conference* on Jun. pp. 267-274 . IEEE.

Lanzon, Alexander. 2005. « Weight Optimisation in Script Hsignloop-shaping ». *Automatica,* vol. 41, nº 7, p. 1201-1208.

Lavretsky, E., et K. Wise. 2012. *Robust and Adaptive Control: With Aerospace Applications*. Springer London. 454 p.

Lee, C. S., W. L. Chan, S. S. Jan et F. B. Hslao. 2011. « A Linear-Quadratic-Gaussian Approach for Automatic Flight Control of Fixed-wing Unmanned Air Vehicles ». *Aeronautical Journal,* vol. 115, nº 1163, p. 29-41.

Lim, Andrew E. B., et Xun Yu Zhou. 1999. « Stochastic Optimal LQR Control with Integral Quadratic Constraints and Indefinite Control Weights ». *IEEE Transactions on Automatic Control,* vol. 44, nº 7, p. 1359-1369.

Lofberg, J. 2004. « YALMIP : a Toolbox for Modeling and Optimization in MATLAB ». In *2004 IEEE International Symposium on Computer Aided Control Systems Design* (Taipei, Taiwan, 2-4 Sept. 2004.), p. 284-290. Coll. « *2004 IEEE International Symposium on Computer Aided Control Systems Design (IEEE Cat. No.04TH8770)* »: IEEE.

Mack, L. M. 1975. « Linear Stability Theory and the Problem of Supersonic Boundary-layer Transition ». *AIAA Journal*, vol. 13, no 3, p. 278-289.

Magni, J.-F. 2006. « Linear Fractional Representation Toolbox for Use with Matlab ». February 2006, with the SMAC Toolbox. En ligne < http://w3.onera.fr/smac/lfrt.>

Manocha, Amit, et Abhishek Sharma. 2009. « Three Axis Aircraft Autopilot Control Using Genetic Algorithms: An Experimental Study ». In *Advance Computing Conference, 2009. IACC 2009. IEEE International*. (Patiala, India, March 6-7, 2009), p. 171-174. IEEE.

Marcos, Andrés, Joost Veenman, Carsten Scherer, G Zaiacomo, David Mostaza, Murray Kerr, H Koroglu et Samir Bennani. 2010. « Application of LPV Modeling, Design and Analysis Methods to a Re-entry Vehicle ». *AIAA Paper No. AIAA-8192*.

Mario, G Perhisnschi. 1999. « Parameter Optimization via Genetic Algorithm of Fuzzy Controller for Autonomous Air Vehicle ». In *AIAA Guidance, Navigation, and Control Conference and Exhibit,* (Portland, OR,USA. Aug.9-11, 1999),vol. 9. no 11. 4084 p.

Menon, Prathyush P., Declan G. Bates et Ian Postlethwaite. 2007. « Nonlinear Robustness Analysis of Flight Control Laws for Highly Augmented Aircraft ». *Control Engineering Practice*, vol. 15, no 6, p. 655-662.

Mitsukura, Y., T. Yamamoto et M. Kaneda. 1997. « A Genetic Tuning Algorithm of PID Parameters ». In. (New York, NY, USA) Vol. vol.1, p. 923-8. Coll. « *1997 IEEE International Conference on Systems, Man, and Cybernetics. Computational Cybernetics and Simulation (Cat. No.97CH36088-5)* »: IEEE. < http://dx.doi.org/10.1109/ICSMC.1997.626222 >.

Mukherjee, I. S., et J. K. Pieper. 2000. « Adaptive LQR Gain Sheduling Applied to an Experimental OHS Aircraft ». In *AIAA Guidance, Navigation, and Control Conference and Exhibit 2000,* (Dever, CO, United states Aug. 14-17, 2000.). Coll. « *AIAA Guidance, Navigation, and Control Conference and Exhibit* »: American Institute of Aeronautics and Astronautics Inc.

Murrieta-Mendoza, Alejandro, et Ruxandra Botez. 2015. « Aircraft Vertical Route Optimization Deterministic Algorithm for a Flight Management System ». In *SAE AeroTech Congress and Exhibition, AEROTECH 2015,* (Seattle, WA, United states, September 22-24, 2015.), September Vol. 2015-September. Coll. « *SAE Technical Papers »:* SAE International. < http://dx.doi.org/10.4271/2015-01-2541 >.

Murrieta-Mendoza, Alejandro, Ruxandra Mihaela Botez et Roberto S. Felix Patron. 2015. « Flight Altitude Optimization Using Genetic Algorithms Considering Climb and Descent Costs in Cruise with Flight Plan Information ». *In SAE AeroTech Congress and Exhibition, AEROTECH 2015*, (Seattle, WA, United states Sept. 22-24, 2015.), September Vol. 2015-September. Coll. « *SAE Technical Papers* »: SAE International. < http://dx.doi.org/10.4271/2015-01-2542 >.

Boely, Nicolas, Ruxandra Mihaela Botez et Gabriel Kouba. 2009. « Identification of a Nonlinear Model Between Control and Structural Deflections of an F/A-18 Aircraft ». *In 47th AIAA Aerospace Sciences Meeting including the New Horizons Forum and Aerospace Exposition*, (Orlando, FL, United states, January, 5-8, 2009). American Institute of Aeronautics and Astronautics Inc.

Neath, M. J., A. Swain, U. Madawala et D. Thrimawithana. 2013. « An Optimal PID Controller for a Bidirectional Inductive Power Transfer System Using Multi-objective Genetic Algorithm ». *Power Electronics, IEEE Transactions on,* vol. PP, nº 99, p.1-1.

Nelson, R.C. 1998. *Flight Stability and Automatic Control*. Coll. « Aerospace Science & Technology ». McGraw-Hill International Editions, 441 p.

Osinuga, M, Sourav Patra et Alexander Lanzon. 2012a. « State-space Solution to Weight Optimization Problem in $\mathcal{H}\infty$ Loop-shaping Control ». *Automatica,* vol. 48, nº 3, p. 505-513.

P.Albertos, and A.Sala. 2004. *Multivariable Control Systems*. Springer. 342 p. En ligne. < http://f3.tiera.ru/2/E_Engineering/Albertos%20P.,%20Sala%20A.%20Multivariable%20Control%20Systems..%20An%20Engineering%20Approach%20(Springer,2002)(ISBN%201852337389)(358s)_E_.pdf >. Consulté le 10 mai 2014.

Pahle, Joseph W, Keith D Wichman, John V Foster et W Thomas Bundick. 1996. « An Overview of Controls and Flying Qualities Technology on the F/A-18 High Alpha Research Vehicle ». 27 p. En ligne. < https://www.nasa.gov/centers/dryden/pdf/88435main_H-2123.pdf >. Consulté le 06 Novembre 2015.

Papachristodoulou, A., et S. Prajna. 2002. « On the Construction of Lyapunov Functions Using the Sum of Squares Decomposition ». In *Proceedings of IEEE Conference on*

Decision and Control, (Las-Vegas, USA, Dec. 10-13, 2002). (Piscataway, NJ, USA) vol.3, p. 3482-7.: IEEE. < http://dx.doi.org/10.1109/CDC.2002.1184414 >.

Perhinschi, Mario G, Giampiero Campa, Marcello R Napolitano, Marco Lando, Luca Massotti et Mario L Fravolini. 2002. « A Simulation Tool for on-line Real Time Parameter Identification ». In *AIAA Modeling and Simulation Technologies Conference and Exhibit 2002*,. (Monterey, CA, United states, Aug. 5-8, 2002).: American Institute of Aeronautics and Astronautics Inc.

Perhinschi, M. G., M. Lando, L. Massotti, G. Campa, M. R. Napolitano et M. L. Fravolini. 2002. « Online parameter estimation issues for the NASA IFCS F-15 fault tolerant systems ». In *Proceedings of 2002 American Control Conference*,. (Danvers, MA, USA, May,8-10,2002), vol.1, p. 191-196. American Automatic Control Council. < http://dx.doi.org/10.1109/ACC.2002.1024802 >.

Perhinschi, Mario G, Marcello R Napolitano, Giampiero Campa, Brad Seanor, Srikanth Gururajan et Gu Yu. 2005. « Design and Flight Testing of Intelligent Flight Control Laws for the WVU YF-22 Model Aircraft ». In *AIAA Guidance, Navigation, and Control Conference 2005*,. (San Francisco, CA, United states. Aug. 15-18, 2005), vol. 8, p. 5925-5936. American Institute of Aeronautics and Astronautics Inc.

Poodeh, M. B., S. Eshtehardiha, A. Kiyoumarsi et Mohammad Ataei. 2007. « Optimizing LQR and Pole Placement to Control Buck Converter by Genetic Algorithm ». In *Control, Automation and Systems, 2007. ICCAS '07. International Conference on*. (Ceox, Seoul, Korea, Oct. 17-20, 2007), p. 2195-2200. IEEE.

Popov, Andrei V, Lucian T Grigorie, Ruxandra M Botez, Mahmood Mamou et Youssef Mébarki. 2010. « Real Time Morphing Wing Optimization Validation using Wind-Tunnel tests ». *Journal of Aircraft,* vol. 47, nº 4, p. 1346-1355.

Poussot-Vassal, C., et C. Roos. 2011. « Flexible Aircraft Reduced-order LPV Model Generation from a Set of Large-scale LTI Models ». In *American Control Conference (ACC), 2011*. (San Francisco, CA, USA. June 29-July 1 2011), (Piscataway, NJ, USA), p. 745-750.IEEE.

Poussot-Vassal, C., et C. Roos. 2012. « Generation of a rRduced-order LPV/LFT Model from a Set of Large-scale MIMO LTI Flexible Aircraft Models ». *Control Engineering Practice,* vol. 20, nº 9, p. 919-930.

Pratt, R., 2000. *Flight control systems: practical issues in design and implementation* No. 57. Iet. pp. 382.

Price, K. V. 1996. « Differential Evolution: a Fast and Simple Numerical Optimizer ». In *Fuzzy Information Processing Society, 1996. NAFIPS., 1996 Biennial Conference of the North American*. (Berkeley, CA , USA, Jun. 19-22 1996), p. 524-527. IEEE

Puyou, G. 2007. *COFCLUO deliverable D1.1.1 - part 1. Report Describing the Selected Clearance Problem*. France SAS: Technical Report. En ligne< http://erprojects.gf.liu.se/main.php/projects/45b09cc684 >.

Puyou, Guilhem, et Yannick Losser. 2012. « Clearance Benchmark for a civil aircraft ». In *Optimization Based Clearance of Flight Control Laws*. p. 11-36. Springer.

Rahimian, M. S., et K. Raahemifar. 2011. « Optimal PID Controller Design for AVR System using Particle Swarm Optimization Algorithm ». In *Electrical and Computer Engineering (CCECE), 2011 24th Canadian Conference on*. (Niagara Falls, ON, Canada, May, 8-11, 2011), p. 000337-000340. IEEE.

Rogalsky, T., S. Kocabiyik et R. W. Derksen. 2000. « Differential Evolution in Aerodynamic Optimization ». *Canadian Aeronautics and Space Journal,* vol. 46, nº 4, p. 183-190.

Roskam, Jan. 1988. *Airplane Design: Deternination of Stability, Control and Performance Characteristics: FAR and Military Requirements*, 7. Roskam Aviation and Engineering Corp. 351 p.

Rugh, Wilson J. c1996. *Linear System Theory* Upper Saddle, N.J. : Prentice-Hall. p.581.

Saad, M. S., H. Jamaluddin et I. Z. M. Darus. 2012. « PID Controller Tuning Using Evolutionary Algorithms ». *WSEAS Transactions on Systems and Control,* vol. 7, nº 4, p. 139-149.

Samad, Tariq, et Anuradha Annaswamy. 2011. « The Impact of Control Technology: Overview, Success Stories, and Research Challenges ». *IEEE Control Systems Society*. 231 p.

Schirrer, A, C Westermayer, M Hemedi et M Kozek. 2010. « Robust H∞ Control Design Parameter Optimization via Genetic Algorithm for Lateral Control of a BWB type Aircraft ». *IFAC Proceedings Volumes,* vol. 43, nº 22, p. 57-63.

Seiler, Peter, Gary J. Balas et Andrew K. Packard. 2012. « Assessment of Aircraft Flight Controllers using Nonlinear Robustness Analysis Techniques ». *Lecture Notes in Control and Information Sciences,* vol. 416, p. 369-397.

Shi, Yang, Weiqi Qian, Qing Wang et Kaifeng He. 2006. « Aerodynamic Parameter Estimation using Genetic Algorithms ». In *2006 IEEE Congress on Evolutionary Computation, CEC 2006*,. (Vancouver, BC, Canada, July 16- 21, 2006), p. 629-633. Inst. of Elec. and Elec. Eng. Computer Society.

Shuai, Dong, Wang Zhisheng, Wang Yongji, Liu Lei et Ou Liuli. 2013. « Tracking Performance Analysis of Flight Control System Based on *H-infinity* Theory ». *International Journal of Modelling, Identification and Control,* vol. 19, nº 3, p. 290-8.

Skogestad, Sigurd, et Ian Postlethwaite. 2005. *Multivariable Feedback Control: Analysis and Design*, 2. Wiley New York. p. 592.

Standard, Military. 1990. *Flying Qualities of Piloted Aircraft*. MIL-STD-1797A, Department of Defense.

Stevens, Brian L., et Frank L Lewis. c2003. *Aircraft Control and Simulation*. Hoboken, N.J. : John Wiley, 664 p.

Storn, R., et K. Price. 1996. « Minimizing the Real Functions of the ICEC'96 Contest by Differential Evolution ». In *Evolutionary Computation, 1996., Proceedings of IEEE International Conference on*. (Nagoya, Japan 20-22 May 1996), p. 842-844. IEEE.

Storn, Rainer, et Kenneth Price. 1997. « Differential Evolution–a Simple and Efficient Heuristic for Global Optimization over Continuous Spaces ». *Journal of global optimization,* vol. 11, nº 4, p. 341-359.

Szabó, Zoltán, Andrés Marcos, David Mostaza Prieto, Murray L Kerr, Gábor Rodonyi, József Bokor et Samir Bennani. 2011. « Development of an Integrated LPV/LFT Framework: Modeling and Data-based Validation Tool ». *IEEE Transactions on Control Systems Technology,* vol. 19, nº 1, p. 104-117.

Tan, M. K., Y. K. Chin, H. J. Tham et K. T. K. Teo. 2011a. « Genetic Algorithm Based PID Optimization in Batch Process Control ». In *Computer Applications and Industrial Electronics (ICCAIE), 2011 IEEE International Conference on*. (Penang, Malysia, Dec. 4-7 2011), p. 162-167.

Tang, J., C. Wei et W. Meng. 2011. « Robustness Analysis of Unmanned Helicopter Flight Control Law using μ-analysis Techniques ». In *2011 6th IEEE Conference on Industrial Electronics and Applications*. (Beijing, China, June, 21-23, 2011), p. 1283-1287.

Tijani, I. B., Rini Akmeliawati, Ari Legowo, Mahmud Iwan et A. G. Abdul Muthalif. 2011. « Robust *H-infinity* Controller Synthesis using Multi-objectives Differential Evolution Algorithm (MODE) for Two-mass-spring System ». In *2011 4th International Conference on Modeling, Simulation and Applied Optimization, ICMSAO 2011,*. (Kuala Lumpur, Malaysia, Apr.19-21, 2011). IEEE Computer Society. < http://dx.doi.org/10.1109/ICMSAO.2011.5775610 >.

Tischler, MB. 1996. *Advances in aircraft flight control*. CRC Press; Jun 28, pp. 750.

Toh KC, Todd MJ, Tütüncü RH. 2012. *On the Implementation and Usage of SDPT3–a Matlab Software Package for Semidefinite-Quadratic-Linear Programming, version 4.0*. Coll. « In Handbook on semidefinite, conic and polynomial optimization »: Springer US, pp. 715-754 p.

Turoczi, Antal. 2009. « Flight Control System of an Experimental Unmanned Quad-Rotor Helicopter ». In *10th International Symposium of Hungarian Researchers on Computational Intelligence and Informatics, CINTI 2009,*. (Budapest, Hungary, Nov. 12-14, 2009), p. 777-789. Budapest Technical College.

Varga A, Hansson A, Puyou G. 2012. *Optimization Based Clearance of Flight Control Laws*, vol. 416. Coll. « A Civil Aircraft Application ». Berlin Heidelberg: Springer, 419 p.

Varga, A., et G. Looye. 1999. « Symbolic and Numerical Software Tools for LFT-based Low Order Uncertainty Modeling ». In *Proceedings of the 1999 IEEE International Symposium on Computer Aided Control System Design,* (Kohala Coast, HI, USA, Aug. 22-27, 1999). (Piscataway, NJ, USA), p. 1-6. IEEE. < http://dx.doi.org/10.1109/CACSD.1999.808615 >.

Varga, Andras, Gertjan Looye, Dieter Moormann et G Gräbel. 1998. « Automated Generation of LFT-based Parametric Uncertainty Descriptions from Generic Aircraft Models ». *Mathematical and Computer Modelling of Dynamical Systems,* vol. 4, nº 4, p. 249-274.

Vincent, Jean Baptiste, Ruxandra Mihaela Botez, Dumitru Popescu et Georges Ghazi. 2012. « New Methodology for a Business Aircraft Model Hawker 800 XP Stability Analysis using Presagis FLsim ». In *AIAA Modeling and Simulation Technologies Conference 2012,*. (Minneapolis, MN, United states, Aug. 13-16, 2012). American Institute for Aeronautics and Astronautics (AIAA). < http://dx.doi.org/10.2514/6.2012-4564 >.

Walker, DJ, MC Turner et AW Gubbels. 2001. *Practical Aspects of Implementing H-infinity Controllers on a FBW Research Helicopter*. LEICESTER University (UNITED KINGDOM) Dept of Engineering

Wang, Fan, et Venkataramanan Balakrishnan. 2002. « Improved Stability Analysis and Gain-Scheduled Controller Synthesis for Parameter-dependent Systems ». *IEEE Transactions on Automatic Control,* vol. 47, nº 5, p. 720-734.

Wang, Hai-Tao, Shu-Wei Guo, Peng Guo et Zi-Zeng Qin. 2010a. « Application of Genetic Algorithms for Aerodynamic Parameter Estimation of Large Parachute ». *Yuhang Xuebao/Journal of Astronautics,* vol. 31, nº 4, p. 981-985.

Wongsathan, Chaiporn, et Chanapoom Sirima. 2009. « Application of GA to Design LQR Controller for an Inverted Pendulum System ». In *2008 IEEE International Conference on Robotics and Biomimetics, ROBIO 2008,*. (Bangkok, Thailand, Feb. 21-26, 2009), p. 951-954. IEEE Computer Society. < http://dx.doi.org/10.1109/ROBIO.2009.4913127 >.

Wu, C. Y., et K. Y. Tseng. 2010. « Stress-based Binary Differential Evolution for Topology Optimization of Structures ». *Proceedings of the Institution of Mechanical Engineers, Part C: Journal of Mechanical Engineering Science,* vol. 224, nº 2, p. 443-457.

Wu, Jun Feng, et Le Xiao. 2010. « Research on LQR Control Optimized by Elitist Preserving Genetic Algorithm ». In *2nd International Conference on Information Science and Engineering, ICISE2010,*. (Hangzhou, China, Dec. 4-6, 2010), p. 5327-5329. IEEE Computer Society. < http://dx.doi.org/10.1109/ICISE.2010.5689281 >.

Xiaohu, Li, Du Haifeng, Zhuang Jian et Wang Sunan. 2008. « A PID Parameters Tuning Algorithm Inspired by the Small World Phenomenon ». In *4th International Conference on Intelligent Computing, ICIC 2008*. (Shanghai, China, Sept. 15-18, 2008), p. 817-24. Springer-Verlag.

Xiong, Xin, et Zhou Wan. 2010. « The Simulation of Double Inverted Pendulum Control Based on Particle Swarm Optimization LQR Algorithm ». In *2010 IEEE International Conference on Software Engineering and Service Sciences, ICSESS 2010,*. (Beijing, China, July 16-18, 2010), p. 253-256. IEEE Computer Society. < http://dx.doi.org/10.1109/ICSESS.2010.5552427 >.

Yan, Wei-Yong, et John B Moore. 1996. « Stable Linear Fractional Transformations with Applications to Stabilization and Multistage H^2 Control Design ». *International Journal of Robust and Nonlinear Control,* vol. 6, nº 2, p. 101-122.

Yang, Shi, Qian Weiqi, Wang Qing et He Kaifeng. 2006. « Aerodynamic Parameter Estimation Using Genetic Algorithms ». In *2006 IEEE Congress on Evolutionary Computation*, (Vancouver, BC, Canada,16-21 July 2006). (Piscataway, NJ, USA), p. 629-633. IEEE.

Yoon Joon, Lee, et Cho Kyung Ho. 1997. « Determination of the Weighting Parameters of the LQR System for Nuclear Reactor Power Control using the Stochastic Searching Methods ». *Journal of the Korean Nuclear Society,* vol. 29, nº 1, p. 68-77.

Yu, Wei-Jie, et Jun Zhang. 2012. « Adaptive Differential Evolution with Optimization State Estimation ». In *14th International Conference on Genetic and Evolutionary*

Computation, GECCO'12,. (Philadelphia, PA, United states, July 7- 11, 2012), p. 1285-1291. . Association for Computing Machinery. < http://dx.doi.org/10.1145/2330163.2330341 >.

Zakaria, M. Z., H. Jamaluddin, R. Ahmad et A. H. Muhaimin. 2011a. « Effects of Genetic Algorithm Parameters on Mmultiobjective Optimization Algorithm Applied to System Identification Problem ». In *2011 Fourth International Conference on Modeling, Simulation and Applied Optimization (ICMSAO 2011),* (Kuala Lumpur, Malaysia, April, 19-21, 2011). (Piscataway, NJ, USA), p. 5 pp. IEEE. < http://dx.doi.org/10.1109/ICMSAO.2011.5775624 >.

Zames, G. ; Francis, B.A. « Feedback, Minimax Sensitivity, and Optimal Robustness ». *Automatic Control, IEEE Transactions* vol. 28, nº 5. p. 585-601.

Zames, G., et L. Y. Wang. 1991. « Local-global Double Algebras for Slow H∞ Adaptation Inversion and Stability ». *IEEE Transactions on Automatic Control,* vol. 36, nº 2, p. 130-142.

Zeng, Xianqiang, Lan Jing, Zeen Yao et Yuhui Guo. 2012. « A PSO-based LQR Controller for Accelerator PWM Power Supply ». In *2nd International Conference on Mechatronics and Intelligent Materials 2012, MIM 2012*. (GuiLin, China, May 18-19, 2012) Vol. 490-495, p. 71-75. Coll. « Advanced Materials Research »: Trans Tech Publications. < http://dx.doi.org/10.4028/www.scientific.net/AMR.490-495.71 >.

Zhi, Wei, QingSheng Luo et JianFeng Liu. 2012. « An Improved PID Tuning Algorithm for Mobile Robots ». In *Electronic Commerce, Web Application and Communication, ECWAC 2012,* (Wuhan, China. March 17- 18, 2012.), vol. 148 AISC, p. 345-353. Coll. « Advances in Intelligent and Soft Computing »: Springer Verlag. < http://dx.doi.org/10.1007/978-3-642-28655-1_55 >.

Zhou, Kemin, John Comstock Doyle et Keith Glover. 1996. *Robust and Optimal Control*, 40. Prentice Hall New Jersey. 596 p.

Zhu, Jinghao, et Kangdi Li. 2003. « An Iterative Method for Solving Stochastic Riccati Differential Equations for the Stochastic LQR Problem ». In *Special Issue part I*. 6 I vol. 18, p. 721-732. Coll. « Optimization Methods and Software »: Taylor and Francis Inc. < http://dx.doi.org/10.1080/10556780310001636657 >.